Development, optimisation and application of novel thermal probe techniques for the study of biological systems

by

Zdravka Yordanova Dragnevska

Thesis submitted for the degree of Doctor of Philosophy

School of Pharmacy
University of East Anglia
Norwich, Norfolk
NR4 7TJ

August, 2011

Abstract

Atomic Force Microscopy (*AFM*) in combination with Micro/Nano-Thermal Analysis and Infrared Spectroscopy (*Photothermal Microspectroscopy*) has been shown to be a unique experimental approach that can be used not only for high-resolution imaging, but also to simultaneously study interactions between different material systems. These techniques have been successfully applied to a number of model systems, including Paracetamol & Polystyrene spheres, but more importantly in the study of the interactions of *E.coli* bacterial cells with pharmaceutically relevant materials, such as antibiotics (Ampicillin). In this largely experimental research it was clearly demonstrated that the use of a lock-in amplifier leads to a significant reduction in the signal to noise ratio, which leads to an increase in the sensitivity of the probes used. This would undoubtedly provide greater confidence and improved consistency in any measurements carried out using AFM. *Thermal* Force Distance Curves (*t*-FDC) from *E.coli* cells were obtained for the first time ever in this study. Furthermore, it was shown that within a narrow temperature range there is a step decrease in the adhesive force representing the cell-tip interaction, which can be associated with structural changes occurring in the individual cells. Photothermal Microspectroscopy (PTMS) was also successfully developed and used in the study of treated and untreated with antibiotics bacterial cells. The findings in this study provided conclusive evidence that PTMS may not only be used to examine cell cycle associated intracellular structural changes, but also interactions between cells and pharmaceutically relevant materials. It is strongly believed that these findings would constitute a novel approach in the use of Microspectroscopy.

Acknowledgments

First of all I would like to thank my supervisor Prof Duncan Craig for giving me the opportunity to do a PhD course at the University of East Anglia and for his useful input and advice on my writing. Special thanks go to my co-supervisor Prof Mike Reading for his enormous help with my experimental work, for being there for me every time I needed help, for the useful discussions that we had in the lab and for teaching me everything that I know about AFM.

Special thanks go to Dr Graeme Hill for the technical support and also for the helpful discussions over the years; Dr Patrick Gunning (IFR) for helping me with the preparation of the E.coli cells for imaging; Dr Anja Muller for teaching me how to grow my cells; Dr Jonathan Moffat for the help with the IR techniques and Dr Klaus Wellner (IFR) for supplying the samples for the PTMS studies. I would also like to thank all my colleagues from the research group and all the technical stuff in the School for their help over the years.

My deepest thanks go to my family in Bulgaria, especially my dad Yordan for his priceless help with my children, my mum Gergana for not-stop believing in me and my sister Olga for being there for me.

Finally, I would like to thank my husband Kalin for his love and support, and for being there for me all the way. Without him, any of this wouldn't happen…

Zdravka Dragnevska

To my two beautiful angels Yvonne and Daniel

"There is neither happiness nor misfortune in this world, there is merely the comparison between one state with another, nothing more."

"Until the day when God deigns to unveil the future to mankind, all human wisdom is contained in these two words: 'wait' and 'hope'!!!'"

(from the letter of Edmond Dantès to Maximilien Morrel)

The Count of Monte Cristo

Alexandre Dumas (Père)

Table of Contents

List of Figures

Figure 4.4 Pulse Force Mode (PFM) images of aggregated HB101 E.coli cells **(a)** low and **(b)** high magnification (top – internal sensor, bottom – topography)

Figure 4.5 PFM AFM images of MG16SS E.coli cells prior to treatment with Ampicillin; (a) low magnification images of aggregated of E.coli cells and (b) higher magnification images of individual bacterial cells (top – adhesion, bottom – topography)

Figure 4.6 PFM AFM images of MG16SS E.coli cells after 5 hours of treatment with Ampicillin; **(a)** 2 cells in contact with each other and **(b)** high magnification image of an individual cell (left – topography, right – adhesion)

Figure 4.7 PFM AFM images of MG16SS E.coli cells after 8 hours of treatment with Ampicillin; **(a)** low and **(b)** high magnification (left – topography, right – adhesion)

Figure 4.8 High **(a)** and low **(b)** PFM AFM images of MG16SS E.coli cells taken with conventional probes after 12 hours of treatment with Ampicillin. Significant cell degradation can clearly be seen (top – adhesion, bottom – topography)

Figure 4.9 Representative AFM image of E.coli cells after 12h exposure to 25mg/ml concentration of Ampicillin (*after Perry et al., 2009*)

Figure 4.10 Thermal images of HB101 E.coli bacterial cells obtained with Wollaston wire probe at **(a)** 30^0C and **(b)** 70^0C (left – topography, right – internal sensor)

Figure 4.11 PFM images of untreated MG16SS E.coli bacterial cells obtained using heated nano tips at **(a)** 30^0C and **(b)** 70^0C (top – adhesion, bottom – topography)

Figure 4.12 PFM images of treated with Ampicillin MG16SS E.coli bacterial cells (12h) obtained using heated nano tips at **(a)** 30^0C and **(b)** 70^0C, top – adhesion, bottom – topography

1. Introduction

The development of Scanning Probe Microscopy (SPM) began in the early 1980s through the invention of the Scanning Tunnelling Microscope (STM) by the Nobel Prize winners Binning and Rohrer (Binnig *et al.*, 1986). In Scanning Tunnelling Microscopy the surface structure of the material is interogated by scanning it with a sharp probe and measuring the electron tunnelling between the surface and the probe. Later that year the second member of the SPM family, the Atomic Force Microscope (AFM) was announced by Binning, Quate and Gerber and commercial Atomic Force Microscopes became available in the early 1990s.

Atomic Force Microscopy creates images by "feeling" rather than "looking" at samples, much like one would read Braille (Round *et al.*, 1999). This novel imaging method results in magnification range spanning that associated with both the Optical and the Electron Microscopes. This experimental technique presents the opportunity to image systems, such as biological materials, in real time under natural conditions, with molecular or sub-molecular resolution. The AFM is perhaps the most widely used, and certainly the most versatile, member of the Scanning Probe Microscopy family. As the name suggests, probe microscopes share as a common feature a probe that interacts with the sample in one way or another. Since its invention, the Atomic Force Microscope has evolved as a powerful technique that not only offers the advantage of obtaining high resolution images, but also to simultaneously study their mechanical response produced from the interaction with the probe. The technique is currently being applied to a wide range of pharmaceutical and biological systems.

In the early 90s and 00s the technique was further developed to incorporate the use of heated probes as means of scanning the sample surface. Pylkki *et al* (1994) used a probe made of Wollaston wire, whereby the tip could be used not only as a thermometer, but also as a heat source. In this way it was possible to perform not only Scanning Thermal Microscopy, but also Localised Thermal Analysis. This experimental methodology was further developed incorporating it with Modulated Thermal Differential Scanning Calorimetry (Hammiche *et al.*, 1996) and the newly invented instrument was commercially launched in 1998 by TA Instruments, Inc. as a Micro Thermal Analyzer.

The latest development in Scanning Probe Microscopy – Photothermal Microspectroscopy (PTMS) was introduced by Hammiche and co-workers in the late 90s early 00s. The basis of this approach is the combined use of a FT-IR spectrometer with an AFM equipped with a thermal probe (Hammiche *et al.*, 1996). The technique allows measurements of spatially resolved IR spectra in inhomogeneous samples at a spatial resolution greater that the diffraction limit (Hammiche *et al.*, 2003).

This research project was aimed at further developing and optimising the use of Atomic Force Microscopy in the study of biological systems, predominantly E.coli cells, and their interactions with pharmaceutically relevant materials. A combination of AFM and Infrared Spectroscopy (PTMS) was also used in order to provide further insight into the structure, composition and interactions of the studied systems.

2. Literature Survey

2.1. Introduction

The purpose of the chapter is to highlight the areas of relevance to the work that was undertaken for this research project and to review current theory. Firstly, the principles and applications of AFM will be considered. This is followed by a presentation of the principles and applications of Microthermal Analysis (μTA). Special emphasis is placed on the applications of the above technique to pharmaceutical and biological systems, as these are currently one of the most widely studied, but yet not fully examined materials systems.

2.2. Atomic Force Microscopy (AFM)

2.2.1. Principles

AFM generates images by "feeling" the specimen; a good analogy is that of a blind person using their fingers to feel Braille characters (Round *et al.*, 1999). In AFM the images are generated by feeling the surface of the specimen using a sharp probe (**Figure 2.1**). The probe is attached to a spring or cantilever that is positioned close to the surface of the sample (Binnig *et al.*, 1982). In the normal mode of operation the probe is close to the surface of the sample and there is a repulsive interaction between the surface and the probe and this repulsion causes the bending of the cantilever to which the probe is attached. As the surface of the sample is scanned beneath the probe the roughness of the surface causes the repulsive force to vary. These variations

in repulsive force are detected by monitoring the degree of bending of the cantilever, and this can be used to generate an image of the surface (Binnig *et al.*, 1986).

Modern Atomic Force Microscopes use wide range of techniques to generate images of sample surfaces. An example of a detection method is the optical lever method, where a laser beam is reflected off the back of the cantilever onto a photodiode detector (**Figure 2.1**). Probe-cantilever assemblies are constructed using modern micro-fabrication methods such as the ones used to make integrated circuits. The cantilevers are generally made of silicon nitride or silicon, as these materials are both very hard and wear resistant, making them ideal for micro-fabrication. The scanning of the tip relative to the sample surface is controlled using piezoelectric transducers (Morris *et al.*, 1999).

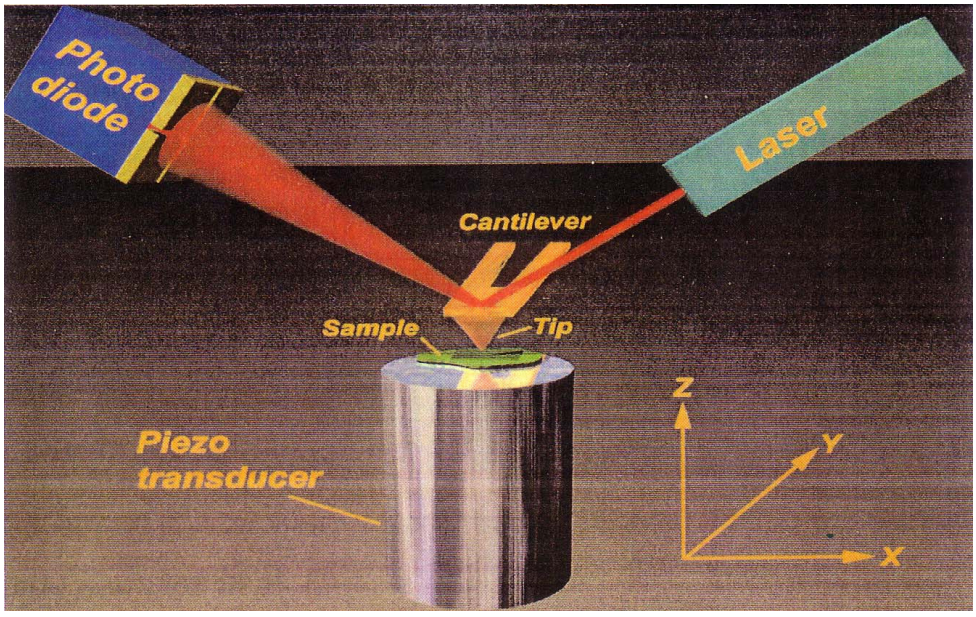

Figure 2.1 Schematic representation of the Atomic Force Microscope (*after Morris et al.*, 1999)

Modes of operation

The AFM can be operated in many different modes depending on the nature of the studied system and the required information, three of these being contact or dc, non-contact or tapping and pulse force mode (PFM). The contact and tapping modes (**Figure 2.2**) are generally methods most commonly applied to biological systems (Adams, 2001) and hence are discussed here in more detail.

Contact mode

In contact mode, the tip is in continuous contact with the surface as it scans over the sample (the tip-sample interaction is repulsive). This process can be performed either in air or under a liquid, such as a biological buffer or precipitant. This imaging mode is also known as "constant force mode" as the imaging force is pre-set using the instrument software. This is equivalent to scanning the sample with the cantilever bent to a small but a fixed amount (Bhushan, 1999). By adjusting the force it is possible to optimise the image contrast and minimise damage to the sample. When using contact mode in air at normal Relative Humidity (RH) a layer of water condenses on the surface. This water forms a strong liquid meniscus that pulls the tip down towards the sample, giving rise to capillary forces. This effectively "glues" the tip to the sample and disrupts or displaces the macromolecules being imaged. This may lead to damaging of soft or fragile samples due to scraping. The elimination of the adhesive force between the tip and substrate can be achieved by imaging under liquids (Atomic force microscopy - Pulsed force mode Operation Manual, 2000).

Tapping mode

This is one of the non-contact modes used in AFM imaging. In tapping mode, the cantilever is exited by electrical oscillator to amplitudes of up to approximately 100nm, so it effectively "bounces" up and down or taps as it scans the surface. Tapping mode reduces the lateral force on the sample because the tip spends less time in contact with the surface, a useful feature when imaging delicate samples. The tapping mode in air also prevents the AFM tip being trapped by capillary forces caused by an extremely thin film of water surrounding samples in air (Aoki *et al*., 1997).

(i) Constant-force mode

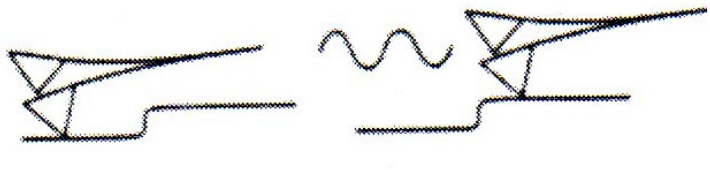

(ii) Tapping mode

Figure 2.2 Different AFM imaging modes *(after Adams*, 2001)

Pulse Force Mode (PFM)

Pulsed force mode is generally considered as an intermittent contact mode AFM that is able to separate stiffness and adhesion data that are collected as separate images. It was introduced by Rosa-Zeiser and co-workers (1997).

In PFM-AFM images are constructed from force distance curves (see Section 2.3) – the process being repeated with a set frequency while the tip is raster scanned over the sample surface (**Figure 2.3**). A tip is oscillated perpendicular to the surface, with the tip being pulled into the sample and then retracted with a typical frequency of 0.1-2 kHz and amplitude of 10-500 nm (Murray *et al.*, 1998, Pollock and Hammiche, 2001).

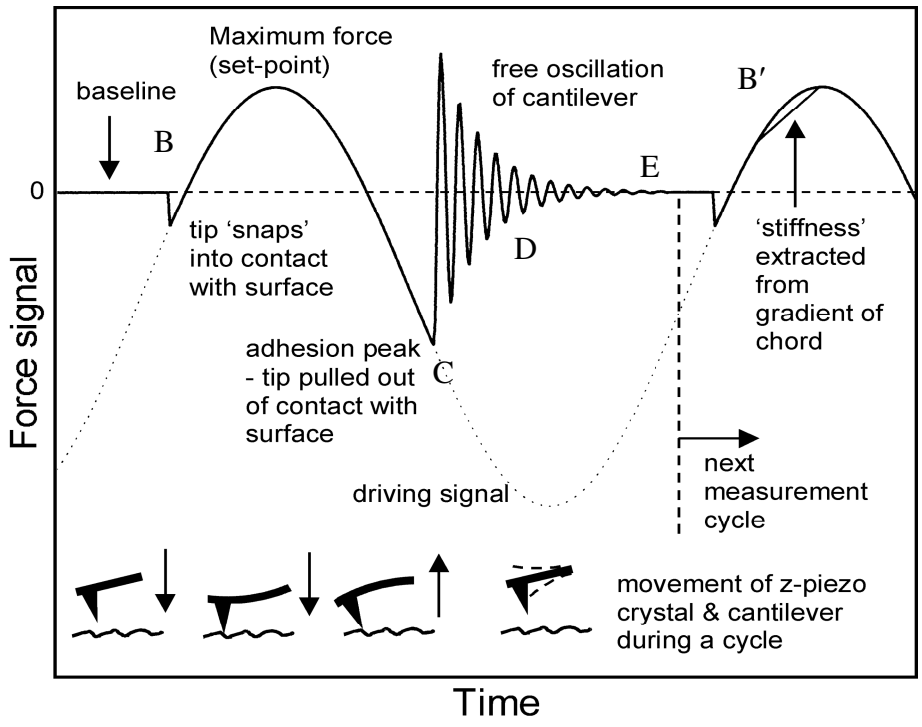

Figure 2.3 Operation of PFM-AFM *(after Grandy, 2002)*

Figure 2.3 shows the operation of PFM-AFM. The contact part of the cycle is exaggerated in comparison with the non-contact part for clarity. The solid line shows the variation of force with time during a measurement cycle, while the dotted sinusoidal trace shows the driving voltage applied to the cantilever. Initially, the tip is above the sample surface. As the probe gets closer to the sample surface, the attractive forces bring the tip into contact (point A). The tip is pushed further into the sample and the repulsive forces reach a maximum (point B). After this point, the probe is pulled away with the attractive forces taking over again due to the adhesive interaction between the sample and the tip. At point C, the tip loses contact as the force exerted by the bending of the cantilever exceeds the attractive force. The subsequent free oscillation of the probe is damped towards the baseline (point D) before the cycle starts again (Grandy, 2002).

AFM image types

Different types of images can be created by AFM depending on what sample properties are most relevant. The main types of images created by AFM are topographical, internal sensor and adhesion (in the case of Pulse Force Mode AFM). Examples of these are presented in **Figure 2.4**. Topographical images are the most common way of recording AFM images. The information used to create a topographical image is simply the vertical movement of the piezoelectric tube. From this type of image it is possible to measure the heights of molecules in the imaging modes. As the cantilever bends, the reflected laser “spot” moves across the

photodiode and the consequent displacement signal is used by a feedback loop to generate the image.

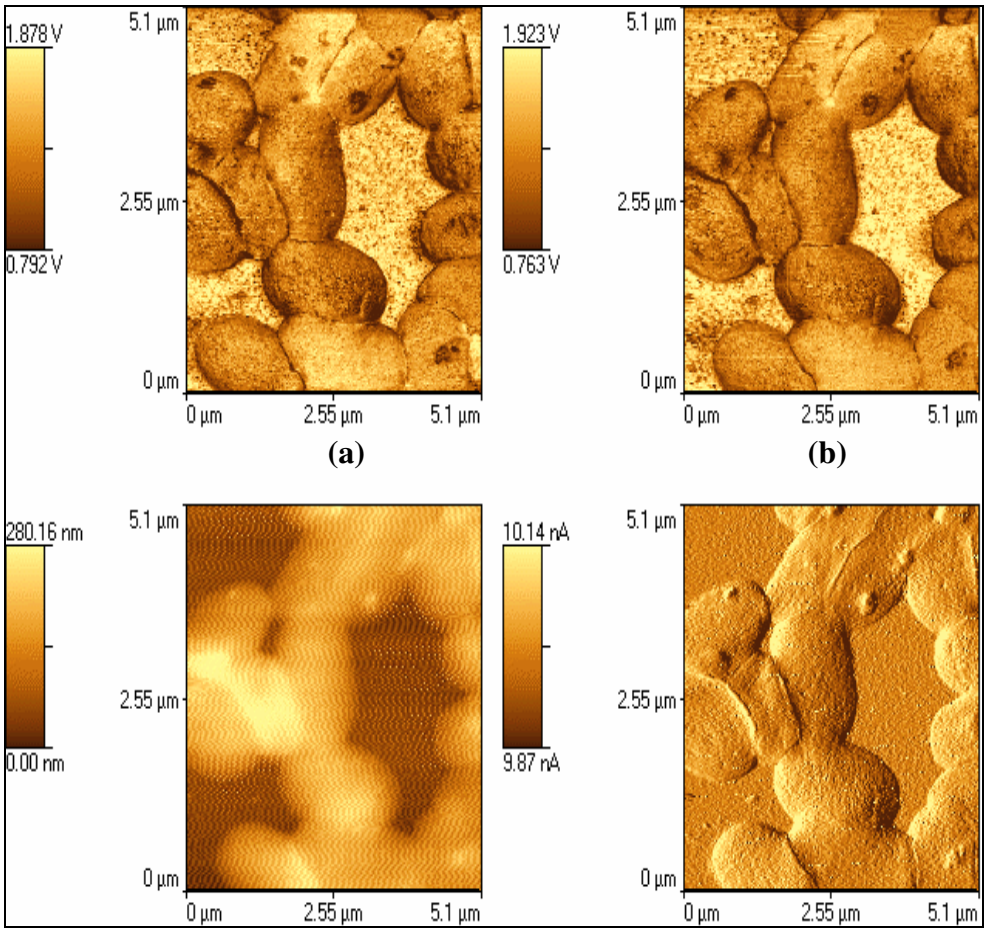

Figure 2.4 Examples of different AFM images of E.coli cells obtained in this study; **(a)** adhesion image forward, **(b)** adhesion image reverse, **(c)** topography image and **(d)** internal sensor image

The sample is scanned line-by-line until a two–dimensional map is created with height information presented in the operator choice of colour. Constant force

conditions are attained by using a feedback system that monitors the deflection of the cantilever that under ideal conditions approximates the force between sample and tip. The feedback loop has a finite frequency response and does not respond instantly to a deviation from the set point; the force can fluctuate briefly before equilibrium is restored. These changes can be monitored and used to generate an internal signal image. The internal signal can be used to generate an image that reveals the edges and therefore considerably more detail of the surface topography.

2.2.2. Application of AFM to biological systems

Since its invention, AFM, with its wide range of applications, has been extensively used in the study of a number of material systems and hence there is a large library of information available to the research community. Due to the nature of this research project, in this part of the literature survey only the more significant and relevant advances in biological systems will be considered. The areas of interest, examples of which are discussed here include bacterial cells, DNA molecules, cancer cells and plants.

Bacterial Cells

Since the early 90's Atomic Force Microscopy with its high resolution and unique features has been extensively used to obtain three-dimensional images of a wide variety of biological samples, ranging from living cells to individual macromolecules (Putman *et al*., 1992; Bustamante *et al*., 1992, Shao *et al*., 1996). Here, as suggested

above, some of the more recent and significant ones will be discussed. These are presented in chronological order.

The main benefit of this technique undoubtedly lies in its ability to characterize viable cells in real time. Unlike other high-resolution microscopy methods that require dehydrating and essentially killing cells (like SEM and TEM), AFM can image living cells sustained in liquid media with nanometre resolution. Also when used in different AFM modes can resolve exquisite subcellular structures, such as function proteins, or even defective domains of pathologic proteins.

Yu and Ivanisevic (2004) used tapping mode AFM to study the morphological and adhesion properties of encapsulated human platelets and *B. subtilus* spore cells coated with different numbers of polymer layers. They successfully mapped out the properties of the encapsulated cells in sufficient details and were able to design lithographic approaches that utilize the tip to pattern onto soft, biomimetic surfaces. In their study it was clearly demonstrated that the roughness of the encapsulated cells increased as the number of adsorbed polymer layers increased. As a result it was suggested that the encapsulated cells' morphology and roughness together with their other characteristics could qualify them as a good choice for the design and the construction of templated biomimetic architectures, where AFM can be used as the primary tool to do the fabrication.

In the same year Milani *et al* (2004) compared the performance of different high-resolution microscopy techniques in the study of *Saccharomyseces Cerevisiae* yeast

cells, a well known sample of most certainly great biological interest. These included Soft X-ray Contact Microscopy (SXCM), Atomic Force Microscopy (AFM), Focused Ion Beam (FIB) and Transmission Electron Microscopy (TEM). It was shown that AFM is a technique which allowed the cell surface to be directly imaged and probed and also to evaluate its dimensions in 3D. The authors also suggested that AFM allowed them to "navigate", i.e. to choose a single cell among a population of cells simply deposited on a substrate. The only disadvantage reported was that the tip jumps were found to be limited to 2-3 μm in height; therefore only rather flat samples can be analyzed. However, ultimately it was suggested, quite reasonably, that obviously yeast cells are not completely representative of the very many different biological samples and the optimal choice of the imaging technique would depend on the type of biological sample as well as on the goal of the research.

Poole *et al* (2004) used AFM to investigate whether raft lipids of Madin-Darby canine kidney cells (MDCK) cells play any role in microvilli maintenance. The authors showed that imaging, at low forces, low speed and under optimized conditions allowed visualization of the surface structures correspond that to microvilli. However, it was reported that the individual microvilli appeared clustered. This was thought to be due to the fact that AFM imaging relies on a mechanical interaction with the sample also results in the bending of flexible surface structures in the scanning direction of the AFM stylus. Nevertheless the data obtained from this study suggested that raft lipids are essential for microvilli maintenance, possibly by providing the membrane architectures necessary for cytoskeletal organization.

Based on near-field metallic-tip enhanced microscopy and frequency-domain finite element method (FEM) simulation Hu *et al.* (2004) developed and applied a combined approach using AFM and optical microscopy to investigate the correlated topographic and spectroscopic information of nanoparticle and biological systems **Figure 2.5**. Fluorescence lifetime images (FLIM) of living cells showed high promise of biological optical imaging beyond the diffraction limit, providing information that is not obtainable using non-correlated and far-field imaging approaches. The only major difficulty of AFM imaging of live bacteria cells was reported to be the issue of physically fixing their motions for a long enough time.

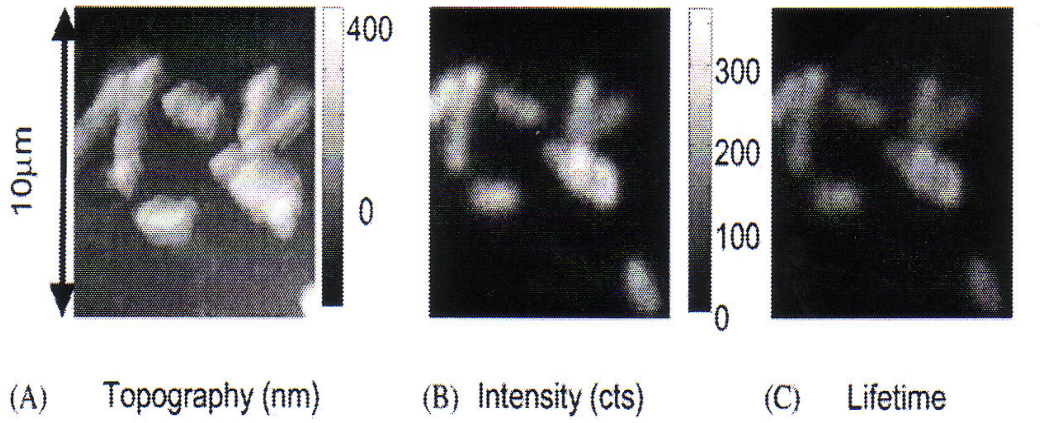

Figure 2.5 Composite correlated AFM-confocal (FLIM) image of *S. oneidensis* bacterial cells on poly lysine surface: (A) topographic AFM image, (B) confocal fluorescence intensity, and (C) confocal fluorescence lifetime image (*after Hu et al.*, 2004)

Later, Pelling *et al* (2005) used high resolution AFM imaging combined with in vivo force spectroscopy to characterize the social bacterium *Myxococcus xanthus* which led to the revelation of not only the cell coordination and organisation in a social

gliding group (**Figure 2.6**), but also the morphological details of extracellular ultrastructure under native conditions and at a resolution comparable to Electron Microscopy (EM). In addition to high-resolution imaging the mechanical properties of the *Myxococcus xanthus* cells were investigated with AFM in aqueous conditions. It is not unreasonable to suggest that these findings provided the basis for AFM to become a useful tool for investigating microbial-surface ultrastructure and nanomechanical properties under native conditions.

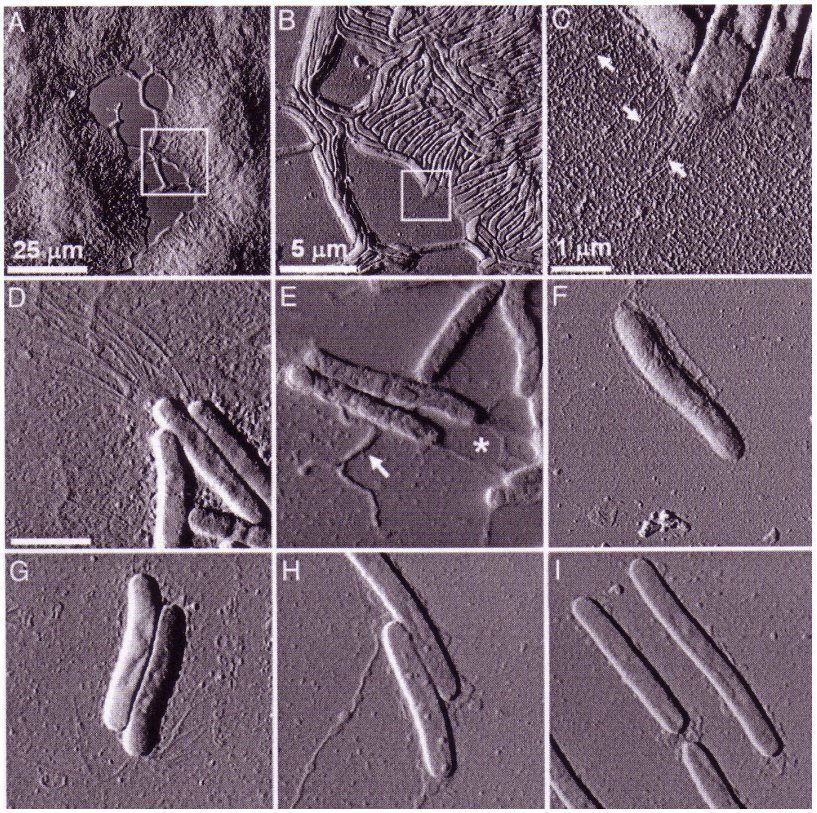

Figure 2.6 AFM deflection-mode images of large socialgroups (A-C) and individual *M.xanthus* cells (D-I) in air (*after Pelling et al.*, 2005)

The more recent AFM studies in cell biology appear to be focused on developing new and improvement of the existing methods for cell immobilization. Kailas *et al.*

(2009) introduced a novel method for immobilizing coccoid bacteria on inert surfaces for in vivo AFM imaging. They used lithography to develop patterned surfaces with hole arrays for the mechanical entrapment of live bacterial cells. This method allows the cells to continue with their cellular processes and gives control over the size, shape, and depth of the holes, as well as reduces the vertical height to be traversed by the AFM probe to scan over the cell diameter.

In another interesting recent study, Zhao *et al* (2009) immobilized live bacteria by means of antibodies that act against bacterial surface antigens. Their results suggest that this method is effective when the antibody used for bacterial immunoimmobilization targets a surface antigen which extends out from the bacterial surface and is tightly attached to the bacterial cell wall.

DNA Molecules & Cancer Cells

Avramovivic *et al* (2005) used AFM to study the interaction between adriamycin (ADR) and DNA leading to ADR antitumour activity in malignant cells *in vitro*. This work is of great significance as ADR is the first anthracycline drug that has been used in clinical practice since 1960's and still remains the most widely used anticancer therapeutics. AFM was used to study this interaction in DNA samples extracted from ADR–treated and non-treated Ehrlich tumour cells. The AFM images of the DNA samples showed significant difference in the morphology of the chromatin of non-treated and adriamycin-treated cells. Therefore, it can be suggested that AFM also

proves to be a unique tool in the investigation of drug treatment of cancer cells and can be of great importance for the future development of anticancer therapeutics.

Other earlier significant studies on DNA include an earlier one carried out by Oberringer *et al* (2003), which focused on the combination of biochemical and nanomanipulation techniques, which enable both nanodissection and nanoextraction of chromosomal DNA. The standard methods of imaging chromosomes from metaphase preparations are based on conventional light microscopy. However, the resolution of light microscopy is by far not good enough to analyze the fine structure of chromosomes. The higher resolution of AFM allows a more precise localization compared to standard techniques, and the extraction of very small amounts of chromosomal DNA by the scanning probe is possible. By using AFM, complete metaphase plates showing 46 chromosomes can easily be visualized in detail. A typical image is shown in **Figure 2.7**.

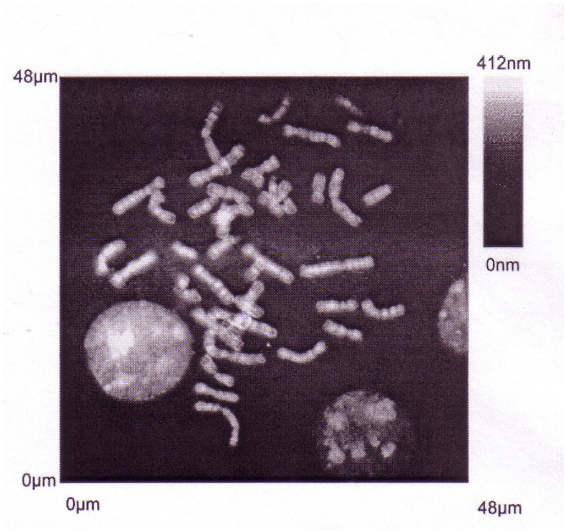

Figure 2.7 GTG-banded human metaphase chromosomes of one cell and several nuclei visualized by AFM (*after Oberringer et al*., 2003)

A higher resolution within a certain band will offer the possibility to extract chromosomal material under better-defined conditions. Usually, complete chromosomes bands are extracted by the method of conventional microdissection using piezo-driven manipulation tools and glass fibres. However, the extraction of small parts of chromosomal G-bands is not possible with this method. By performing controlled tip movements, the above researchers managed to successfully separate single DNA areas (**Figure 2.8**) and therefore proposed that AFM is not only useful tool to visualise well-defined chromosomal areas within bands, but can also be used to modify DNA with the intention to extract chromosomal DNA. The authors also showed that it was possible to dissect chromosomal regions of variable size.

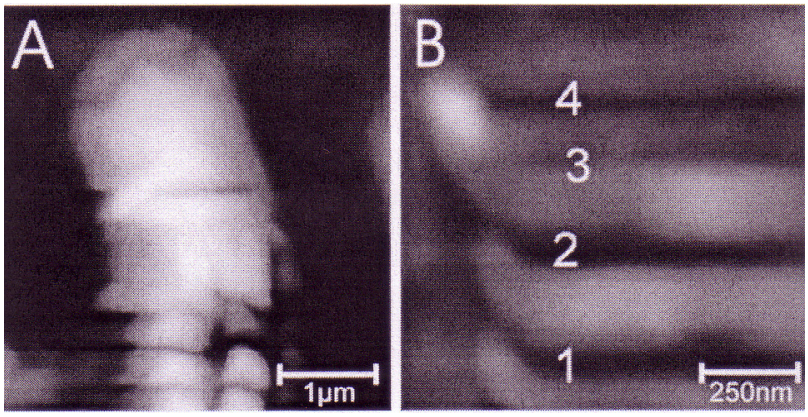

Figure 2.8 A Separation of DNA blocks by AFM. **B** Corrugations in the chromosome surface introduced by AFM (*after Oberringer et al*., 2003)

Finally, Yang *et al* (2010) used Atomic Force Microscopy (AFM) in combination with Fluorescence Microscopy (FM) for the investigation of non-Hodgkin's type B cells lymphoma after antibody treatment with Rituximab, which is commonly used in the treatment of this cancer type. This is a chimeric monoclonal antibody directed

against the protein Cluster of Differentiation 20 (CD20), which is expressed on mature B cells. In this study the authors applied anti-CD20 antibody to the B lymphoma cells that was labelled with fluorophore. Simultaneous imaging was then performed by both FM and AFM. Immunofluorescence imaging confirmed the binding of Rituximab to the CD20 protein; while the AFM imaging revealed changes in lymphoma cells in terms of mean cell height and cell surface roughness. It can therefore be proposed that AFM imaging and measurements may provide biomarkers of cell behaviour and may facilitate the treatment of lymphoma clinically as a pre-test to determine the effectiveness of the drug Rituximab on lymphoma cells from individual patients.

Plants

One of the more significant studies, carried out in the past few years in the area of plant science is by Gradinaru *et al* (2004) who investigated the unstacking of grana membranes in the envelope-free plant chloroplasts. They combined for the first time the superior spatial resolution of AFM with the high sensitivity and discrimination power of a confocal two-photon microscope. The multiplexing allows finding the target objects by rapidly acquiring a fluorescence map over a very large area and then selecting a region of interests for finer scanning with the AFM tip. The AFM allowed direct comparison between the cell morphology and then distribution of the signalling protein H-Ras in living cells, i.e. mouse fibroblasts. In this case the power of AFM was improved with the chemical identification capabilities of optical techniques,

which opens up interesting possibilities in various areas of research including material and life sciences.

In summary it can be said that in the past few years AFM has become versatile tool for imaging cellular surfaces at high resolution and under different conditions. It is likely that morphology probing on living cells will be more frequently employed in the future as the instrumentation is further developed and optimized. Through modification of the AFM tip, it is also possible to investigate many forms of interactions between different material systems. Combinations of AFM with other complementary techniques, such as Fluorescence Microscopy or different types of Spectroscopy, have been developed and are undoubtedly currently being considered by many researchers working in this area. Overall, it is strongly believed that AFM-based measurements will continue to play an important role in future research in biology, and improve the understanding of the structures and properties of microbial cell surfaces for example and the mechanisms involved in their behaviour.

2.3. Measurements of molecular forces and physical properties of biological systems using Atomic Force Microscopy – Force Distance Curves (FDC)

During the past decades, the initial step of microbial adhesion and aggregation processes has been described in the light of classical physico-chemical approaches, i.e. the Derjaguin-Landau-Verwey-Overbeek (DLVO) theory of colloid stability (Hermansson, 1999). However, these approaches are limited by the fact that they consider the surfaces as being smooth, rigid and chemically homogeneous, which is clearly a rough approximation. Most microbial surfaces bear appendages in the form

of fmbriae, pili, fibrils, flagella. The nature of these appendages and their specific chemistry enable microorganisms to adhere to different types of substrate or to aggregate despite the fact that overall electrostatic interactions are generally not favourable for microbial adhesion to occur. Hence, there is a need to develop methods capable of probing the surface properties of microbial cells at the (supra) molecular scale in order to refine our 'classical view' of microbial adhesion processes (Dufrene *et al*., 2001).

2.3.1. Principles of FDC

In recent years Force Distance Curves (FDC) have emerged as a valuable technique to measure local physical properties and interaction forces (Pollock *et al.*, 1995). AFM force-distance curves (**Figure 2.9**) are obtained by monitoring the cantilever deflection (d) as a function of the vertical displacement of the piezoelectric scanner (z). To monitor the cantilever deflection, a laser beam is focused on the free end of the cantilever and the position of the reflected beam is detected by a position sensitive detector (PSD). The cantilever deflection is converted into a force (F) using the Hooke's law ($F = -k \times d$, where k is the cantilever spring constant). The curve can be corrected by plotting F as a function of (z-d). At large probe-sample separation distances, the force experienced by the probe is null (A). As the probe approaches the surface, the cantilever may bend upwards due to repulsive forces (B) until the probe jumps into contact when the gradient of attractive forces exceeds the spring constant plus the gradient of repulsive forces (C). The approach portion of the force-distance curve can be used to measure a variety of surface forces, including van der Waals,

electrostatic, solvation, hydration and steric/bridging forces. When the force is increased in the contact region, the shape of the approach curve may provide direct information on the viscoelasticity of the sample. Finally, upon retracting the probe from the surface, the curve often shows a hysteresis referred to as the adhesion 'pull-off' force (D).

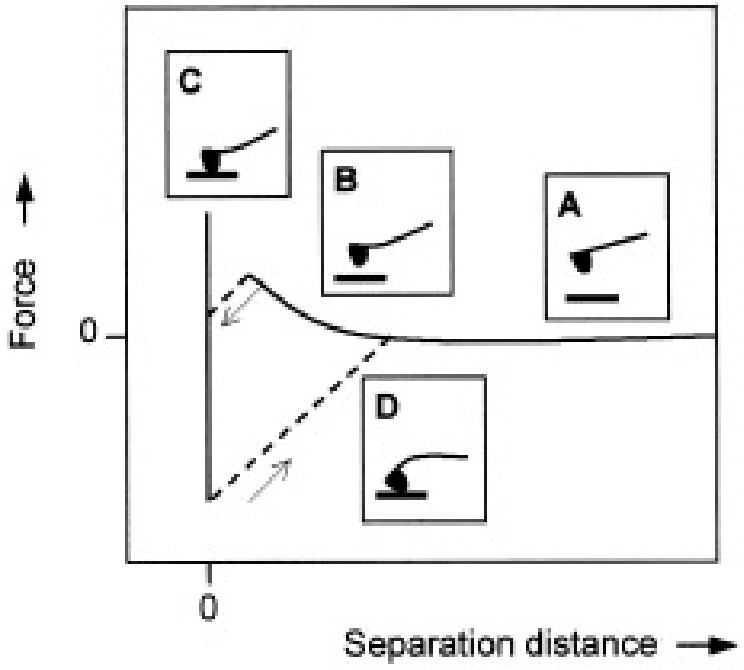

Figure 2.9 Typical parts of an AFM force-distance curve. (*after Dufrene et al.*, 2001)

It should be kept in mind that force-distance curve measurements present some limitations. First, AFM does not provide a direct measurement of the probe-sample separation distance; therefore, in the presence of repulsive forces and when no jump to contact is observed upon approach, defining the zero separation may be difficult. Second, for soft samples, separating the relative contributions of surface forces and sample deformation may be a delicate task (Dufrene *et al.*, 2001, Bolshakova *et al.*, 2004).

2.3.2. AFM adhesion studies of biological systems

As already suggested earlier in this Chapter, since its invention, AFM, with its wide range of applications, has been extensively used in the study of a number of materials systems and hence there is a large library of information available to the research community. Hence in this part of the Literature Survey only what are believed to be the more significant and relevant advances of AFM adhesion biological studies will be considered. These are presented in chronological order.

It is well-known that spatial and temporal changes of the mechanical properties of living cells reflect the overall complex underlying physiological processes. Therefore, following these changes would undoubtedly provide valuable insight into the biological importance of cellular mechanics and their regulation. As already shown earlier in this chapter, the tip of an AFM can be used to indent soft samples and the force versus indentation measurement could provide information about their mechanical properties, for example local viscoelasticity, and hence address the above scientific issues.

Hassan *et al* (1998) developed an experimental approach, using AFM, which they described as Force Integration to Equal Limits (FIEL) mapping, to produce robust, internally quantitative maps of relative elasticity of living Madine-Darby canine kidney (MDCK) cells. By collecting FDC on a time scale where viscous contributions are small, it was found that the forces measured were dominated by the elastic properties of the sample. It was further shown that FIEL mapping has the

advantage of essentially being independent of the tip-sample contact point and the cantilever spring constant. FIEL maps of living Madine-Darby canine kidney (MDCK) cells showed that elasticity is uncoupled from topography and revealed a number of previously unseen features.

Later, Patel *et al* (1999) showed that AFM can be a sensitive technique in the study of adhesion of biopolymers onto buccal cell surfaces. Changes in surface topography were indicative of the presence of bound polymer, whose ability to adsorb onto buccal cell surfaces were previously identified using direct staining and lectin-binding inhibition technique. It was suggested that this is the first time AFM has been used in this way (Patel *et al*., 2000).

Lo *et al* (2001) used AFM to study the dynamic force spectrum of the biotin-streptavidin bond strength in solution by measuring the unbinding forces between biotin and streptavidin complexes. This is an important example for the application of AFM, because it is well-known that noncovalent ligand-receptor interactions are critical to life because of their important roles in governing numerous biological events and processes. In their study both the AFM tip and the glass substrate were first functionalized with biotinylated bovine serum ablumin (BBSA). The tip (or vice versa) was further incubated in streptavidin solution to produce a streptavidin-modified tip surface (**Figure 2.10**). Specific FDC was observed with multiple steps in the retracting process which may be attributed to multiple or sequential breaking of interacting bonds between the probe and the substrate.

In 2002, Ahimou *et al* used AFM with chemically functionalized probes to investigate the surface charges of yeast cells. Cell surface charge plays an important role in controlling cell adhesion and aggregation phenomena, as well as antigen-antibody, cell-virus, cell-drug, and cell-ions interactions.

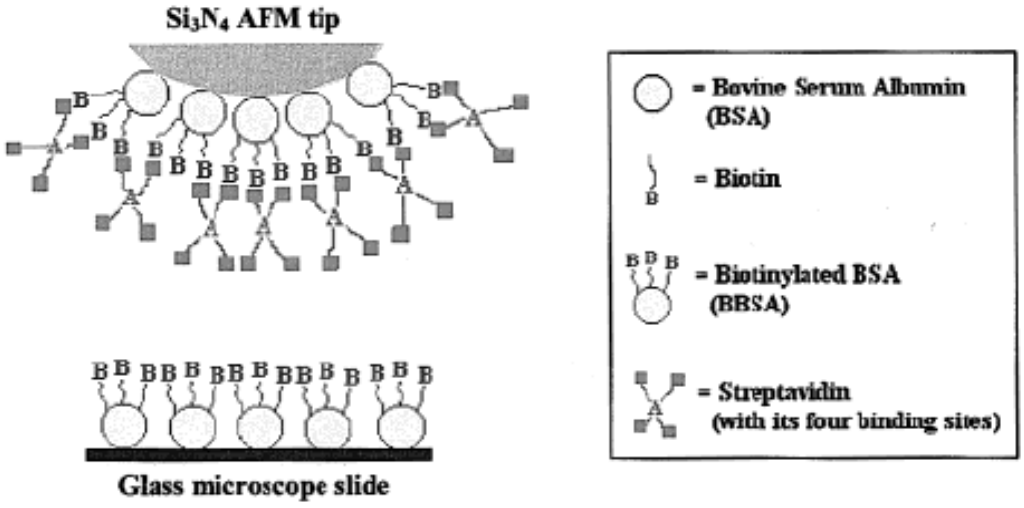

Figure 2.10 Schematic representation of the biotin-streptavidin experimental system (*after Lo et al*., 2001)

FDC and adhesion maps were recorded with probes terminated with ionisable carboxyl groups: while no adhesion was measured at neutral/alkaline pH, multiple adhesion forces were recorded at pH≤5. The AFM results indicated that the changes were related to differences in the ionisation state of the cell surface functional groups. It can therefore be suggested that AFM with chemically modified probes is a valuable approach in microbiology and biophysics for probing the local electrostatic properties of microbial cell surfaces.

Touhami *et al* (2003) used AFM to measure individual lectin-carbohydrate interactions involved in the reversible aggregation of yeast cells, a process referred to as yeast flocculation (**Figure 2.11**) which has been reported to be of particular importance in fermentation processes, such as brewing and wine-making. Carbohydrate-coated and lectin-coated AFM probes were made and used to record FDC on living yeast cells in buffered solutions. It was reported that specific interaction forces were not observed in non-flocculating conditions, i.e. in the presence of mannose or when using non-flocculating cells, pointing to their involvement in yeast flocculation.

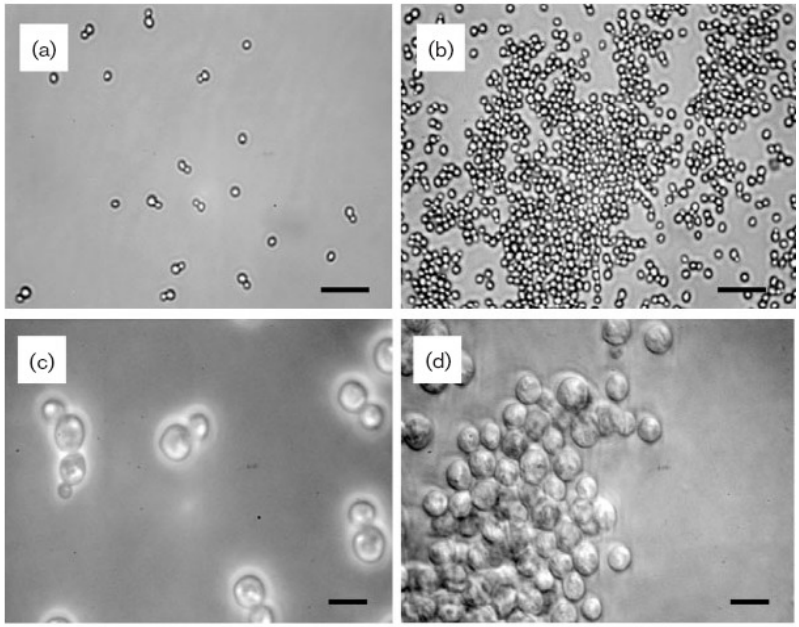

Exponential cells Stationary cells

Figure 2.11 Flocculation of yeast cells through specific lectin-carbohydrate interactions (a-d). Optical micrographs of *S. carlsbergensis* cells in exponential phase (a, c) and in stationary phase (b, d). Bars, 20 mm (a, b) and 10 mm (c, d) (*after Touhami, et al*., 2003)

Schaer-Zammaretti and Ubbnik (2003) studied the adhesion of lactic acid bacteria to the intestinal epithelium which is one of the most important factors determining probiotic ability of a bacterial strain. The observation of the surface topography of bacteria from the species *L. crispatus*, *L. helveticus* and *L. johnsonii* showed major differences between bacteria having a crystalline-like protein layer as part of the cell wall and those without such layers. After the collection of the AFM FDC it was found that bacteria covered with S-layer proteins have properties similar to spores having a crystalline-like surface and the surface properties are spatially highly uniform. In contrast, bacteria with a surface predominantly based on polysaccharides or peptidoglycans showed a soft gel-like behaviour and in most cases, significant spatial heterogeneities in surface properties are observed.

Arce *et al* (2004) employed AFM to compare the adhesion of Navicula species I diatoms to surfaces of a hydrophobic elastomer, Intersleek, and a hydrophilic mineral, mica using tipless atomic force microscopy cantilevers functionalized with live diatom cells (**Figure 2.12**). Force versus distance curves generated during these experiments revealed comparable cell adhesion strengths on Intersleek and mica, indicating that Navicula diatoms secrete extracellular polymeric substances with hydrophobic and hydrophilic properties.

Han *et al* (2005) proposed a new application for AFM involving a cell manipulation system. In their study the objective molecules, for example, genes or proteins, were immobilized on an ultra thin needle.

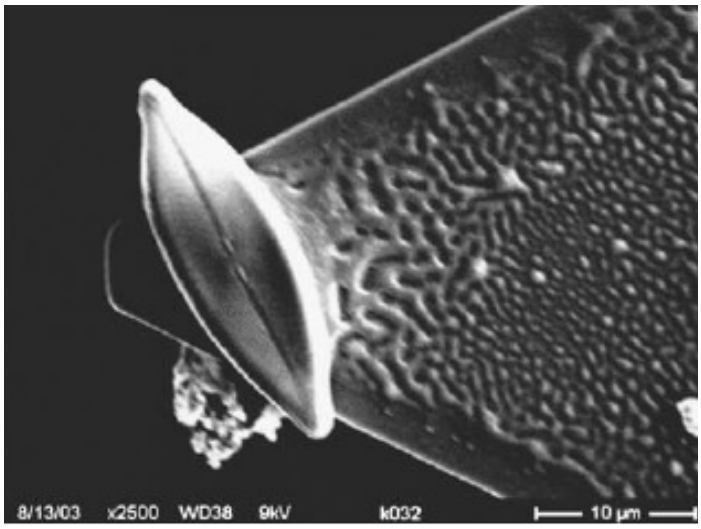

Figure 2.12 SEM micrograph of a single diatom cell attached with an epoxy glue to an AFM tipless cantilever (*after Arce, et al.*, 2004)

The gene-immobilized needle was then inserted into a single living cell. The cell damage by insertion can be reduced compared to microinjection because the diameter of needle is quite thin, 200 nm, the so-called nanoneedle (**Figure 2.13**). It was shown that the information from the insertion of the needle into the cell can be monitored as the signal of the force applied to the cantilever. The inserted depth of the nanoneedle can also be monitored and controlled by using the AFM FDC. This appears to be a very attractive point in cell science because it makes possible the accurate delivery of for example nucleic acids and proteins into the nucleus or cytoplasm without causing critical cell damage.

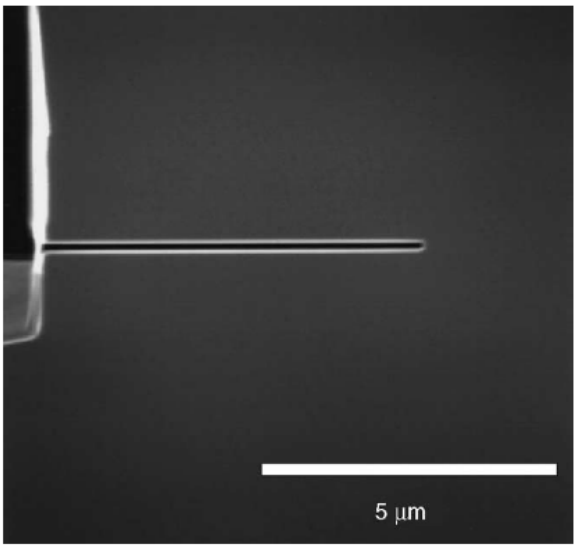

Figure 2.13 SEM image of a nanoneedle (*after Han, et al*., 2005)

Nguyen *et al* (2007) investigated the binding forces between λ-DNA and several types of substrates, including glass, mica, and Si. This is an important study, because binding forces connecting bio-molecules to solid substrates have a strong influence on both atomic force microcopy (AFM) imaging and force spectroscopy. It was found that the interaction forces were in the range of pN for DNA on mica and glass, and nN for DNA on Si. In addition, the force-distance curve showed different features depending on the position of the cantilever tip on the DNA.

In summary it can be said that Force Distance Curves have been and undoubtedly are currently extensively used in studying a variety of biological systems and associated processes many of which are relevant to everyday life. It is also strongly believed that the ability not only to image, but also to obtain data for the mechanical properties of the sample under investigation offers great potential for providing further insight into

the complex interactions taking place between for example pharmaceuticals and bacterial cells. This will provide useful information about the nature of the above and may aid further development and optimisation of existing and novel systems used for example in the treatment of infections.

2.4. AFM applications in the study of Escherichia coli (E.coli)

The aim of this part of the literature survey is to present the up to date research carried out on E.coli bacterial cells. This is due to the fact that this biological system was also used in the current study. In a similar pattern these will be presented in chronological order. Further details about this widely studied bacterial system are provided in the Materials & Methods Section of the thesis.

One of the first reports on the use of AFM to study E.coli bacterial cells came in the late 90's. Razatos *et al* (1998) reported on the development of a methodology whereby by modifying the atomic force microscope tip it was possible to determine whether bacteria are attracted or repelled by virtually any biomaterial of interest. This information is of critical importance when designing materials that are resistant to bacterial adhesion. In their study, Razatos *et al* (1998) showed that AFM can be used to analyze the initial events in bacterial adhesion with unprecedented resolution. Interactions between the cantilever tip and isogenic strains of E.coli mutants exhibiting subtle differences in cell surface composition were measured. It was shown that the adhesion force is affected by the length of core lipopolysaccharide

molecules on the E. coli cell surface and by the production of the capsular polysaccharide, colonic acid.

One year later, Ong *et al* (1999) immobilized E.coli cells onto the tip of a standard atomic force microscope cantilever (**Figure 2.14**), and performed force measurements by approaching the modified cantilever onto mica, hydrophilic glass, hydrophobic glass, polystyrene, and Teflon. It was shown that bacterial adhesion is indeed enhanced by the surface hydrophobicity of the substrate. However, the adhesive behavior of E. coli strains with more complex cell surface structures was found to be more difficult to model because of the possible involvement of steric and bridging effects or specific receptor-ligand interactions that remain to be resolved.

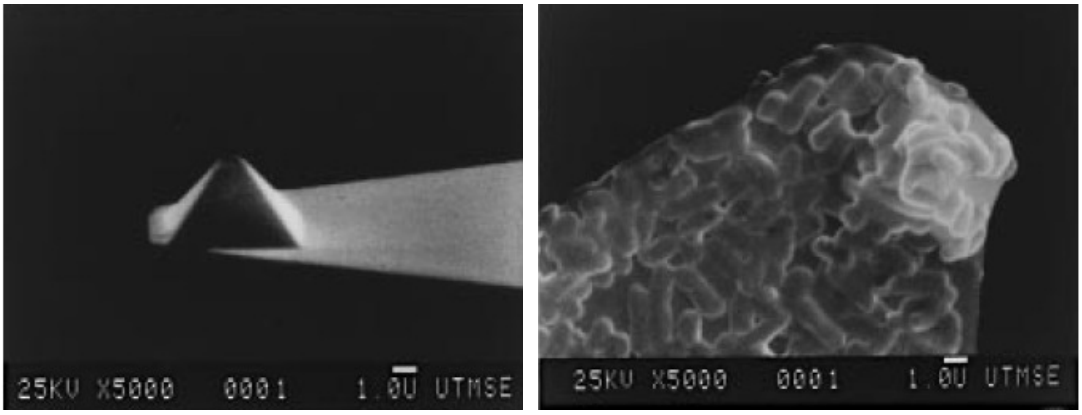

Figure 2.14 SEM micrographs of a standard AFM cantilever with a microfabricated Si_3N_4 tip and a cantilever tip coated with E. coli D21 cells (*after Ong et al*., 1999)

In a further study, Razatos *et al* (2000) used AFM to directly measure the forces of interaction between E.coli D21 bacteria and hydrophilic glass or hydrophobic *N*-octadecyltrichlorosilane (OTS)-treated glass substrates coated with the block

copolymers, poly (ethylene glycol) (PEG)-lysine dendron or Pluronic F127 surfactant, respectively. It was found that polymeric brush layers appear to not only block the long-range attractive forces of interaction between bacteria and substrates, but also to introduce repulsive steric effects.

In a separate study carried out in the same year, Lower *et al* (2000) directly measured interfacial and adhesion forces between living, unmodified bacterial cells (E.coli) and mineral surfaces (muscovite, goethite, and graphite) in aqueous solution using a force microscope. Adhesion forces, up to several nanoNewtons in magnitude and exhibiting various fibrillation dynamics showed the complex interactions of structural and chemical functionalities on the bacteria and mineral surfaces.

In 2003, Velegol *et al* used AFM to study polyethylenimine immobilised E.coli bacterial cells. In their study it was shown that the relatively large height and compliance of the bacterium led to the generation of imaging artefacts. The AFM images of E.coli K12 were consistently found to contain image shadows that were oriented in parallel lines 27° from the direction of the cantilever tilt, regardless of the scan direction. The authors described these artefacts as appearance of 'excess material' alongside the cell (**Figure 2.15**) and suggested that this was caused by the height of the specimen and the tip geometry.

In the same year, Doktyez *et al* (2003) investigated the effects of immobilising agent on the image quality of E.coli bacterial cells. In this study it was demonstrated that Sigma gelatine is a suitable candidate for live cell immobilisation and follow on AFM

imaging. It was also claimed that Sigma gelatin is superior compared to poly-L-lysine, which is another commonly used cell immobilisation agent, especially in Electron Microscopy.

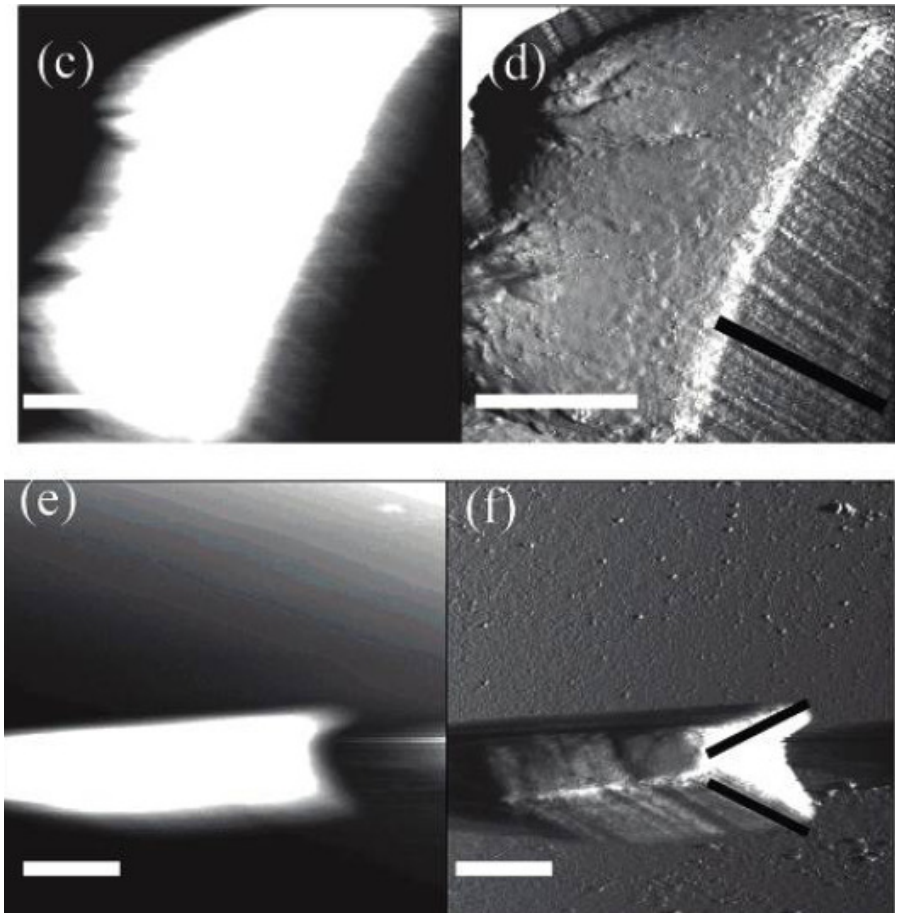

Figure 2.15 Examples of tapping mode AFM images of E.coli cells showing line artefacts (*after Velegol et al., 2003*)

Hanna *et al* (2003) used AFM to directly measure the reversible physiochemical and specific binding interactions between isogenic uropathogenic E.coli strains that differed in colanic acid expression and various substrates as bacteria initially approach the interface (**Figure 2.16**). These studies were carried out with the aim of providing more information about, urinary tract infections, which are the most

common urologic diseases in the United States and one of the most common bacterial infections of any organ system. The AFM results indicated that electrostatic interactions were not solely responsible for the repulsive forces between the colonic acid mutant strains and hydrophilic substrates. Moreover, hydrophobic interactions were not found to play a significant role in adhesion of the colanic acid mutant strains.

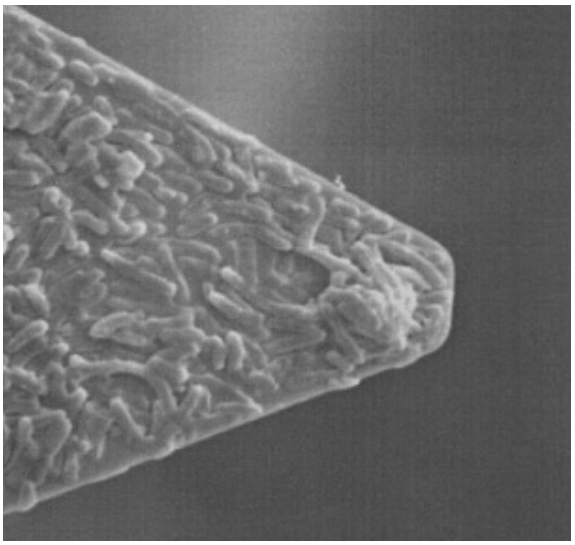

Figure 2.16 SEM micrograph of an AFM cantilever tip coated with E. coli C97 bacteria (*after Hanna et al*., 2003)

Cao *et al* (2005) studied the adhesion of *E.coli* (JM 109) on modified silicone surfaces with different biopolymers, silane (heparin, hyaluronan, self-assembled octadecyltrichlorosilane (OTS) and fluoroalkylsilane (FAS) using AFM and scanning electron microscopy (**Figure 2.17**). AFM probes were coated with E.coli and the force measurements between the bacteria immobilized tip and various materials surfaces were obtained while approaching to and retracting from the surfaces. It was

found that hydrophobicity cannot be used as a criterion to predict bacterial adhesion. The study also showed that AFM force measurements can be used as primary indicator in predicting bacterial adhesion. Both the native properties of the individual strain of bacteria and the specific functional structure of the surfaces determine the strength of force interaction, and thus the extent of adhesion. It was suggested that the nature of the functional group on the surface appears to be the principal factor defining the interaction between substrates and bacteria.

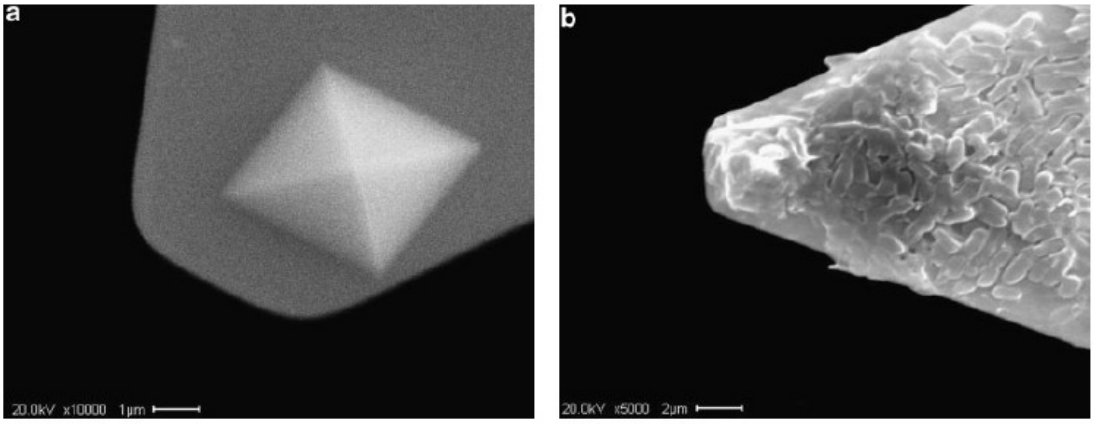

Figure 2.17 SEM photograph of a standard AFM silicon nitride tip (a) before and (b) after being coated with E. coli JM 109 bacteria (*after* Cao *et al.*, 2005)

Morrow *et al* (2005) used AFM to measure nanoscale interaction energies between different biobarrier materials of varied surface characteristics (dolomite, R-alumina, silica, pyrophyllite, and Pyrax (a composite form of pyrophyllite, mica, and silica)) and several E.coli strains in macroscale continuous-flow columns. The observed behaviour of the various E. coli strains and the selected mineral surfaces was

consistent with the DLVO predictions and Pyrax was determined to be an excellent biobarrier material for E. coli deposition and capture.

More recently, Wright and Armstrong (2007) developed a number of different types of functionalised tips (e.g. E.coli cell probes) that can be used for AFM studies including single-molecule force spectroscopy and lateral force measurement (**Figure 2.18**).

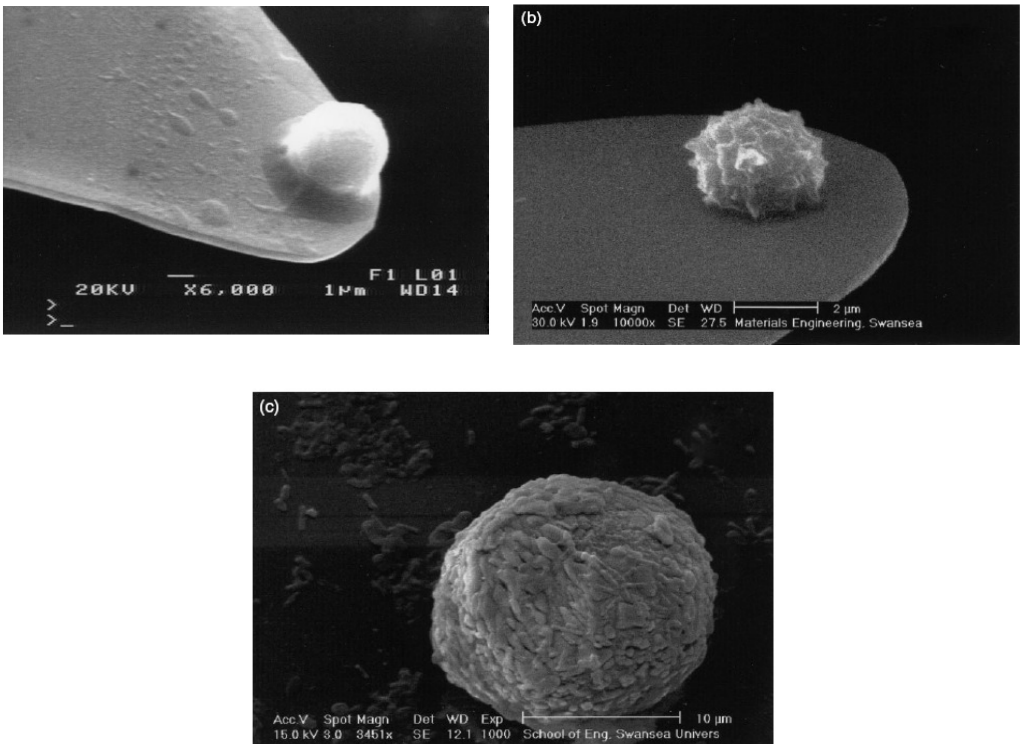

Figure 2.18 Scanning electron micrographs of the different microbial probes that can be constructed to study the interactions of microbial cells. (a) *S. cerevisiae* cell probe. (b) *A. niger* spore probe. (c) Coated colloid probe with a lawn of *S. putrificaens* (*after Wright and Armstrong*, 2007)

Very recently, Perry *et al* (2009) used AFM to study the effects of Ampicillin and Garlic extract on the mechanisms of membrane disruption of E.coli bacterial cells. This study is indeed of great importance as the antibiotic was also used to in this research. It was shown that both pharmaceuticals led to cell death after approximately 12h of treatment. It was also suggested that that this process occurred via the creation of pores on the cell walls and further leakage (**Figure 2.19**).

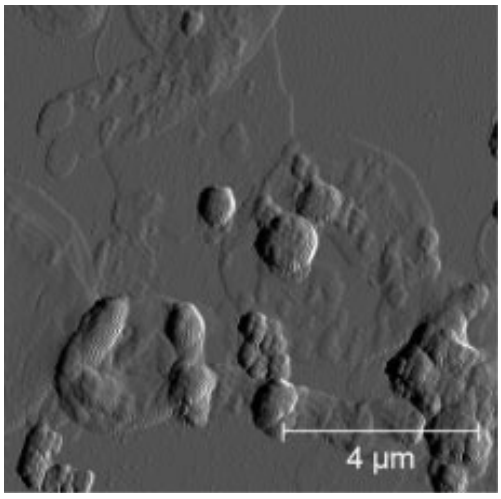

Figure 2.19 Example AFM image of E.coli cells treated with Ampicillin (*after Perry et al., 2009*)

In summary it can be said that over the past few years there has been significant research activity into the areas of AFM and E.coli bacterial cells. It was shown that most of the recent studies have been focussed on investigating interaction between the cells and different substrates (i.e. adhesion studies) rather then on exploring alternative imaging modes (e.g. PFM AFM). However, it would appear that there are still areas within this field that can be explored in order to get further insight into the

morphology and interactions of these unique biological species. For example, the use of novel heated nano-probes is yet to be investigated.

2.5. Thermal probe AFM techniques - Microthermal Analysis (μTA)

2.5.1. Principles

Microthermal analysis is a recently introduced thermoanalytical technique that combines the principles of scanning probe microscopy (SPM) with thermal analysis via replacement of the probe tip with thermistor. This allows samples to be spatially scanned in terms of both topography and thermal conductivity, by placing the probe on a specific region of a sample and heating. It is also possible to perform localised thermal analysis experiments on those regions.

The method represents a development of the family of techniques known as scanning thermal microscopy whereby the thermal properties of the surface of a sample such as thermal conductivity are measured as a function of temperature and mapped (Craig, 2002). The basis of the analysis is a modification of a typical SPM. In SPM, the tip cantilever is attached to a piezoelectric scan head which can control the position of the tip in three axes (*x, y, z*). X-Y piezoelectric actuators are used to scan the tip across the sample surface either in hard contact with surface (contact mode), intermittent contact with the surface (for example pulse force mode, force modulation) or a constant distance from the surface, interacting with near-surface forces (non-contact node). The tip usually scans across the surface in a raster pattern,

while an optical lever measures the deflection of the cantilever in the z-axis and controls the height of the tip via force-feedback loop (MicroThermal Analyzer - Operator's Manual, 2000).

In Scanning Thermal Microscopy the conventional SPM ultra sharp tip is replaced by a so-called thermal probe. Originally, for μTA, this was achieved using a Wollaston wire (Pylkki *et al.,* 1994). The Wollaston wire is composed of a fine platinum/rhodium alloy wire (3-5 μm in diameter) coated by a sheath of silver approximately 75 μm thick (Pollock and Hammiche, 2001, Bond *et al.*, 2002). This wire is bent into a V-shape and the silver sheath etched away at the apex to expose the platinum core, forming a tip with diameter in the region of 1 μm (**Figure 2.20**). A mirror attached to the back of the wire serves as the fulcrum of the optical lever, such that the tip can be controlled in such manner as a conventional sharp cantilever tip but with lower spatial resolution because of the increased dimensions of the thermal probe tip. Typically the resolution is in the region of 100nm-10μm (Sanders *et al.*, 2000 & Fischer, 2005). The exposed platinum tip has a much higher resistance than the intact Wollaston wire (approximately 2 Ω) and associated connections. The application of a current across the assembly results in Joule heating of the tip which provides a controlled heating signal that can be applied to a highly specific region. For isothermal studies, the probe may be used in two basic modes: constant temperature mode, requiring the use of a feedback loop to control the tip temperature, or constant current mode, whereby a small current is applied to the probe which subsequently acts as a thermometer. In constant temperature mode the thermal element acts as a resistive heater and forms part of a Wheatstone's bridge circuit,

with an identical, but remote tip held at constant temperature used as a reference. When in contact with a heterogeneous sample surface, the amount of heat flow into the sample will vary according to the thermal properties. The applied current is adjusted to compensate for the variations in heat flow, hence the temperature of the tip remains constant and the required feedback voltage may be measured as a function of position and used to create contrast between regions. Similarly, in constant current mode, the feedback loop will allow the temperature of the material to be assessed as a function of position. The heat transfer conditions are not as fully characterised as in conventional differential scanning calorimetry (DSC), because of the uncontrolled losses/gains from surrounding regions of the sample. In addition, the apparent thermal conductivity may be a reflection of surface topography due to the differences in the contact area between the probe and the sample at different positions on the sample surface. For example, if the probe is in contact with the "peak" in the sample topography, then the contact area will be less than if the probe is in the "valley". This effect causes an apparent increase in thermal conductivity of valleys compared with peaks and is a difficulty that is currently the subject of intense investigation (Craig *et al.*, 2002 & Grandy, 2002).

The technique is usually used as a semiquantitative method to distinguish components in a single surface. However, there has been considerable interest in developing these isothermal approaches as means of obtaining quantitative information of the sample surface (Craig *et al.*, 2002).

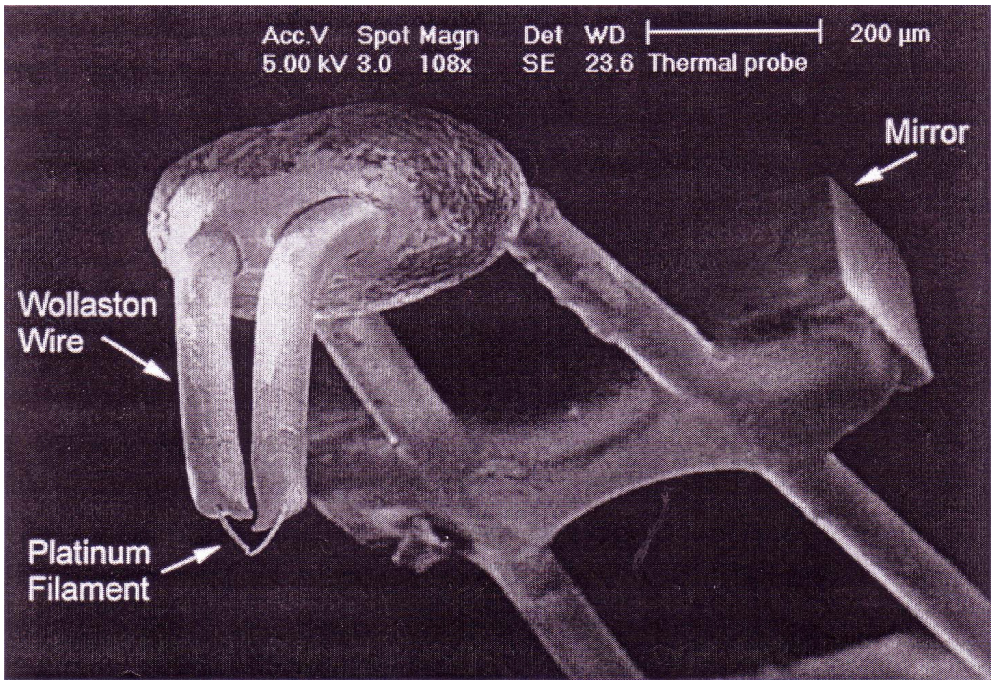

Figure 2.20 SEM image of the Microthermal analysis tip (*after Royall et al., 2001*)

A further analytical possibility which can be achieved by using this method, as mentioned above, is the application of a scanning heating signal to a small area of the sample surface, thereby allowing thermal analysis to be performed on specific regions. This mode is known as Localized Thermal Analysis (LTA) and has been shown to allow measurement of phase transition temperatures of specific sample regions (Harding *et al.*, 2007). The instrument may also collect mechanical data related to the sample's response to the thermal program via the force feedback control unit, an approach known as micro-thermomechanical analysis (Hammiche *et al.*, 2000, Odlyha *et al.*, 2003, Oulevey *et al.*, 2000). The information is related to events such as thermal expansion of the sample or indentation of the probe tip into the sample surface during events such as softening at glass-rubber transitions or melts. The effect of tip impingement into the sample surface after a thermal event is visible

in subsequent topographical analysis as a crater. The size of the crater may itself be an indication of the local behaviour of the sample and is indicative of the volume of the sample that has been investigated by the preceding thermal analysis (Reading and Price, 2003).

A final technical point regards the speed with which scanning thermal analysis can be performed, compared with macro-scale analysis of similar samples. Because of the very small size of the thermal probe tip, heating rates in the order of 10-20 K per second are usual; slower rates would simply result in heat transfer through wide regions of the sample. This allows rapid experiments to be carried out and raises the possibility of batch monitoring in an industrial processing environment (Craig *et al.*, 2002).

Microthermal analysis was originally the name given to the combination of localized thermal analysis with near-field microscopy. In its wider sense this includes any form of localized characterisation or analysis combined with microscopy, which uses a near-field thermal probe. Microthermal analysis was launched commercially in March 1998 (μTA^{TM} Microthermal Analyser (TA Instruments, New Castle, USA)), and two aspects of its development encourage the development of future variants.

The particular advantages of the technique are that the thermal imaging contrast can reveal spatial variations in the thermal conductivity and diffusivity of the sample and is able to detect subsurface structure. The source of thermal excitation may be the near-field thermal probe itself, used both as a heater and as a thermometer, for

localised application of temperature programmes. Localized thermal analysis builds upon this near-field thermal imaging technique (Pollock *et al*., 2001).

Finally, like its parent instrument the SPM, μTA can be coupled with additional instrumentation to investigate the same sample. For example, a μTA can be positioned above a sample mounted for surface plasmon resonance analysis, or placed above a sample on the stage of an inverted light microscope chassis (Harding, 2007).

Microthermal analysis combines and provides a versatile set of technologies for material characterisation on the micro- nano-scale. As described above, it combines the imaging power of atomic force microscopy with the ability to analyse physical, mechanical, thermal and chemical characteristics at a specific point of interest on the surface of a material. The μTA unit (**Figure 2.21**) is a fully functional AFM with a temperature stage that cools to -70^0C and heats to over 300^0C (TA instruments Instruction Manual). The different imaging modes can also be used to provide complimentary information about the change in mechanical properties as a function of temperature. Microthermal analysis measurements are based on a probe that incorporates a thin platinum resistance thermometer that enables the probe to act as a heater and a thermal sensor simultaneously. Current commercial thermal probes are made from Wollaston wire. New probes based on a platinum filament (as small as 200nm at the tip) are now available that enable thermal measurements at a spatial resolution below 100nm (Reading, 2003). Further details for these can be found in Materials and Methods chapter as these where extensively used for the experiments carried out in this research. However, here it is important to mention that these have

been successfully used for the first time ever in the study of pharmaceuticals (Harding, 2007), but their application is yet to be explored in the investigation of biological systems, e.g. E.coli cells.

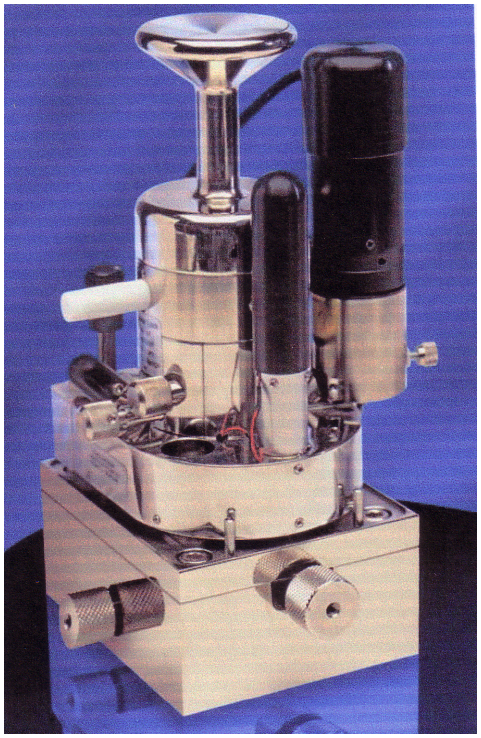

Figure 2.21 Photograph of the TA Instrument Inc. µTA™ 2990, Microthemal Analyzer (*courtesy of* TA Instruments)

The Microthermal Analyzer system developed by TA in 1998, shown in **Figure 2.21**, consists of a Topometrix Explorer™ AFM which uses thermal probes, as well as conventional AFM topology probes, and control units for piezoelectric and temperature feedback. The figure shows the major piezoelectric assembly in the centre, the laser probe and a video camera for positioning and direct observation of sample and probe on the side, all placed on the cell base, which allows placement and

coarse positioning of the sample. The V-shaped tip is shown in **Figure 2.22**. It is made of 200 µm length platinum-core wire which extends from silver jacket of the Wollaston wire and is the most resistive part of the probe. By measuring the electrical resistance of the overall Wollaston wire, the average temperature of the platinum-wire tip can be determined. The mirror attached to the cantilever arms serves to reflect the laser beam for the usual, piezoelectric control for the positioning of the platinum tip (Moon *et al.,* 2000).

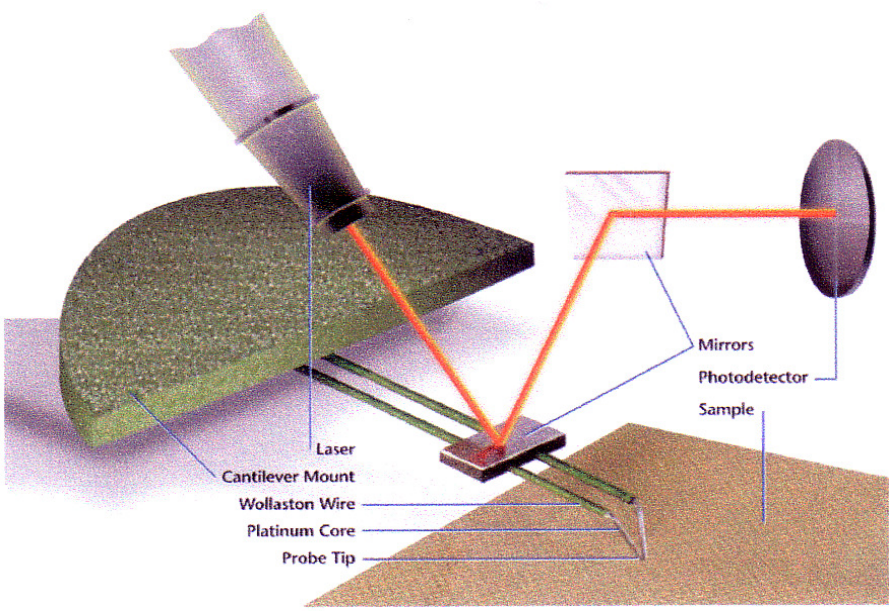

Figure 2.22 Schematic of the thermal probe (*courtesy of* TA instruments)

2.5.2. Application to pharmaceutical and biological systems

Although the use and potential of µTA is yet to be fully explored within the pharmaceutical sciences, a number of studies have now been completed that have identified the basic strengths and weaknesses of the approach. Up to date it appears that the key application for the above technique is the potential ability to not only

discriminate between different materials or physical forms, within a complex system, but also to perform in-situ characterisation studies on individual component.

Royal *et al* (2001) clearly demonstrated the ability of the micro-thermal analysis to differentiate between the coat and the core of commercial sugar coated ibuprofen tablet in order to characterise the thermal properties of both components using localised thermal analysis. The technique of micro-thermal analysis (MTA) again allows discrimination between different phases, with thermal responses seen that corresponded to the melting of the coat and core. The study has highlighted the strengths and weaknesses of using micro-thermal analysis as means of studying sugar coats on tablet surface. In addition, the technique may be used to asses the thermal properties of individual components within mixtures, but in this case it is essential to consider the scale of scrutiny of the measurement with reference to the size of the regions under study.

Six *et al* (2002) indicated that micro-thermal analysis makes it possible to characterise separate phases of itraconazole and Eudragit^{R} E100, thereby confirming the MTDSC results on phase separation. If more than one structure is present within the region, the LTA profile may appear as an intermediate softening between the values of the individual components. This is an important limitation of the technique and must be considered in using the approach to study drug dispersions in matrices. Overall, the study has showed that in characterising glassy materials by MTA, it is helpful to consider the fragility of that material when interpreting data.

There has been considerable recent interest in the preparation and behaviour of amorphous low molecular weight materials such as pharmaceuticals and food constituents. This interest has arisen for two principal reasons: in the first instance, there are many circumstances where the preparation of glassy dosage form has advantages over the equivalent crystalline system. However, it is now recognised that the accidental generation of amorphous material on particle surfaces during processing (e.g., mixing, milling) may result in significant changes to the behaviour of the studied system. Both issues are illustrated by the study of Royall *et al* (2001) who explored the strengths and weaknesses of microthermal analysis, particularly as a means of characterising low molecular weight drugs such as the drug *indometacin* in the amorphous or crystalline forms. The method is clearly able to differentiate between these two forms in a physically multicomponent system. Therefore, the study has demonstrated that the technique has considerable potential for the characterisation of recrystallisation processes in low molecular weight materials.

A further important issue is to distinguish and identify mixes of polymorphs in a single sample. Sanders and Roberts (2000) explored the novel use of scanning thermal microscopy (SThM) and localized thermal analysis to distinguish and identify polymorphic forms of the drug *cimetidine*. The LTA and SThM revealed that a sample of 50:50 mixture cimetidine polymorphs contains regions of different thermal conductivity, corresponding to the different polymorphs. This study and other work (Price *et al*., 1999) show that localized thermal analysis is a powerful tool capable of distinguishing and identifying polymorphic forms.

There have also been considerable interests in using μTA within the polymer science field, as it represents a unique method of performing thermal analysis on highly specific regions of a sample without the necessity of heating the material entirely. Royall and Hill (2001) investigated the ability of the technique to perform localized thermal analysis on the surface of progesterone-loaded microspheres.

Galop *et al* (2005) successfully applied the technique of μTA to the physical characterisation of solid dispersions. They reported that LTA offers a unique way to probe a selected area on the surface of the sample and it is capable of melting the drug locally without melting the excipient. μTA yet again proves to be a sensitive tool for measuring local properties where conventional macrotechniques usually fail.

There is also a persistent need within the pharmaceutical field to characterze the physical and structural properties of powder batches, particularly in terms of issues such as polymorphic forms and degree of crystallinity. A number of techniques are available including DSC, X-ray diffraction and Fourier transform infrared/Raman spectroscopy (FTIR). However all these methods rely on assessing a mass of powder (usually in range of 5-20mg) and accepting the response as being representative average of the properties of the individual powder particles. Murphy and Andrews (2003) studied the potential use of μTA as a novel means of characterising the thermal properties of individual powder particles. The method allowed identification and characterisation based on melting behaviour with reasonably good precision. The approach may also be used for samples showing more complex thermal behaviour but

in cases it is necessary to perform the data interpretation with care, particularly bearing in mind the possible effects of the high scanning speed.

Royal and Craig (1999) described the use of μTA as a novel means of differentiating between components in a model tablet formulation. The study highlighted some of the strengths and weaknesses of μTA approach with references to the study of pharmaceutical compact ibuprofen. The technique has been shown to be capable of resolving the constituents of the tablets on then basis of their response to a heating signal. It is possible to map not only the topology, but also the thermal conductivity of the sample. Furthermore, it is possible to apply a heating signal to the material and to perform thermal analysis on highly specific regions of the sample. However, the highlighted disadvantages included the semi-quantitative nature of the technique, the limitations of resolution and the difficulties in differentiating between materials with similar thermal conductivity.

Microthermal analysis by scanning thermal microscopy is being used increasingly for the analysis of pharmaceutical dosage forms, but there is currently little evidence to show that microthermal analysis data can compare directly with that from the established approach of DSC. However, Bond *et al* (2002) compared the DSC and MTA data from an active vitamin B6 analogue, pyridoxal hydrochloride, and two commonly used pharmaceutical excipients, Mannitol and Avicel^{TM} which are used in its formulation. It was found that MTA provides precise and accurate microthermal analytical data with 0.1 K thermal sensitivity, which is comparable to that obtained by DSC measurements of bulk samples. It is also shown that μTA offers the

opportunity to study single particles and the interfacial region between particles, data that is currently inaccessible through the DSC technique.

The applications of μTA in biology are yet to be explored, and hence there is very little information available in the literature at present. That is the reason why, here only the work of Hashimoto *et al* (2003) will be discussed. The cryopreservation of biological tissues is an indispensable technique in biological engineering. The control of intracellular ice formation or glass formation and dehydration with an extracellular solution are important for cryopreservation, because biological cells are easily damaged by the volume change of ice formation. The recent advance in infrared (IR) cameras enables the microscale thermographical study of biological materials with high response and high spatial resolution. The advantage of these cameras is that they are also seen as noncontact sensors for calculating radiation temperature after correcting emissivity. Hashimoto *et al* (2003) proposed the two-dimensional microscale thermal analysis for the measurements of the latent heat released from biological cells during freezing by use of high-speed infrared focal plane arrays. Onionskin cells were selected as specimens of a typical plant cell consisting of a cell wall, a cell membrane, a nucleus, a Golgi apparatus, cytoplasm, a mitochondrion and other parts. It is clear that temperature increase caused by a release of latent heat in a biological cell follows the rule of intercellular thermal diffusion. This will provide valuable information for the study of microscale thermal analysis in the freezing of biological cells.

2.6. Photothermal Microspectroscopy (PTMS)

The final part of the Literature survey considers the principles and recent applications of Photothermal Microspectroscopy (PTMS). PTMS is a recently developed SPM-based technique that allows measurements of spatially resolved IR spectra in inhomogeneous samples at a spatial resolution greater that the diffraction limit (Hammiche *et al.*, 1996). The technique was used in this research to further investigate the interactions between living cells (e.g. E.coli and pharmaceutically relevant materials (e.g. Ampicillin) in an attempt to gain further insight into the mechanisms of these.

2.6.1. Principles of PTMS

It is well known that when electromagnetic waves pass through a sample, absorption of certain frequencies occurs, leading to the molecular vibrations as illustrated in **Figure 2.23** (Williams and Fleming, 1997). The energy of most molecular vibrations of organic materials corresponds to that of the IR region of the electromagnetic spectrum. The absorption spectrum produced is unique for each molecule, thus IR spectroscopy is indeed a powerful tool for the identification of organic compounds. IR spectra are also extremely useful in the elucidation of unknown structures, as certain chemical groups give characteristic absorption bands that are consistent in wavelength and intensity. However, conventional vibrational micro-spectroscopy, using conventional IR microscopes, is diffraction-limited. The maximum achievable spatial resolution is of the order of a few micrometres. In order to overcome this problem, PTMS was developed.

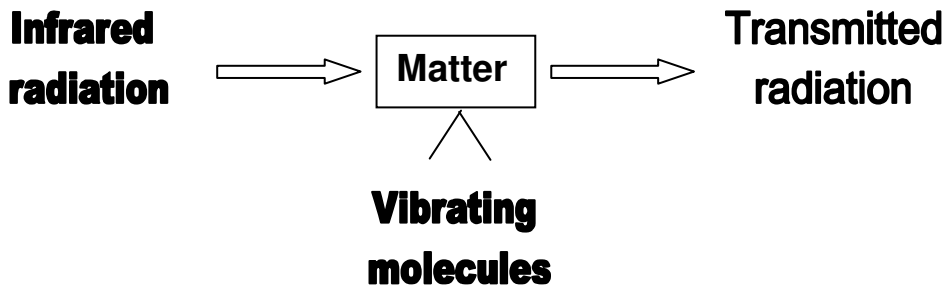

Figure 2.23 Interaction of radiation with matter (*after Bozec et al., 2003*)

The PTMS technique is based on the so-called photothermal effect. A photoinduced change in the sample, due to the retention of absorbed electromagnetic energy, results in sample heating (**Figure 2.24**). This heating causes measurable changes in a number of thermodynamic parameters, which form the basis for photothermal spectroscopy. By modulating the frequency of the excitation radiation, a spatial resolution smaller than the diffraction limit can be achieved (Bialkowski, 1996).

The basis of this approach is the combination of a FT-IR spectrometer with an atomic force microscope equipped with a thermal probe (Hammiche *et al.*, 2003, 2004). Sensitivity of the technique is assessed by recording infra-red spectra from small quantities of analytes and thin films. In order to reduce heat loss effects, which lower temperature and degrade the signal-to-noise ratio, if practically possible, analytes should be picked up by the probe and measured away from any substrate.

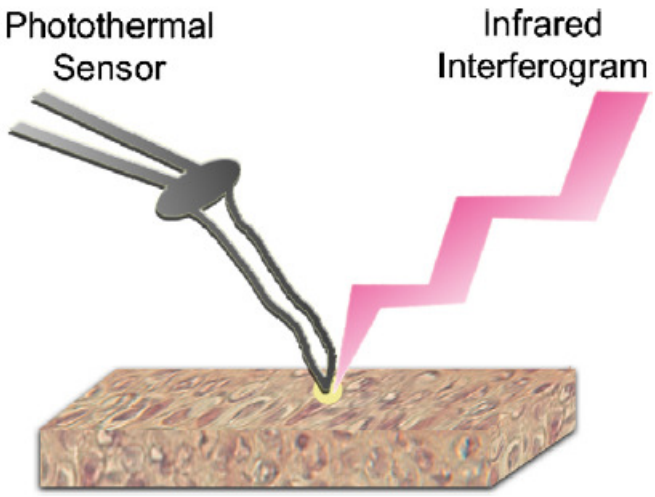

Figure 2.24 Schematic illustration of the principles involved in PTMS. Mid-infrared radiation is generated and it is focused onto the biological sample via custom-built optical interface. IR absorption-associated heat release at the IR focal point (in yellow) is detected with a photothermal sensor (*after Grude et al., 2009*)

The two instruments are integrated using a dedicated optical interface. The interface is placed in the chamber compartment of the spectrometer. A schematic diagram of the set-up is shown in **Figure 2.25**. The thermal tip of the MTA which can be operated as heat source or temperature sensor, is used in its passive mode. As the sample absorbs the IR radiation, it heats up. The resulting temperature rise of the probe induces changes in its electrical resistance, which are measured. Resistance changes, and therefore temperature variations, are measured using a Wheatstone-bridge based pre-amplifier developed by Specac Ltd. This amplified probe signal is fed into the external input of the spectrometer, and a Fourier transform algorithm is performed on this signal after digitization.

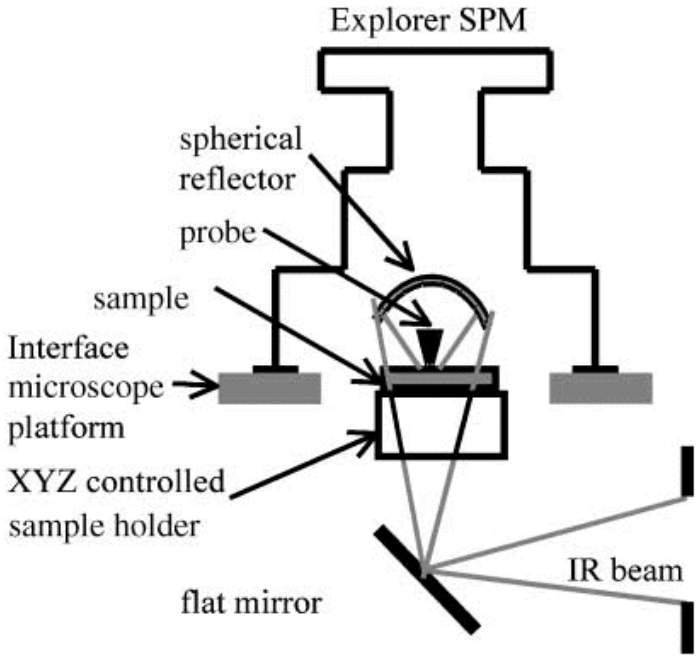

Figure 2.25 The near-field photothermal Fourier transform infra-red microspectroscopy set-up - a schematic diagram illustrating details of the probe and IR beam focus (*after Hammiche et al., 2003*)

Peaks on the resulting spectrum represent peaks of absorption by the sample. A background signal, with the probe lifted away from the sample surface but still exposed to the beam, and a sample signal recorded when the probe is in contact with the sample surface are recorded. The background spectrum is then subtracted from the contact spectrum so as to remove any traces of the spectral contents of the probe. The spatial resolution of this technique depends on the contact area between the tip and the sample – submicron spatial resolution was reported (Price *et al.*, 2001).

With the use of PTMS it is not only possible to monitor spectral changes at a location on a surface, but also to pick up individual particles or abstract small quantities of material from a surface using a thermally assisted nanosampling technique (Reading *et al*., 2002). Using this approach, small samples of a material can be picked up by the tip by carrying out MTA on the surface of the specimen; this melts the material beneath the tip and a small amount often adheres to the probe when it is retracted. The spectrum of the material attracted to the probe can be obtained by placing the tip in the focussed IR beam. This approach has been successfully used in the study of Metal Chelating Materials (Moffat *et al*., 2010), Polymers (Reading *et al.*, *2002*) and Pharmaceuticals (Harding, *et al*., 2007).

2.6.2. PTMS applications to biological systems

Although at this point PTMS is at a fairly early stage of development and application to biological systems, there have been a few studies that have undoubtedly demonstrated its strength and future capabilities.

Hammiche *et al.*, 2005 employed the technique to examined MCF-7 cells and IR spectra corresponding to proteins, DNA, RNA, glycoproteins, carbohydrates, lipids were obtained in spectral regions (900–2000 cm^{-1}). Experiments were carried out in the absence or presence of lindane, a pesticide known to induce G1-arrest in MCF-7 cells. Significant elevations in spectral intensities were associated with exponentially growing cell populations, predominantly in S-phase or G2-phase, compared to more quiescent populations predominantly in G1-phase. These results seem to suggest that

intracellular bulk changes, associated with transit through the cell cycle, can be tracked using this technique. **Figure 2.26** shows a typical absorption spectrum of a sample of MCF-7 cells after 24-h culture.

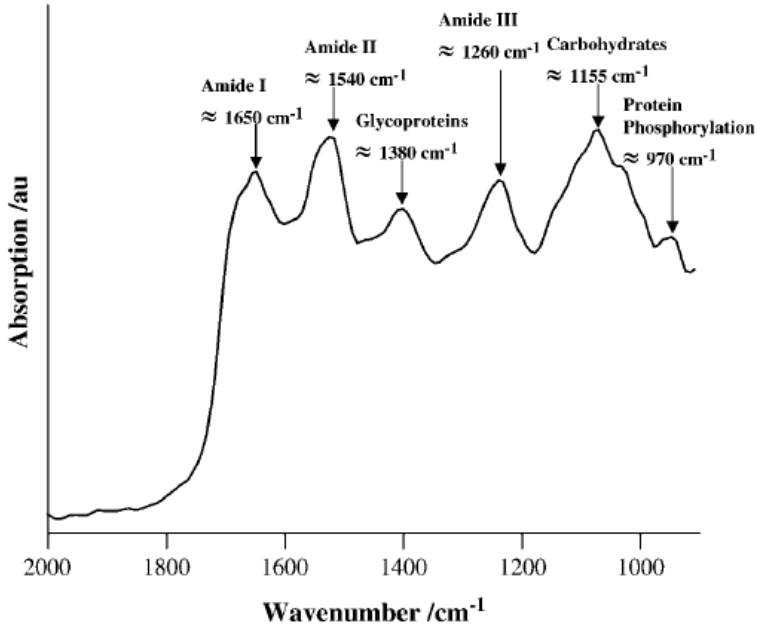

Figure 2.26 Spectral regions of interest in a typical absorption spectrum (2000-900cm^{-1}) of MCF-7 cells after 24h incubation (*after Hammiche et al., 2005*)

More recently, Walsh *et al* (2007) reviewed the evidence supporting PTMS's diagnostic potential in cancer biology. This is of significant importance as cervical cancer is the most common female cancer in the developed world. And although in recent years there have been a number of screening programmes adopted, there are a number of limitations to the smear test that remain and a need for a novel approaches such as methods that exploit infrared (IR) microspectroscopy were proposed to be

one of the possibilities to allow efficient and objective interrogation of exfoliative cytology.

A year later, Walsh *et al* (2008) used PTMS to "fingerprint" locations along the length of human small and large intestinal crypts. IR spectra were collected using globar FTIR microspectroscopy in reflection mode, synchrotron FTIR microspectroscopy in transmission mode or near-field photothermal microspectroscopy. Dependent on the location of crypt interrogation, clear differences in spectral characteristics were noted. This study is highly promising, as it demonstrates that the biomolecular characteristics of locations associated with the small and large intestinal crypts can be spatially segregated based on their IR spectral characteristics.

Grude *et al* (2007) also showed that it is possible to use this technique to identify adult stem cells in a model system and has great potential for the identification of adult stem types for use in regenerative medicine.

The technique has also been used in the study of more complex system, such as the brain where a better understanding of neural stem-cell proliferation could be invaluable in the treatment of neurodegenerative disease (Fullwood, 2007). PTMS in this study appeared to be more sensitive than synchrotron radiation FTIR spectroscopy in distinguishing between stem cells, TA cells and TD cells in tissue sections.

In 2009, Grude *et al* further showed that PTMS can also be used for characterisation of stem cells (SCs) and differentiated cells in tissue sections of human cornea. Stem cells have great potential in clinical medicine. It was reported that each PTMS spectrum provides a broad range of biomolecular information, in contrast to the techniques which identify cells on the basis of the presence or absence of single molecular groups. The work of Grude and co-workers is of significant importance with respect to the development of PTMS as a sensitive technique over existing FTIR spectroscopy methods where high spatial resolution is a requirement.

In summary, it can be said that up to date it has been clearly demonstrated that the PTMS technique does offer some possible advantages over other commercially available methodologies. Firstly, it is evident that its working principle circumvents the diffraction limitations that restrict the spatial resolution obtainable with all-optical detection systems. With PTMS, spatial resolution is limited by the dimensions of the tip of its thermal sensing probe only. PTMS measurements are unaffected by IR opacity of the sample, giving the method a further edge in comparison to FTIR spectroscopy. The future developments will be focussed on achieving subcellular resolution with the use of micromachined near-field probes that are currently under development (Anasys Instruments, USA.). However, it is also evident that the capabilities of this technique are yet to be fully explored and appreciated in the field of biology and for that reason its use was further investigated in the current research project.

2.7. Conclusions of the literature survey

1. In recent years AFM has become one of the most rapidly developing imaging method and has a number of potentially important applications within the biological sciences.

2. AFM has been applied to most biological materials with results that are not attainable with other methods and has become a powerful addition to the range of techniques that are available to investigate the structure, properties and functions of biological systems.

3. Methods have been introduced in order to make the technique suitable for quantitative force measurements.

4. AFM can visualize membrane proteins at sub-nanometre resolution, monitor conformational changes in single molecules. Observation of the surface of living cells with unprecedented resolution and structural changes as the cells grow or interact with their environment is also possible with AFM.

5. μTA provides a unique blend of thermal analysis and microscopy in a single instrument. It has achieved the status of a reliable general and simple to use tool, due to a variety of factors including: resolution, specificity, sample preparation and the amount of time required to acquire high resolution images. It has the

advantage to characterise the morphology of different materials, such as pharmaceutical, foods and biological specimens.

6. It is possible to visualize the topographic and heat transport properties of a surface with high resolution. The technique also offers the possibility to measure local calorimetric and thermomechanical properties that can be used to identify different components.

7. Selected locations may be characterized by thermal analysis, so as to investigate sample heterogeneity, composition or simply to examine specimens that are too small to examine by conventional techniques, such as very thin films and samples buried within composites.

8. Photothermal Microspectroscopy offers advantages over other commercially available techniques. Although this recently developed SPM-based methodology has been successfully applied in the study of a variety of systems its full potential is yet to be fully explored.

3. Materials & Experimental Techniques

3.1. Introduction

This chapter provides details of the materials used and the experimental techniques employed for their analysis and characterisation. Firstly, the pharmaceutical and biological systems studied and their preparation will be described. This will be followed by a description of the imaging, thermal and spectroscopy techniques used in this research.

3.2 Materials

3.2.1. Paracetamol

Paracetamol (acetaminophen; N-acetyl-p-aminophenol; 4'-hydroxyacetanilide; N-(4-hydroxyphenyl) acetamide) is a white crystalline powder, soluble in cold water. It has been shown that its solubility increases considerably as the water temperature is increased (Lund, 1994). The chemical structure of the substance is shown in **Figure 3.1**. Paracetamol is also soluble in methanol, ethanol, dimethylformamide, ethylene dichloride, acetone and ethyl acetate. Paracetamol is widely used as an analgesic and antipyretic and is one of the first line treatments in osteoarthritis. If combined with decongestants the drug can also be used to help relieve the symptoms of common cold, influenza and sinusitis by relieving headache, general aches, nasal congestion and fever (The Merck Index, 2001).

Paracetamol was first prepared by Morse in 1878, and its antipyretic properties were discovered in 1893 (Boldyreva *et al.*, 2002). It was first launched as a drug in 1956 and, as suggested above, is currently the most widely used analgesic and antipyretic drug in the world (Beyer *et al.*, 2001).

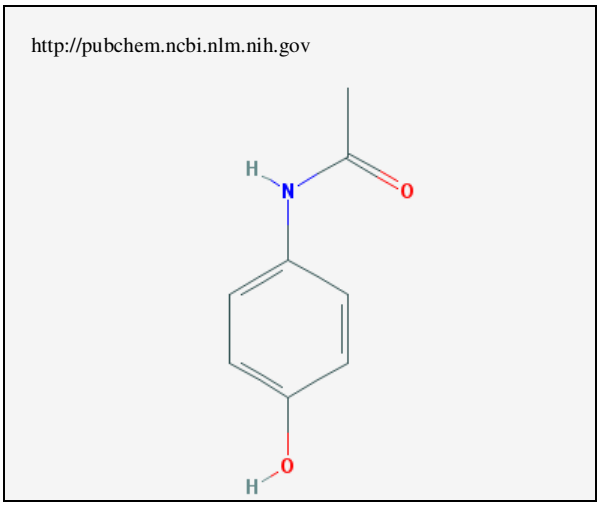

Figure 3.1 Structural formula of Paracetamol

Paracetamol can exist in three polymorphic forms: form I (monoclinic), form II (orthorhombic), and form III, the structure of which has not been elucidated because of its instability. It has been shown that the relative thermodynamic stability of Paracetamol polymorphs is as follows **I>II>>III** (Peterson *et al.*, 2003). The amorphous form can be generated by cooling the material from the melt (Di Martino *et al.*, 1997 & Qi *et al.*, 2008). Form I is the commercially available form and is stable at ambient temperature and pressure (Giordano *et al.*, 2002). The monoclinic form is more stable than the other forms at all temperatures below its melting point (Boldyreva *et al.*, 2002). The melting points of form I and form II are 169^0C (Nichols & Frampton, 1998) and 157^0C (Di Martino *et al.*, 1997), respectively.

Over the years there has been a considerable interest in the generation and stability of Paracetamol polymorphs. Some of the more significant research showed that the orthorhombic form of Paracetamol exhibits better compression characteristics and has a faster dissolution rate in water (Di Martino *et al.*, 1996, de Wet *et al.*, 1998). Furthermore, it was reported that Form I to form II transition can occur as a result of grinding and compaction (Boldyreva *et al.*, 2002).

In this research project, Paracetamol tablets were used as a model system with the aim to develop a suitable methodology for obtaining force distance curves and also to compare the results with data already available in the literature. This was thought to be necessary to be done in order to ensure that the methodology used is robust enough and delivers consistent and reproducible data, especially when further used in the study of bacterial cells. The Paracetamol tablets were prepared from powders obtained from Rhodia Organique by using a using a 13 mm evacuable IR sample press (Specac, UK). For the making of the tablets, approximately 400mg of material was weighed and poured into a die, to which a pressure of around 10 Tonne was applied for a period of 3 minutes.

3.2.2. Ampicillin

Since the early 1960's, Ampicillin has become one of the most commonly used antibiotics in the treatment of bacterial infections. The chemical structure of this beta-lactam antibiotic is shown in **Figure 3.2** (American Society of Health-System Pharmacists, 2006). Ampicillin, originally known as '*Penbritin*', is not only effective

against Gram-positive organisms, such as *staphylococci* and *streptococci*, but also has demonstrated activity against Gram-negative organisms such as *H. influenzae*, *coliforms*. Ampicillin is part of the aminopenicillin family and has been shown to be almost equivalent to its amoxicillin in terms of spectrum and level of activity (Gordon, *et al.*, 1972). It is relatively non-toxic and adverse effects of a serious nature are encountered only infrequently. If used as a powder Ampicillin's appearance is white with slight yellow cast and is readily soluble in water (MSDC, Fisher Scientific).

In the late 80's it was shown that Ampicillin acts as a competitive inhibitor of the enzyme transpeptidase, which is needed by bacteria to make their cell walls. It was found that it inhibits the third and final stage of bacterial cell wall synthesis, which ultimately leads to cell lysis. The holes that appear in the cell walls allow the body's immune system to take over and fight off the bacteria (Drug Information, 2006).

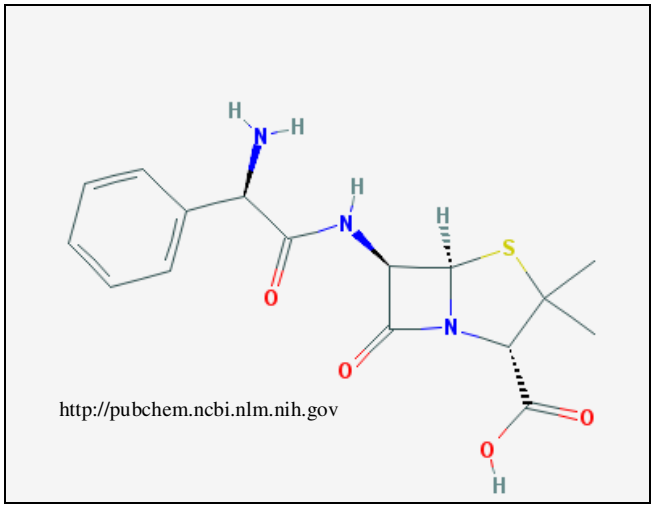

Figure 3.2 Chemical structure of Ampicillin

Ampicillin, like other β-lactam antibiotics, not only blocks the division of bacteria, but also the division of chloroplasts of the Glaucophytes (called cyanelles) and chloroplasts of the moss *Physcomitrella patens*, a bryophyte (Machinda *et al.*, 2006).

Ampicillin is also often used as a selective agent in molecular biology for the selection and confirmation of the uptake of genes by bacteria (e.g. *E. coli cells*). Usually, a gene that inserted into the studied bacterial system is coupled to a gene coding for an Ampicillin resistance (in *E. coli*, usually the (TEM-1) gene, coding for β-lactamase). The treated bacteria are then grown in a medium containing Ampicillin. It has been shown that in this way only the bacteria that successfully take up the desired genes become resistant to the Antibiotic used for treatment, and therefore contain the other desired gene as well (Pasquali *et al.*, 2005).

In this research project Ampicillin was used to treat E.coli cells with the aim to investigate its structural effects on the bacterial system by means of Atomic Force Microscopy and Photothermal Microspectroscopy. The Ampicillin powder, obtained from Sigma-Aldrich, was diluted with distilled water to a concentration of 100mg/ml. Approximately 1ml from the freshly prepared solution was then simply poured over the clearly seen colony of bacterial cells. Specimens from the cells treated with antibiotics were then examined after different periods of time in order to study the effects of the antibiotics.

3.2.3. E.coli

Undoubtedly, in the world of bacteria, the spotlight for biologists has for a long time been Escherichia coli (**Figure 3.3**). This small gram-negative rod-shaped bacterial cell, usually abbreviated to E. coli, was first discovered by Theodor Escherich, a paediatrician and bacteriologist, who devoted his life and research in the areas of improving child and infant hygiene and nutrition. The bacteria are a normal part of the gut flora and are commonly found in the lower intestines of animals and humans. Nevertheless, it has been shown on a number of occasions that it can be easily grown in a simple nutrient broth (e.g. Luria Broth) in a culture bottle (Bertani, 2004).

The E.coli bacterial cells are part of the Enterobacteriaceae family, which is a large class of bacteria which also includes the familiar pathogen – Salmonella, and are commonly used as model organisms for bacteria in general. As mentioned above, members of the Enterobacteriaceae are rod-shaped, and are their typical length is in the region of 1-5μm and their diameter is approximately 0.5 μm. They are non-spore forming and have many flagella which aid their movement. The genetic instructions of these bacterial cells are contained in a single circular molecule of DNA (Alberts *et al.*, 2002).

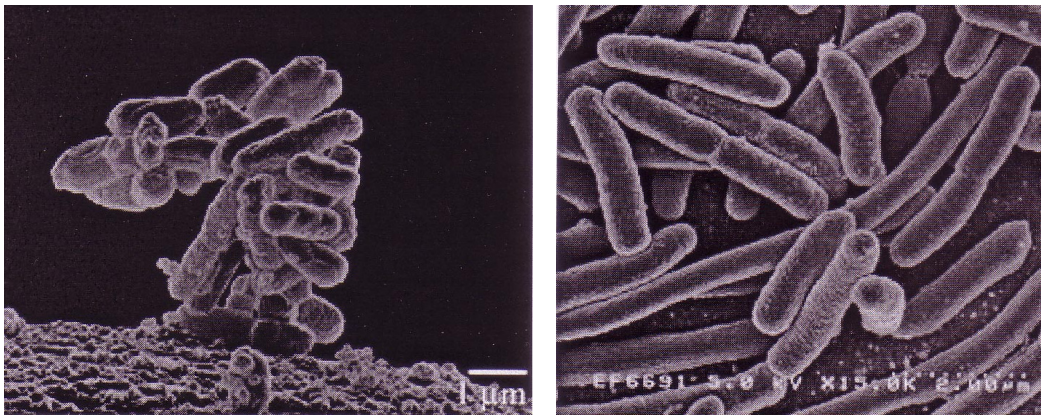

Figure 3.3 SEM images of E.coli cells at different magnifications

(*after Erbe, E. & Pooley, C, 2005*)

The typical inner structure of the E.coli cells is shown in **Figure 3.4**. It consists of a Cytoplasm region that encapsulates the DNA molecule, which as explained above is representative of the genetic code of the bacterial cells. The assembly is held together by the cell membrane to which are attached a number of Flagella.

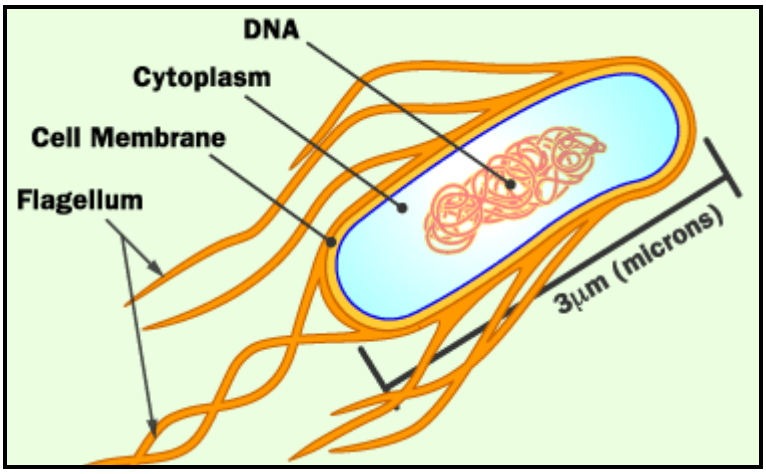

Figure 3.4 The structure of the *E.coli* bacterial cell (*after Marler, 2009*)

An important structural feature of these gram-negative bacterial cells is their cell membrane, commonly referred to as a cell wall. In contrast to the gram-positive bacteria, which have a single plasma membrane surrounded by a thicker wall (**Figure 3.5a**), the gram-negative bacteria have a dual membrane system (**Figure 3.5b**) in which the plasma membrane is surrounded by a permeable outer membrane (Cooper & Hausman 2009).

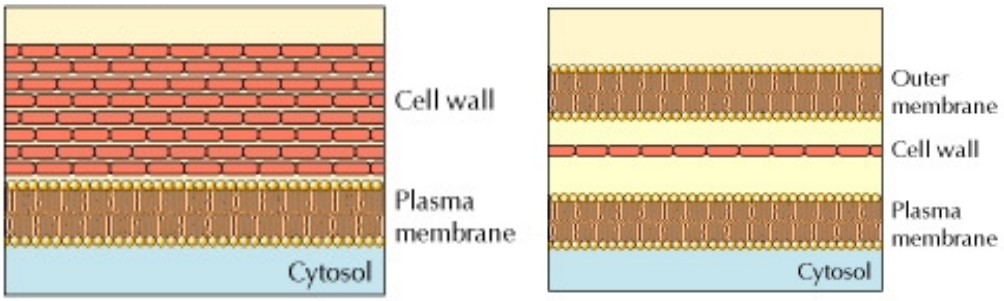

Figure 3.5 The structures of Gram-positive **(a)** and Gram-negative **(b)** bacterial cells (*after Cooper & Haunsman, 2009*)

The latter is composed of phospholipids and lipopolysaccharides, whereas the inner side of the wall is made of peptidoglycans (**Figure 3.6**). The carbohydrates are of great importance, as it has been shown that the so-called LPS or endotoxin layer is associated with the pathogenic capability of the bacteria (Salton & Kim, 1996). In humans, it has also been reported that LPS triggers an innate immune response characterized by cytokine production and immune system activation. Inflammation is a common result of cytokine production, which can also produce host toxicity.

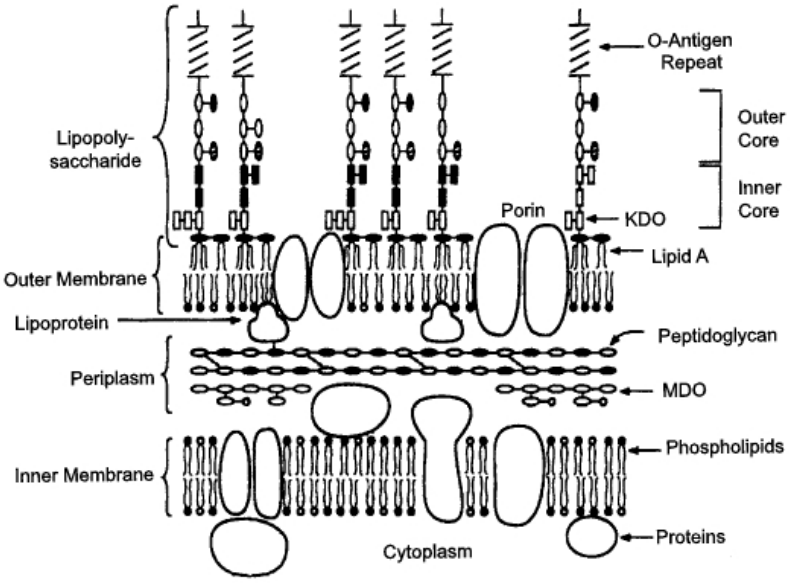

Figure 3.6 The structure of the outer and inner membranes of a gram-negative cell wall (*after Varki et. al., 1999*)

It has been found that this outer lipopolysaccharide rich membrane protects the bacteria from several antibiotics, dyes and detergents (e.g. lysozyme & penicillin) that would normally be expected to damage the inner membrane. However, alternative medicinal treatments, including the antibiotic Ampicillin, have been developed and successfully used to combat the protective outer membrane of this gram-negative organism (Woese, 1987). The actual detrimental effect of the β-lactam on E. coli cells was recently investigated by Yang *et al.*, (2006). The results from their study suggested that cell division is inhibited by the creation of nanopores at the apical ends of the cells. Furthermore, the authors reported that there was an apparent leakage of the cell contents. It was therefore proposed that the damage to the cell wall structure would create an imbalance between the inner and outer osmotic pressures of the cell, resulting in the loss of inner contents and consequent cell death.

It is thought that the use of the AFM-PTMS approach would provide additional and new information about the effects of the studied antibiotic on the bacterial cells and any associated changes taking place on structural and sub-structural levels.

The E.coli bacterial cells exhibit a typical cell-cycle, a schematic representation of which is shown in **Figure 3.7**. The individual growth phases are labelled on the curve and briefly described below.

- ***Lag phase***: associated with the production of new enzymes needed for growth;
- ***Log phase***: also known as exponential growth phase associated with a maximum cell growth;
- ***Stationary phase***: during this phase essentially growth becomes equal to death, or in other words the nutrients and/or waste products become limiting factors to growth;
- ***Death phase***: in this phase the lack of nutrients and accumulation of waste products becomes prevalent, which results in killing cells.

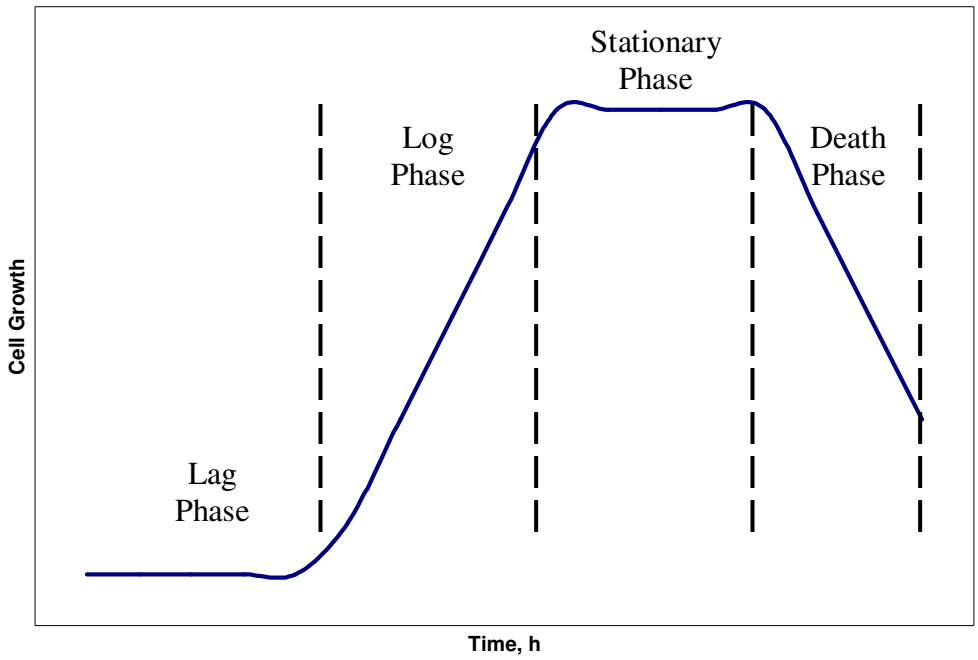

Figure 3.7 Typical Growth curve of E.coli bacterial cells

Apart from, as already mentioned, being one of the most studied cellular systems in recent years, E.coli bacterial cells have also found useful applications in processes such as water purification and expectedly in diseases. This are considered briefly below.

Role in water purification and sewage treatment

In the fields of water purification and sewage treatment, E. coli was chosen very early in the development of the technology as an "*indicator*" of the pollution level of water, which essentially provides information of the amount of human faecal matter in it. The main reasons for using E. coli are that there are a lot more coliforms present than individual types of pathogenic bacteria and these can be tested relatively easily (Seidel, 1976).

Role in diseases

Unfortunately, certain strains of this relatively harmless bacterial cell can be the primary cause to a number of intestinal and extra-intestinal infections such as urinary tract infections, meningitis, peritonitis, mastitis, septicaemia and gram-negative pneumonia. However, E. coli are extremely sensitive to antibiotics such as streptomycin or gentamicin, so treatment with antibiotics of the above infections is generally very effective (Wong *et al.*, 2000, Rolhion *et al.*, 2007).

Here, it is also important to note that certain strains of E.coli are toxigenic and produce a toxin very similar to that seen in dysentery, which can cause food-poisoning usually associated with eating contaminated meat. The severity of the illness varies considerably; but can be fatal, particularly to young children and the elderly (Robins-Brown *et al.*, 2004).

In this research project E.coli bacterial cells were used as the main model biological system in an attempt to not only further develop and optimise the use of the Atomic Force Microscopy techniques described below, but also to try and provide further insight into the inner structure and interactions of the biological system with pharmaceutically relevant materials. The general preparation methodology used involved the following few steps. The E.coli bacterial cells (strains MG16SS, and HB101 obtained from IFR and School of Biological Sciences, UEA) were grown from overnight cultures at 35^{0}C with mild shaking at 150 rpm in Luria Broth (Sigma, UK) medium (tryptone 10g l^{-1}, yeast extract 5g l^{-1}, NaCl 5g l^{-1}) to stationary growth phase. These were then harvested by centrifugation at 9000 rpm for 3 min and then

washed three times with phosphate-buffer saline (PBS). Details of any further preparation methodologies and treatment of the studied biological system are provided in the following chapters prior to the relevant experiments carried out using them.

3.3. Experimental techniques

The second part of this chapter provides details about the experimental techniques and conditions used. Firstly, the Atomic Force Microscopy image types will be considered. This will be followed by a description of the experimental set up for performing Force Distance Curve (FDC) measurements. Finally, details of the Photothermal Microspectroscopy (PTMS) experimental set up used in this research will be given.

3.3.1. AFM imaging

3.3.1.1. Tapping mode

One of the most commonly used AFM modes is tapping mode (*see Chapter 2*). In this mode of operation, a schematic representation of which is shown in **Figure 3.8**, the cantilever is oscillated above the sample surface at or near its resonant frequency. As the probe gets closer to the sample surface, the forces between the tip and the sample change the oscillation amplitude and phase of the tip. Either of these can be detected and used by the feedback loop to track the surface and hence map the topographic data. Amplitude detection is the tapping mode method usually used for high-amplitude oscillation and for phase imaging. The term '*phase imaging*' refers to the

use of amplitude detection for the feedback-control loop while simultaneously monitoring phase change to produce an image.

Because tapping mode eliminates strong lateral forces between the tip and the sample surface, it has been suggested to be ideal for scanning soft and/or adhesive samples such as polymers. It has also been shown to produce high-resolution images of hard materials, such as silicon, where permanent tip-sample contact would blunt the tip, this giving rise to poor lateral resolution and damage to the tip. This method is also well suited for scanning materials that exhibit a strong attractive force with the tip (*Veeco Instruments Ltd., UK - Caliber Operation Manual, 2006*).

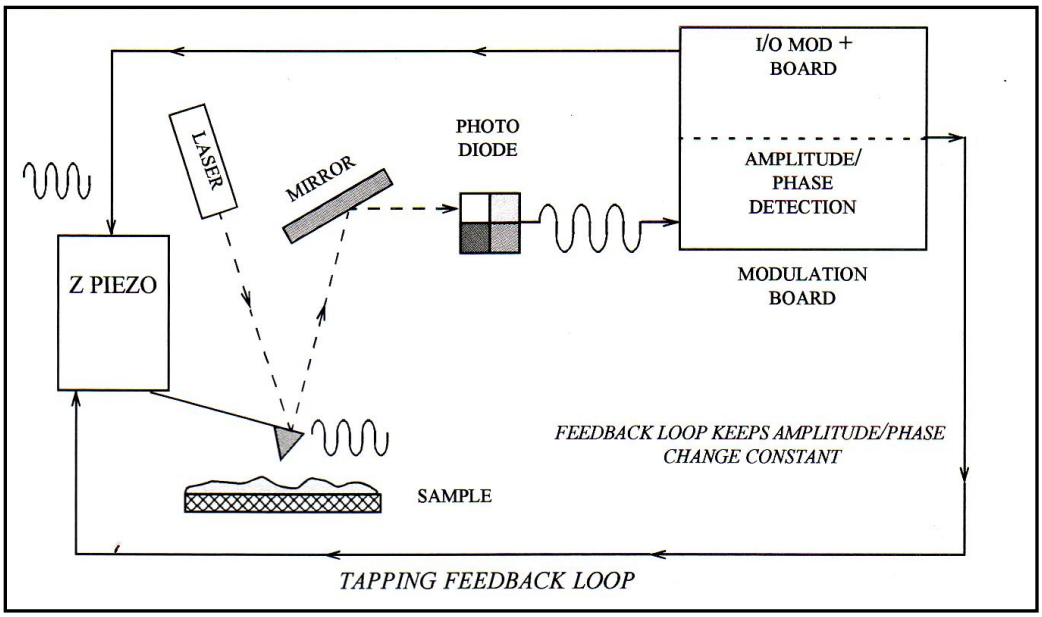

Figure 3.8 Schematic diagram of tapping mode operation/procedure (*courtesy of* Veeco Instruments Ltd., UK)

3.3.1.2 Pulse Force Mode (PFM) Imaging

The Pulse Force Mode (PFM) image mode, as suggested before, extends the capabilities of the AFM, simply by measuring topography. It allows additional properties like local stiffness and adhesion to be determined. A schematic representation of the typical force-time curve for this image mode, showing the force signal over a complete modulation period, as viewed with an oscilloscope is presented in **Figure 3.9**.

It can be clearly seen that after about 0.2ms the tip snaps into contact with the sample, which is due to the negative force acting between tip and sample. The piezo then pushes the tip further to the sample and the positive force reaches a maximum (*point 1 in Figure 3.7*). The piezo pulls back and the tip looses contact. The probe is damped towards the baseline. After this, the cycle starts again (Grandy, 2002)

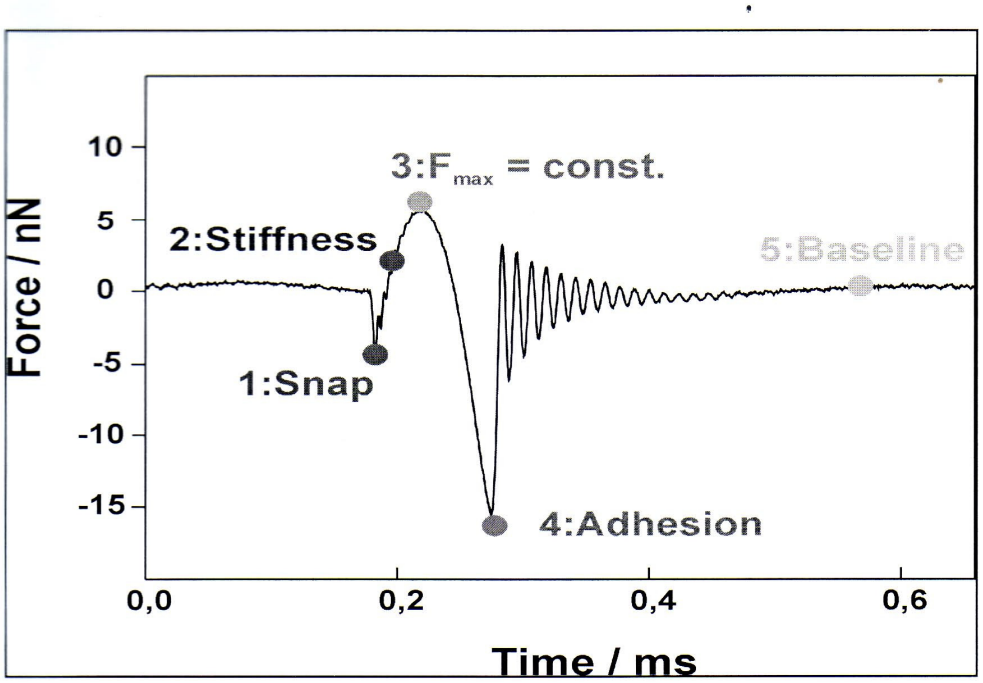

Figure 3.9 Typical force/time curve (Grandy, 2002)

The baseline is an important feature, because due to long range electrostatic forces, the position of the baseline may vary from point to point. Therefore, all other features are related to this baseline. Secondly, the maximum force at point 1 is extracted and fed back to the control circuits of the AFM to keep the force at this point constant and to measure the topography. The setpoint of the AFM controls the difference between baseline and maximum force. The maximum adhesion force at point 4 is recorded by the PFM and can be fed into additional analog input channel of the AFM, forming the adhesion image of the sample. The force difference between point 1 and 2 is related to the local stiffness of the sample. On hard samples this difference is larger than on soft ones. This is recorded by the AFM and forms the stiffness image *(Veeco Instruments Ltd., UK - Explorer Operation Manual, 2000*).

3.3.1.3. Force distance curves

The principles of these measurements have already been described in detail in the previous chapter of the thesis and therefore here only a brief summary will be given. AFM force-distance curves are obtained by monitoring the cantilever deflection as a function of the vertical displacement of the piezoelectric scanner. To monitor the cantilever deflection, a laser beam is focused on the free end of the cantilever and the position of the reflected beam is detected by a position sensitive detector (PSD). The cantilever deflection is converted into a force (F) using Hooke's law

$$F = -k \times d$$

where k is the cantilever spring constant.

As the probe approaches the surface, the cantilever may bend upwards due to repulsive forces until the probe jumps into contact when the gradient of attractive forces exceeds the spring constant plus the gradient of repulsive forces. Finally, upon retracting the probe from the surface, the curve often shows a hysteresis referred to as the adhesion 'pull-off' force. An example of the Force Distance Curves obtained in this study is provided in **Figure 3.10**.

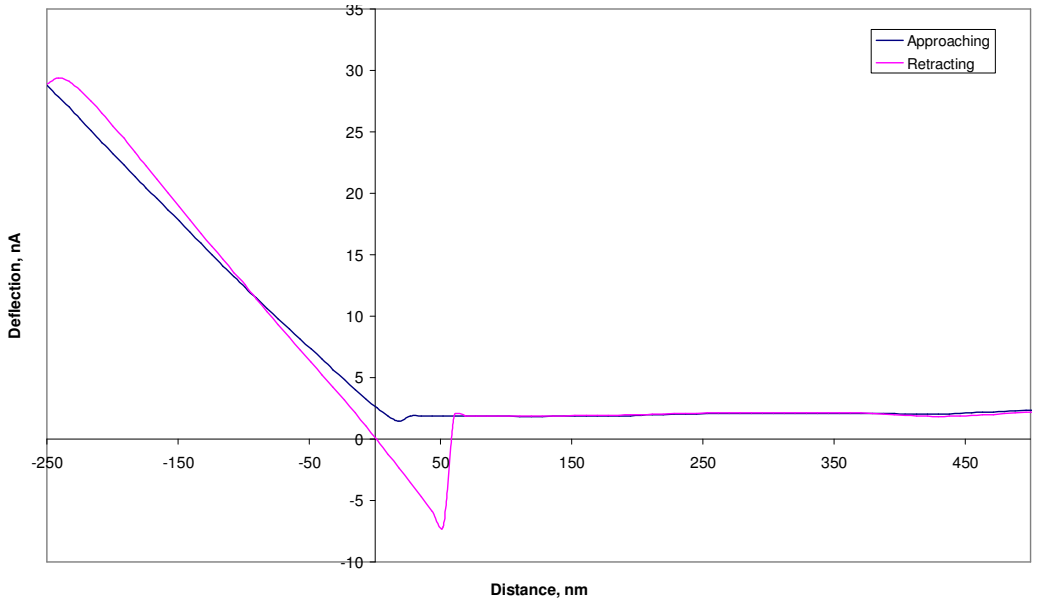

Figure 3.10 Example of a Force Distance Curve obtained in this study from a model system – Paracetamol tablet

3.3.2. Microthermal (MT) & Nanothermal (NT) Analysis

The theoretical background of these techniques has already been described in the previous chapter of the thesis and therefore here only the experimental set up employed in this study will be considered. The instrumentation (**Figure 3.11**) is based on that of a standard Atomic Force Microscope, but the standard AFM silicon probes, is replaced by a thermal probe, which can act as a near-field temperature detector and a source of heat. The thermal probe is composed of a Wollaston wire (made of platinum/10% rhodium core surrounded by a silver sheath) which is bent to a V shape. The silver at the tip of the loop is etched away to reveal a platinum/10% rhodium core, which results in higher resistance at the tip than in the remaining wire (Pollock *et al.*, 2001). A mirror was attached to the back of the probe thus allowing

the position to be monitored and controlled via laser reflection. The electric current passed through the probe results in Joule heating of the exposed platinum/10% rhodium tip, thus allowing heating of the sample in a controlled manner whilst simultaneously measuring its mechanical or thermal parameters.

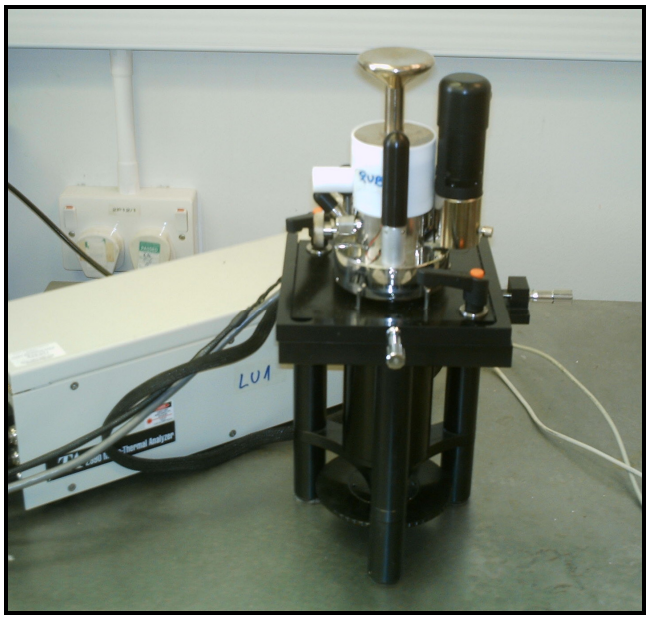

Figure 3.11 Photograph of a TA Instruments 2990 Microthermal Analyser with a Thermomicroscopes Explorer AFM head combined with a hot/cold stage

A lock–in amplifier (**Figure 3.12**) was used to detect and measure the very small signals generated. These types of instruments employ a technique known as phase-sensitive detection, which singles out the component of the signal at a specific reference frequency and phase. Noise signals at frequencies other than the reference frequency are rejected and hence do not affect the measurements.

However, the most important part of the open loop interface circuit/control unit, which allowed accurate measurements to be taken using the Atomic Force Microscope, is the Wheatstone bridge, a schematic representation of which is shown in Figure 3.13. It is used to measure an unknown electrical resistance by balancing two legs/arms of a bridge circuit, one leg/arm of which includes the unknown component or in the case of the AFM the actual sample probe.

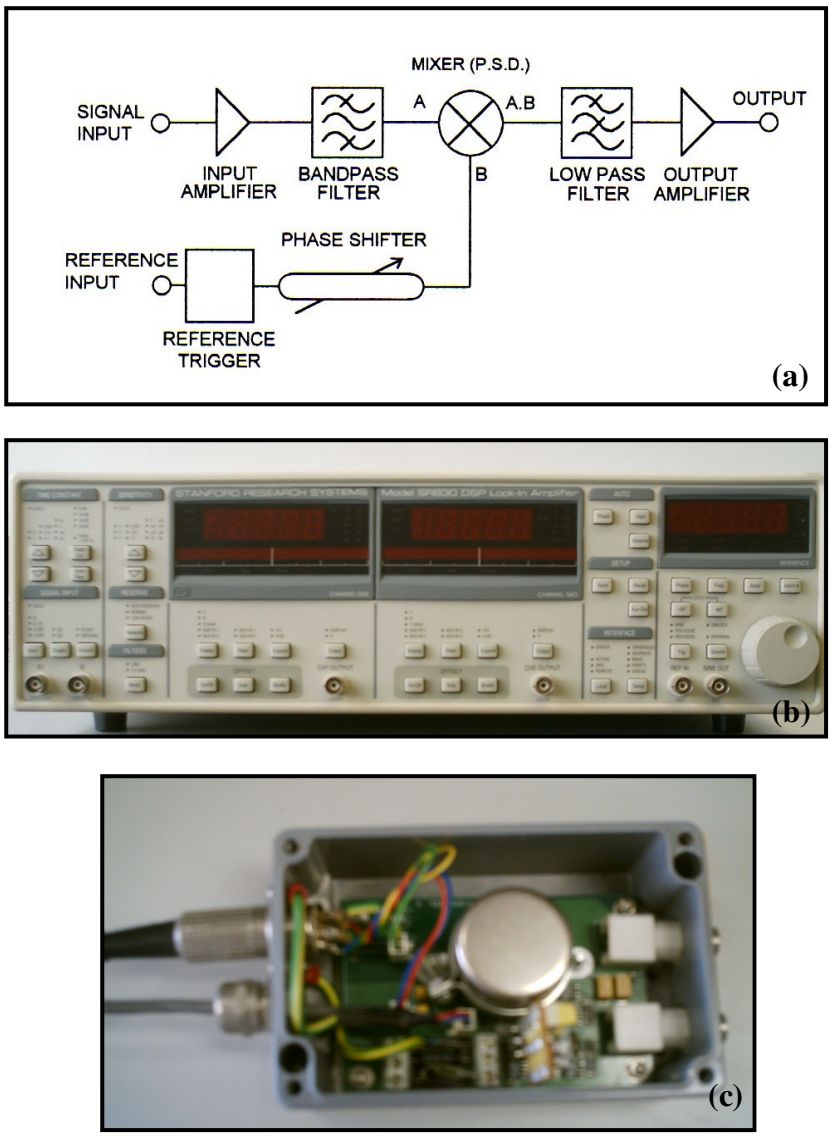

Figure 3.12 Basic elements of a lock-in amplifier: **(a)** Block diagram of a typical lock-in amplifier, **(b)** Photograph of a front panel, **(c)** Pre-amplifier box

In this instrument the voltage difference between the two arms of the bridge is determined by the resistance components and the applied voltage. In **Figure 3.13**, R_p is the unknown resistance to be measured, in our case the resistance of the sample-probe; R_1, R_2 and R_c are resistors of known resistance and the resistance of R_c is adjustable/variable. If the variable resistor R_c, is controlled to produce a nearly zero voltage between the two midpoints of the bridge then the resistance of the sample probe R_p, is given by the simple equation:

$$R_p = \frac{R_1}{R_2} R_c$$

Therefore the bridge-balancing condition is maintained by controlling only the variable resistance R_c. Or in other words, if the ratio of the two resistances in the known leg/arm of the bridge (R_1/R_2) is equal to the ratio of the two in the unknown leg/arm (R_p/R_c), then the voltage between the two midpoints will be zero and no current will flow between the midpoints.

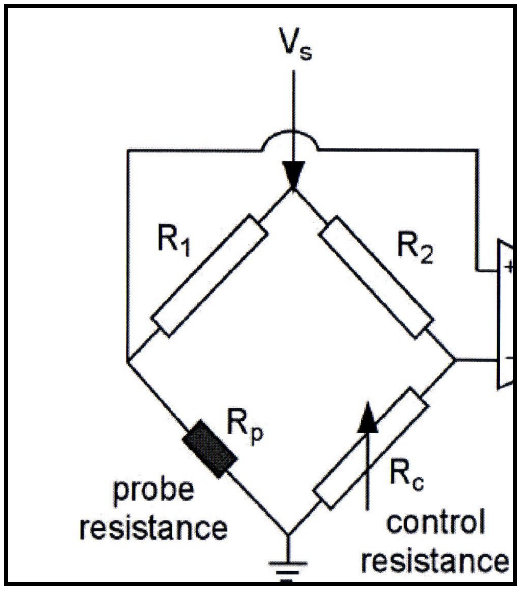

Figure 3.13 Schematic diagram of a Wheatstone bridge

The adjustable resistance R_c can be varied until this condition is reached. The current direction indicates if R_c is too high or too low. If R_1, R_2, R_c are known to high precision (e.g. measured by using galvanometer), then R_p can be measured to high precision as well. The very small changes in R_p disrupt the balance and are readily detected.

Another set of instrumental equipment used in this research project in conjunction with the Micro and Nano-thermoanalytical investigations was the Veeco diCaliber Atomic Force Microscope and the nano-TA system. The main advantages that the instruments offer are briefly described below.

Veeco diCaliber

The Veeco diCaliber AFM (**Figure 3.14a**) is able to perform a variety of SPM applications (Contact Mode, Tapping Mode, Force Distance Curves and Force Spectroscopy) on samples of various sizes for materials, such as polymers and biologicals. The AFM can also image large samples without having to cut them down. The sample stage (**Figure 3.14b**) has a mount that allows users to scan and rescan the sample at the same location and also uses pre-mounted tips. The system utilizes integrated optics with a colour camera that can enable easy judgment of tip-sample separation (*Veeco Instruments Ltd., UK-Caliber Operation Manual, 2006*).

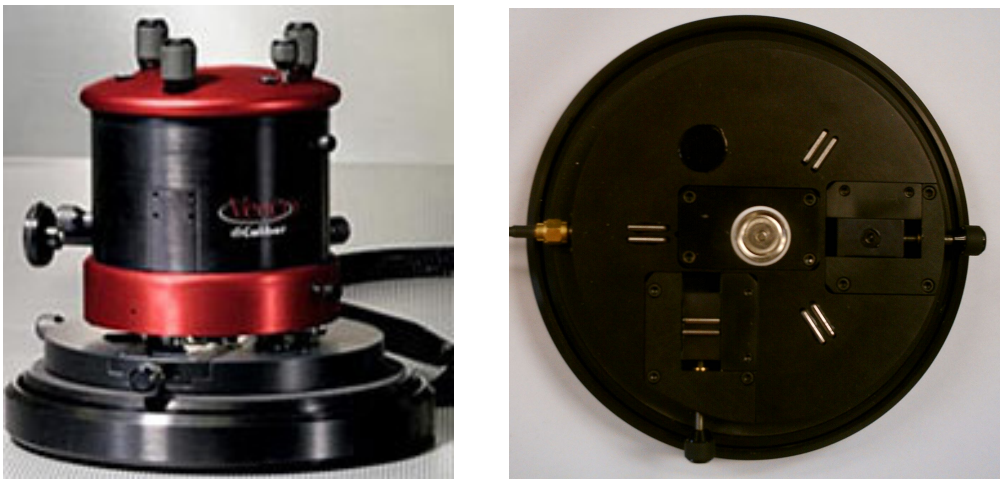

(a) **(b)**

Figure 3.14 Photograph of Veeco diCaliber **(a)** and the stage **(b)**

(*courtesy of* Veeco Instruments Ltd., UK)

Nano-TA system

The Nano-TA^{TM} Controller can be used in conjunction with a suitable AFM microscope, such as the one described above. The system is used to obtain images not only on the basis of topography, but also, for certain types of thermal probe, on the thermal properties of the sample. The resistive thermal probe can be placed at specific locations and in order and the images obtained can then be used to identify domains, features, and phases. In this mode, the system acts as a nanothermal analyser to obtain the characterization of the sample. As the chosen region of the sample is heated by the probe, temperature-dependent properties, such as softening and melting can be measured. This process is commonly referred to as *Localized Thermal Analysis*.

The Nano-TA^{TM} system consists of three boxes, shown in (**Figure 3.15a**) and special connectors. The boxes are the Power Supply, TMA Controller and CAL Controller. The Power Supply supplies +/-15 V and +5 V to the two other boxes through a 6 pin black cable. The TMA Controller box is responsible for communicating with the computer, ramping the voltage applied to the probe and reading the signals which will are displayed in the software. The CAL Controller has analogue electronics, which allow the measurement of the voltage across the sample probe, the resistance and power in the single probe mode and the power difference in the dual probe mode. The CAL Controller is set to a particular mode, either single probe or dual probe mode.

The bridge box (**Figure 3.15b**) holds the two other resistors for the bridge circuit. This box has two cables on one end with 2 socket connectors, one being red and the other black. The red connector is for the reference probe and should only be used if the system is in the dual probe mode. The black connector is for the sample probe and should be connected to the probe that makes contact to the sample surface whether in the dual or single probe mode (*nano-TA^{TM} User's Manual, 2006*).

The Nano-TA system uses the new generation of micromachined thermal probes that can achieve a spatial resolution for imaging that is 100x better than the conventional Wollaston probes. The products, supplied by Anasys Instruments are commonly referred to as nanoprobes. Nanoprobes are manufactured using boron- or phosphorus-doped silicon that renders the probe electrically conductive. The free end of the cantilever is doped with a lower level of contaminant than the legs (King, 2005),

hence it has a higher electrical resistance than the legs. An electrical current running through the cantilever causes resistive heating at the tip end.

Anasys Instruments provides two styles of nanoprobe: the GT style, with a shorter tip (~1 µm) and the AN style probes with taller tips (3-5 µm). Only the AN probes were used in this work (**Figure 3.15c**). The probes have a length of 200-300 µm, a thickness of 1-2 µm and a total width of ~60 µm. The resistance of the nanoprobes is typically in the range from 0.5 to 6 kΩ. AN style probes can achieve a maximum temperature of 250^0C. Nanoprobes are more sensitive to cleaning and this function should only be used as a last resort to clean the probe.

Nanoprobes offer several advantages over the conventional Wollaston probes. Probes are capable of imaging in all AFM modes (contact, non-contact and intermittent contact mode) with spatial resolution comparable to conventional AFM probes, excellent repeatability can be achieved and the temperature drift is avoided. There are, however, some disadvantages associated with the use of these probes. Nanoprobes are much more fragile than conventional thermal probes – therefore careful handling is a necessity.

(a)

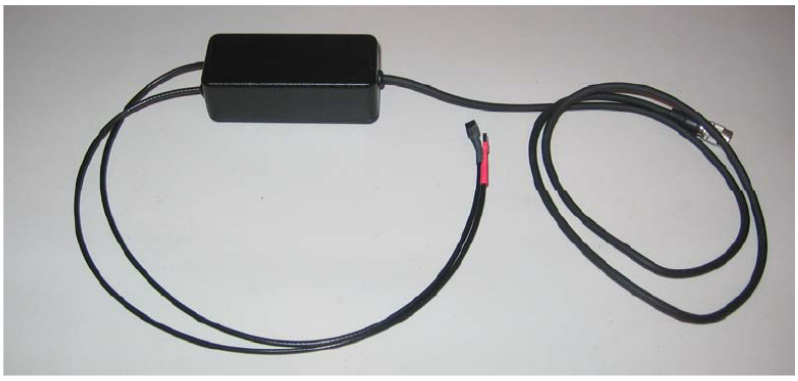

(b)

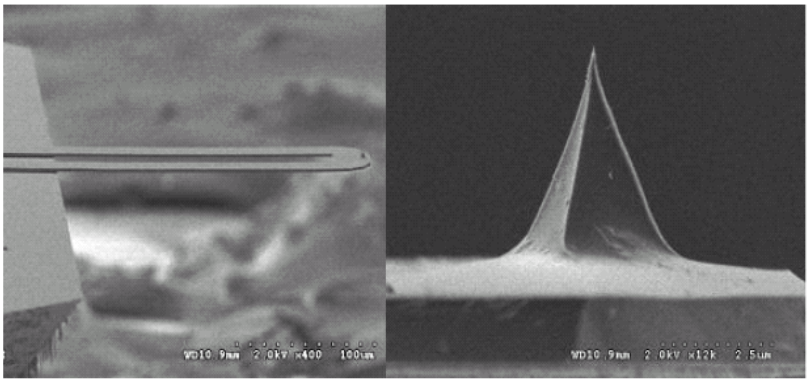

(c)

Figure 3.15 Photograph of the three components of the Nano-TA system **(a)**, the bridge box **(b)** and **(c)** SEM micrograph of AN style nanoprobes (*courtesy of* Anasys Instrumnet Inc., USA)

3.3.3. Photothermal Microspectroscopy (PTMS)

Photothermal Microspectroscopy is a technique based on the absorption of electromagnetic radiation and detection of associated temperature rise. The theoretical background and its up to date applications have already been described in detail in the previous chapter. Therefore, here only a description of the experimental set up used in this research project will be considered. In this study the Photothermal Microspectroscopy set up was implemented by combining a Scanning Probe Microscope (Explorer AFM, Veeco Instruments, UK) equipped with a Wollaston wire thermal probe together with a Fourier Transforming Infra Red (FTIR) Spectrometer (Bruker Optics Ltd., Coventry, UK). The two systems were integrated using a dedicated optical interface obtained from Specac, Orpington, UK. A photograph of the set up is shown in **Figure 3.16**.

As explained before, in this research Photothermal Microspectroscopy was mainly used in an attempt to characterise any structural changes taking place in untreated and treated (with Ampicillin) E.coli bacterial specimens. The methodology was also applied in a preliminary study of food systems including wild and mutant types of maize.

Unless otherwise stated in the following chapters, all spectra from the experiments were recorded at 16 cm^{-1} spectral resolution, 2.2 kHz mirror speed and consist of 1000 co-additions. The spectra were obtained from two sets of measurements. Firstly, a background measurement was obtained with a clean probe. The measurement of the sample spectrum was performed next. The sample spectrum was divided by the

background spectrum and scaled using the CO_2 absorption band at approximately 2350 cm^{-1}. The background spectrum was then subtracted from the sample spectrum to remove any traces that were due to the probe's own absorption and heating of the surrounding air.

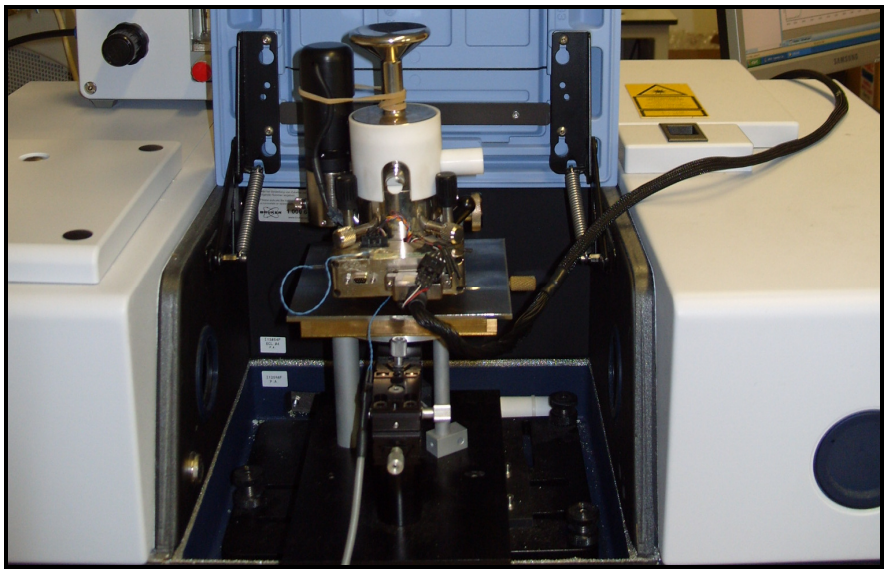

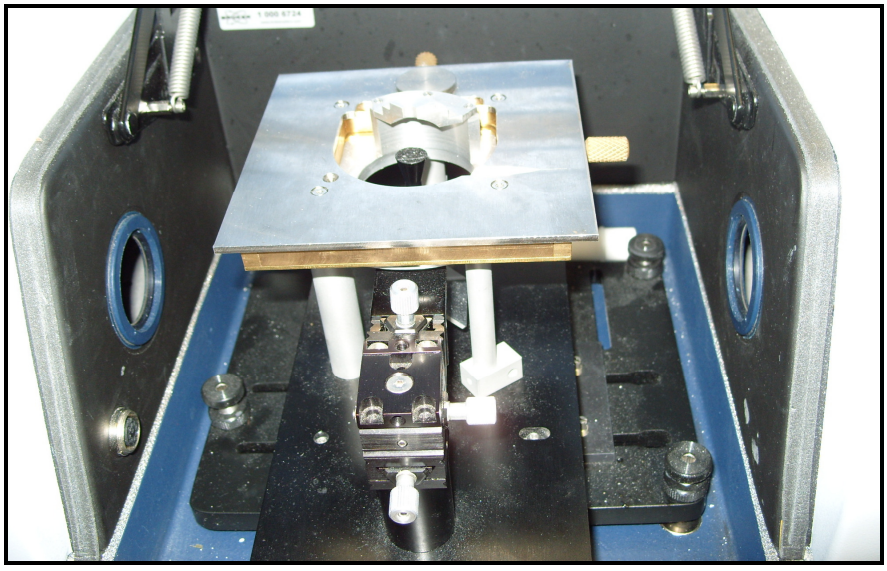

Figure 3.16 Photographs of the experimental set up used to perform the Photothermal Microspectroscopy experiments on the treated and untreated E.coli bacterial cells

3.3.4. Environmental Scanning Electron Microscopy

Environmental Scanning Electron Microscopy (ESEM) was used in this study for comparative purposes and to confirm the presence of cells on the AFM tips. This technique offers the possibility of imaging 'wet' and insulating materials in their natural hydrated state, and has been successfully used in the study of a number of systems and dynamic processes (Donald, 2003). Unlike conventional Electron Microscopy, where high vacuum is maintained throughout the instruments, ESEM is based on the use of a multiple aperture graduated vacuum system, which allows specimens to be imaged under water vapour or other auxiliary gases, such as nitrogen or nitrous oxide (**Figure 3.17a**). In this way, the chamber can be held at pressures of up to 40 Torr, while the gun and column remains at pressures of ~7.5×10^{-7} Torr (Meredith & Donald, 1996). Moreover, by using a correct pumpdown procedure and by controlling the temperature of the specimen, which in the ESEM is usually done by using a Peltier stage, dehydration can be inhibited and hence samples can be imaged in their 'natural state' (Cameron & Donald, 1994).

The microstructural analysis was carried out on an FEI XL-30 Environmental Scanning Electron Microscope (**Figure 3.17b**), equipped with a Peltier stage and linked to an EDAX Energy Dispersive X-ray (EDX) analysing system. Specimens from the studied systems were placed onto the cooling stage in the microscope chamber at a temperature of ~273 K. An evaporation-inhibiting pumpdown sequence was then performed with the ambient air progressively replaced by water vapour, in order to minimise sample evaporation during the initial pumpdown. Once the purging

cycle was completed, water vapour pressures and working distances of 1.5 – 3.5 Torr and 9.5 – 11.5 mm respectively were set, which provided suitable imaging environments.

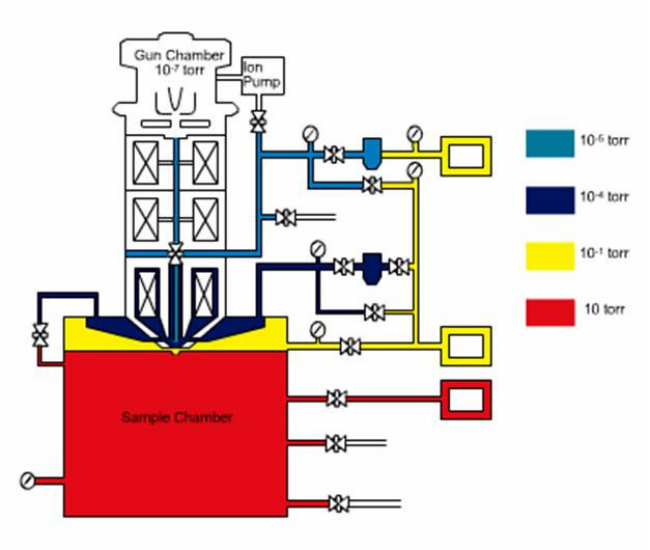

(a)

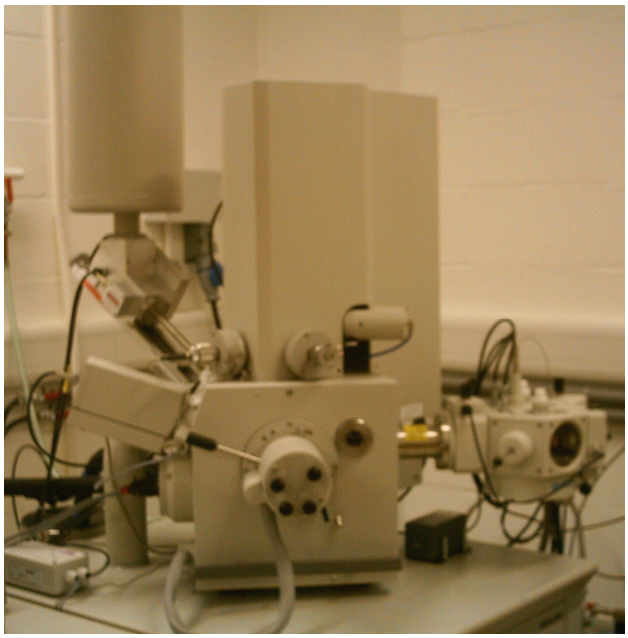

(b)

Figure 3.17 Schematic diagram **(a)** and photograph **(b)** of the FEI XL-30 Environmental Scanning Electron Microscope

4. Imaging of E.coli bacterial cells

4.1. Introduction

As already mentioned, the principal aim of this research is to develop a novel SPM-based approach whereby we are able to detect and quantify interactions between pharmaceutically relevant materials and biological cells. In order to do that it is not only important to understand and optimise the sensitivity of the probe used, but also to develop suitable protocols for imaging of the studied bacterial systems. This is necessary to be done in order to get better understanding of the morphology and the changes taking place in the E.coli cells. This part of the thesis considers the results from the sample preparation technique employed and the images obtained by using different modes of operation on untreated E.coli cells and those treated with Ampicillin. The effects of use of different types of heated probes (Wollaston wire and novel nano probes) on the quality of the obtained images are also considered. The data obtained from this work is also discussed in terms of previously published work in this research area some of which has already been highlighted in the Literature Survey chapter.

4.2. Sample preparation methodology

As described previously in the Materials and Methods chapter the E. coli bacterial cells were grown from overnight cultures at 35^{0}C with mild shaking at 150 rpm in Luria broth medium (tryptone 10g l^{-1}, yeast extract 5g l^{-1}, NaCl 5g l^{-1}) to stationary growth phase (Sezonov *et al.*, 2007). These were then harvested by centrifugation at

9000 rpm for 3 min and then washed three times with phosphate-buffer saline (PBS). 50μL of the cell suspension was placed on a glass slide coated with poly-L-lysine solution followed by incubation, rinsing and drying. It is important to note at this stage that poly-L-lysine solution is widely used in the preparation of biological specimens mainly for Electron Microscopy examination. The imaging of the cells was carried out in tapping, pulsed force and thermal modes using a Veeco diCaliber AFM (Veeco Instruments Ltd., UK). Details of the microscope used and its modes of operation can be found in Materials and Methods chapter.

4.3. AFM imaging of E.coli bacterial cells

Tapping and pulse force mode imaging

In the first part of the chapter the results obtained using tapping and pulse force mode (PFM) imaging are considered. A series of tapping mode images of E.coli bacterial cells obtained by using the above described sample preparation method are presented in **Figures 4.1**. From the results it is clearly seen that by using the above described sample preparation technique it is possible to obtain high quality images of individual and aggregates of E.coli cells. From the images obtained using tapping mode it is also possible to extract information about the size and shape of the E.coli cells. The rod shaped bacterial cells are of length in the region of 2.5-5.0 microns and 1.0-2.5 microns width. These dimensions are consistent with many of the previously published results, examples of which include the work of Velegol *et al.*, 2002, Doktyez *et al.*, 2003 and more recently Perry *et al.*, 2009. This is also confirmative of

the fact that the bacteria have been grown to stationary phase. An AFM example image of E.coli bacterial cells from the earlier studies is provided in **Figure 4.2**.

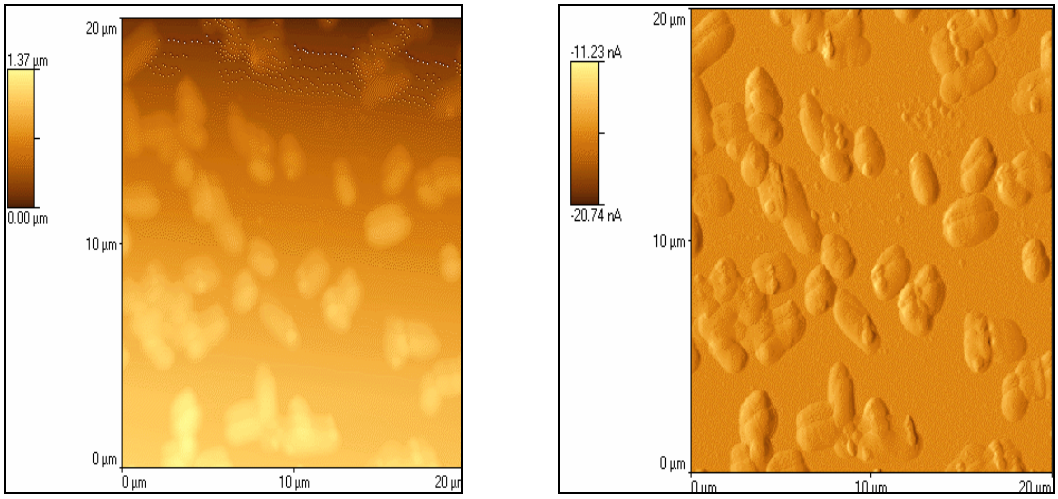

(a)

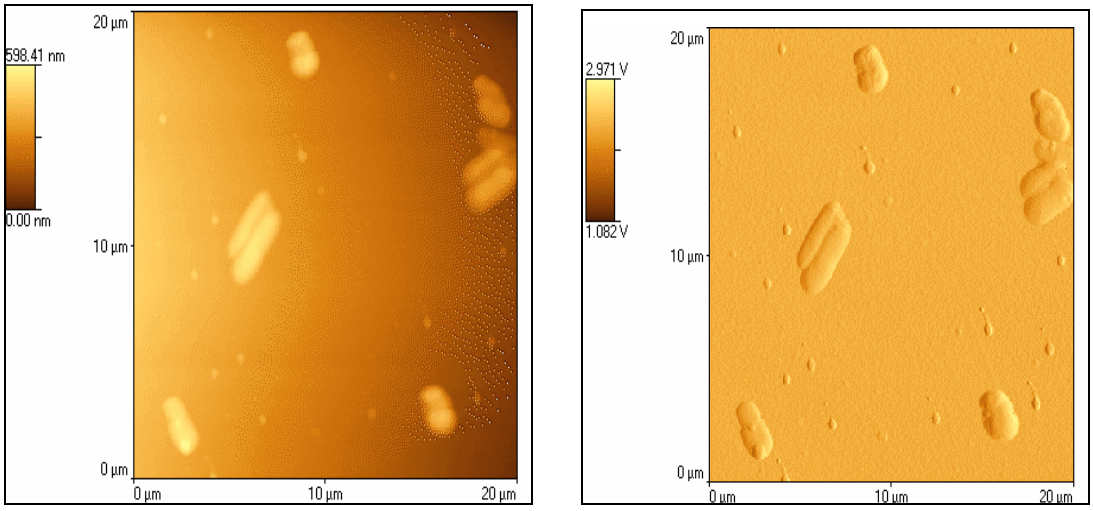

(b)

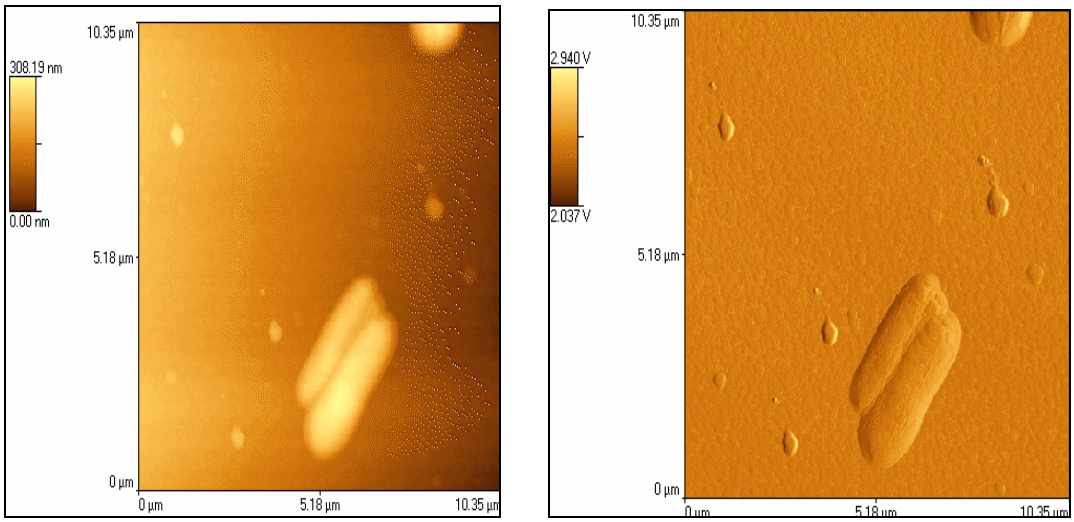

(c)

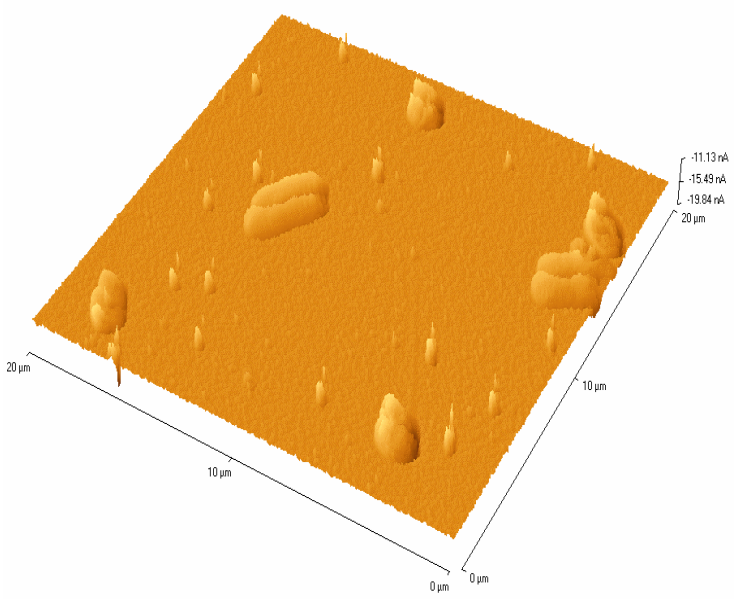

(d)

Figure 4.1 Tapping mode images of HB101 E.coli cells obtained at different magnifications **(a)** aggregates of E.coli cells, **(b)** individual randomly distributed cells, **(c)** higher magnification image of 2 E.coli cells in contact with each other and **(d)** a 'place fit' image of the 2 cells in contact with each other, confirming that there are no 'double tip' artefacts that can be associated with this AFM imaging mode (left – topography image, right – internal sensor image)

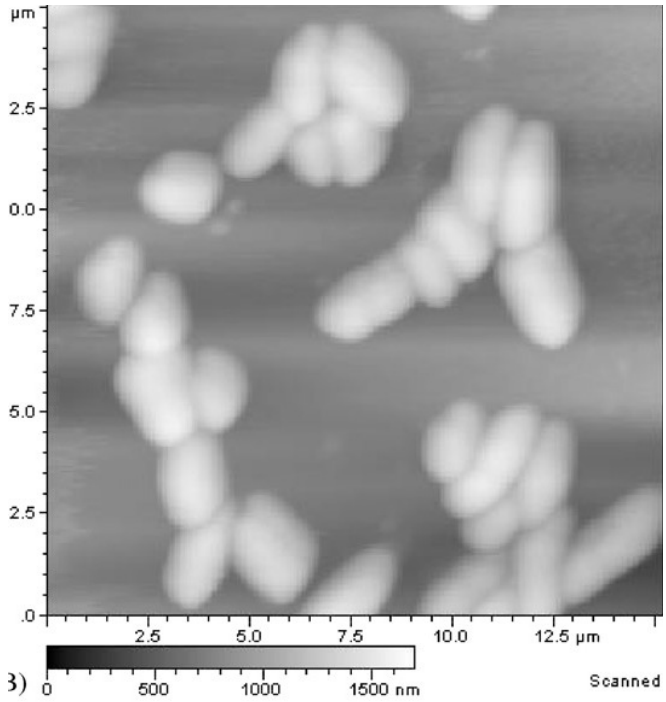

Figure 4.2 Example of a tapping mode AFM image of E.coli bacterial cells. In contrast to this study the cells here have been immobilised on Sigma gelatin coated surfaces, rather than poly-L-lysine (*after Doktyez et al., 2003*)

As annotated above in the example provided, the E.coli cells in this particular study have been immobilised on Sigma gelatin coated surfaces, rather than poly-L-lysine. This obviously is an alternative method for sample preparation which has also been shown to be effective when trying to immobilize live bacterial cells (Doktyez *et al.*, 2003). In their study the authors further claimed that Sigma gelatine is superior to poly-L-lysine. However, this suggestion was not supported by conclusive evidence and furthermore by comparing the images obtained in this study to those obtained in theirs it is obvious that this may not necessarily be the case. It is believed that here it is clearly demonstrated that by using the above described sample preparation technique it is possible to obtain high quality tapping mode images of individual and

aggregates of E.coli cells. Also, here it is important to mention that none of the images obtained from the cells immobilised by using poly-L-lysine contained line artefacts (**Figure 4.3**), which are commonly found in bacterial specimens prepared by using polyethylenimine (Velegol, *et al.*, 2003). This artefact appears as 'excess material' alongside the cell and is thought to be caused by the height of the specimen and the tip geometry. However, as none of these were varied in this study it is not unreasonable to suggest that the actual sample preparation technique may also have an effect. This is also suggestive of the fact that poly-L-lysine is not only a suitable immobilisation agent that can be used for AFM imaging of E.coli bacterial cells, but it would also appear that its use may not introduce unwanted artefacts within individual cell images, which can undoubtedly lead to difficulties and/or misinterpretation of the results.

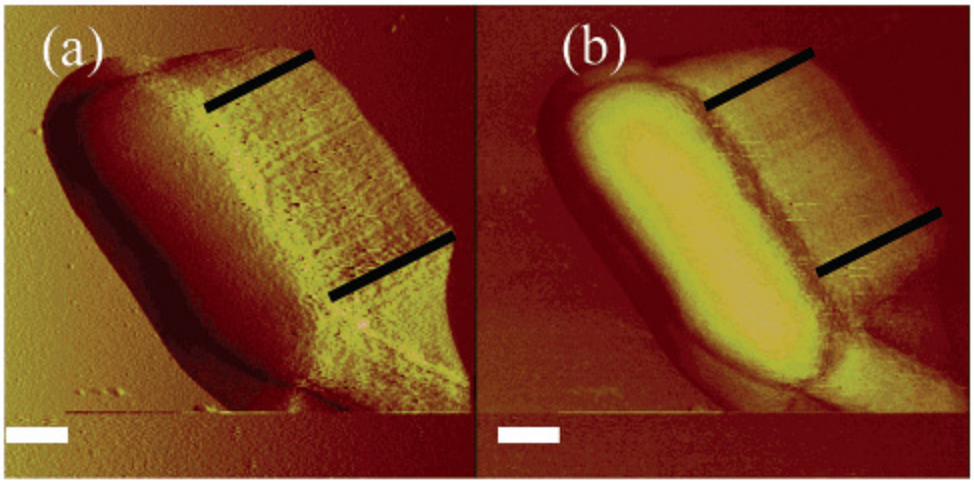

Figure 4.3 AFM tapping mode line artefacts observed in E.coli bacterial specimens; **(a)** amplitude and **(b)** phase (*after Velegol, et al., 2003*)

The next part of this chapter considers the results obtained using Pulse Force Mode (PFM) imaging. Up to now it was clearly demonstrated that while the tapping mode images provide useful information of the shape and size of the studied bacterial cells, they do not appear to be very representative of the topography, or in other words the overall surface relief of the cells. In contrast, the Pulse Force Mode (PFM) images (**Figure 4.4**) do not only give information of the dimensions of the individual and/or aggregated bacterial cells, but also provide additional information about the surface morphology of the system, which can be clearly seen from the images in the figure below. The results presented here are believed to be of significant importance as Pulse Force Mode AFM is currently not widely used in the study of biological systems and hence there is lack of information in the literature. It is also important to note that the PFM-AFM approach of analysis provides important information on sample mechanical properties (e.g. adhesion) that cannot be obtained from topography imaging. Therefore it may not be unreasonable to suggest that this imaging mode may indeed be very suitable for the investigation of interactions of cellular systems and for that reason it was used for the imaging of the treated E.coli bacterial cells.

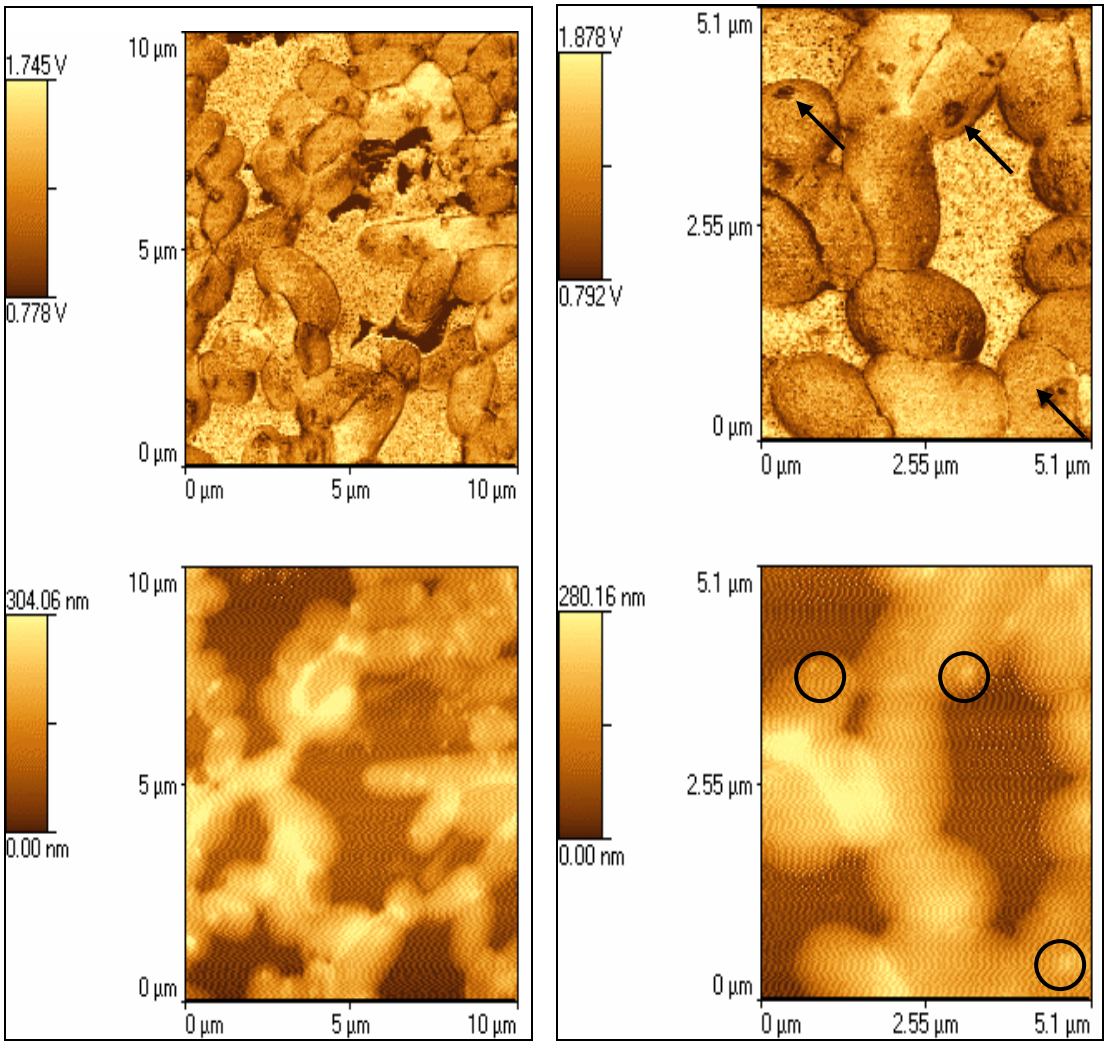

(a) **(b)**

Figure 4.4 Pulse Force Mode (PFM) images of aggregated HB101 E.coli cells **(a)** low and **(b)** high magnification. Surface features present on the surfaces of the individual bacterial cells can clearly be seen. Some of these have been indicated by the arrows and circles in the images. Here, it is important to note that such features were not present in the tapping mode images (top – internal sensor, bottom – topography)

So far, it has been demonstrated that the sample preparation technique and AFM imaging parameters employed in this research can be successfully used for obtaining high quality images of the studied bacterial system. The next part of this chapter considers the results obtained from the treated E.coli cells. As explained earlier, this is thought to be an essential and important step in the development of SPM based protocols for studying the interactions of living cells and pharmaceutically relevant materials, in this case Ampicillin, which is still one of the most commonly used antibiotics in the treatment of bacterial infections. The actual treatment of the cells, as described in the Materials and Methods chapter, was done simply by adding a pre-made solution of concentration 100mg/ml to the media containing bacteria. A sequence of images obtained from E.coli cells prior to and after treatment with Ampicillin using, as suggested above, PFM mode are presented in **Figures 4.5, 4.6**, **4.7** and **4.8**. Here it is important to note that the images were then taken after different periods of treatment in an attempt to investigate the effect of Ampicillin as a function of time and to observe any structural changes that were taking place within the individual bacterial cells.

From the images of the untreated cells (**Figure 4.5**) it is clearly seen that as before it is possible to easily extract information about their shape and size. The MG16SS strain rod shaped cells are of similar length and width when compared to the HB101 strain. However, it is evident from the images that this strain has an additional structural feature – flagellum, which in the adhesion images can clearly be identified.

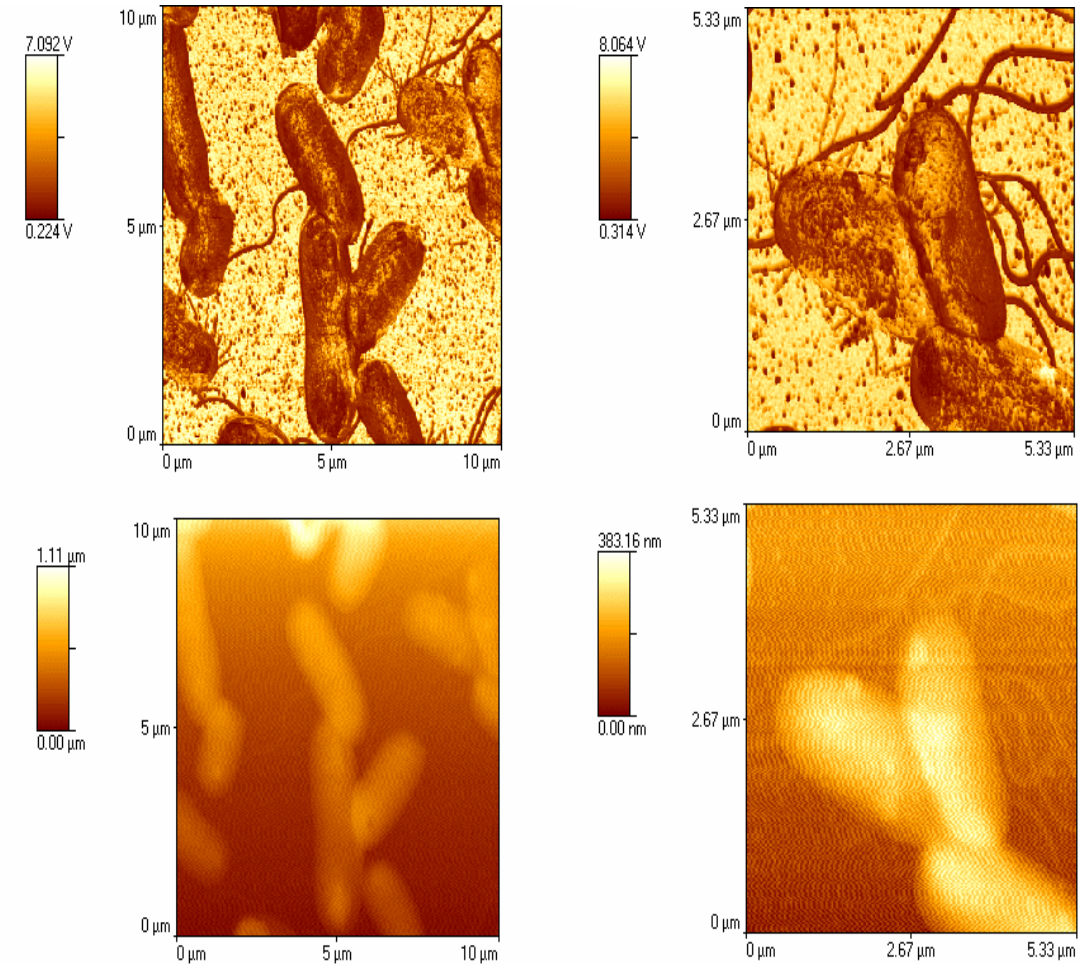

(a) **(b)**

Figure 4.5 PFM AFM images of MG16SS E.coli cells prior to treatment with Ampicillin; **(a)** low magnification images of aggregated of E.coli cells and **(b)** higher magnification images of individual bacterial cells (top – adhesion, bottom – topography)

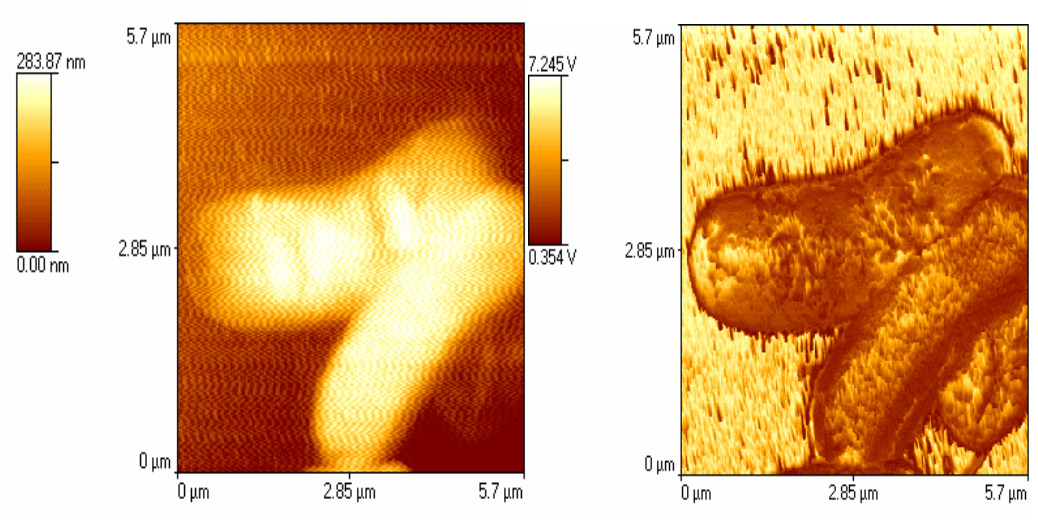

(a)

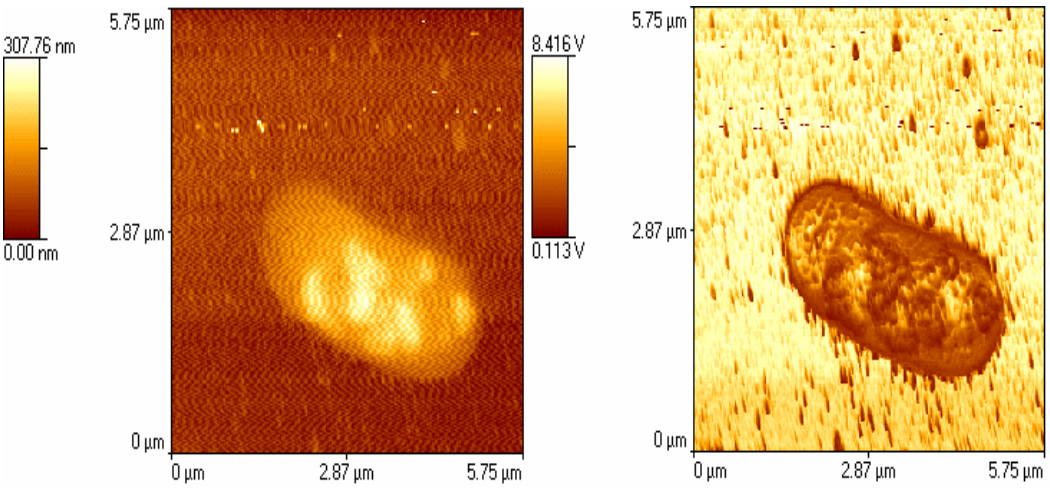

(b)

Figure 4.6 PFM AFM images of MG16SS E.coli cells after 5 hours of treatment with Ampicillin; **(a)** 2 cells in contact with each other and **(b)** high magnification image of an individual cell. After 5 hours of treatment it appears that there are no visible changes to the cell surface or its shape (left – topography, right – adhesion)

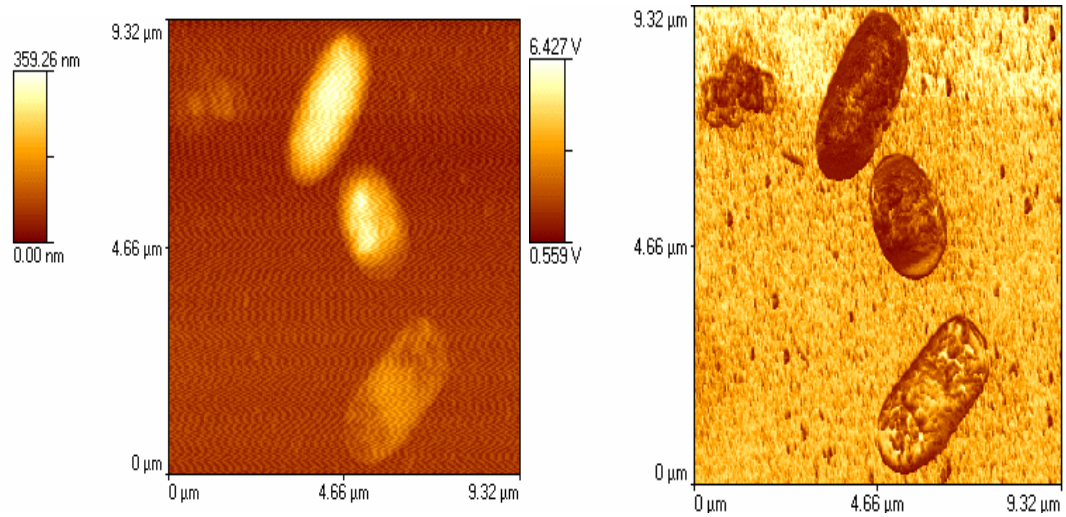

(a)

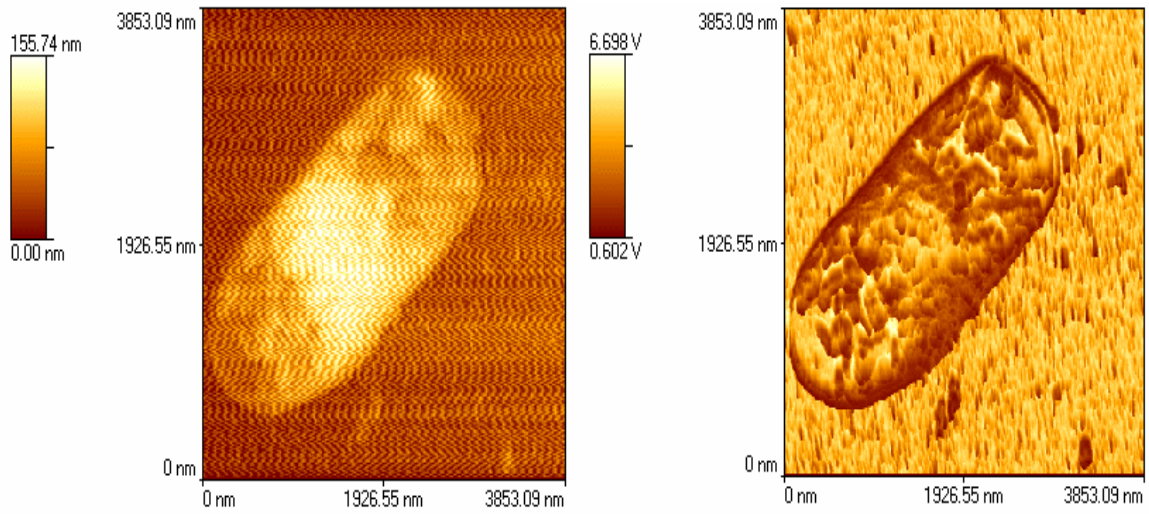

(b)

Figure 4.7 PFM AFM images of MG16SS E.coli cells after 8 hours of treatment with Ampicillin; (a) low and (b) high magnification. Changes in the cell wall and the overall cell shape appear to have started taking place (left – topography, right – adhesion)

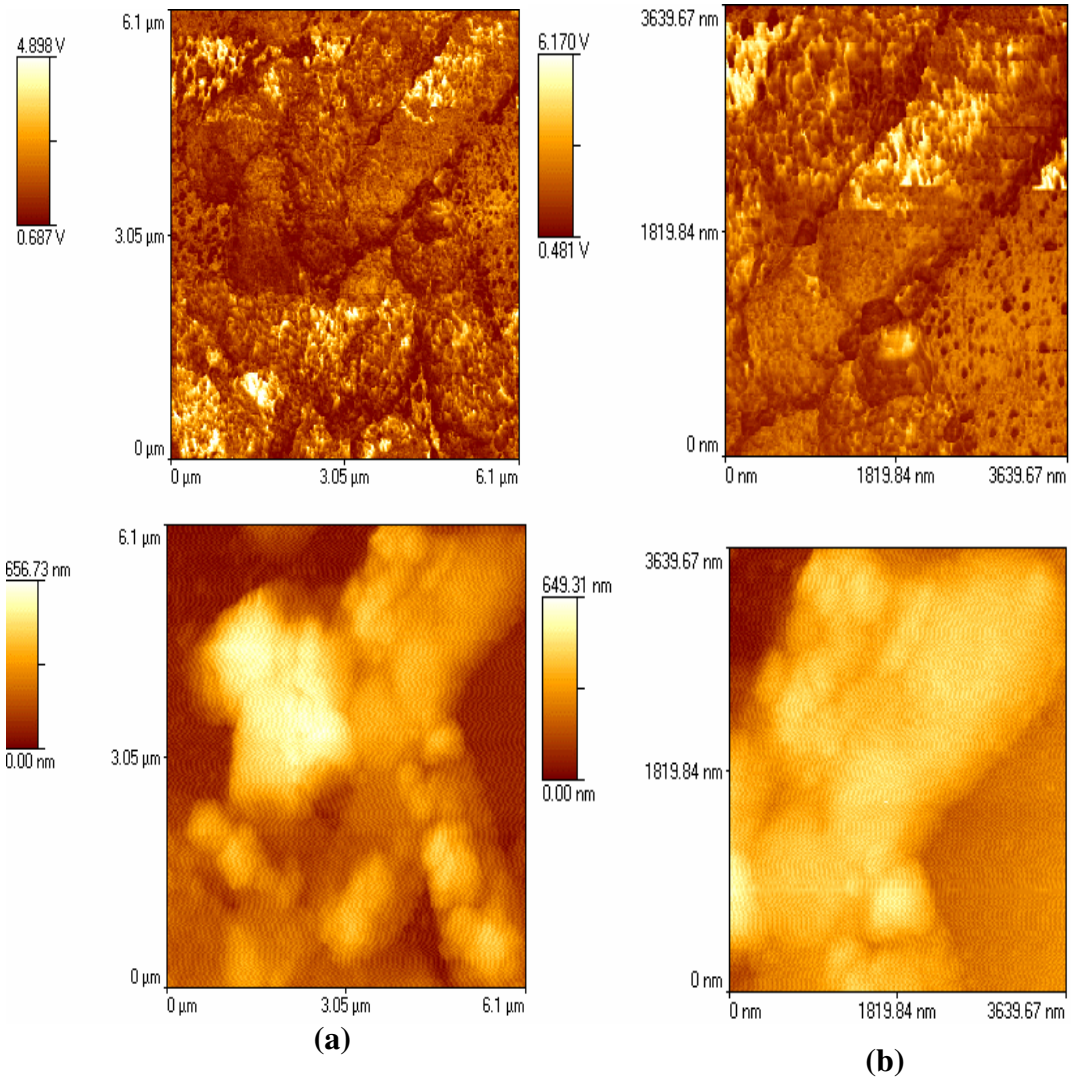

Figure 4.8 High **(a)** and low **(b)** PFM AFM images of MG16SS E.coli cells taken with conventional probes after 12 hours of treatment with Ampicillin. Significant cell degradation can clearly be seen (top – adhesion, bottom – topography)

Before the effect of Ampicillin is considered, here it is important to mention yet again that the sample preparation technique employed in this study proved to be successful also for imaging cells treated with antibiotics. From the images of the treated cells it is evident that in the early stages of the treatment (**Figure 4.6**) there are no obvious

changes to the overall structure of the individual cells. However the flagellum appears to have been destroyed by the antibiotic. After approximately 8 hours of treatment (**Figure 4.7**) it is apparent that changes to the cell wall and their overall shape begin to take place; and after 12 hours of treatment the degradation of the cell wall and membrane has progressed to a very advanced stage so that it becomes difficult to distinguish individual cells (**Figure 4.8**). The process of degradation can be associated to the production of nanopores and further leakage from the inside.

The actual detrimental effect of β-lactams, such as Ampicillin, on E. coli bacterial cells was recently investigated by Yang *et al* (2006) who proposed two main reasons leading to the death of these species. Firstly, it was reported that cell division is inhibited by the creation of nanopores at the apical ends of E. coli cells. Secondly, the authors reported that there was an apparent leakage of the cell contents. It was therefore proposed that the damage to the cell wall structure would create an imbalance between the inner and outer osmotic pressures of the cell, resulting in the loss of inner contents and consequent cell death.

Furthermore, very recently, Perry *et al* (2009) investigated the effects of Ampicillin and Garlic extract on E.coli bacterial cells and reported similar observations for the case of the antibiotic (**Figure 4.9**). More interestingly, they observed cell death after 12h of treatment which is consistent with the results from this study. However, here it is important to note that the concentration of the Ampicillin used was 25mg/ml, whereas the one used in this study was 100mg/ml. Therefore it may not be unreasonable to suggest that there may be a range of antibiotic concentrations that

have similar effect when used on bacterial cells. Hence, it seems plausible that AFM may also find useful application in the determination of the optimum antibiotic concentration needed for the treatment of for example bacterial infections.

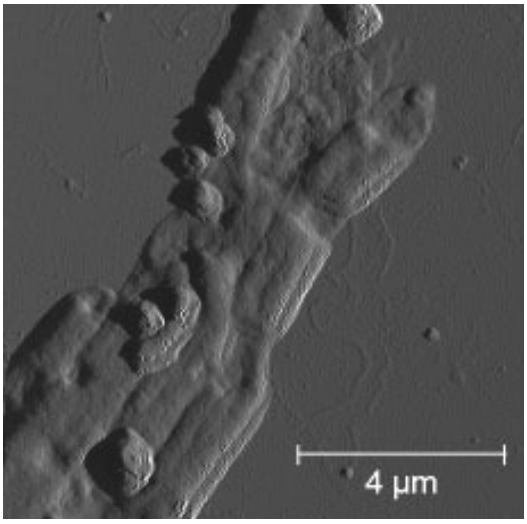

Figure 4.9 Representative AFM image of E.coli cells after 12h exposure to 25mg/ml concentration of Ampicillin (*after Perry et al., 2009*)

Thermal imaging

This part of the Chapter presents the results from the thermal mode imaging of the studied bacterial system. Here it is important to note that as this is a reasonably new imaging mode, which undoubtedly is being used by a number of researchers for different investigations, there is still no information available in the literature of its application in the study of E.coli cells. Therefore it can be claimed that the images presented below are the first ever images of this type of cell obtained using thermal probes. Here the effect of the type of probe (e.g. Wollaston wire, nano-probe) and temperature on the quality of the obtained images will also be considered.

Examples from the images obtained in thermal mode using the classical Wollaston wire probe are shown in **Figure 4.10**. The images were obtained at probe temperatures in the region 30^0C – 70^0C. The temperature range was chosen in an attempt to investigate the effect of probe temperature on the overall mechanical properties in the viable cell temperature range and at slightly elevated temperatures, but not completely detrimental to the cells or immobilisation media (e.g. 300^0C). From the images presented in the figure below it is clearly seen that although informative they appear to be quite noisy, which is most probably due to the fact that the tip is heated during the process of image acquisition. Also, due to the size of the tip, which exceeds the size of the E.coli cells, the shape and size of individual bacteria can not be easily determined. From the images it is also evident that the temperature of the probe has little or no effect on the image quality. This again is likely to be due to the size of the probe. Nevertheless, the results still indicate that this mode of operation can be used for imaging of bacterial cells, especially if for example processes and/or interactions are investigated at elevated temperatures. It is believed that the Wollaston wire probe will be useful in the study of biological species that exceed its size, i.e. are larger than 5 microns.

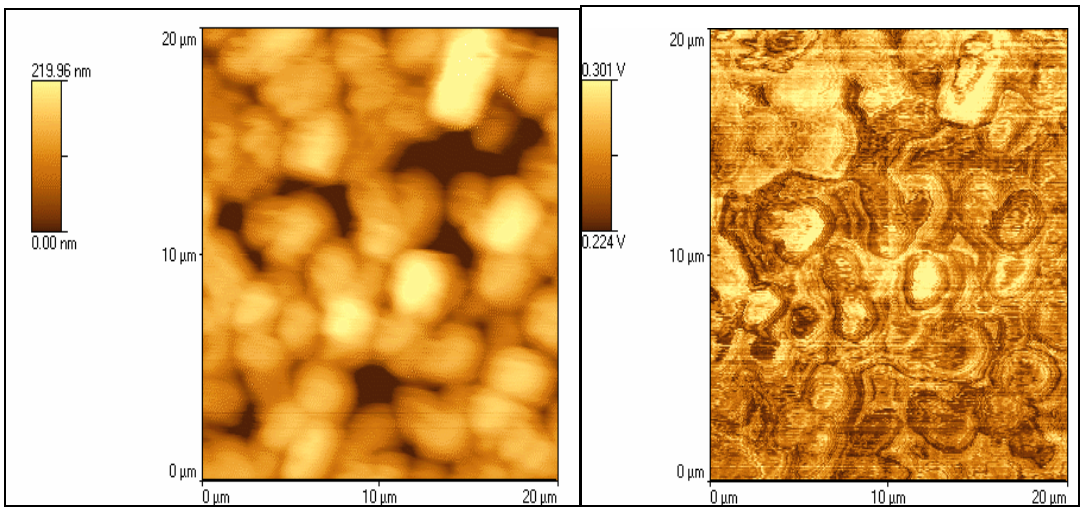

(a)

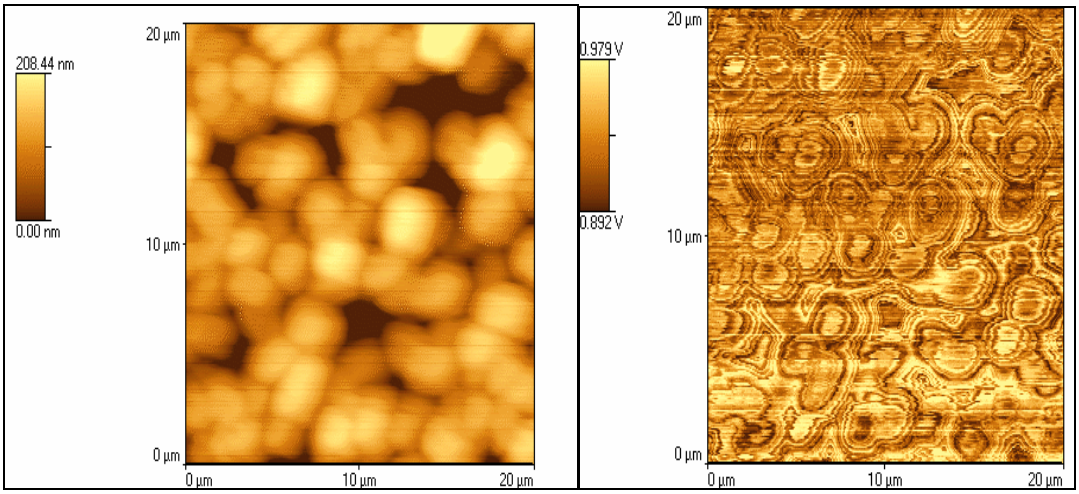

(b)

Figure 4.10 Thermal images of HB101 E.coli bacterial cells obtained with Wollaston wire probe at **(a)** 30^0C and **(b)** 70^0C. Although informative the images are quite noisy, which is thought to be due to the size and shape of the tip used in the imaging process (left – topography, right – internal sensor)

However, it was found that the image quality can be greatly improved by using the recently developed nano-probes. This is most probably due to the fact that the size of these novel nano-tips is in the nanometre region and hence the spatial resolution is greatly improved by at least one to two orders of magnitude compared to the Wollaston probes. Typical examples from the images obtained in this study using the above AFM tips are shown in **Figure 4.11**.

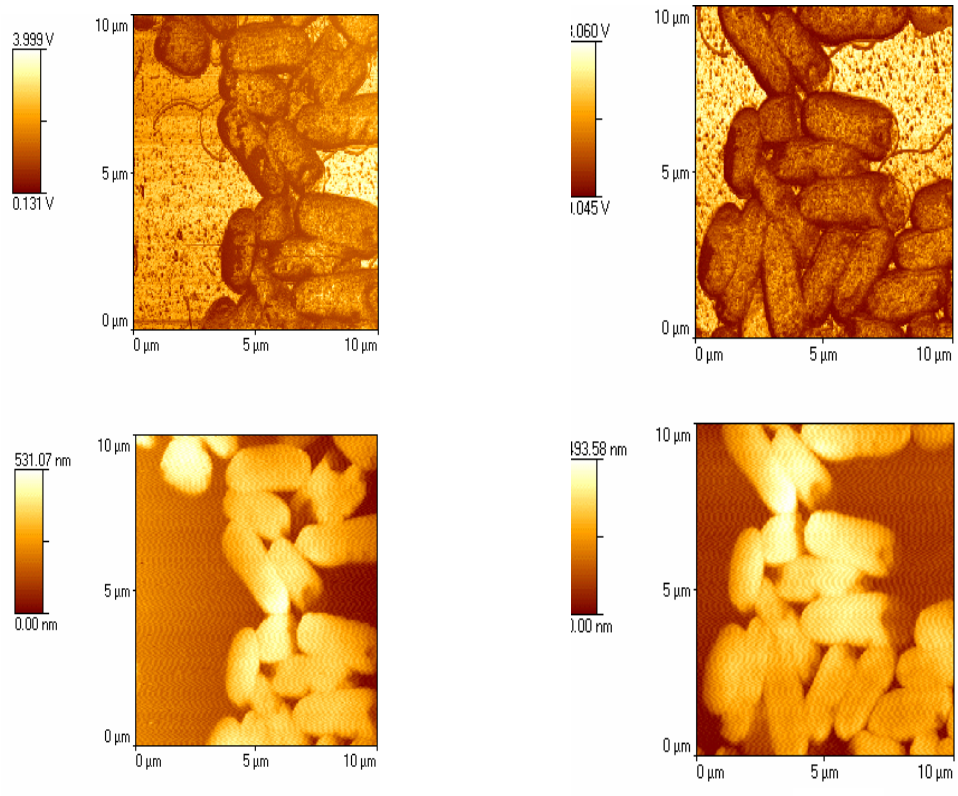

(a) **(b)**

Figure 4.11 PFM images of untreated MG16SS E.coli bacterial cells obtained using heated nano tips at **(a)** 30^0C and **(b)** 70^0C. The quality of the images is much better compared to the ones obtained using the conventional Wollaston wire probes. From these it is also seen that the shape and size of the bacterial cells can easily be determined and that these are similar to those observed with tapping and conventional PFM modes (top – adhesion, bottom – topography)

From the results presented in the figures above it is clearly seen that the use of heated nano-tips results in the generation of images of much higher quality and contrast in comparison to those obtained using the Wollaston wire probes. In this case the individual bacterial cells can easily be determined and their shapes and sizes accounted for. Moreover, it was found that image quality of the samples obtained at higher temperatures (**Figure 4.11b**) was better that the ones obtained at lower. Similar observations were made by Harding (2006) when studying interactions between pharmaceutical materials. The origins of this effect are yet to be fully understood.

Finally, in a similar pattern, the heated nano-probes were also used for imaging of bacterial cells treated with antibiotics. Examples from the images obtained from these are presented in **Figure 4.12**. Similar to the previous observations can be made or in other words it is clearly evident that after 12 hours of treatment the degradation of the cell wall and membrane has progressed to such an advanced stage so that it becomes difficult to distinguish individual cells. Again, here it can be said that the actual process of degradation can be associated to the production of nanopores and further leakage from the inside (Yang, 2006). In the example provided below, this is further confirmed by the presence of detached flagellum of the E.coli cells.

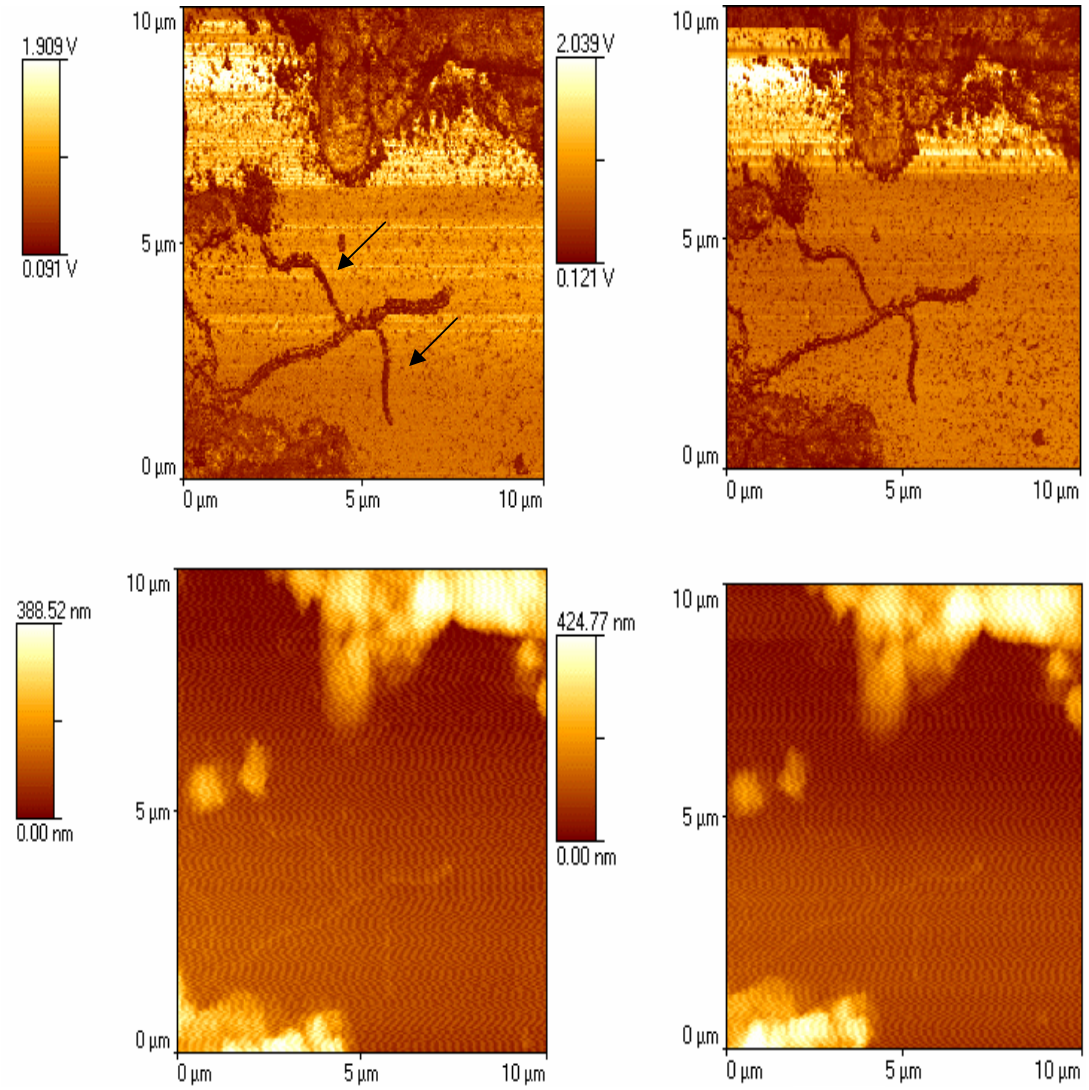

Figure 4.12 PFM images of treated with Ampicillin MG16SS E.coli bacterial cells (12h) obtained using heated nano tips at **(a)** 30^0C and **(b)** 70^0C. As before, it is evident that after 12 hours of treatment the degradation of the cell wall and membrane has progressed to such an advanced stage so that it becomes difficult to distinguish individual cells. For this particular strain, the degradation is also further emphasized by the detachment if flagellum (indicated by the arrows); top – adhesion, bottom – topography

4.4. Force-Volume imaging of E.coli cells

Force volume imaging is another imaging mode available to the Atomic Force Microscope, which was also tried as means of studying the biological system under investigation. The principals of the technique are briefly described below.

It is a well known fact that any small particle that approaches a surface experiences a number of forces before and after contact with the surface. Hence, using an Atomic Force Microscope (AFM) tip, or a small particle attached to an AFM cantilever, it becomes possible for the instrument to be used to probe these forces between the tip (or particle) and the surface in question. This is usually done by recording the cantilever deflection as the tip approaches, contacts, and retracts from a surface and then plotting a force curve as a function of the approach-retract travel distance. These types of force measurements can contain information about the electrostatic, chemical, and magnetic properties of surfaces and materials. Because most surfaces being examined are not homogeneous, it is often of interest to collect an array of force curves. Such an array produces information about the lateral distribution of different surface and/or material properties (*Veeco Instruments Ltd., UK - Explorer Operation Manual, 2000*).

A force volume contains an array of force curves over the entire sample area. Each force curve is measured at a unique x-y position in the area, and force curves from an array of x-y points are combined into a three-dimensional array, or "volume," of force data (**Figure 4.13**).

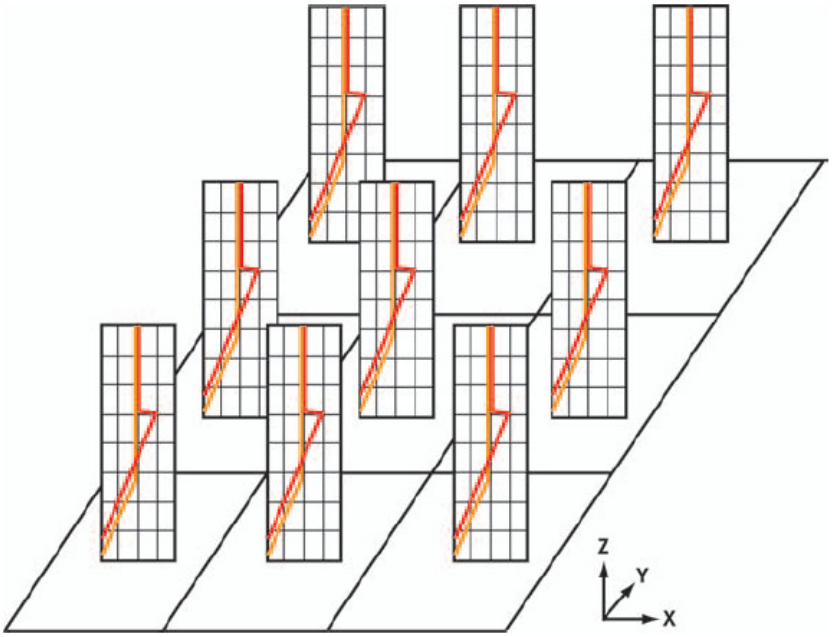

Figure 4.13 An example of a force volume data set – an array of regularly spaced force curves yields three-dimensional force information (*Veeco Instruments Ltd., UK - Explorer Operation Manual, 2000*)

A typical force volume image obtained from an E.coli sample after 12h treatment with antibiotics is shown in **Figure 4.14**. From the image it is clearly seen that the quality of the images obtained using tapping and especially PFM mode are far more superior compared to the Force Volume image and it is obvious that no additional information can be extracted from it. Furthermore, it was also found that the technique is very time consuming and hence the method was deemed unsuitable for further studies.

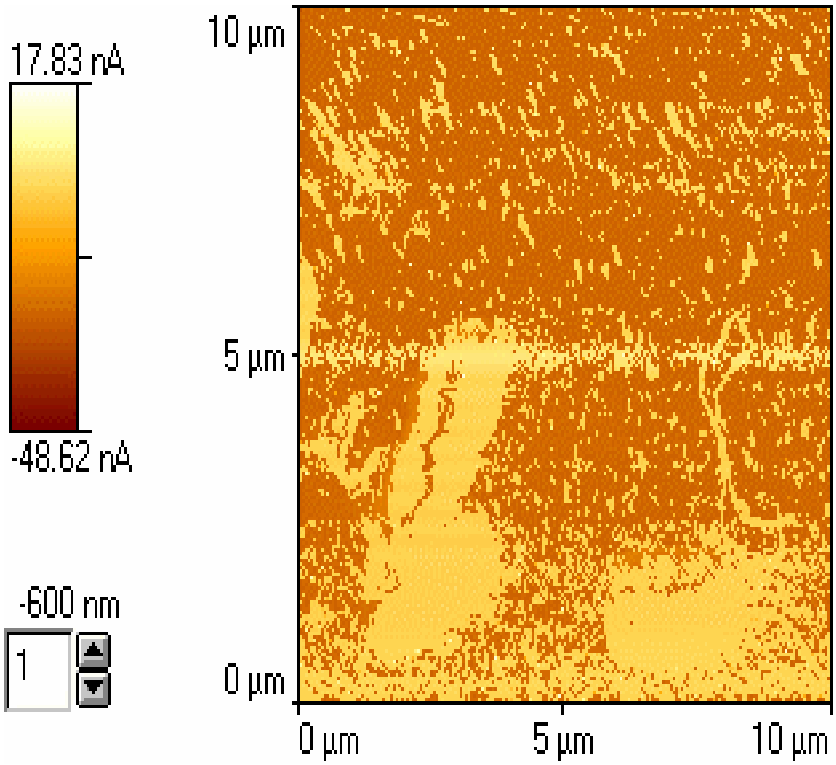

Figure 4.14 Force volume image of MG16SS E.coli cells treated with Ampicillin

4.5. ESEM imaging of E.coli cells

As described in the Materials and Methods Chapter, Environmental Scanning Electron Microscopy (ESEM) is an alternative Electron Microscopy technique, which allows imaging of insulating materials in their natural hydrated state without the need for conductive coatings or other extensive sample preparation. This imaging method was employed in this study as a comparative technique for examining the E.coli specimens. The results from the microstructural investigations are presented in **Figures 4.15** and **4.16** for the cases of untreated and Ampicillin treated bacterial cells.

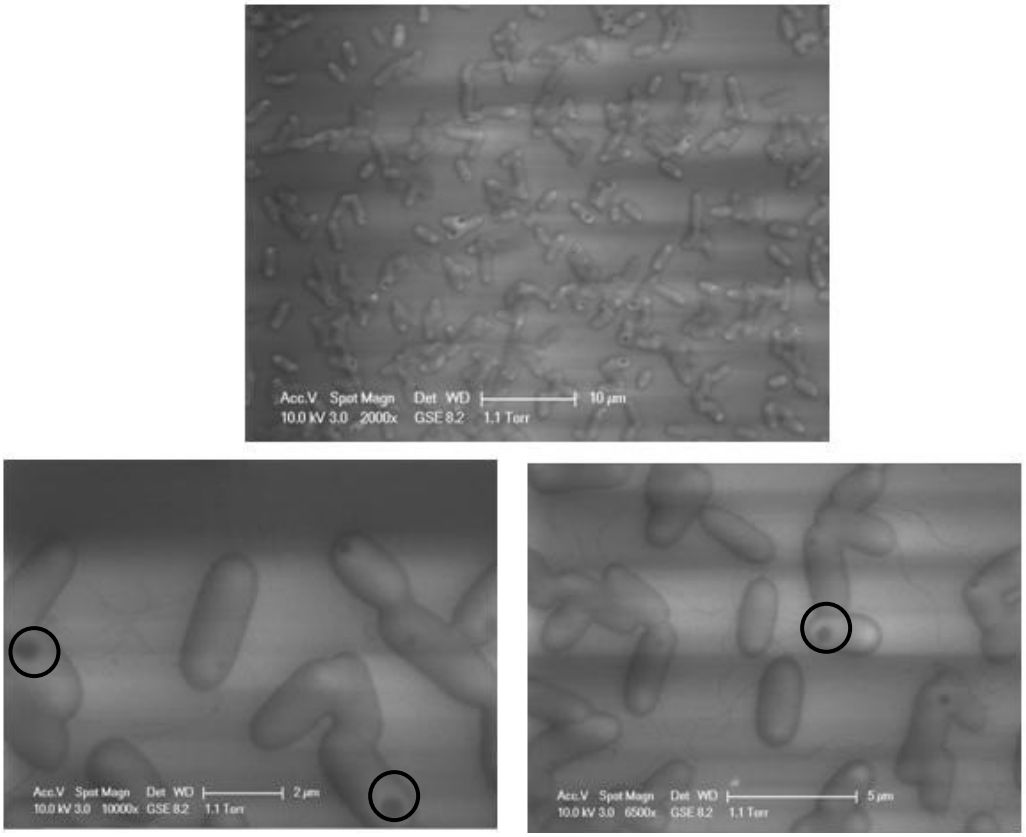

Figure 4.15 ESEM images of untreated MG16SS E.coli cells at various magnifications. Surface features present on the surfaces of the individual bacterial cells can clearly be seen. Some of these have been indicated by the circles in the images. These are comparable to the AFM images

From the electron images it is evident that the cells appear to be of the same shape and size as the ones observed using AFM. However, it was found that imaging could not be carried out for prolonged periods of time as the electron beam started to damage the surface of the cells. Also the cell topography seen in the PFM AFM images is not identifiable in the ESEM ones.

The images of the cells treated with antibiotics are also similar to those observed using AFM. However, in none of the examined specimens it was possible to observe the flagellum of the individual cells, which would suggest that AFM offers better resolution than ESEM when imaging E.coli bacterial cells, which makes it overall the more attractive imaging methodology.

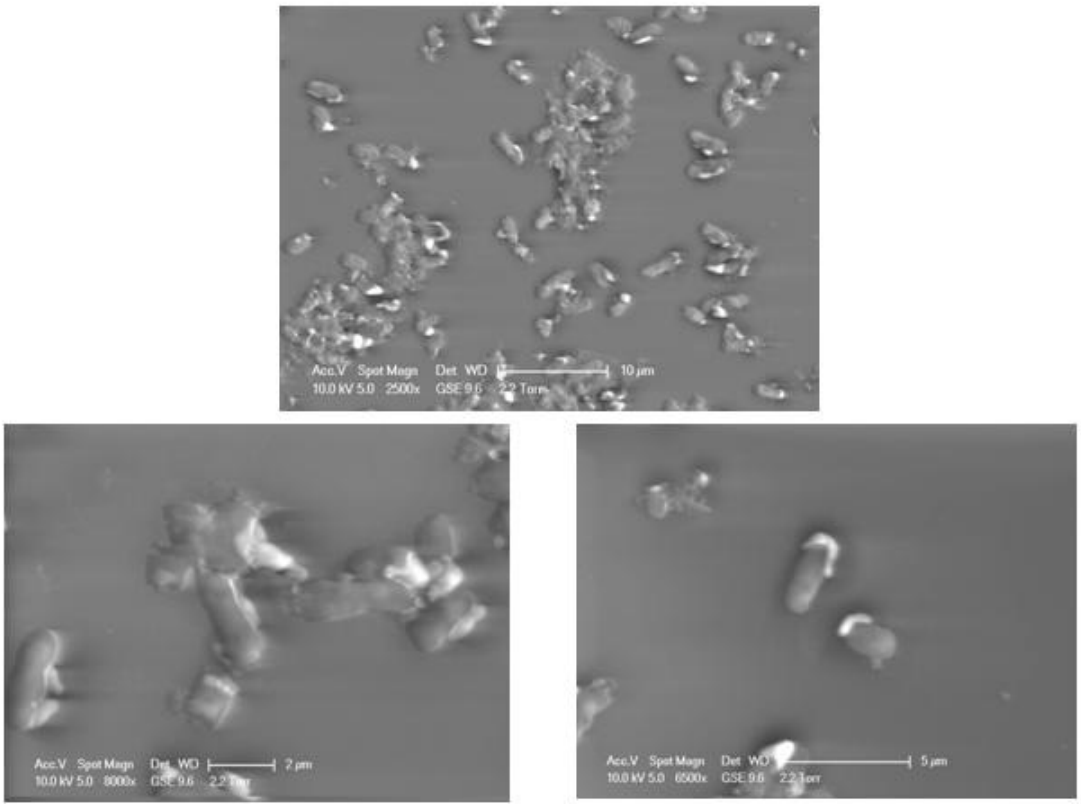

Figure 4.16 ESEM images of treated MG16SS E.coli cells at various magnifications

4.6. Summary of observations

Overall it can be said that the sample preparation and treatment technique employed in this study gives reproducible results and also offers the opportunity to generate images of excellent quality in all AFM modes used. From the images presented and discussed above it was also evident that the best contrast achieved in this study was in Pulse Force Mode, which surprisingly is rarely used for imaging of bacterial cells.

From the images of the treated cells it was evident that in the early stages of the treatment there were no obvious changes to the structure of the individual cells. However, after approximately 8 hours of treatment it is thought that changes to the cell wall have started taking place; and after 12 hours of treatment the degradation of the cell wall and membrane had progressed to a very advanced stage so that it became difficult to distinguish individual cells. The results presented and discussed here are also thought to confirm the recently proposed mechanism by Yang *et al* 2006 for the effect of □-lactams for species of the studied type. These are also supported by the even more recent study carried by Perry *et al* 2009 which was discussed earlier in the chapter.

These observations were re-confirmed by the PFM images obtained with heated nano probes for the first time from the studied biological system. It was also demonstrated that imaging at increased probe temperatures results in higher quality images. Based on the results, it is strongly believed that PFM imaging at elevated probe temperatures together with its ability to provide data for the mechanical properties of

the studied biological system is indeed a unique methodology which would undoubtedly provide further insight to understanding the phenomenon of adhering of E.coli to surfaces, for example hospital equipment as also recently suggested by Zalas-Wiecek *et al* 2009 and Amalaradjou *et al* 2010.

Finally, it was shown that Atomic Force Microscopy offers greater potential and flexibility for cell examination compared to an alternative Electron Microscopy technique.

5. The study of physical interactions between model systems and E.coli cells

5.1. Introduction

The purpose of this chapter is to present and discuss the results from the Force Distance measurements carried out during this research. The principal aim of these experiments was to, on the one hand, evaluate the use of novel heated probes in the study of their interactions with pharmaceutical and biological systems and on the other to demonstrate whether these can be used to detect any structural and/or morphological changes taking place during the process of localised heating. Firstly, the Force Distance Curves (FDC) obtained for what is here defined as a model system, Paracetamol tablets, will be presented. This will be followed by a presentation of the results for the main biological system used in this study, E.coli bacterial cells. The effects of use of different types of heated probes (Wollaston wire and novel nano probes) are also considered.

5.2. The study of physical interactions on model system: Paracetamol tablets

Paracetamol tablets were used as a model pharmaceutical system in order to develop a suitable methodology for obtaining force distance curves and also to compare the results with data already available in the literature. This was considered in order to ensure that the methodology used is robust enough and delivers consistent and reproducible data.

The isothermal FDC measurements were performed, as mentioned above, using a Wollaston wire & novel nano probes and the ‘‘Point Force Spectroscopy’’ menu of the controller program of a Caliber Atomic Force Microscope. The theoretical background of this technique is described in previous chapters (*see Chapters 2 & 3*).

The FDC experiment was started with the probe in contact with the sample surface. The probe was then withdrawn a few nm away from the surface and the recording of a FDC was started. The probe commenced the approach to the sample at a predetermined speed. When the probe was 0 nm into the sample, the approach cycle stopped and the probe retraction started. The probe was retracted 5000 nm away from the surface, recording stopped, and the probe brought back into force feedback. Because of the limitation of the current version of the SPM Lab software which does not allow the temperature of the tip to be controlled during a force distance curve measurement nanoTA^{TM} was used in the study. For the temperature measurements a Wollaston wire probe (Veeco) with an extension cord was mounted on the Caliber and calibrated for temperature using three different calibration samples with known melting points/temperatures: PCL, PE and PET. The data are expressed as equivalent current rather than directly as force, because it is not possible at present to derive reliable values for spring constants for these probes with any confidence (Harding *et al.*, 2007)**.** This is because such correlations require an accurate measure of probe dimensions (length, thickness, height) which is extremely difficult to obtain with the irregularly shaped Wollaston probes. However, as our objective was to provide profiles rather than quantitative mechanical data, this disadvantage was considered to be acceptable in the present context. The tip was brought into contact with the surface

at room temperature and the FDC measurement was initiated. As soon as the probe was retracted off the surface, the temperature of the probe was increased, using the temperature controller in nanoTA^{TM} software. This was done to prevent the hot tip damaging the material's surface before the start of experiment. After the FDC measurement, when the probe was at a maximum distance away from the surface and immediately before returning to force feedback, the heating of the probe was switched off, cooling the probe quickly to room temperature. This step was necessary because the hot probe could otherwise melt through the material in an attempt to achieve the force feedback. After each FDC run, the probe was retracted away from the sample and cleaned by heating the tip up to 600^0C in order to burn off any contaminants. This step is essential for this type of experiment because even thin layers of contaminants could seriously affect the measurement of pull-off forces.

The above described experimental set up as mentioned earlier was firstly used in the study of Paracetamol tablets, here used a model pharmaceutical system.

5.2.1. FDC on Paracetamol with Wollaston wire tip

A series of force distance profiles obtained from Paracetamol tablets, prepared using the methodology described in the Materials and Methods Chapter, are shown in **Figure 5.1**, where each individual case that is representative of different temperatures is labelled accordingly. The pull-off force was measured with the tip temperature set at values from 15 to 140^0C, with 5^0C increments. From the results presented in the graphs below it is evident that the shapes of the Force Distances Curves (FDC)

change significantly with the increase in probe temperature, especially in the vicinity of the transition temperature of the studied pharmaceutical system. At low temperatures, in the region of 15 to 30^0C, the approach and retraction components of the curve follow the same path and the adhesion hysteresis recorded is negligible. However, from the follow on graphs it is clearly evident that by increasing the probe temperature, both curves change their appearance. The slope of the approaching part of the FDC curve is related to the local mechanical properties, surface forces, and the shape of the tip and the sample (Kajiyama *et al.*, 1996). At elevated temperatures in the region of 140^0C the slope of the approach curve begins to change its shape. It can be clearly seen that the adhesion hysteresis of the retraction part of the curve increases dramatically. It was found that this change was reproducible and was observed in all experiments carried our using the Paracetamol tablets. As this was not believed to be a calibration issue, as the tips were fully calibrated using standard procedures, it is therefore not unreasonable to suggest that what is being observed is pre-melting. This process represents loosening of molecular structure at temperatures below the thermodynamic melting point of the sample.

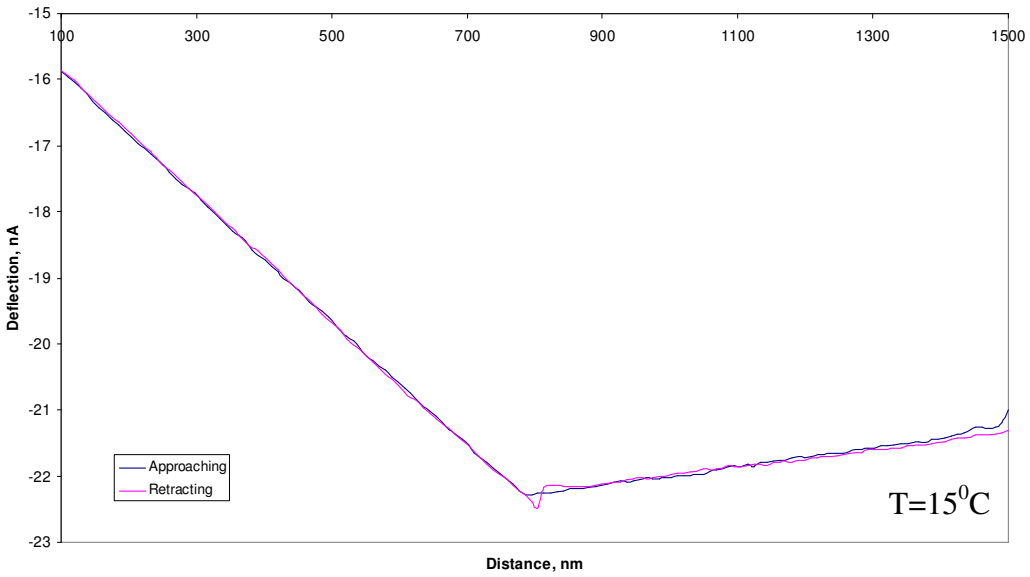
-15
-16
-17
-18
-19
-20
-21
-22
-23
100
300
500
700
900
1100
1300
1500
Deflection, nA
Distance, nm
Approaching
Retracting
T=15^{0}C

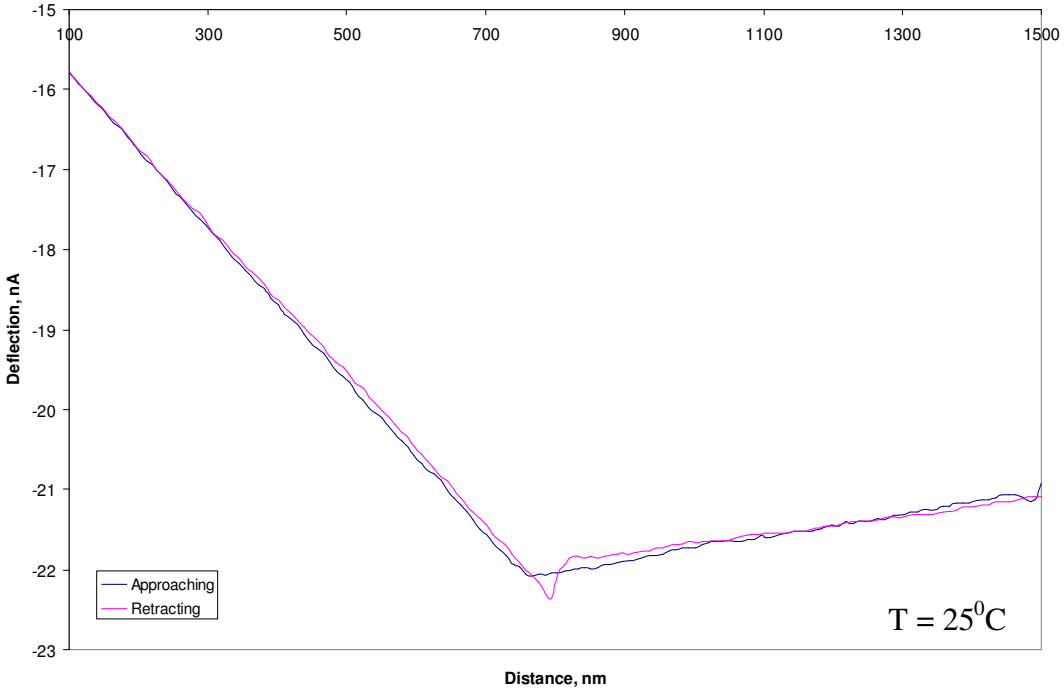
-15
-16
-17
-18
-19
-20
-21
-22
-23
100
300
500
700
900
1100
1300
1500
Deflection, nA
Distance, nm
Approaching
Retracting
T = 25^{0}C

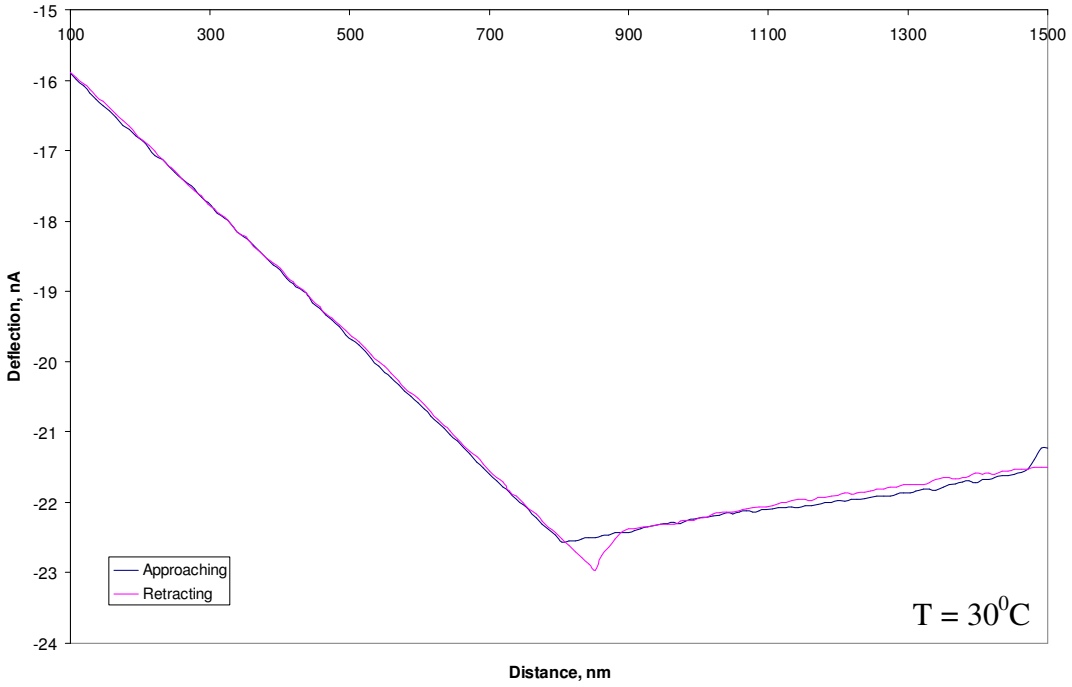
-15
-16
-17
-18
-19
-20
-21
-22
-23
-24
100
300
500
700
900
1100
1300
1500
Deflection, nA
Distance, nm
Approaching
Retracting
T = 30^{0}C

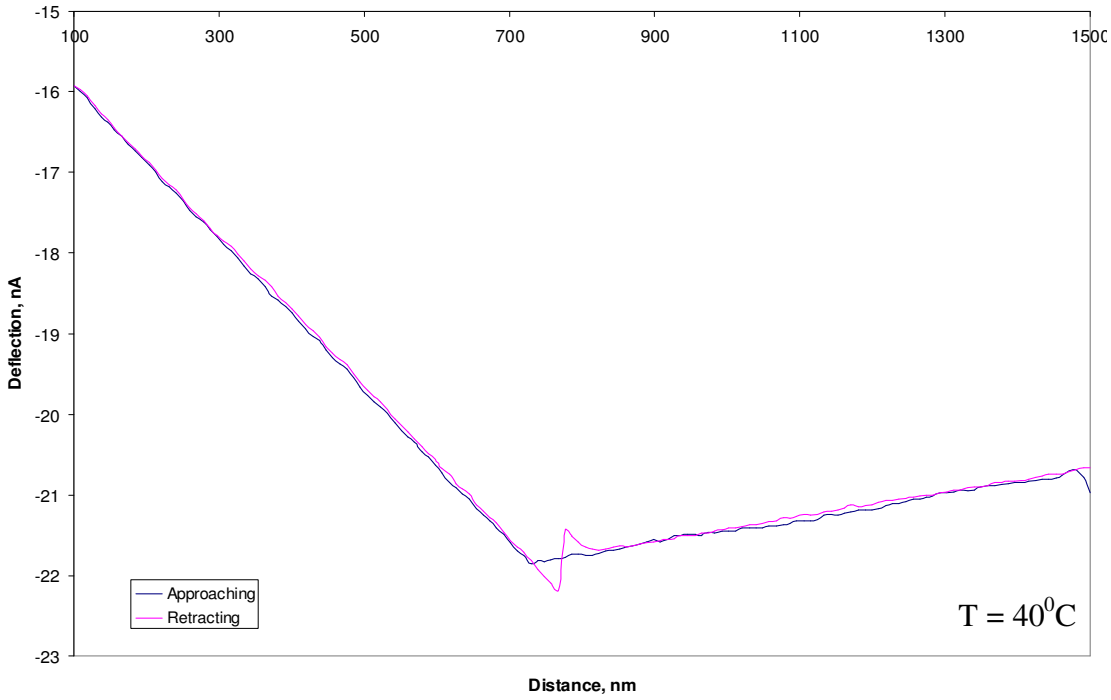
-15
-16
-17
-18
-19
-20
-21
-22
-23
100
300
500
700
900
1100
1300
Deflection, nA
Distance, nm
Approaching
Retracting
T = 40^{0}C

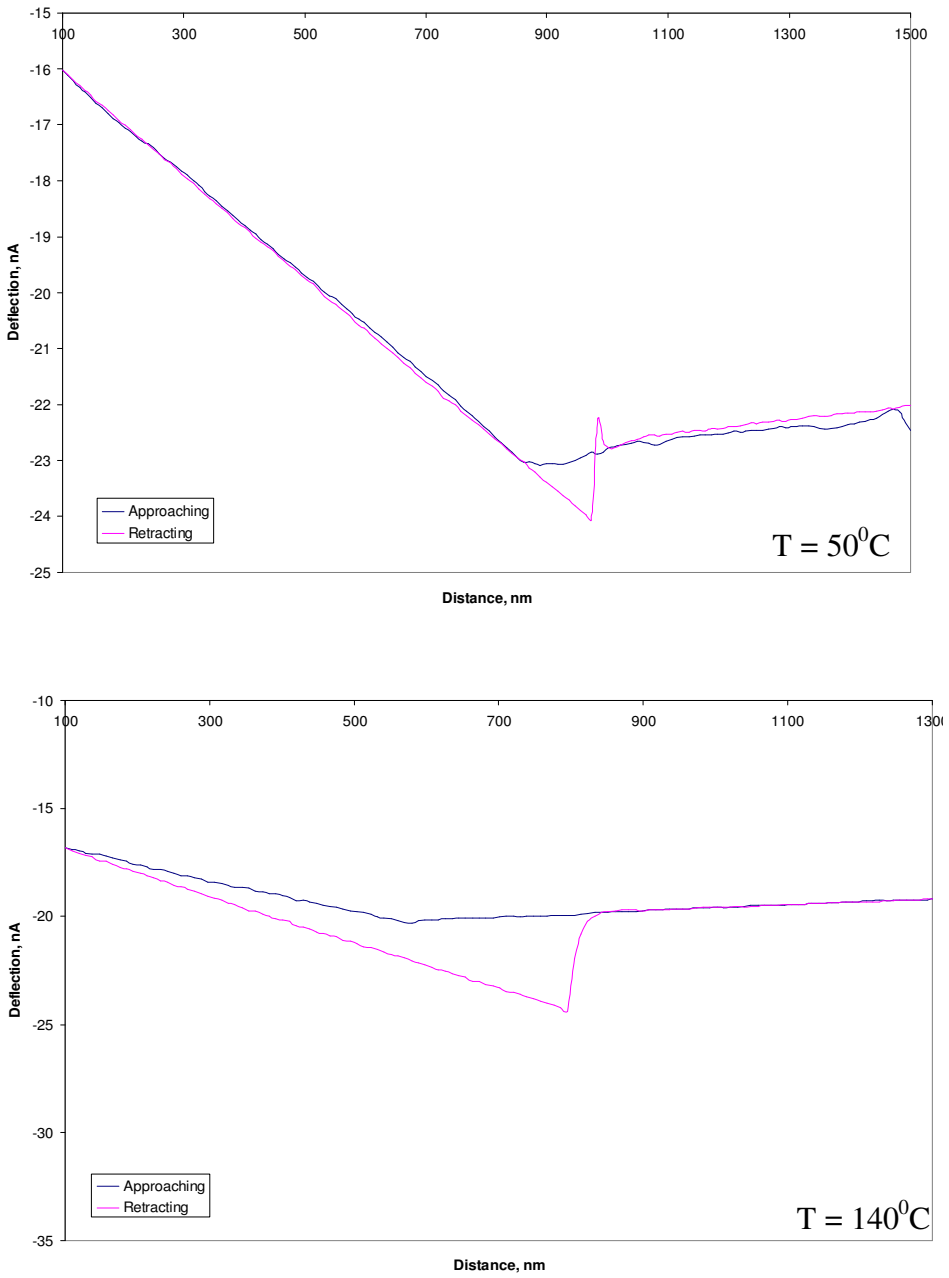

Figure 5.1 FDC on Paracetamol with Wollaston wire tip at different temperatures. It can be clearly seen that at low temperatures the approach and retraction components of the curves appear to follow the same pattern and the adhesion hysteresis is negligible, whereas at higher temperatures the slope of the approach begins to change its shape and adhesion increases dramatically

The results obtained from these experiments are comparable to those published earlier by Harding *et al* (2007). In a similar study the authors examined the effects of probe temperature on the pull off force ad shape of the force distance curve obtained from Paracetamol tablets. The authors observed a similar increase in adhesion hysteresis. Furthermore, it was shown that the increase in adhesion hysteresis peaked at temperatures in the region of just above 160^0C; whereas at higher temperatures the values of adhesion hysteresis showed a decrease. Their proposed explanation for the observed behaviour was that at the beginning of melting process there is only a very thin layer of molten crystallites at the surface. Hence, it can be expected that the thickness of the molten mass will increase with the increase in tip temperature, which would result in the increase in pull-off forces. As the same behaviour was observed in this study, it is not unreasonable to assume that this indeed is the case. For the higher temperatures, which are not covered in this study, Harding and co-authors suggested that the viscosity of the molten material decreases, thereby reducing the pull-off force. The decrease in viscosity results in a decreased ability to hold the cantilever in a negative deflection (i.e. towards the sample) for extended periods of time. Instead, the cantilever springs back to the neutral position.

5.2.2. FDC on Paracetamol with nano tip

The methodology developed and utilised with the conventional Wollaston wire thermal probes was also tested on the same model system using nano probes. The results from the experiments carried out with the novel probes at different temperatures are presented in **Figure 5.2**. From the graphs presented below, it is

clearly seen that the trends observed are very similar to those obtained with the Wollaston wire probe. Again, for the force distance profiles at low temperatures it is evident that the approach and retraction components of the curve follow the same path and adhesion hysteresis is negligible, while at elevated temperatures in the region of 140^0C the adhesion hysteresis of the retraction part of the curve increases drastically, which again is suggestive of pre-melting, i.e. loosening of the molecular structure at temperatures just below the thermodynamic melting point of the studied material system.

Finally, it is important to note that the pull-off forces measured from the experiments carried out with nano probes were much lower, compared to those obtained from the experiments performed with Wollaston wire probes. This is most probably due to the fact the interaction volume in the case of the nano probes is much smaller compared to the one for the case of the Wollaston wire probes.

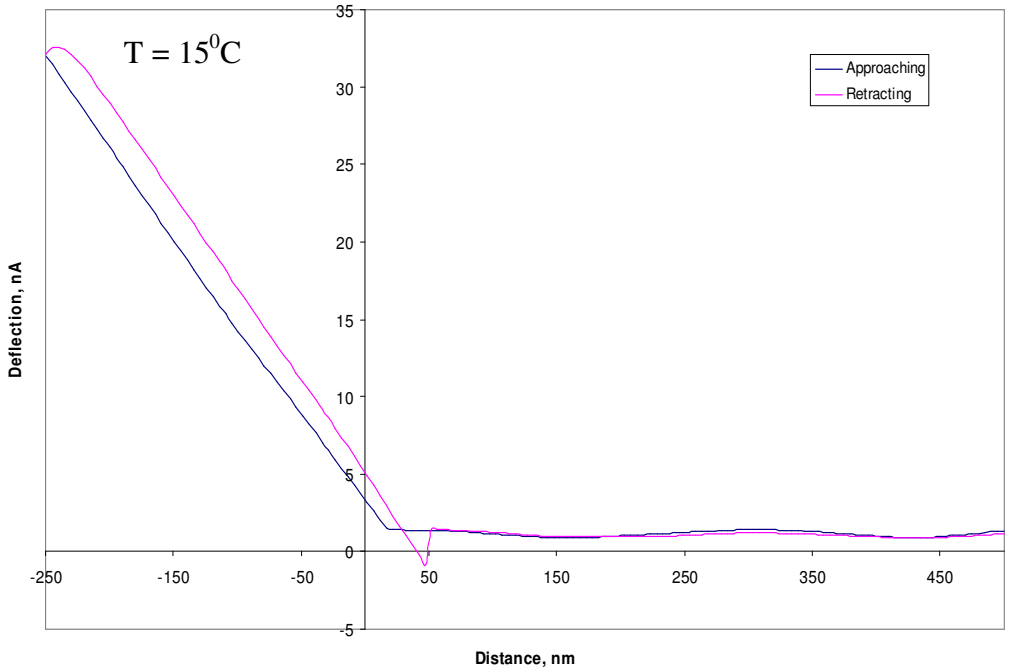
T = 15^{0}C
Approaching
Retracting
Deflection, nA
Distance, nm
35
30
25
20
15
10
5
0
-5
-250
-150
-50
50
150
250
350
450

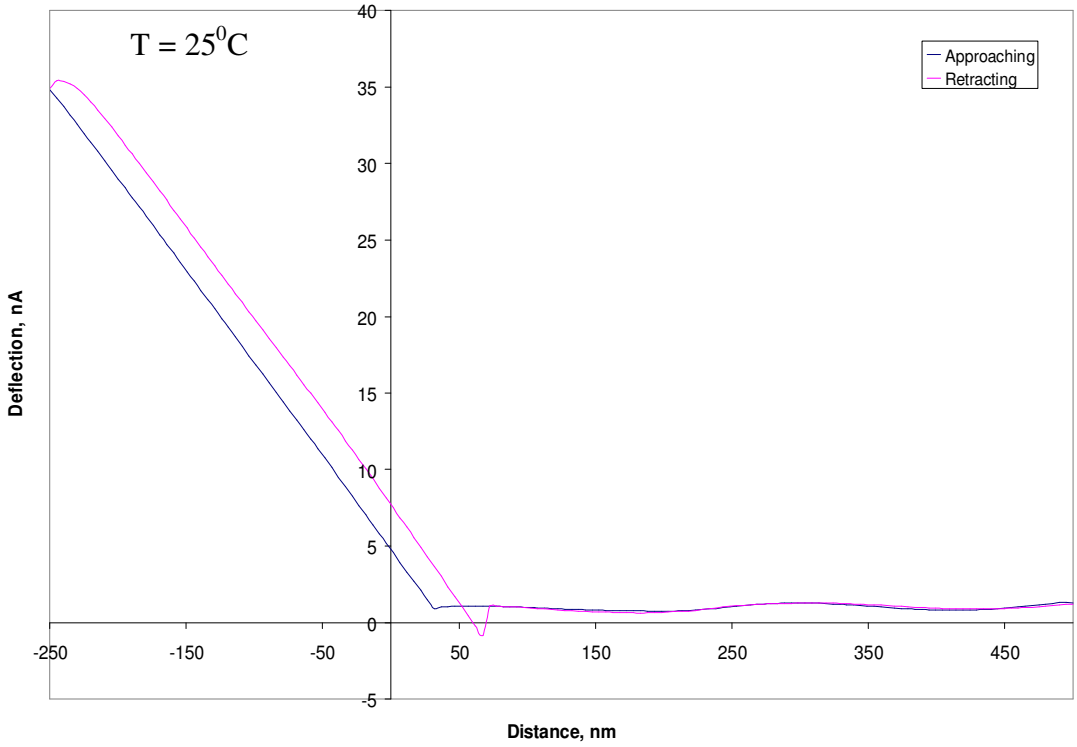
T = 25^{0}C
Approaching
Retracting
Deflection, nA
Distance, nm
40
35
30
25
20
15
10
5
0
-5
-250
-150
-50
50
150
250
350
450

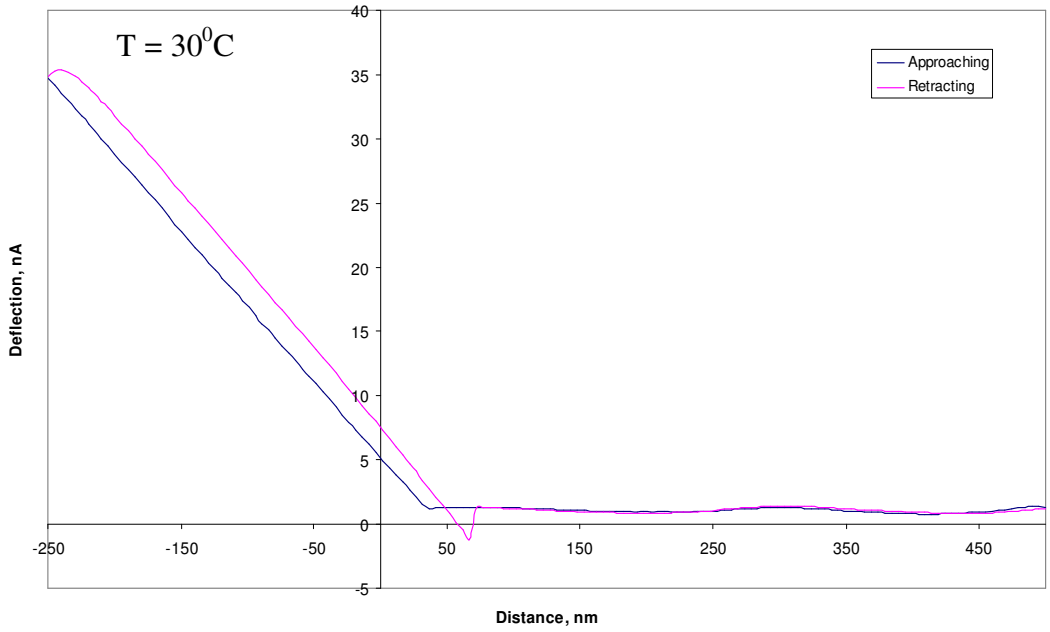
T = 30^{0}C
Approaching
Retracting
Deflection, nA
Distance, nm
40
35
30
25
20
15
10
5
0
-5
-250
-150
-50
50
150
250
350
450

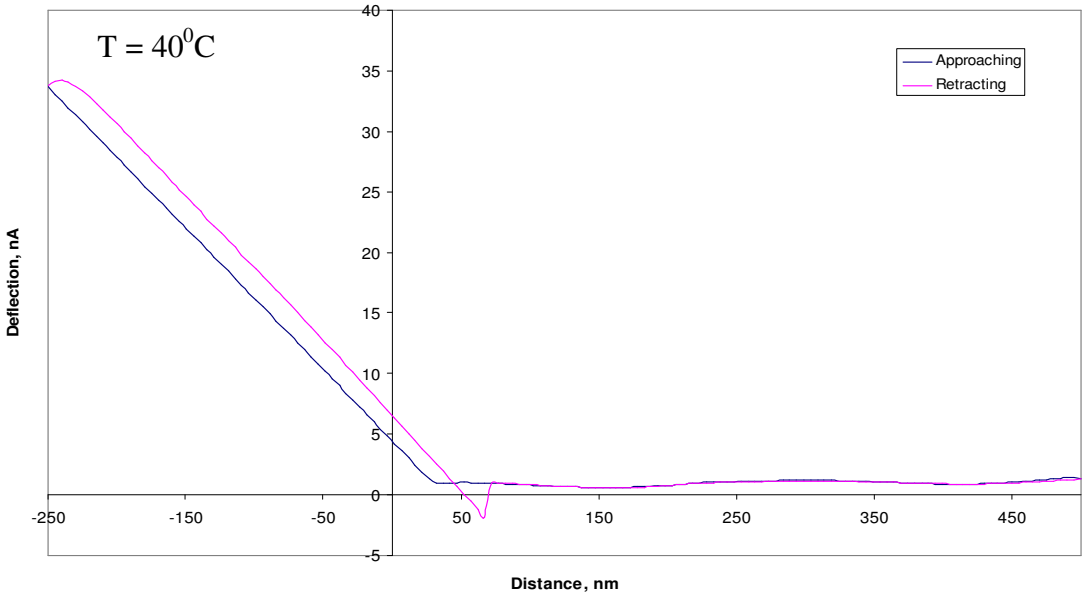
T = 40^{0}C
Approaching
Retracting
Deflection, nA
Distance, nm
40
35
30
25
20
15
10
5
0
-5
-250
-150
-50
50
150
250
350
450

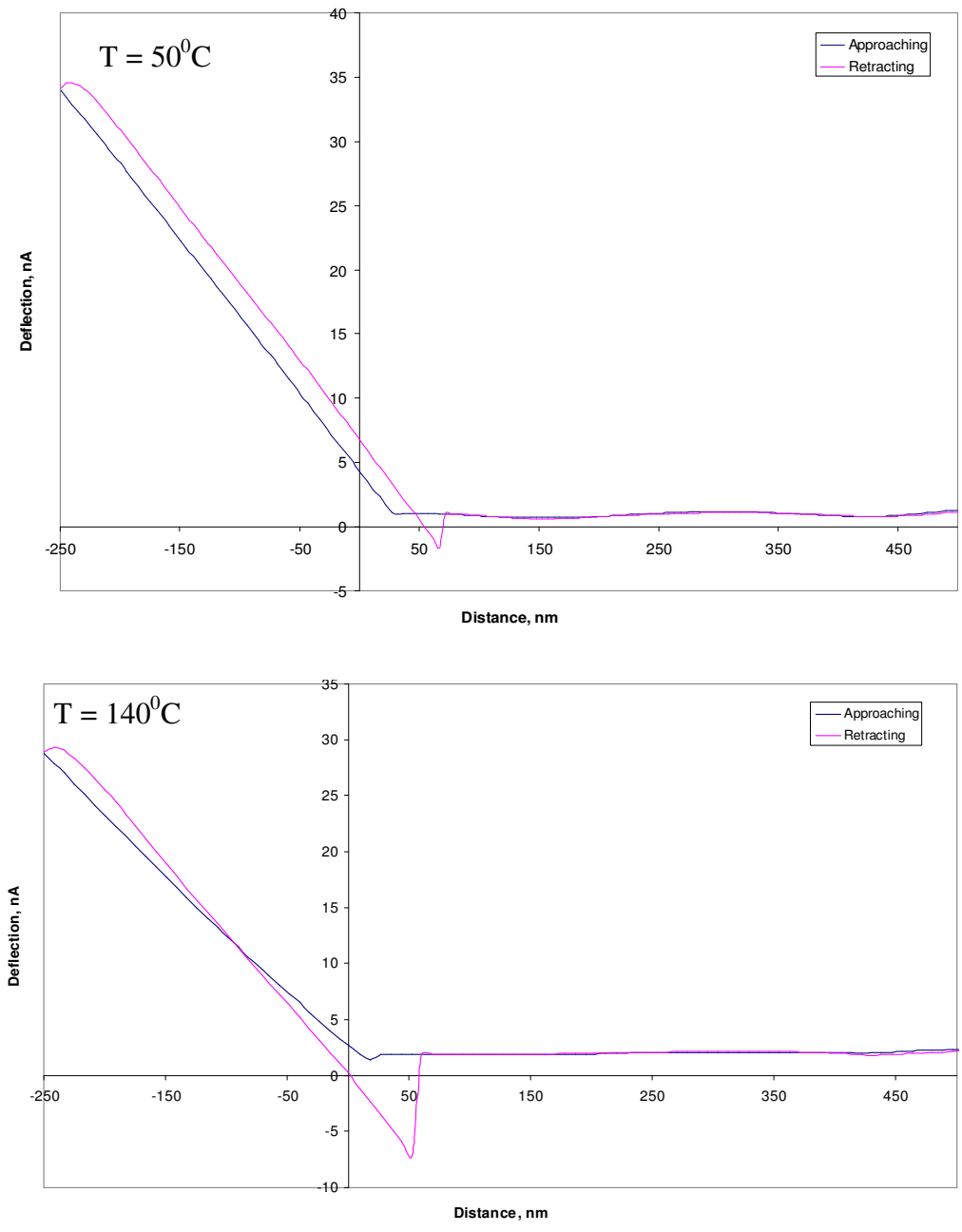

Figure 5.2 FDC on Paracetamol with nano tip at different temperatures. Similarly to the case of the Wollaston wire probe it is seen that at low temperatures the approach and retraction components of the curves appear to follow the same pattern ad the adhesion hysteresis is negligible, whereas at higher temperatures the slope of the approach begins to change its shape and adhesion increases dramatically

In summary, it can be said that the methodology developed and used in the study of the model pharmaceutical system, Paracetamol tablets, resulted in obtaining consistent and reproducible results that are comparable to those already available in the literature. Furthermore, here it is important to note that the data for the adhesive properties of Paracetamol was obtained for the first time using nano tips. The results also clearly demonstrate that the precision and accuracy of the technique is dependent on the type of AFM probe used and its size and geometry. This can be clearly seen by comparing the results obtained at 140^0C with Wollaston wire and nano probes (*see Figures 5.1 and 5.2*).

Here it is important to mention that the origins of the "pull-in" effect were investigated utilising temperature controlled pull-off force measurements, which were performed by measuring force-distance curves with a heated nano tip. The novel approach used in this study differs from the one reported earlier by Marti *et al* (1999), who used conventional AFM tips in combination with a temperature stage which required heating of the whole specimen.

The approach used in this study of measuring pull-off forces at elevated temperature using the probe as a highly localised source of heat is believed to offer a number of advantages compared with the conventional method, where a temperature stage is used. Firstly, temperature calibration is quick and easy, and the risk of thermal decomposition of the whole sample is eliminated (*nano-TA^{TM} User's Manual, 2006*). Furthermore, the probe can be easily decontaminated after each experiment simply by heating it to 300^0C. One of the only encountered drawbacks observed in this study

with the SPM Lab software was the unavailability of the temperature control option. This was overcome by using the new Anasys Instruments software and hardware configuration which in actual fact was recently made commercially available. Finally, with the advent of high resolution thermal probes, this method should be comparable in quality to conventional FDC measurements. With these improvements, it is reasonable to expect that this novel method will find application not just in pharmaceutical materials science, but also in other scientific fields, one of which is explored further in the section below.

5.2.3. Force distance curves of E.coli cells

As seen from the results above the methodology developed and applied in the study of interactions of pharmaceutical materials with various AFM tips at different temperatures provided consistent and reproducible results. This led to the conclusion that the same can be used to study the mechanical response of the chosen biological system, E.coli cells.

The E.coli cells were prepared using the technique described in the Materials and Methods chapter. The Force Distance measurements were performed using conventional Pulse Force Mode tips, Wollaston wire & nano-probes. Here it is important to note that it has been shown (Wright & Armstorng, 2006) that when working with biological samples, the number of force measurements or indentation experiments should be monitored, as the surface can deteriorate and hence become unrepresentative. The authors also demonstrated that with indentation experiments

used to measure the mechanical properties of microbial cells, there is a clear change in the measurements after repeated force measurements, indicating damage of the surface. The number of force measurements that can be carried out without damaging the surface was found to be dependent on the type of microbial sample. However, as mentioned above this number can vary significantly depending on the system studied and has been reported to reach up to 20 (Bowen & Wright, 2000).

The results from the Force distance measurements are presented in the Figures below. Firstly, the data obtained by using conventional Pulse Force Mode tips will be considered. This will be followed by a presentation of the results obtained by using Wollaston wire probes. Finally, the force-distance measurements obtained from the experiments carried out using nano-probes will be discussed.

5.2.3.1 Adhesion studies on E.coli cells using conventional PFM tips

A series of graphs obtained from E.coli cells using conventional Pulse Force mode AFM tips are presented in the **Figure 5.3** below. Prior to each measurement an AFM image of the cell surfaces was obtained. This was necessary to be done in order to ensure that measurements can be carried out on different cells and at different points of individual cells.

From the graphs presented in **Figure 5.3** it is evident that the adhesion forces measured over a number of cells are consistent with a maximum pull-off force in the region of 15 to 16nA. The results are comparable to those in the literature (Wright *et*

al., 2006). However, here it is important to mention that in this study the force distance curves were obtained using conventional PFM tip, whereas most of the results available in the literature were obtained using functionalized tips, i.e. ones pre-coated with cells. Therefore, it is not unreasonable to suggest that the mechanical response of bacterial surfaces can also easily be measured using conventional AFM probes for force distance studies, for example on immobilised bacterial cells fixed on different surfaces.

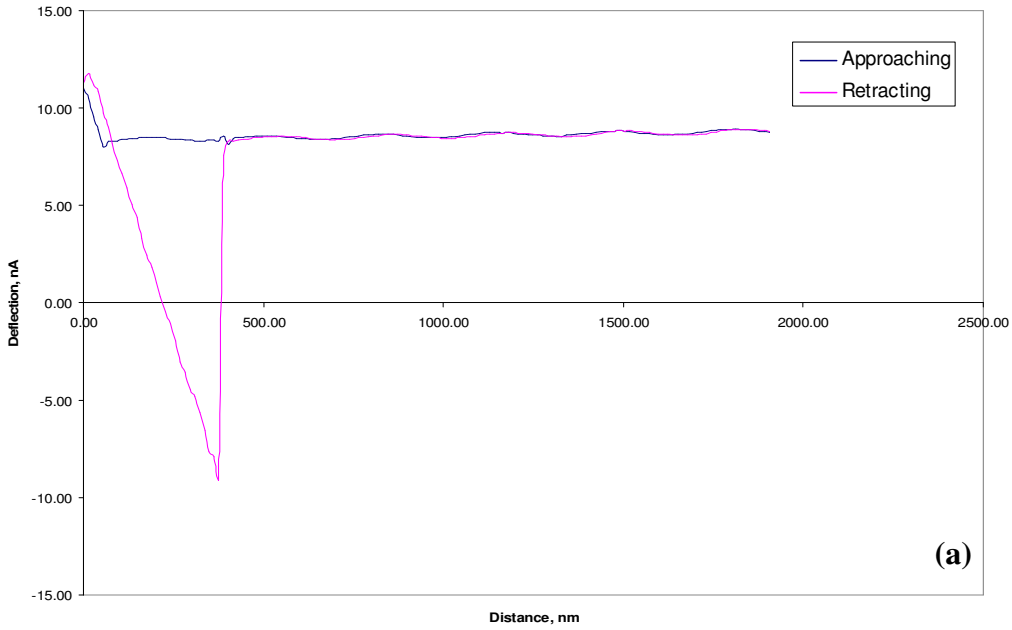

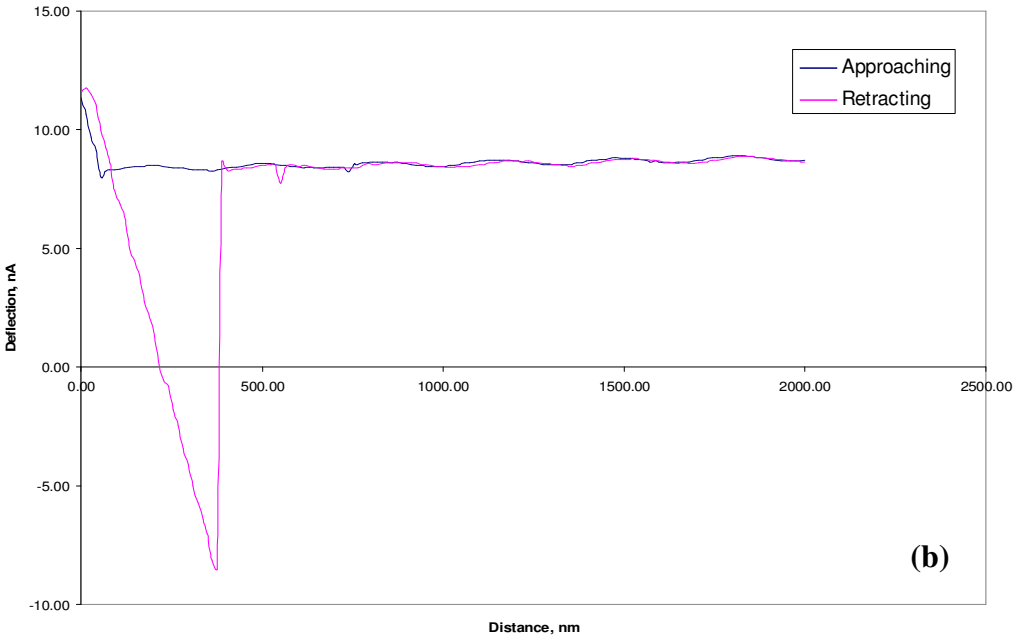
15.00
10.00
5.00
0.00
-5.00
-10.00
0.00
500.00
1000.00
1500.00
2000.00
2500.00
Deflection, nA
Distance, nm
Approaching
Retracting
(b)

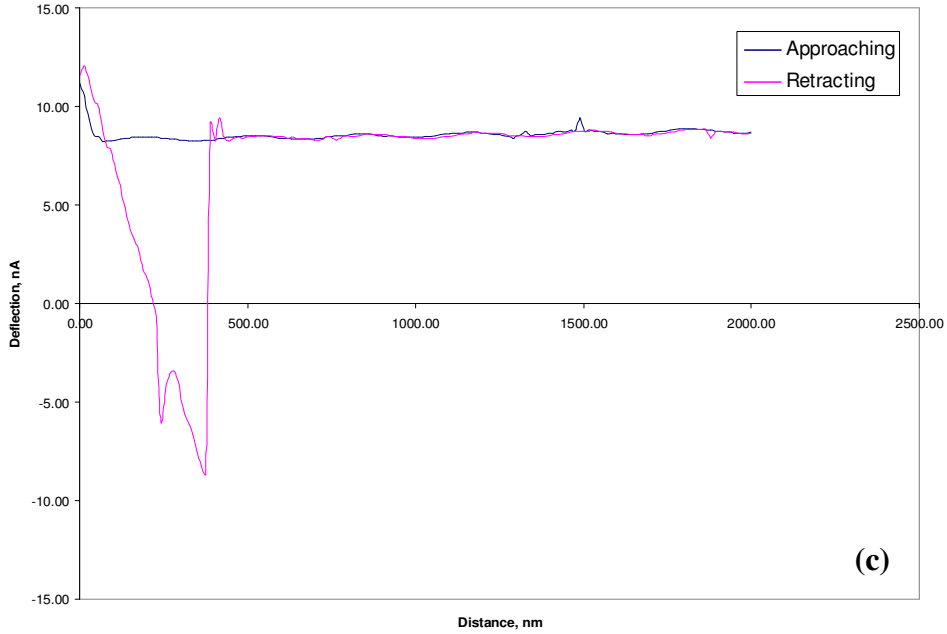
15.00
10.00
5.00
0.00
-5.00
-10.00
-15.00
0.00
500.00
1000.00
1500.00
2000.00
2500.00
Deflection, nA
Distance, nm
Approaching
Retracting
(c)

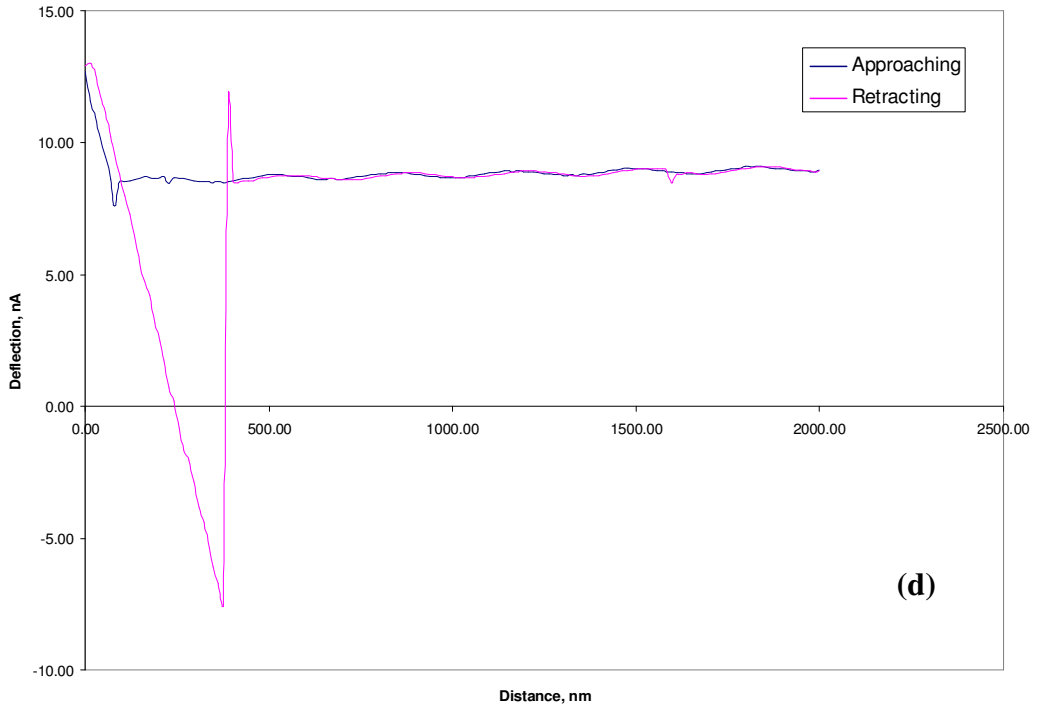

Figure 5.3 FDC curves obtained from different single MG16SS E.coli cells, using conventional PFM AFM tips. From the examples provided, it is evident that the use of conventional pulse force mode AFM tips results in the generation of reproducible force distance curves. The average maximum pull off force measured is in the region of 15 to 16nA. In one of the measurements (graph c) a double peak is observed. This is believed to be caused by an unexpected vibration and/or cell or probe contamination

From the shapes of the curves obtained in this study it is evident that there is no long distance of detachment and sequential breaking which is indicative of a sudden break in contact. Therefore, it can confidently be said that there is no indicative continued stretching of the cell, localised stretching of cell surface regions still in surface contact, stretching and rupturing of adhesive molecules and the 'peeling' of the cell away from the surface. These observations are consistent with the ones made by Ong *et al* (1999), who studied the mechanical response of E.coli coated tips with mica surfaces. In one of the measurements (*see Figure (c)*) a double peak was observed in the Force Distance curve. Similar effect was observed and reported by Dufrene *et al* (2001), **Figure 5.4**. The multiple adhesion forces were thought to be caused by the progressively increasing distances over which the measurements were taken. However, in this case this is believed to be caused by an unexpected external vibration or possible contamination of the cell or tip surface.

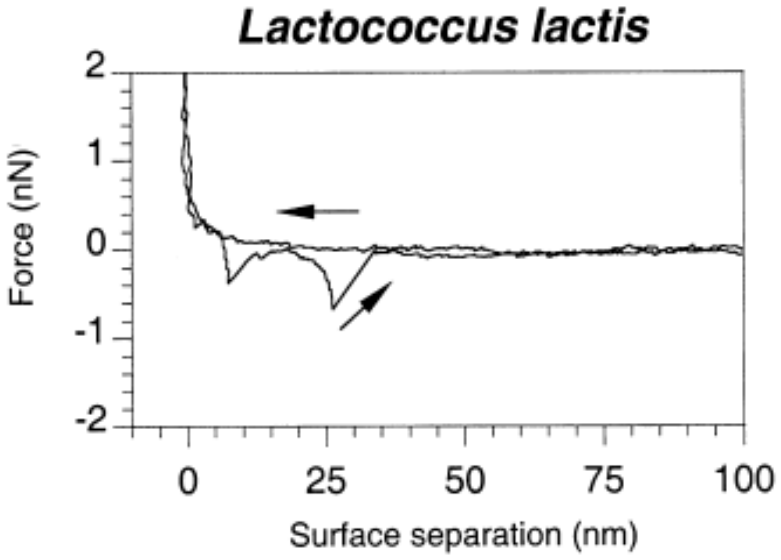

Figure 5.4 Force distance curves recorded under water between a silicon nitride probe and L. Lactus (*after Dufrene et al., 2001*)

5.2.3.2 Adhesion studies on E.coli cells using Wollaston wire & nano probes

Before the next two sets of experimental results are considered, it is important to note that the data presented and discussed here is unique, because of the fact that in this study heated probes were used for the first time in an attempt to obtain mechanical response from bacterial cells.

The experimental methodology followed was as the one described above, with the only difference being the fact that the measurements were made at temperatures in the range 20^0C to 140^0C. Again, prior to each measurement an AFM image of the cell surfaces was obtained. This, as explained before, was necessary to be done in order to ensure that measurements can be carried out on different cells and at different points of individual cells. An example of the AFM image and points of measurements is provided in **Figure 5.5**.

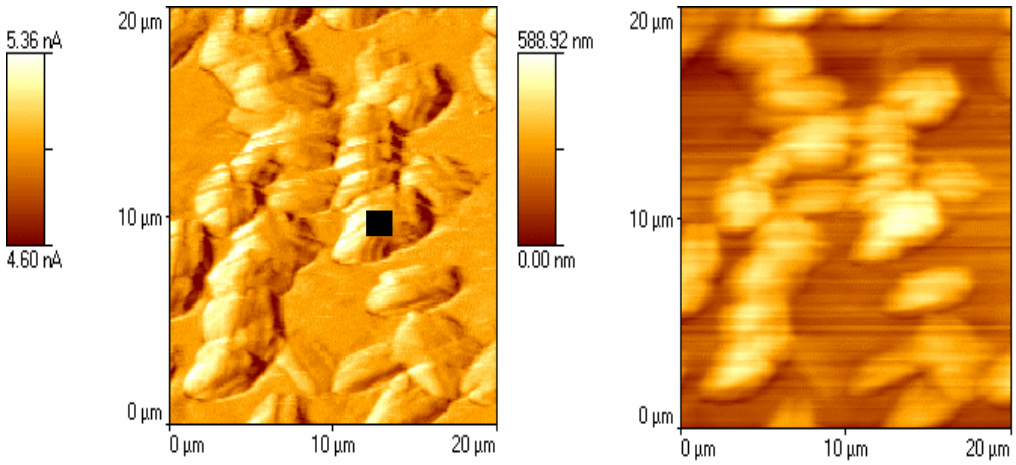

Figure 5.5 Image of MG16SS E.coli cells taken with Wollaston wire tip indicating the point corresponding to the FDC experiment (left – internal sensor, right – topography)

A series of Force Distance curves at different temperatures obtained from E.coli cells using Wollaston wire probes are presented in the graphs in **Figure 5.6** below. From the plots it is evident that the shape of the curves obtained is comparable to the ones obtained using the conventional pulse force mode (PFM) tips. However, the data appears quite noisy and difficult to interpret. As the experiments were conducted following the same methodology it is therefore plausible that the size & shape of the Wollaston wire probe are the most probable factors that have influence on the measurement. Due to the above it would not be unreasonable to suggest that during the measurements it is possible that the tip interacts with the media surrounding the individual cells.

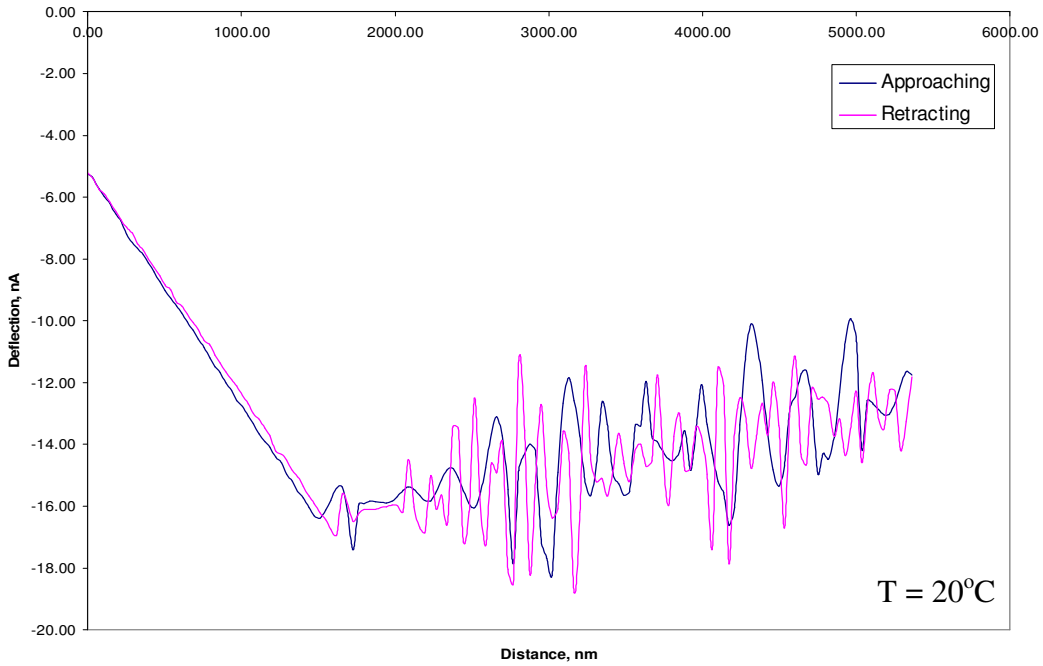

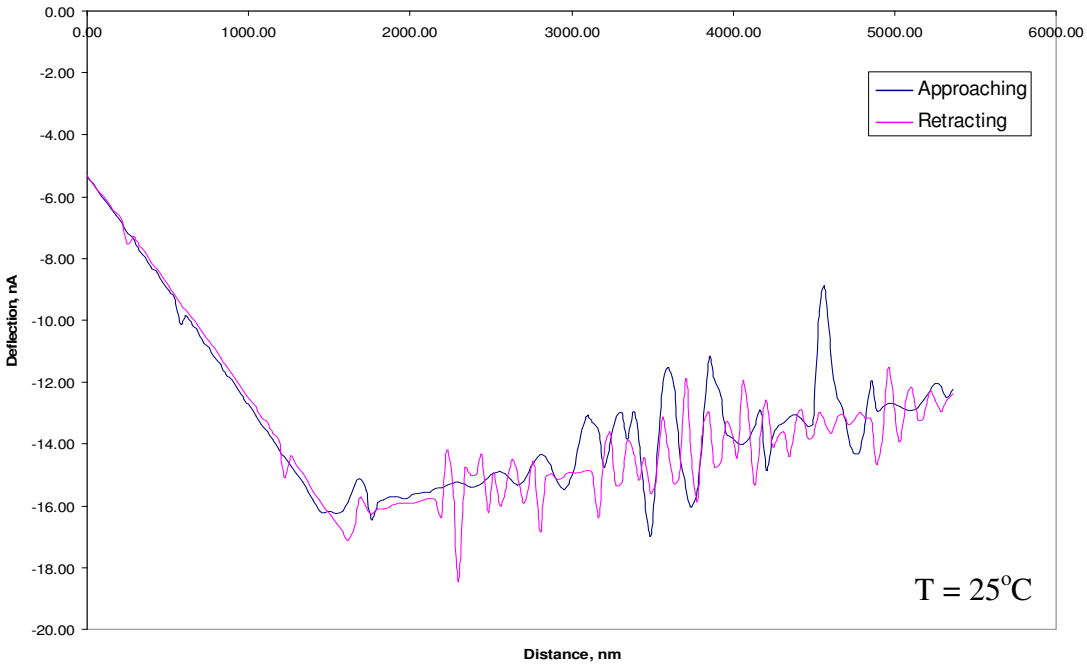
0.00
0.00
1000.00
2000.00
3000.00
4000.00
5000.00
6000.00
-2.00
-4.00
-6.00
-8.00
-10.00
-12.00
-14.00
-16.00
-18.00
-20.00
Deflection, nA
Distance, nm
Approaching
Retracting
T = 25°C

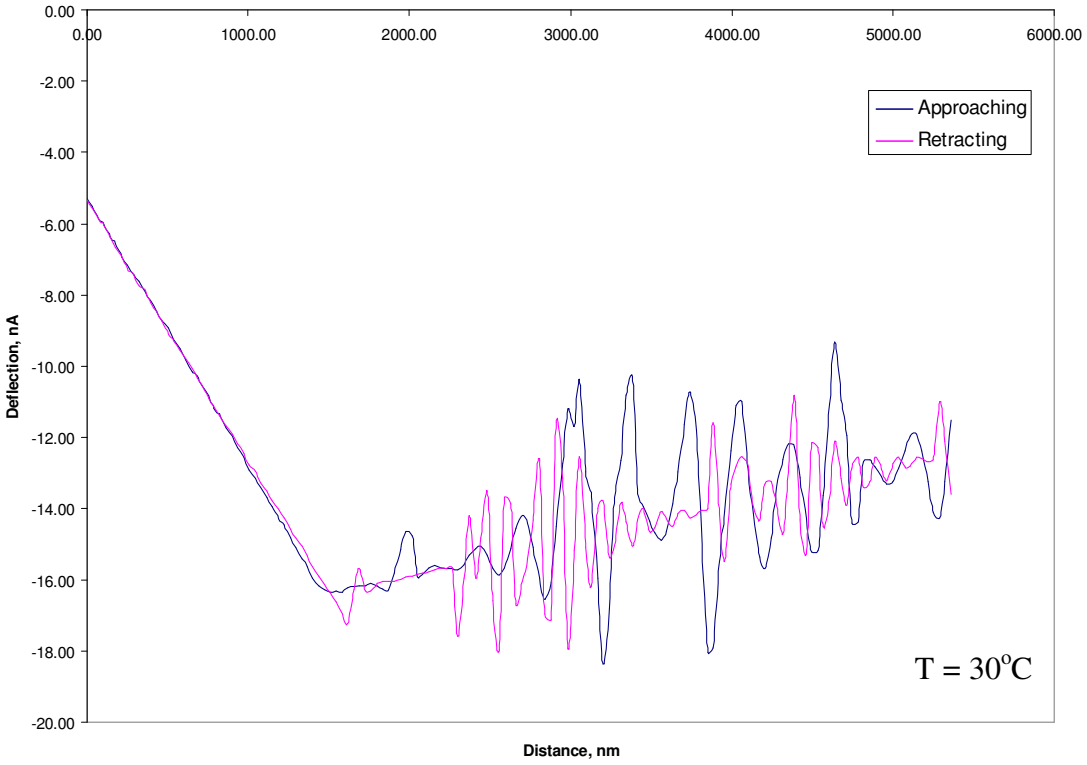
0.00
0.00
1000.00
2000.00
3000.00
4000.00
5000.00
6000.00
-2.00
-4.00
-6.00
-8.00
-10.00
-12.00
-14.00
-16.00
-18.00
-20.00
Deflection, nA
Distance, nm
Approaching
Retracting
T = 30°C

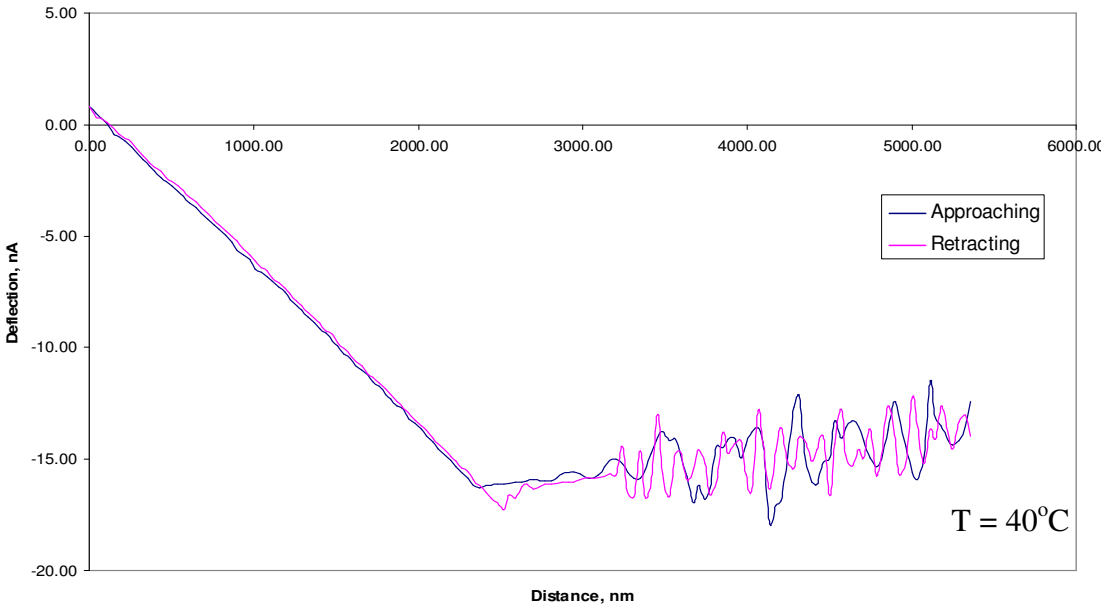
5.00
0.00
-5.00
-10.00
-15.00
-20.00
0.00
1000.00
2000.00
3000.00
4000.00
5000.00
6000.00
Deflection, nA
Distance, nm
Approaching
Retracting
T = 40°C

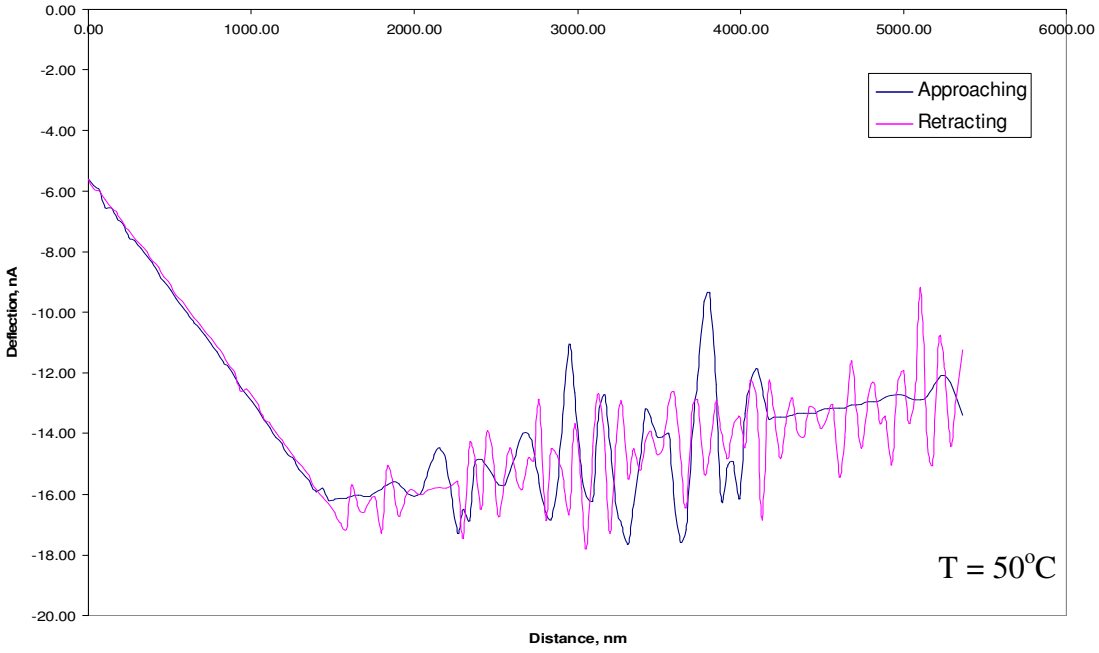
0.00
-2.00
-4.00
-6.00
-8.00
-10.00
-12.00
-14.00
-16.00
-18.00
-20.00
0.00
1000.00
2000.00
3000.00
4000.00
5000.00
6000.00
Deflection, nA
Distance, nm
Approaching
Retracting
T = 50°C

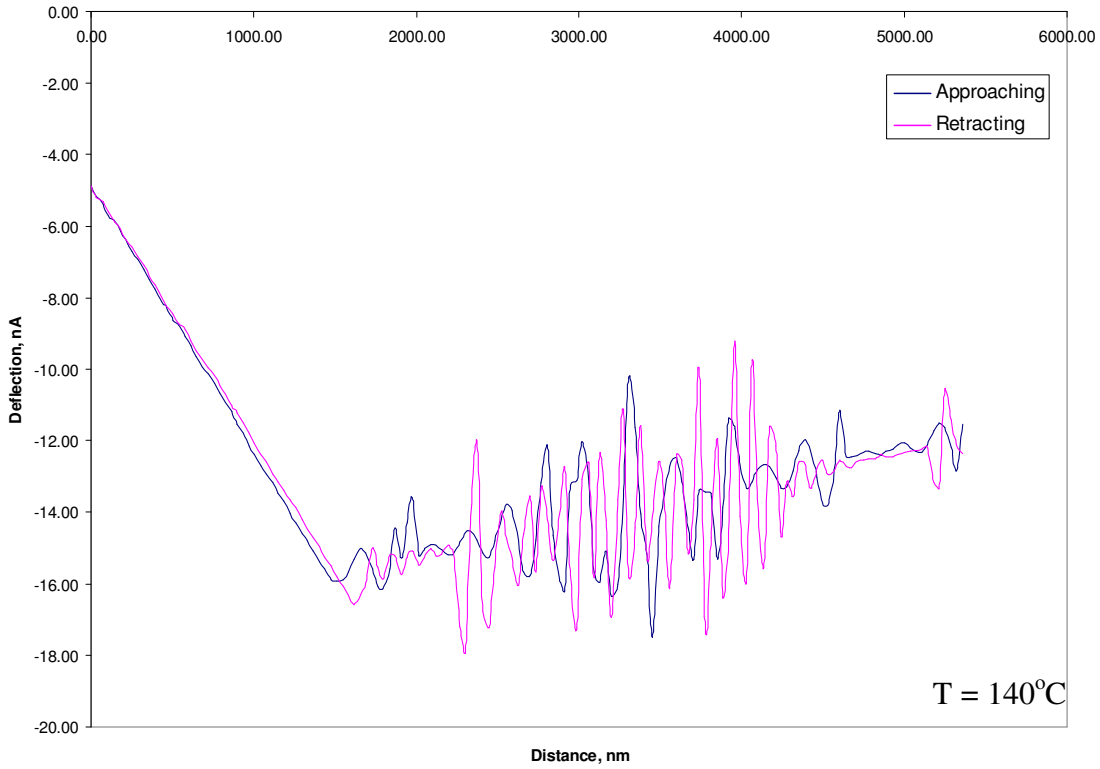

Figure 5.6 Force distance curves of MG16SS E.coli bacterial cells obtained using Wollaston wire tips at different temperatures. It is clearly seen that irrespective of the temperature of the measurements the data obtained from these experiments is quite noisy and difficult to interpret. It can be suggested that due to the shape and size of the Wollaston wire probe additional interactions with the surrounding media and possibly cellular material are taking place leading to the generation of artefacts

Based on the results presented and discussed above and the difficulty to extract any useful information from the obtained force distance profiles, the Wollaston wire probe was deemed unsuitable for use in the study of interactions of E.coli cells at elevated temperatures.

The next part of this chapter considers the results from the force distance measurements obtained from E.coli cells at different temperatures using novel nano probes. These are presented in graphical formats in **Figures 5.8** & **5.9**. An example image with points indicating the positions of the measurement is also shown in **Figure 5.7**.

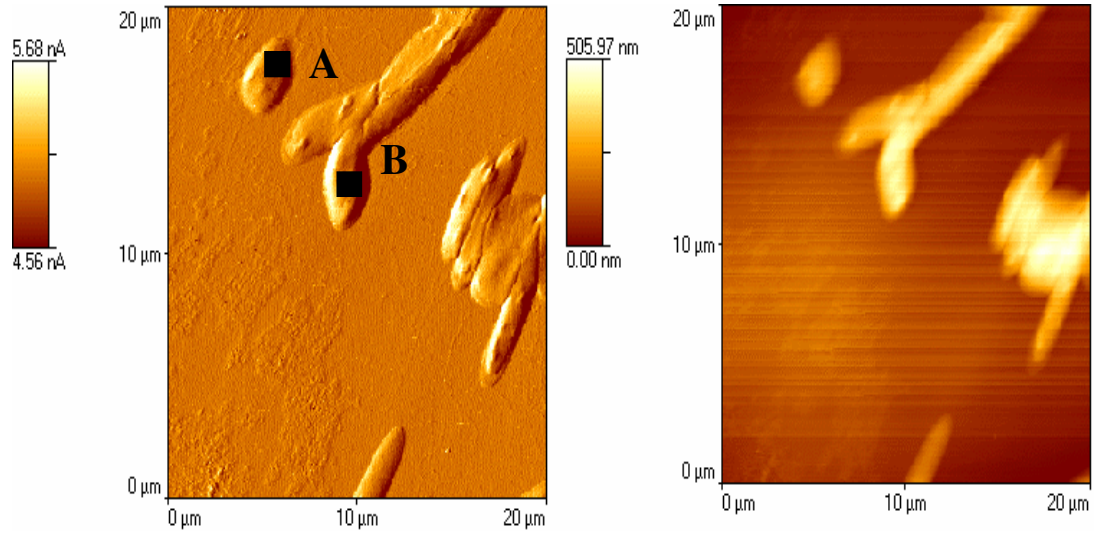

Figure 5.7 AFM images of MG16SS E.coli bacterial cells taken with nano tip with the points of the FDC experiment indicated (left – internal sensor, tight – topography)

From the results it is immediately evident that the data obtained using heated nano probes is essentially noise free, especially when compared to the one obtained using Wollaston wire probes. Despite the fact that there is some waviness and additional peaks present in the plots, which are most probably caused by external noise or specimen artefacts, it is not unreasonable to suggest that heated nano probes can be successfully used in the study of their interactions with E.coli bacterial cells.

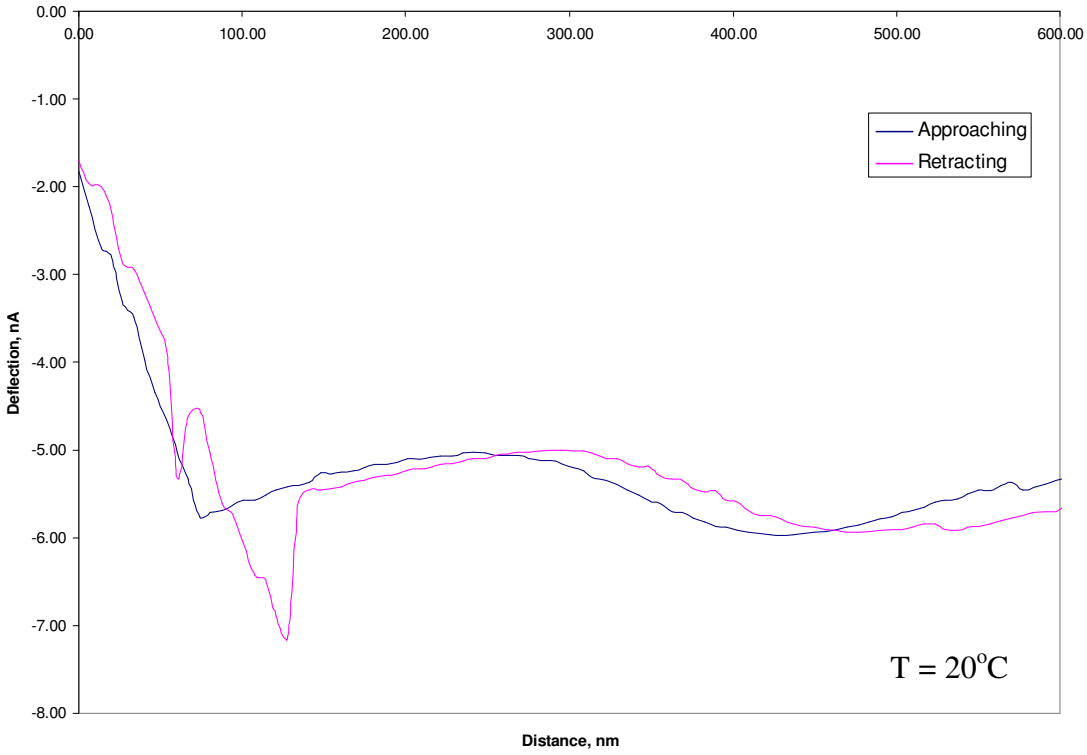

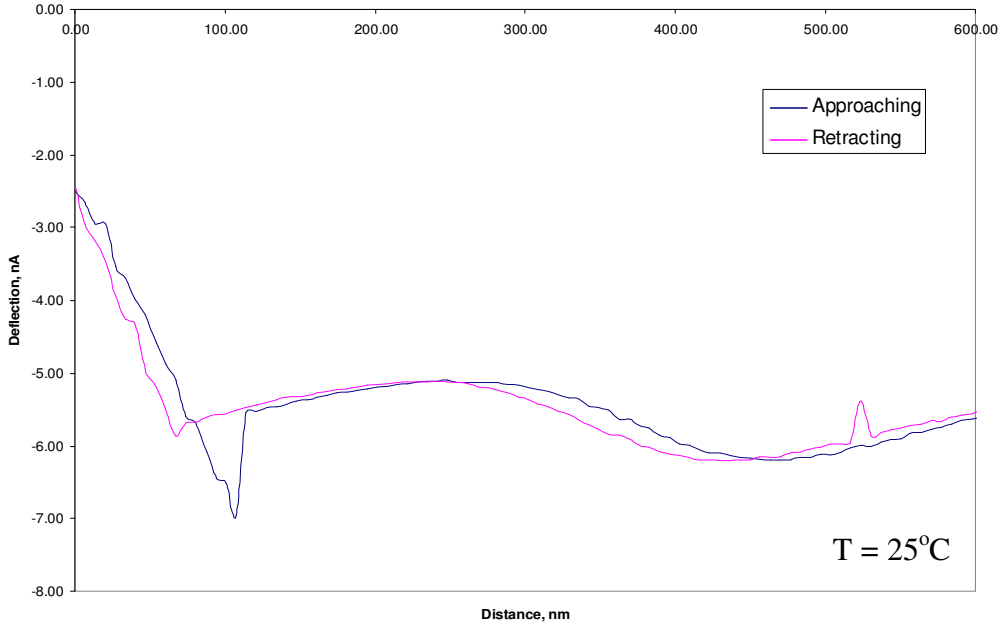
0.00
0.00
100.00
200.00
300.00
400.00
500.00
600.00
-1.00
-2.00
-3.00
-4.00
-5.00
-6.00
-7.00
-8.00
Deflection, nA
Distance, nm
Approaching
Retracting
T = 25°C

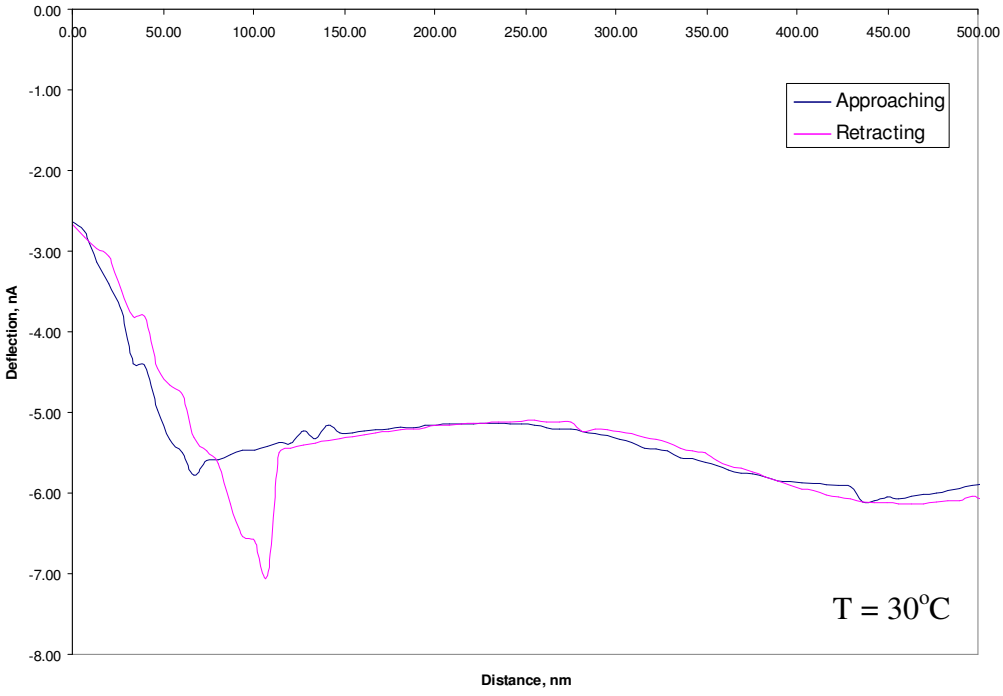
0.00
0.00
50.00
100.00
150.00
200.00
250.00
300.00
350.00
400.00
450.00
500.00
-1.00
-2.00
-3.00
-4.00
-5.00
-6.00
-7.00
-8.00
Deflection, nA
Distance, nm
Approaching
Retracting
T = 30°C

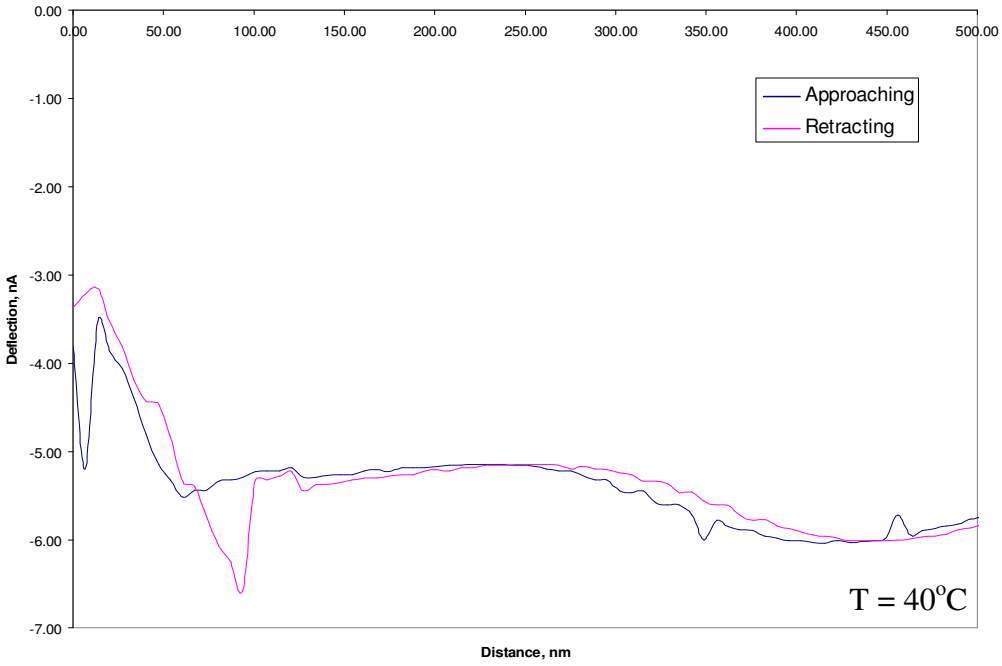
0.00
0.00
50.00
100.00
150.00
200.00
250.00
300.00
350.00
400.00
450.00
500.00
-1.00
-2.00
-3.00
-4.00
-5.00
-6.00
-7.00
Deflection, nA
Distance, nm
Approaching
Retracting
T = 40°C

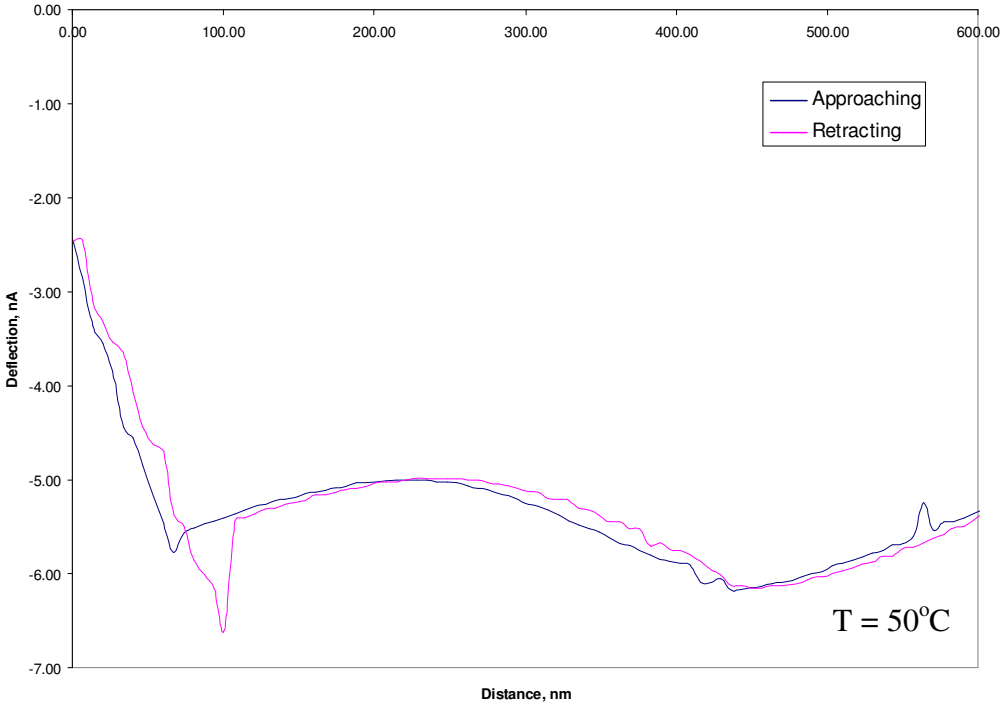
0.00
0.00
100.00
200.00
300.00
400.00
500.00
600.00
-1.00
-2.00
-3.00
-4.00
-5.00
-6.00
-7.00
Deflection, nA
Distance, nm
Approaching
Retracting
T = 50°C

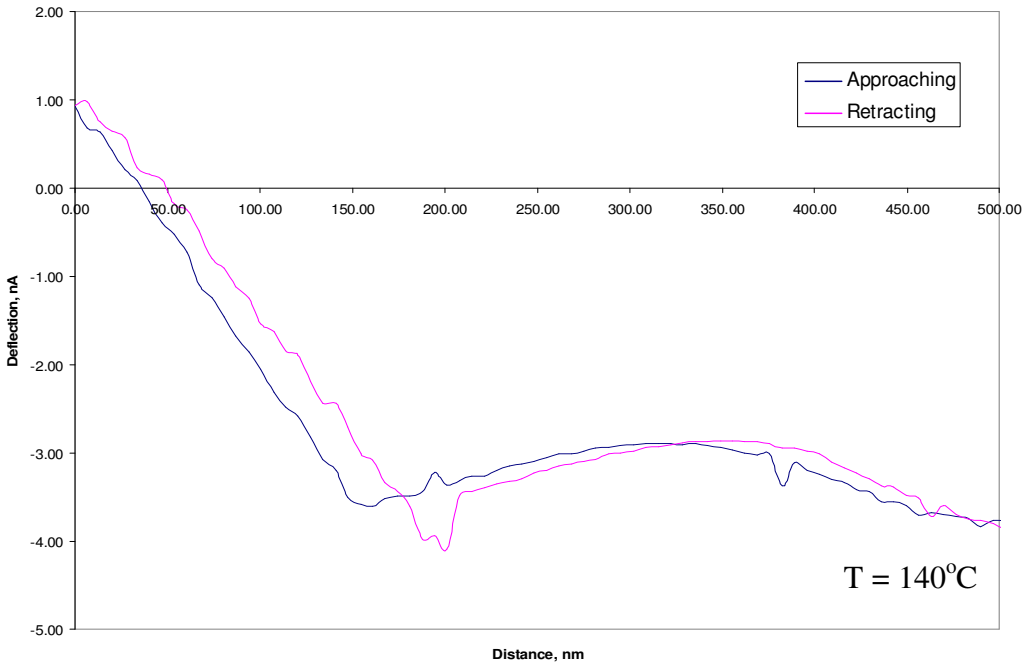

Figure 5.8 Force distance curves of MG16SS E.coli bacterial cells obtained using a nano probe, *point (a)*. From the data it is evident that at low temperatures in the region 20-30^{0}C the maximum pull off force is in the region of 1.7nA. As the temperature of the measurement is increased it is clearly seen that the maximum deflection or pull off force decreases. There is also some waviness and additional small peaks present in the graphs which are believed to be caused by external noise or artefacts

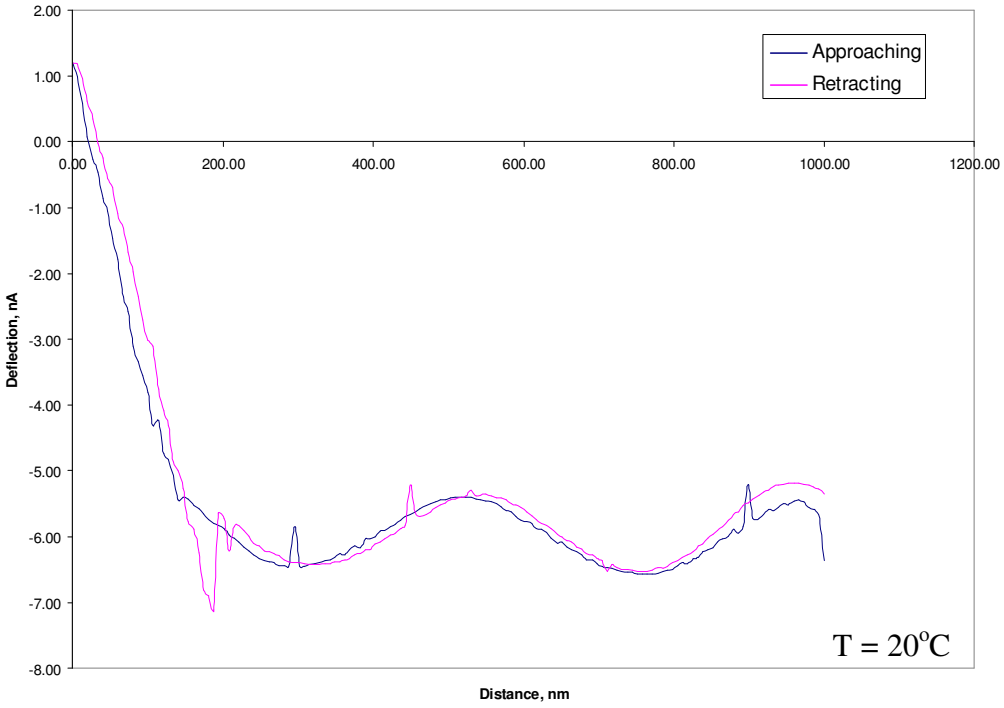
Approaching
Retracting
2.00
1.00
0.00
-1.00
-2.00
-3.00
-4.00
-5.00
-6.00
-7.00
-8.00
0.00
200.00
400.00
600.00
800.00
1000.00
1200.00
Deflection, nA
Distance, nm
T = 20°C

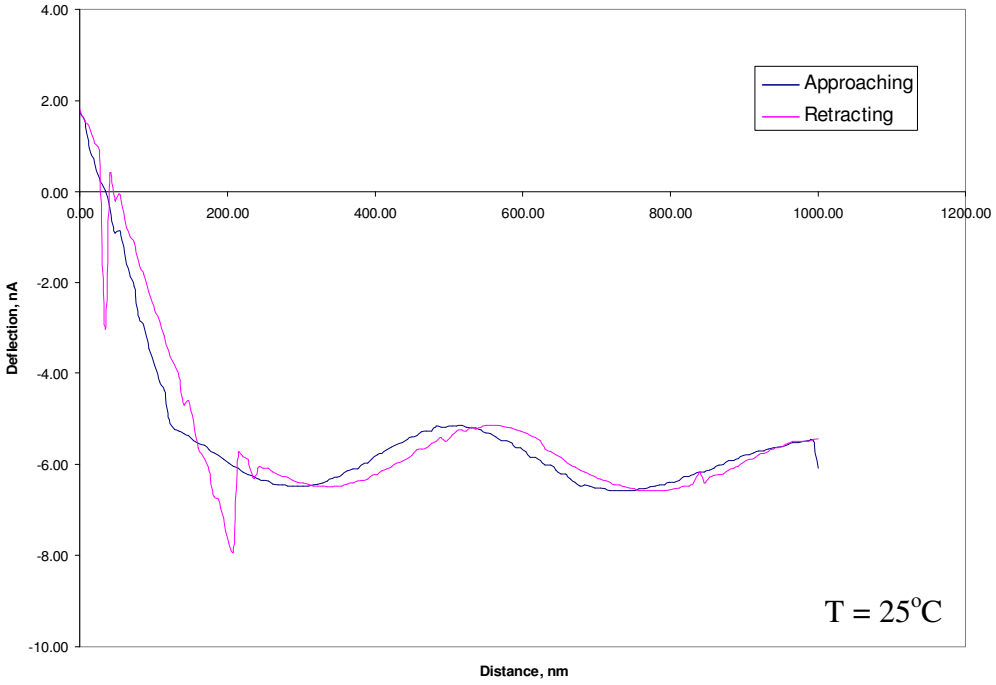
Approaching
Retracting
4.00
2.00
0.00
-2.00
-4.00
-6.00
-8.00
-10.00
0.00
200.00
400.00
600.00
800.00
1000.00
1200.00
Deflection, nA
Distance, nm
T = 25°C

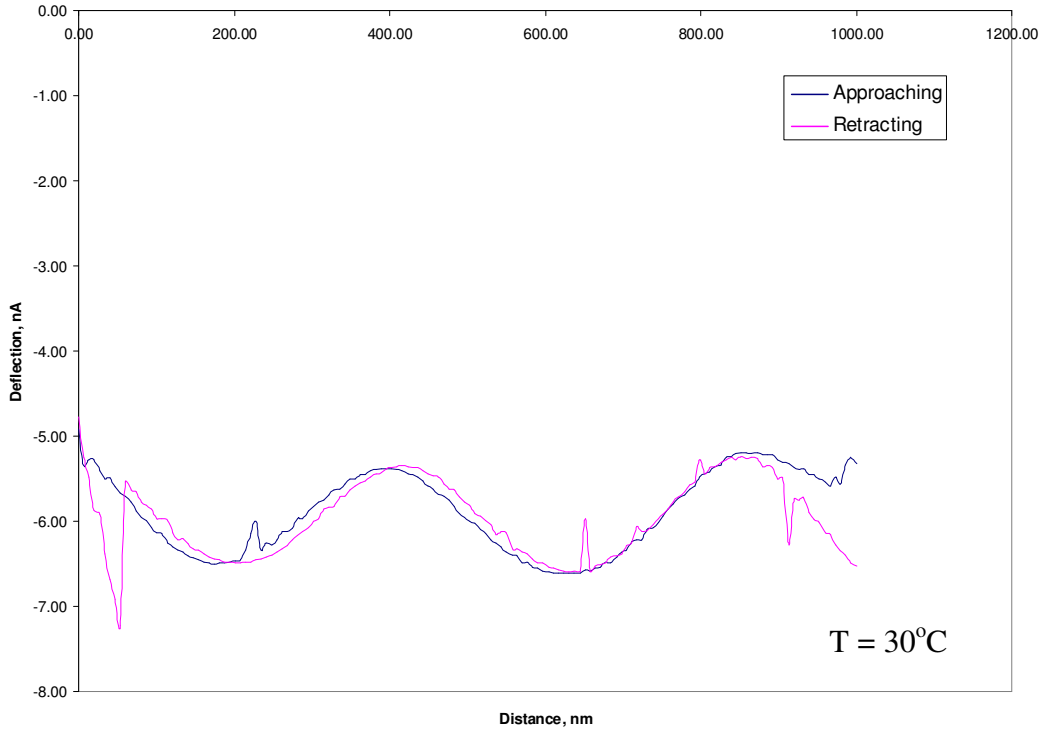
0.00
0.00
200.00
400.00
600.00
800.00
1000.00
1200.00
-1.00
-2.00
-3.00
-4.00
-5.00
-6.00
-7.00
-8.00
Deflection, nA
Distance, nm
Approaching
Retracting
T = 30°C

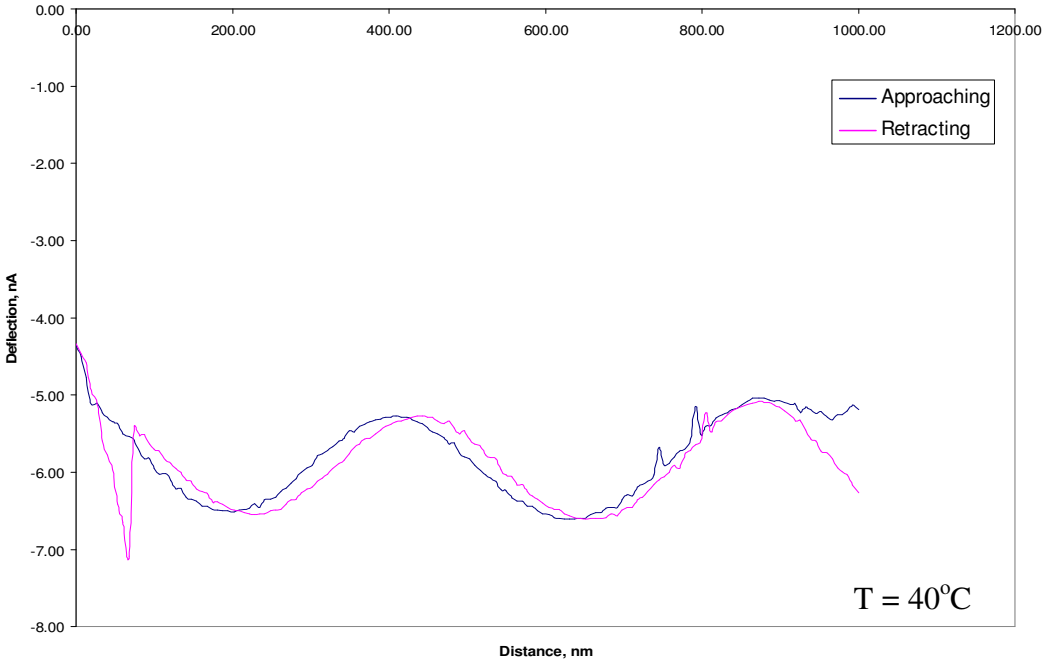
0.00
0.00
200.00
400.00
600.00
800.00
1000.00
1200.00
-1.00
-2.00
-3.00
-4.00
-5.00
-6.00
-7.00
-8.00
Deflection, nA
Distance, nm
Approaching
Retracting
T = 40°C

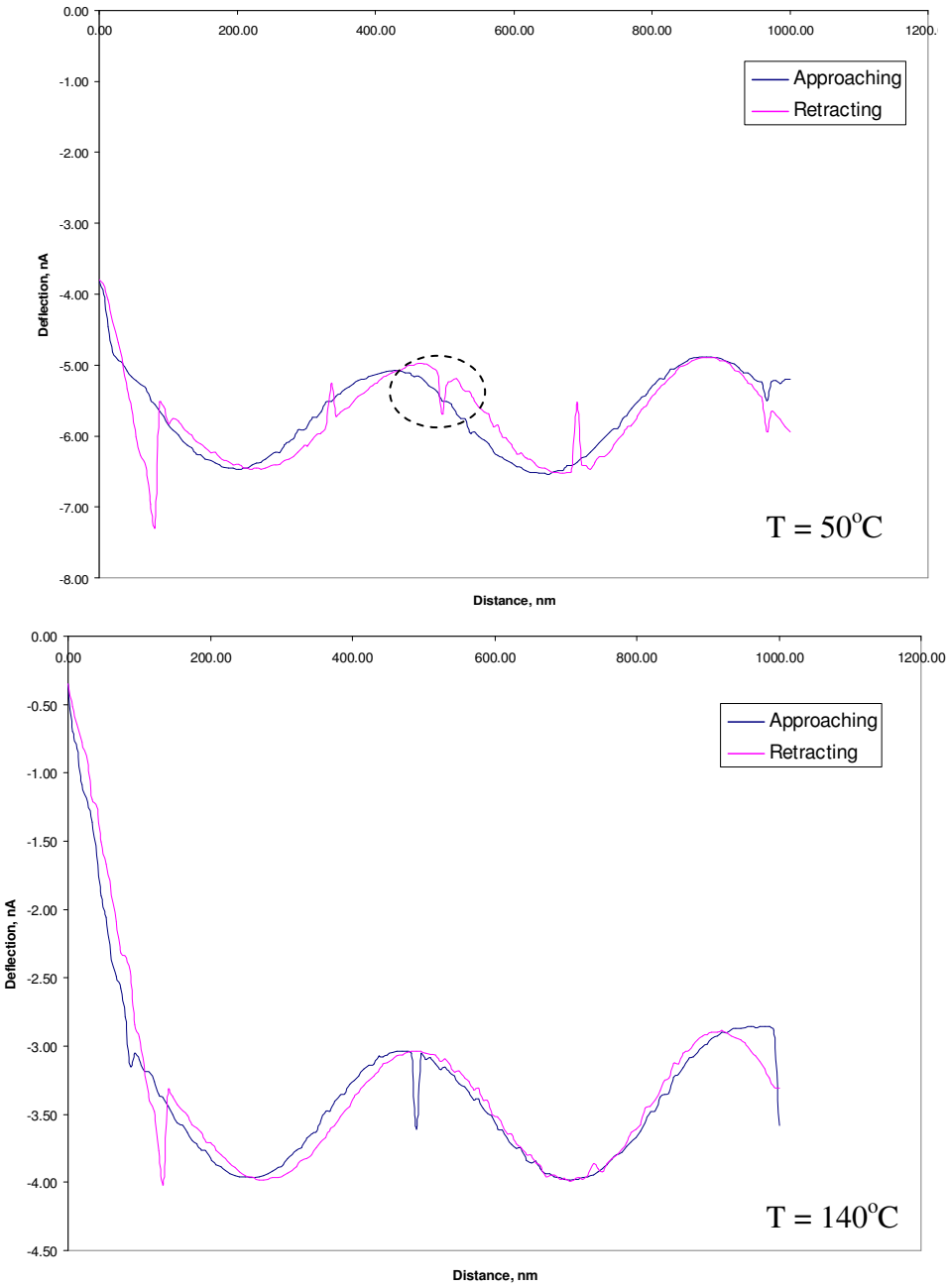

Figure 5.9 Force distance curves of MG16SS E.coli bacterial cells obtained using a nano probe, *point (b)*. Similarly to point (a), from the data it is evident that at low temperatures in the region 20-30^{0}C the maximum pull off force is in the region of -1.7nA. As the temperature of the measurement is increased it is clearly seen that the maximum deflection or pull off force decreases. There is also some waviness and additional small peaks (*see circles in graph above*) present in the graphs which are believed to be caused by external noise or artefacts

From the force distance curves obtained from the E.coli cells it is evident that as the temperature is increased the shape of the curve does not change significantly. This on the one hand is suggestive there is no sudden break in contact, but on the other indicates that no changes in the cell structure can be detected using heated nano probes. However, it is also clearly seen that increasing the temperature of the tip leads to a decrease in the adhesive force obtained, which in the case of the E.coli cells becomes apparent at temperatures above 40^0C. This is more clearly shown in the plot in **Figure 5.10**. This is thought either to be due to softening of the cell immobilizing agent, but can also be due to compositional and/or structural changes taking place within the bacterial cell. This is an important observation, as microstructural changes of the cells were not observed when imaged with heated probes (*see Chapter 4*). Therefore it will not be unreasonable to suggest that these so-called '*thermal force distance curves*' do not only provide information about the mechanical response of the biological system in question, but can also provide information of sub-structural changes that take place as a function of temperature.

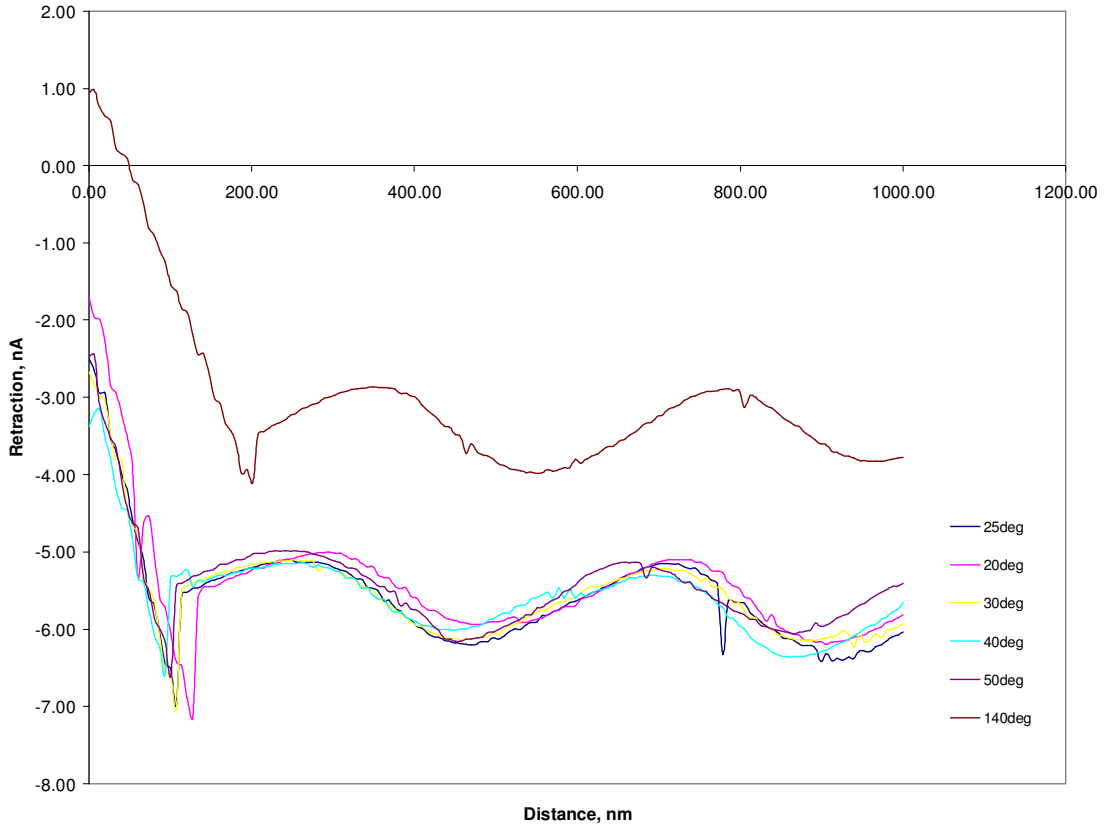

Figure 5.10 Comparative plot of the Force distance curves obtained from E.coli cells using heated nano-probes. The decrease in the maximum pull-off force, which is most probably due to structural changes taking place, can clearly be seen

Figure 5.11 presents an average plot of the maximum pull off forces (five measurements per temperature) measured as a function of temperature for the example point (*a*). From the data it would appear that in the temperature range 30-50^{0}C there is a step change in the values of the maximum pull-off force. As this step transition is observed in the region where the cells are viable, it is yet again not

unreasonable to suggest that this step change may be accompanied by structural changes in the bacterial specimens.

If the data is approximated (**Figure 5.11 solid black line**), it would appear that the relationship between pull-off force and temperature can be described by a simple linear equation of the type below:

$$F = -0.01T + 1.84$$

where F is the pull-off force and T is the temperature at which the measurement was taken. However, on the one hand, considering the complex nature of biological systems, their chemical composition and structure it can be said that it is highly unlikely such a simple model to describe their behaviour; but on the other, hand, if only mechanical interaction is assumed then this well maybe the case. The question although is open whether such a broad temperature range is needed over which mechanical interactions need be investigated. Nevertheless, it is believed that the results presented & discussed here offer enormous potential for future studies to gain further insight into the mechanical interactions of biological systems.

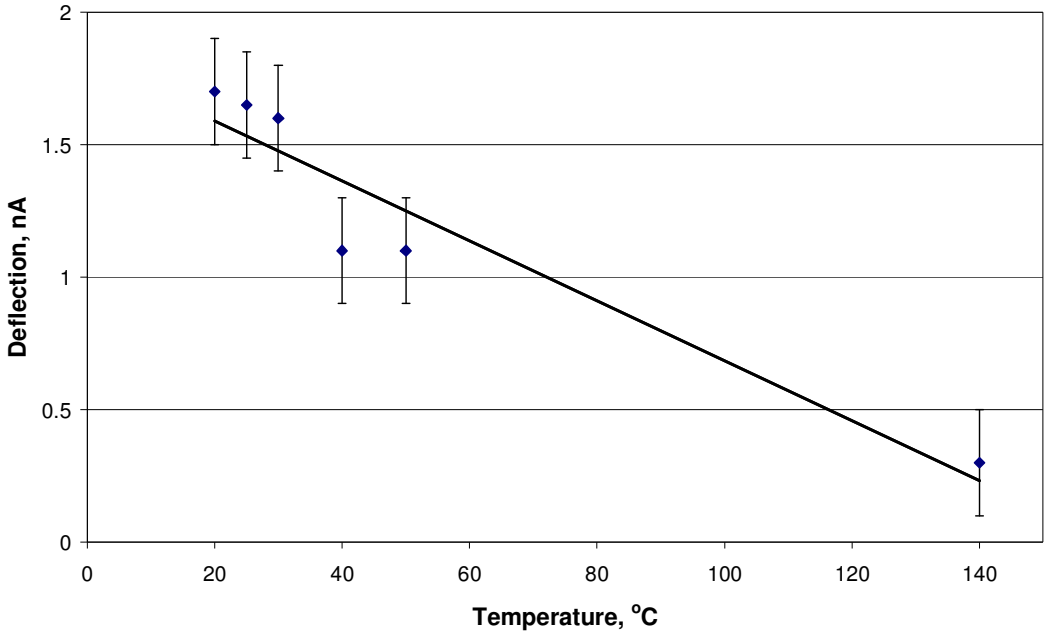

Figure 5.11 Plot of pull-off values against the tip temperature for E.coli bacterial cells (blue diamonds represent the experimental points and the solid black line represents the predicted linear relationship in the values of the maximum pull-off force as a function of temperature). Note the step change in the maximum pull-off force observed in the temperature region 30-50^{0}C

5.2.4. Summary of Experimental Observations

In this part of the thesis it was shown that Atomic Force Microscopy can be successfully employed to measure the interactive forces between different types of probes and a variety of material systems. The developed methodology was initially successfully applied in the study of a model system (Paracetamol tablets). This was then applied in the study of E.coli bacterial cells; where the use of heated probes was also successfully utilised for the first time ever. It was clearly demonstrated that the adhesive forces decrease with increase in temperature. This can also be indicative of structural and/or compositional changes within the systems in question. From the shapes of the obtained curves it was evident that there was no long distance of detachment and sequential breaking, which is indicative of a sudden break in contact. Therefore, there was no indicative continued stretching of the cell, localised stretching of cell surface regions still in surface contact, stretching and rupturing of adhesive molecules and the 'peeling' of the cell away from the surface.

It can be concluded that the AFM force measurement capability offers great opportunities for further investigations into the properties and function of the microbial cell surface and their interactions not only on its own, but also for example with pharmaceutically relevant materials.

6. Development & applications of Photothermal Microspectroscopy on model & biological systems

6.1. Introduction

Photothermal Microspectroscopy (PTMS) is a recently developed technique (Hammiche, *et. al.,* 2003) which combines Atomic Force Microscopy & Infra Red Spectroscopy. The technique is based on the so-called photothermal effect. In this approach a photoinduced change in the sample due to the retention of absorbed electromagnetic energy results in sample heating, which causes measurable changes in a number in a number of thermodynamic parameters. This method, as mentioned before, allows one to simultaneously obtain a high resolution image from a specific region of the specimen, coupled with information of the chemical composition of the material in question. The principal aim of this part of the research project was to evaluate the sensitivity of the thermal probes used in PTMS studies and to develop a robust methodology and apply it in the study of biological systems and their interactions with pharmaceutically relevant materials. Firstly, the results from the preliminary investigations into the sensitivity of the probes used will be considered. Secondly, the methodology developed and used on a model system (Polystyrene spheres) will be discussed. This will be followed by a presentation of the results obtained from untreated and treated with antibiotics E.coli bacterial cells. The final part of the chapter will consider the results from a collaborative research with the Institute of Food Research, Norwich, UK which was aimed at the application of PTMS in the study of food systems.

6.2. Probe sensitivity & its optimisation as a function of Temperature

In the first part of this chapter, as mentioned above, the results from the preliminary investigations into the sensitivity of the Wollaston wire probes as a function of temperature are presented. It is believed that these sets of experiments were necessary to be done in order to confirm whether the tips are sensitive enough for the PTMS studies and whether their performance can be optimised.

6.2.1. Temperature measurements

Temperature measurements were conducted using a TA Instruments (New Castle, DE, USA) 2990 μTA Microthermal Analyzer with a Thermomicroscopes Explorer AFM head combined with hot/cold stage, Linkam TP 93 temperature controller (Linkam Scientific Instruments, UK) and a Wollaston wire thermal probe (Veeco, CA, USA). The instrument was calibrated for temperature and displacement according to the manufacturer's recommendations. Polyethylene terephthalate (PET) was used as a calibrant. The room temperature 'kick-in point' was used as the other known temperature point for a two point calibration. The temperature program is started below ambient, so that the electrical power supplied to the tip is initially zero; then, as the program temperature rises to room temperature, the control system begins to supply power, giving rise to the so-called 'kick-in point'. The vertical displacement of the tip against the force measured by the degree of bending of the cantilever is calibrated using a Topometrix silicon oxide-silicon grid. This hard sample will not deform when the tip is pressed against it. Bringing the tip and the sample into contact will result in bending of the cantilever thereby allowing displacement calibration.

The tip contacts the surface of the stage at a fixed location with a programmed force, controlled by the piezoelectric feedback. An identical reference tip is attached next to the sample tip with its tip floating without contact to the sample. If the probe contacts a sample, two major factors affect the power to maintain the tip temperature constant. The first is the contact area, which is determined by the topography of the sample surface and the second is the thermal conductivity of the sample. Equal currents are applied to both tips and are controlled by the temperature-feedback circuit, to achieve a temperature-ramping speed in the range of 1 to 1, 500 $Kmin^{-1}$. The temperature of the sample tip T_p, can be determined after calibration from the resistance of the sample probe, R_p. Since the resistance of platinum has an almost linear dependence on temperature in the range of 300-600 K, R_p, can be expressed by:

$$R_p=R_{p0}\,[1+\alpha\,(T_s-T_0)],$$

where R_{p0} and α are the resistance and the temperature coefficient of the platinum wire at room temperature, T_0. The resistance of all lead wire and of all Wollaston-portion of the temperature sensor are neglected because of their small resistance when compared to the resistance of V-shaped platinum tip. The magnitudes for R_{p0} and α of the platinum tip are about 3 Ω and 0.004 K^{-1}, respectively (Moon *et al.*, 2000)

It was thought that the following two experiments will provide further information about the sensitivity of the system. The first one examined the sensitivity of the tip as a function of the temperature of the stage at a constant temperature of the tip, whilst the second investigated the sensitivity of the tip as a function of its distance from the

stage at different temperatures of the stage. The results from these experiments are presented and discussed below.

6.2.2. Sensitivity of the tip as a function of the temperature of the stage

After calibration, as mentioned above, a series of measurements were performed at different, but constant temperatures of the tip. These were chosen to be in the range of 25-38^{0}C, which is in line with the viable temperature range for the E.coli cells. During the measurements the Wollaston wire probe was in feedback control and in constant contact with surface of the stage. The temperature of the stage was controlled using a Linkam TP 93 controller (**Figure 6.1**). The experiments were carried out in the following sequence: stage heating from 35^{0}C to 38^{0}C, followed by cooling from 38^{0}C to either 35^{0}C or ambient temperature, with a temperature gradient of 1^{0}C. During each step any changes in the power signals of the probe were recorded as a function of time. Images for each temperature were also taken during the course of the experiment. An example is provided in **Figure 6.2**. After each experiment the data was exported to Excel, using the μTA software. The results from the analysed data are presented in graphical formats in **Figure 6.3**. From the experimental data presented in the figure below it is evident that the power signals of the probe increase with an increase of the temperature of the tip. This is obviously to be expected, as in order to maintain higher temperature of the probe, higher power levels will be needed.

Figure 6.1 Photograph of the Linkam TP 93 temperature controller used in the experiments (*courtesy of* Linkam Scientific Instruments, Ltd.)

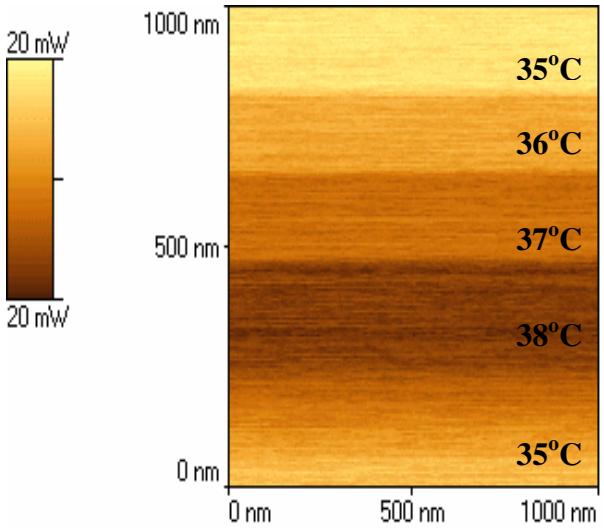

Figure 6.2 Example of the AFM image of the stage obtained during the first set of experiments in case of heating from 35^0C to 38^0C and follow on cooling. From the image it is seen that its brightness changes as the temperature of the stage is increased/decreased

However, from the data it is also clearly seen that increasing the temperature of the stage results in a step decrease in the power output of the sample probe. This is clearly seen in the graph as a function of time for each step associated with an increase in the temperature of the stage. This result can be explained as follows: when the temperature of the stage is increased, even by as little as 1^0C, the feedback system of the Wollaston wire probe detects this increase and adjusts the power signals, in this case decreases them, by the amount required to maintain the desired tip temperature. However, in the follow on cooling sequence, i.e. decreasing the stage temperature from 38^0C to 35^0C, one would expect to see a step increase in the power levels of the probe back to their original values. Although an increase is clearly seen in the plots this signal does not return to its starting point. This is most probably caused by an uneven cooling of the temperature stage. Finally, it is important that it is also evident that for different temperatures of the tip the pattern of the power levels as a function of time is similar.

Overall, it can be said that based on the measurements presented and discussed here, it has been clearly shown that the Wollaston wire probe is indeed sensitive to very small temperature changes and can therefore be successful used in PTMS studies.

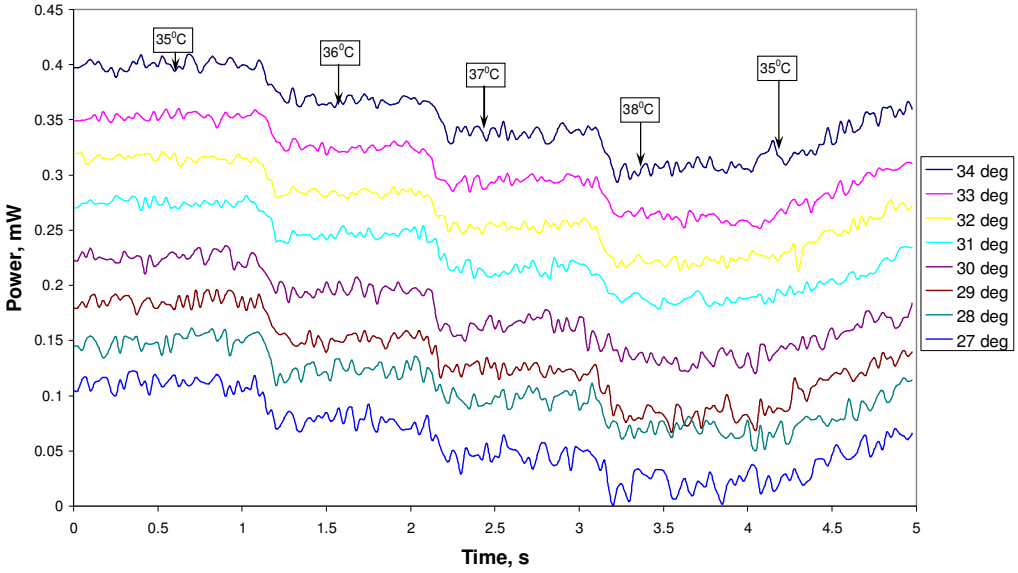

Figure 6.3 Sensitivity of the tip as a function of time and temperature of the stage at a constant tip temperature. From the above graph it can be seen that the power signals increase with an increase of the temperature of the tip. It is also evident that increasing the temperature of the stage results in a step decrease in the power output of the sample probe. It can also be seen that for different temperatures of the tip the pattern of the power levels as a function of time is similar

6.2.3. Sensitivity of the tip as a function of its distance from the stage at different temperatures of the stage

The second series of measurements were performed in two different ways; with and with out the use of the lock in amplifier. The function of the amplifier is described in the Materials and Methods chapter in detail, but in essence its use is expected to improve the signal to noise ratio and the overall stability of the signal. For these

experiments the tip was in passive mode, i.e. just used as a conventional thermocouple and not in feedback. It was noted that at the beginning of each measurement, depending on the temperature of the stage the initial power of the probe was in the range of 0.3-0.6mW. The experiments were carried out in a similar fashion in the following sequence: heating of the stage from 35^0C to 55^0C (still in the viable range of the E.coli cells) with a temperature gradient of 5^0C, followed by moving the tip away from the stage every one second for up to 20 seconds, using the μTA software. After each experiment the data was exported to Excel, using the μTA software. The results from the analysed data are presented in graphical formats in **Figures 6.4** and **6.5**. It is immediately seen that the data obtained from the experiments in which the lock in amplifier was not used does not show any pattern and is quite noisy. Therefore, it can be concluded that if used in this way the Wollaston wire probe will certainly be unsuitable for photothermal microspectroscopy experiments. .

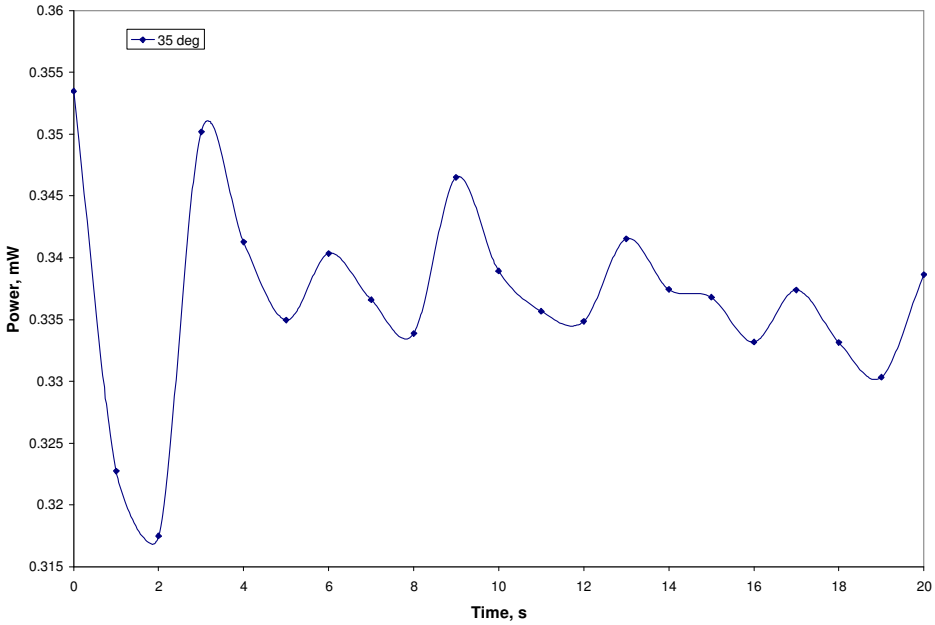
35 deg
Power, mW
Time, s
0.36
0.355
0.35
0.345
0.34
0.335
0.33
0.325
0.32
0.315
0
2
4
6
8
10
12
14
16
18
20

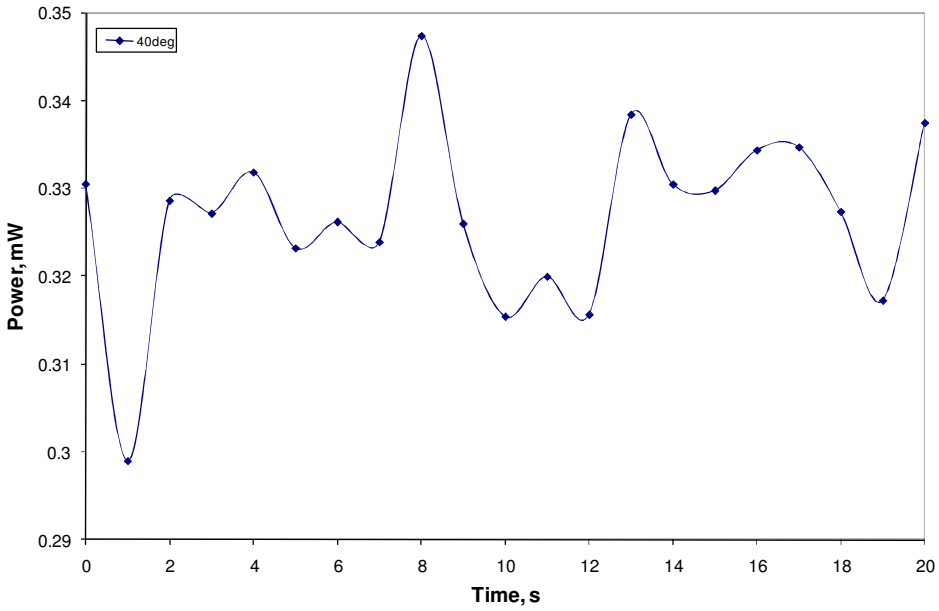
40deg
Power, mW
Time, s
0.35
0.34
0.33
0.32
0.31
0.3
0.29
0
2
4
6
8
10
12
14
16
18
20

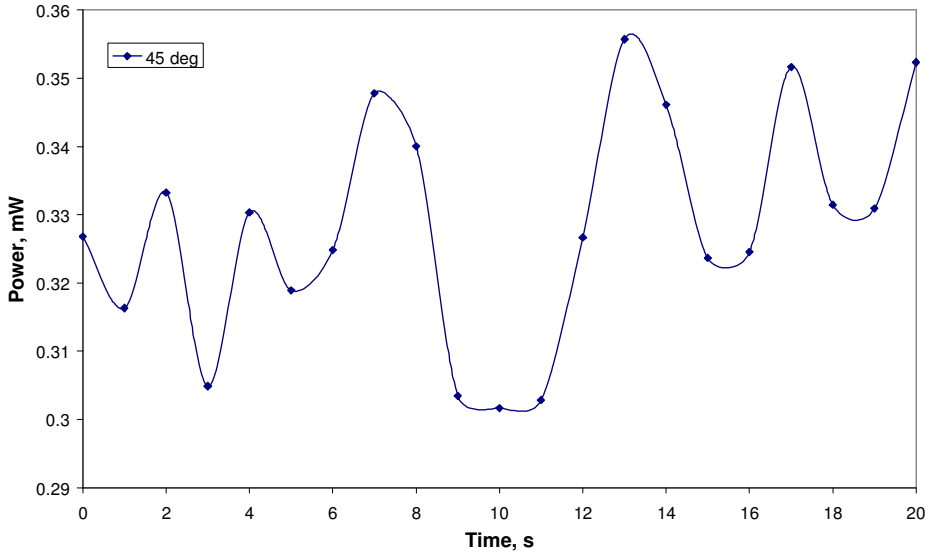
45 deg
Power, mW
Time, s
0.36
0.35
0.34
0.33
0.32
0.31
0.3
0.29
0
2
4
6
8
10
12
14
16
18
20

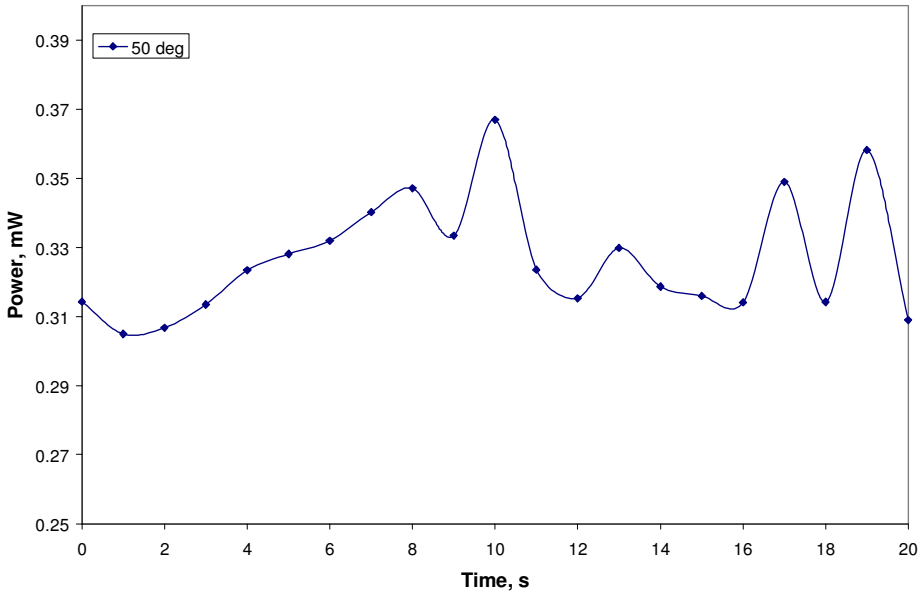
50 deg
Power, mW
Time, s
0.39
0.37
0.35
0.33
0.31
0.29
0.27
0.25
0
2
4
6
8
10
12
14
16
18
20

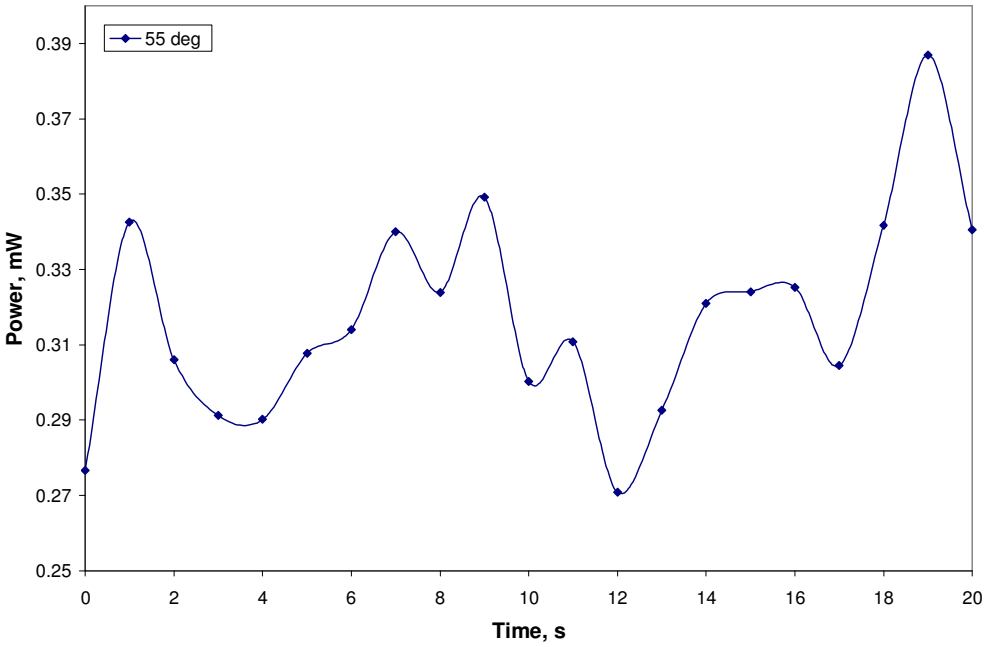

Figure 6.4 Effect of stage temperature on the sensitivity of the tip as a function of time and variable tip distance without the use of the lock-in amplifier. It can be seen that the data obtained from the does not show any pattern and is quite noisy. Therefore, it is suggested that if used in this way the Wollaston wire probe will certainly be unsuitable for photothermal microspectroscopy experiments

However, from the data obtained from the measurements where the lock in amplifier was in use (**Figure 6.5**) it is clearly seen that power in the tip increases as it is moved away from the surface of the stage. This can be explained as follows: as the tip is moved away from the stage a temperature gradient (difference) will be created which is sensed by the Wollaston wire probe and adjusted with the amplifier. Therefore, it is expected that as this temperature gradient changes, with further moving of the tip away from the surface, more power will be needed, which would ultimately result in increased power levels of the probe.

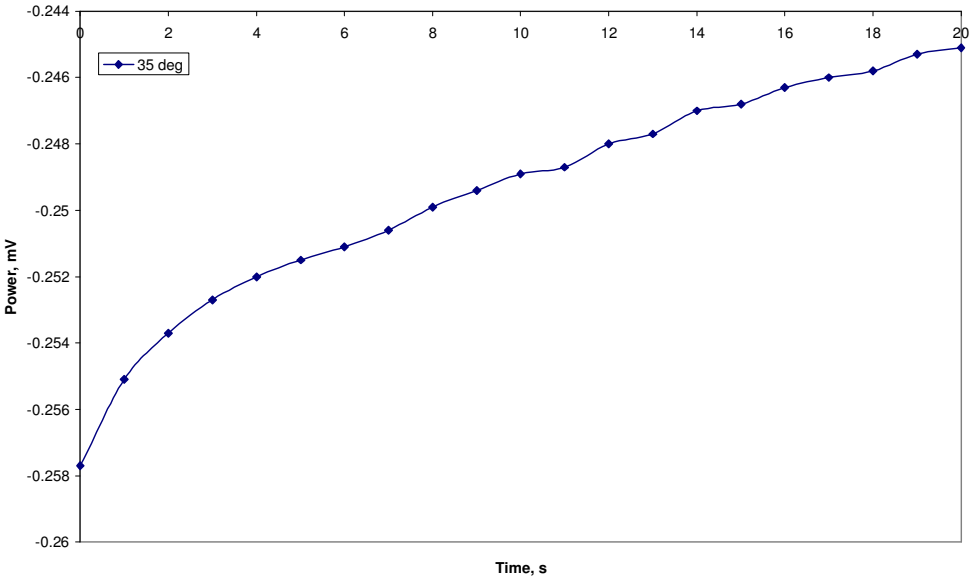
-0.244
-0.246
-0.248
-0.25
-0.252
-0.254
-0.256
-0.258
-0.26
0
2
4
6
8
10
12
14
16
18
20
35 deg
Power, mV
Time, s

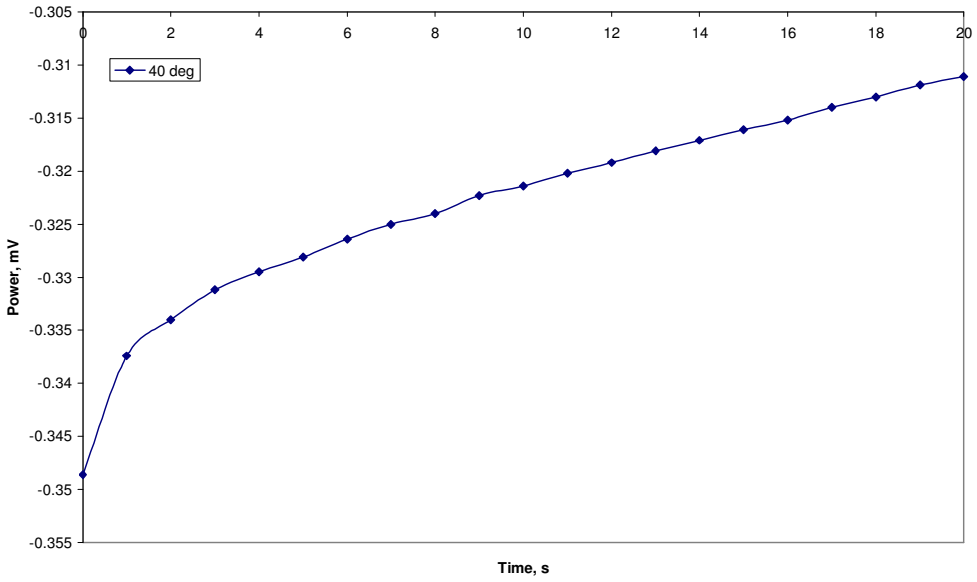
-0.305
-0.31
-0.315
-0.32
-0.325
-0.33
-0.335
-0.34
-0.345
-0.35
-0.355
0
2
4
6
8
10
12
14
16
18
20
40 deg
Power, mV
Time, s

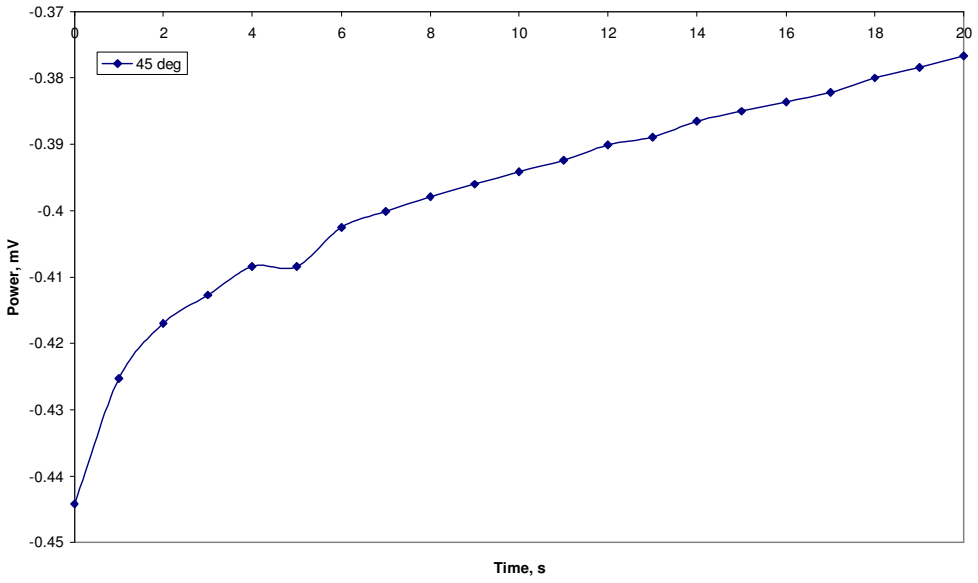
-0.37
-0.38
-0.39
-0.4
-0.41
-0.42
-0.43
-0.44
-0.45
0
2
4
6
8
10
12
14
16
18
20
45 deg
Power, mV
Time, s

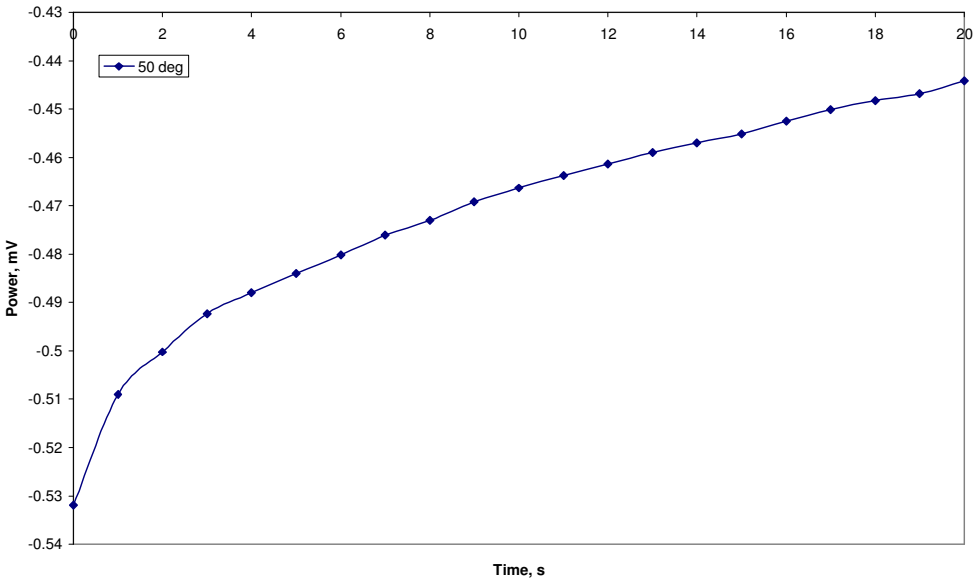
-0.43
-0.44
-0.45
-0.46
-0.47
-0.48
-0.49
-0.5
-0.51
-0.52
-0.53
-0.54
0
2
4
6
8
10
12
14
16
18
20
50 deg
Power, mV
Time, s

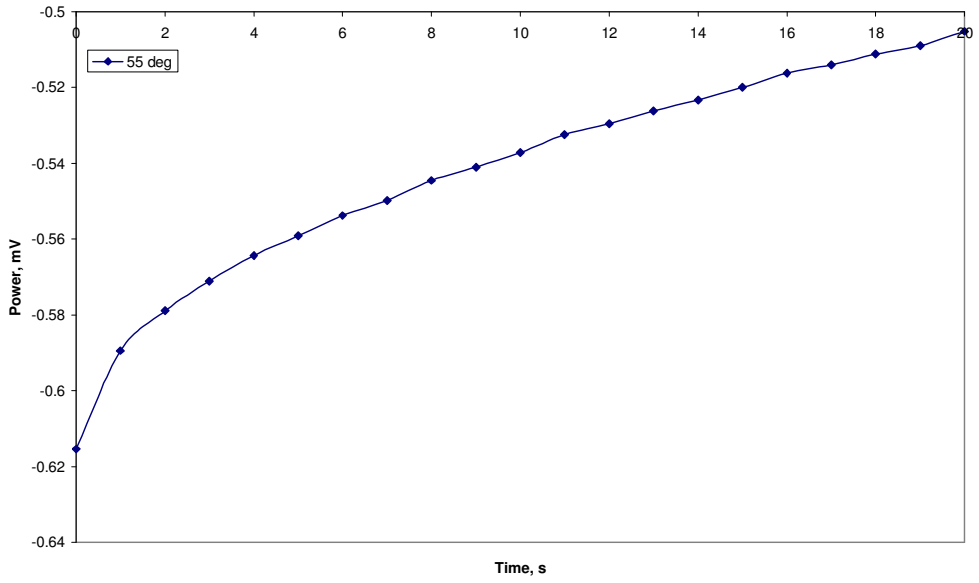

Figure 6.5 Effect of the temperature of the stage on the sensitivity of the tip as a function of time and variable tip distance, using the lock in amplifier. It is evident that power in the tip increases as it is moved away from the surface of the stage

The above results clearly demonstrate that the use of the lock-in amplifier does not only result in a significant reduction in the signal to noise ratio, but also leads to an increase in the sensitivity of the probe used. Therefore, it can be concluded that if used in this way the Wollaston wire probe will be suitable for photothermal microspectroscopy experiments.

In summary it can be said that that the data obtained from both sets of experiments strongly suggests that the Wollaston wire probe is a suitable tool for that can be used for PTMS studies.

6.3. PTMS studies on model system - polystyrene spheres

The next step of this part of the project was aimed at the development of a robust methodology that was then going to be applied in the study of biological systems. As polystyrene spheres, have previously been studied (Hammiche *et. al.*, 2004) it was decided to use them as a model system in this research.

The polystyrene sphere beads (concentration of 10 % w/w solids in water) were purchased from Sigma Aldrich. These were then diluted to a concentration of 0.05% w/w solids with water. A droplet of the solution prepared in the above manner was deposited and dried onto a mica surface. The specimen was then heated to just above its glass transition temperature (~110^0C) in order to ensure complete adhesion to the surface of the mica.

The Photothermal Microspectroscopy was setup by interfacing the Bruker FT-IR spectrometer with an Explorer Scanning Probe Microscope (SPM) equipped with a Wollaston wire thermal probe (Veeco Instruments, Santa Barbara, CA). The probes are constructed from a 75 μm diameter silver wire with a 5 μm diameter platinum/10% rhodium filament core. The SPM was placed on a custom designed optical interface which contains a flat mirror to steer the IR beam to a spherical mirror which condenses the beam to a diameter of ~500 μm. An adjustable platform is employed to position the SPM so that the tip of the probe is located at the focal point of the beam. Samples can be loaded on an *XYZ* controlled stage, and the probe is placed in contact with the sample using the SPM. Alternatively, the probe can be

used to pick up a small amount of the specimen, which can be used to perform measurements in air. For the PTMS measurements, background and sample measurements were taken at a resolution of 16 cm^{-1} for 1000 scans. Photographs of the experimental set up are shown in **Figure 6.6a** & **b**.

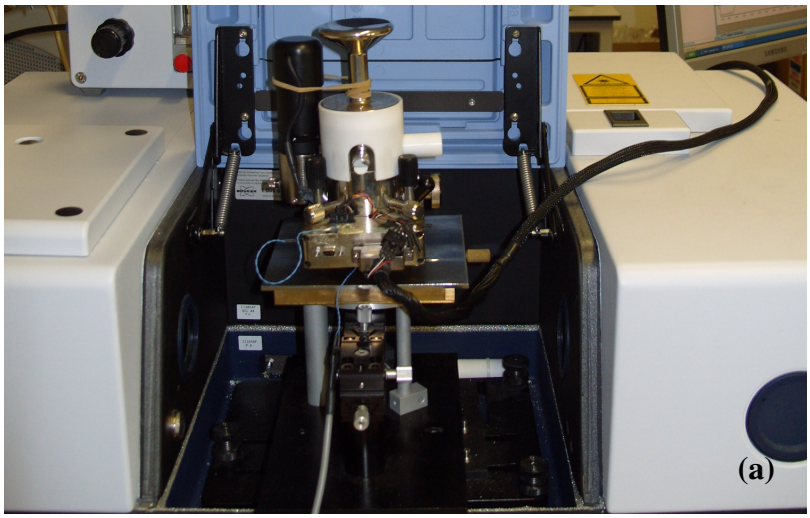

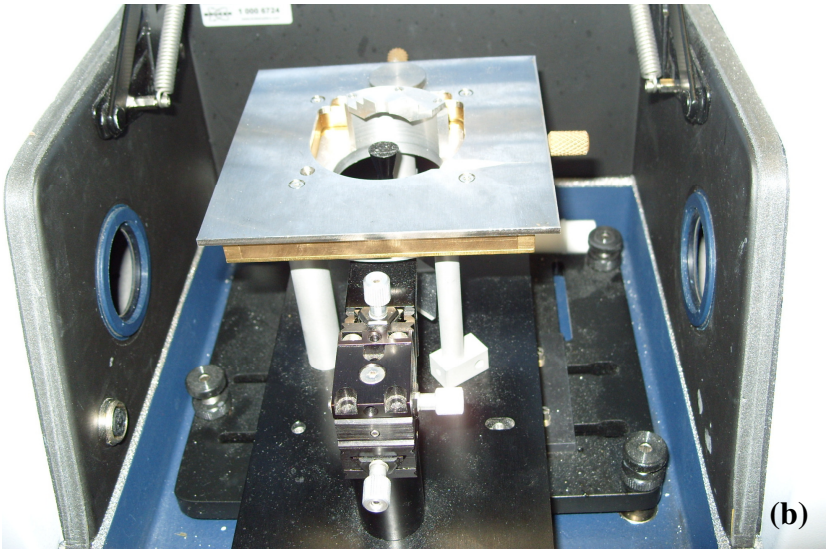

Figure 6.6 Photograph **(a)** and interface **(b)** of the Photothermal Microspectroscopy experimental setup

As mentioned above, the first step of the experiment involved obtaining an image of the polystyrene specimen, example of which is provided in **Figure 6.7**. In this way it was possible to obtain a number of individual spectra from a number of points across the surface of the specimen and mica. These are identified on the image below.

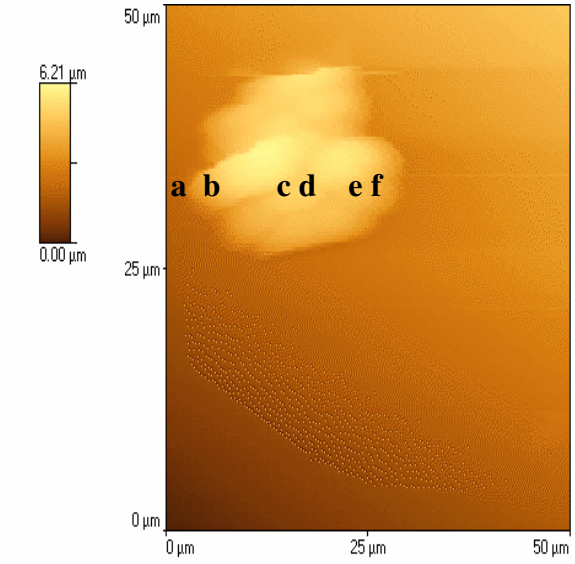

Figure 6.7 Topographical AFM image of polystyrene specimen on mica, taken with a Wollaston wire probe

The results from the spectral measurements are presented in **Figure 6.8**. From the experimental data it is evident that the spectra obtained for the mica and the polystyrene sphere can clearly be identified. This is an important observation, as previous studies (Hammiche *et. al.,* 2004) employed the use of rock salt as a substrate. This can be potentially useful, because salt as a substrate is transparent to IR radiation, thus ensuring that spectral contamination is eliminated. However, for many material systems mica is the preferred substrate surface and hence spectral contamination will always be present. Nevertheless, the results obtained from this study are comparable to those published in the literature (Hammiche *et. al.,* 2004).

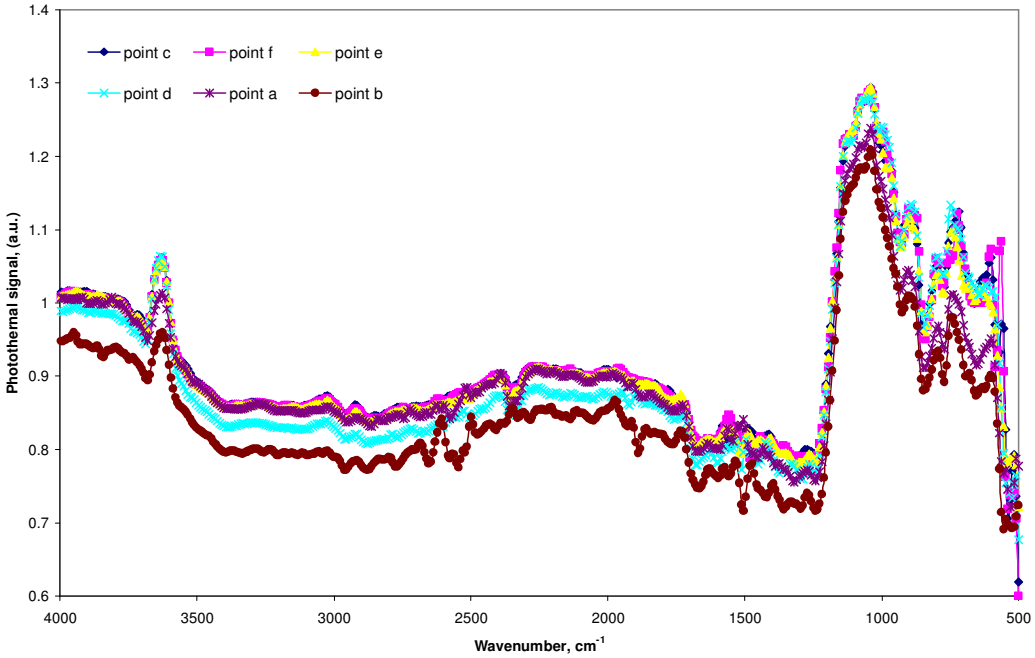

Figure 6.8 PTIR spectra of polystyrene spheres taken with Bruker FTIR corresponding to the points in the topographical image

The results can also be interpreted in terms of the maximum of the Photothermal signal as a function of distance. A representative plot of the above data is presented in **Figure 6.9**. From the data it is evident that the Photothermal intensity is much lower near the edges of the polystyrene specimen, compared to those in the middle.

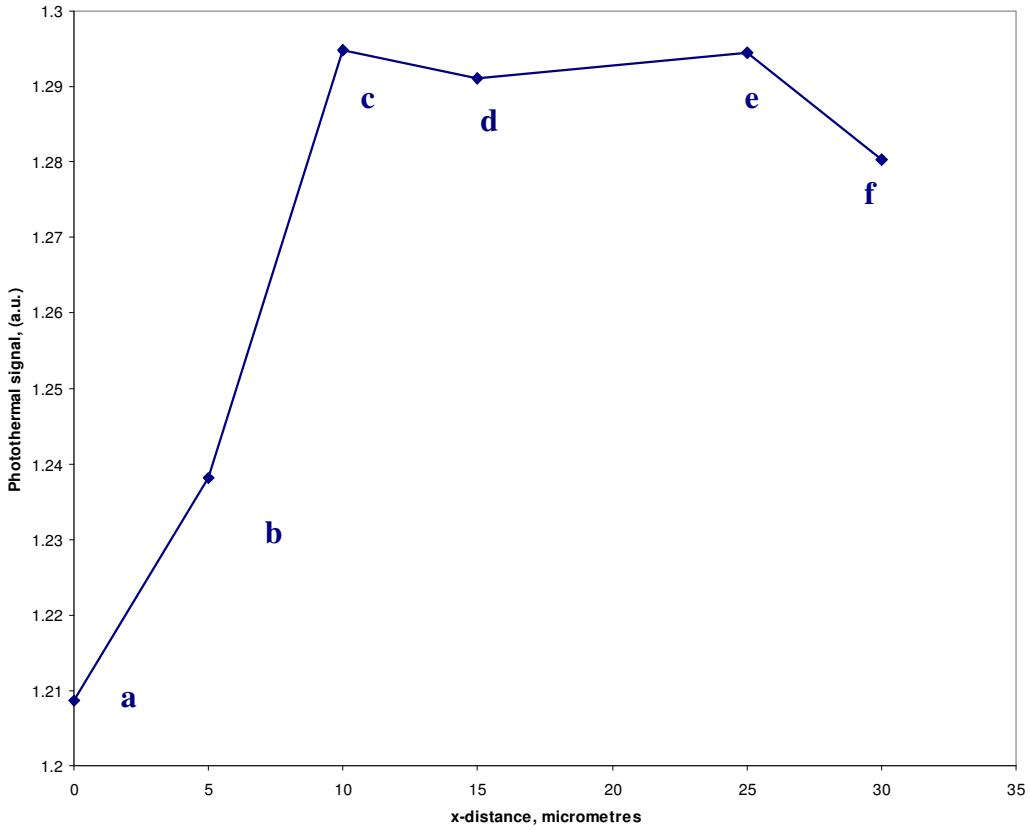

Figure 6.9 Maximum photothermal intensity as a function of distance for a polystyrene specimen adhered to mica

In this study the specimens were adhered to the mica substrate simply by heating them over their glass transition temperature. This method appears to offer an advantage over, for example, mechanically adhered specimens. Earlier work has shown that (Hammiche *et. al.,* 2004) if this is the case then particles during the experiments can become dislodged and/or dragged along by the scanning tip. In summary it can be said that the developed methodology appears to have been successfully applied in the study of the model system polystyrene spheres on mica. It

was clearly shown that the two spectra can be clearly identified and vary significantly in the maximum of the photothermal signal.

6.4. PTMS studies on E.coli cells

As already mentioned a number of times, the strategy for this research project is to investigate interactions between pharmaceutically relevant materials and living cells, by means of novel SPM based techniques. It was already demonstrated that these can be successfully studied by developing suitable sample preparation and imaging protocols and also by measuring the adhesive forces of the systems in question. In this part of the study the results from the near-field Photothermal Microspectroscopy (PTMS) measurements carried out on untreated and treated with Ampicillin E.coli bacterial cells are considered. Due to the fact that the measurements were carried out on a rather complex biological system consisting of a number of substances and in order to avoid misinterpretation of the results, it was necessary to initially obtain spectra of the main component of the studied system; these included agar, LB media and Ampicillin. Representative examples of these are presented and discussed in the figures below.

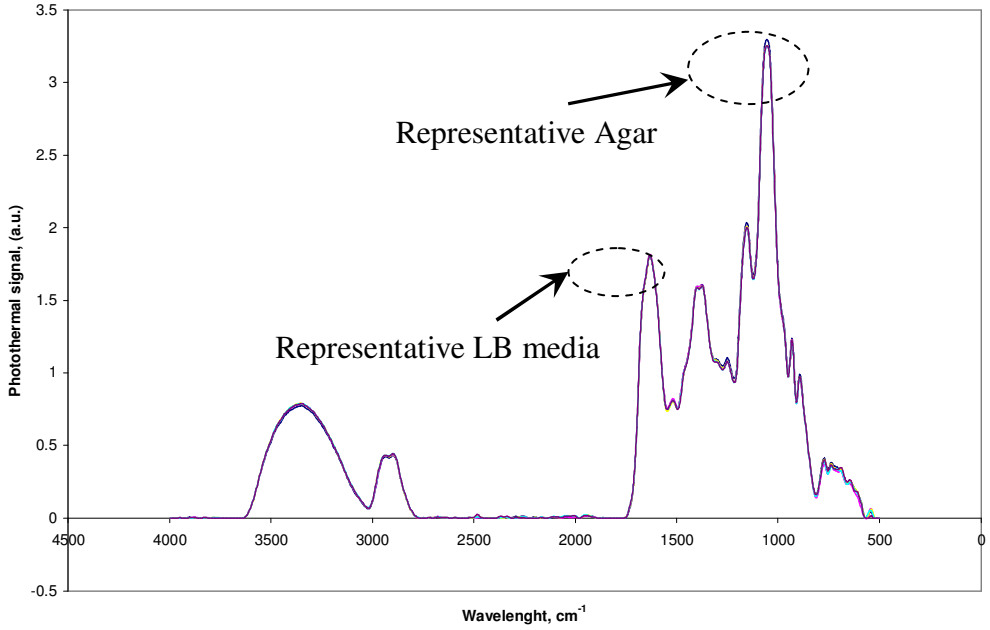

Figure 6.10 Photothermal spectra of LB media and agar obtained with Wollaston wire probe in air 16 cm^{-1}, 1000scans

From the PTMS spectra presented in **Figure 6.10** it is evident that the most prominent band is centered around 1079 cm^{-1}, which is consistent with data from the Raman spectroscopy carried out on agar. This band has contributions from several vibrational modes, namely to the C-O and C-C stretchings and to the C-C-O and C-O-H deformations. According to Pereira *et al* (1999) the 890 cm^{-1} band is also specific for agar and can be attributed to anomeric C-H of galactose residues.

The representative bands for the fatty acids in the Luria Broth media in the region of 2925cm^{-1} and 1658cm^{-1} are weak, whereas the ones for the peptidoglycans/polysaccharides in the region of 1656 cm^{-1} and 1080 cm^{-1} are much more well-defined. Here it is important to mention that it has been reported that the

absorption ratios between these bands can vary depending on the so-called 'freshness' of the media (Filip *et. al.,* 2008).

Figure 6.11 presents typical PTMS spectrum of pure Ampicillin obtained in this study. Ampicillin, as mentioned before, is a common antibiotic that is effective against a wide variety of Gram-positive and Gram-negative organisms. Various hydrated forms of ampicillin have been reported including a monohydrate, dehydrate and trihydrate.

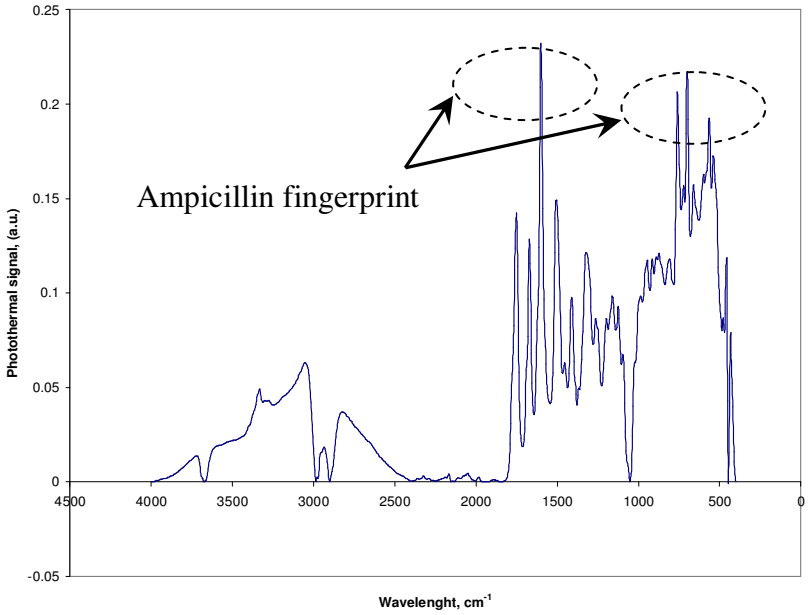

Figure 6.11 PTMS spectra of pure Ampicillin

From the PTMS data of Ampicillin it is evident that the spectrum exhibits a characteristic fingerprint region (1800–600 cm^{-1}), which is consistent with the data available in the literature (Nojavan *et al.*, 2005).

Figure 6.12 reveals the typical PTMS spectrum obtained for the agarized Luria Broth media in the presence of Ampicillin. It can be seen that the fingerprint region of the antibiotic can clearly be identified in the spectrum. The characteristic band associated with the LB media containing agar around 1079 cm^{-1} is also well-defined although not as intense as in the pure state.

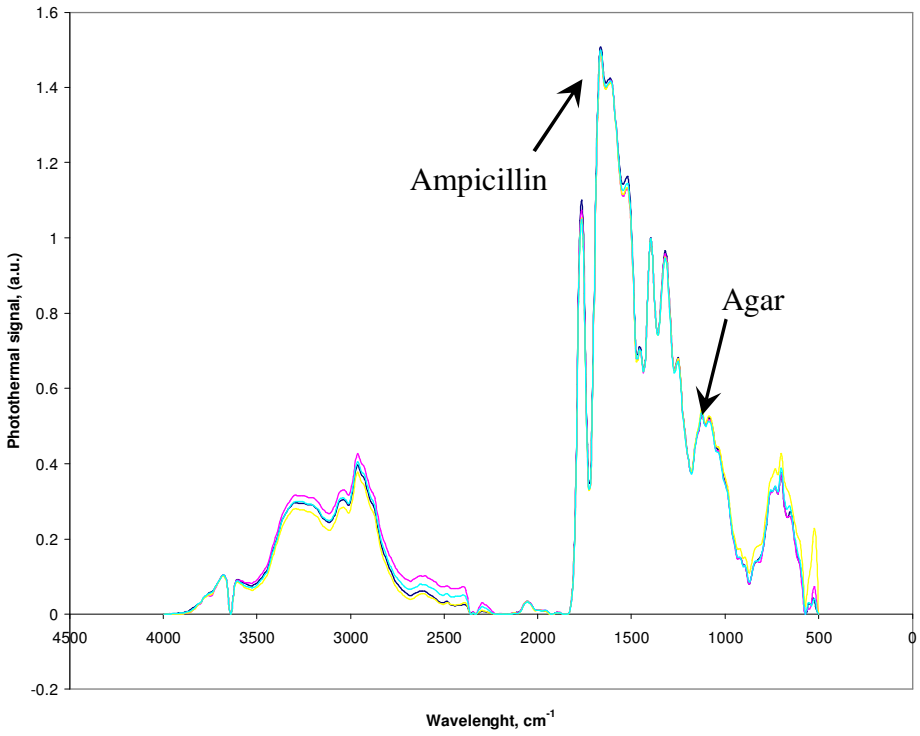

Figure 6.12 Photothermal spectra of the agarized LB media in the presence of the test agent Ampicillin obtained with Wollaston wire probe in air 16 cm^{-1}, 1000scans

Overall, up to now, it is not unreasonable to suggest that the initial PTMS measurements on individual components of the biological system that is to be investigated provide useful information of the bands associated with them which is

likely to allow for accurate interpretation of the data from the measurements carried out using untreated and treated with Ampicillin E.coli bacterial cells.

For the PTMS experiments E.coli bacterial cells were attached to the Wollaston probe tip by simply touching the cells with it and then retracting. Environmental Scanning Electron Microscopy (*please see chapter Materials & Methods*) was used in order to confirm the presence of cells on the actual tip. Images of an uncoated and coated with cells Wollaston wire probe are presented in **Figure 6.13** and **6.14**.

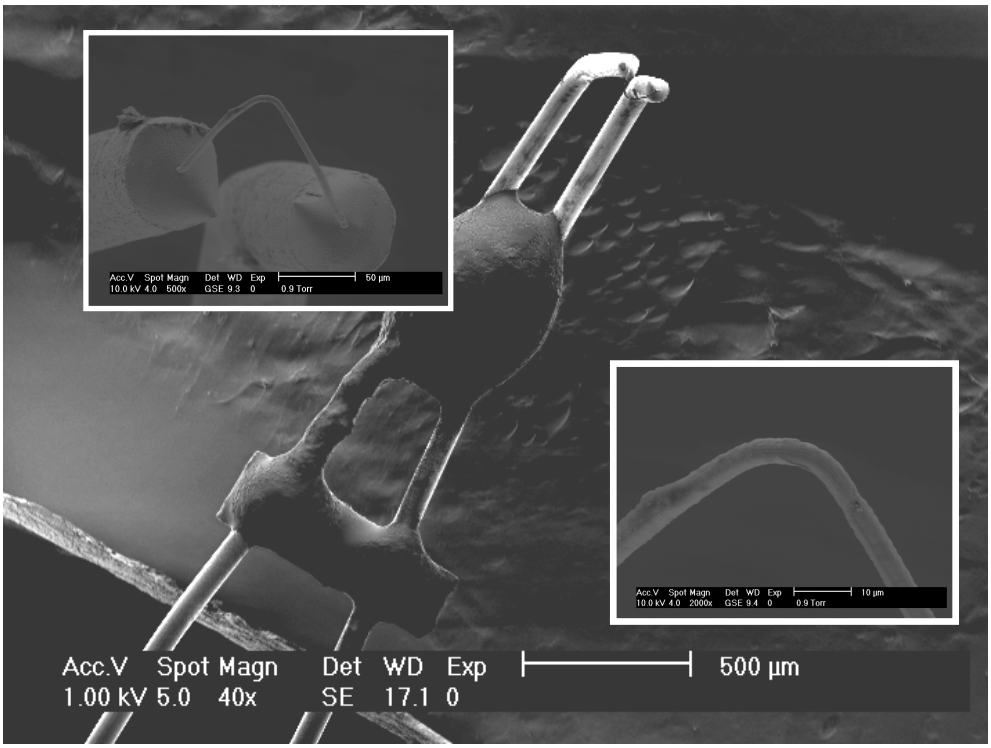

Figure 6.13 ESEM images of an uncoated Wollaston wire probe at various magnifications

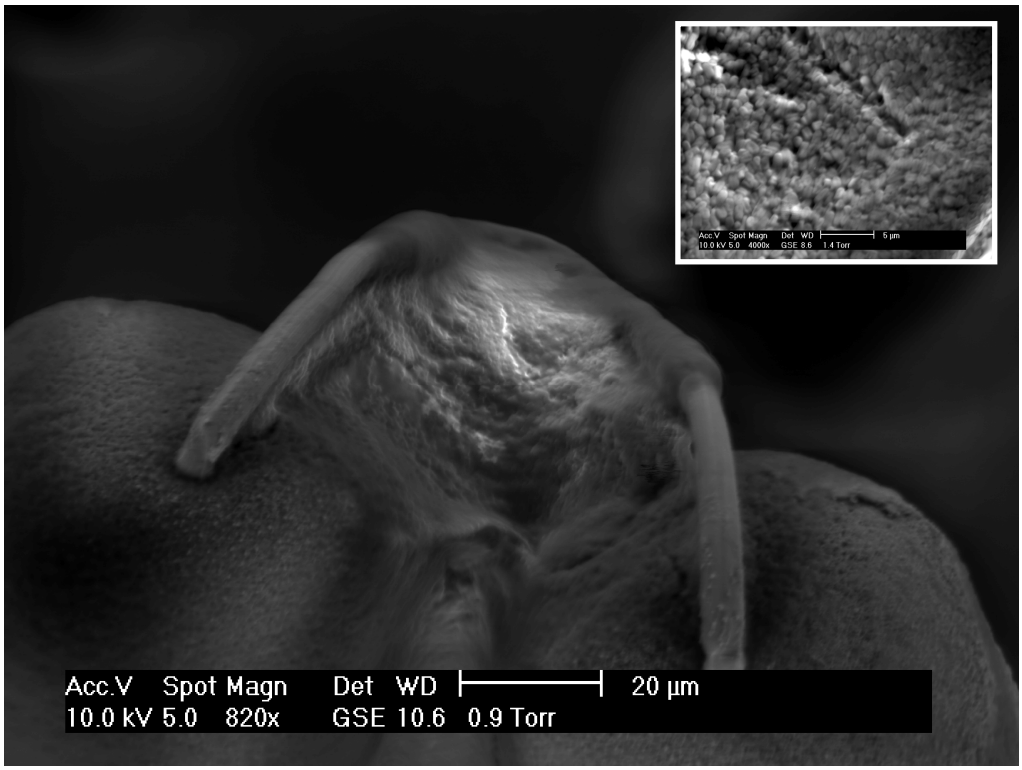

Figure 6.14 ESEM images of a Wollaston wire probe coated with E.coli cells at various magnifications. The E.coli bacterial cells are clearly seen on the tip

The PTMS experiments were performed using the methodology developed and used on the model system. **Figures 6.15a** shows the typical absorption spectra obtained from Wollaston wire probes coated with E.coli cells before treatment with antibiotics. An example of the typical cell structure observed by PFM AFM is also shown (**Figure 6.15b**).

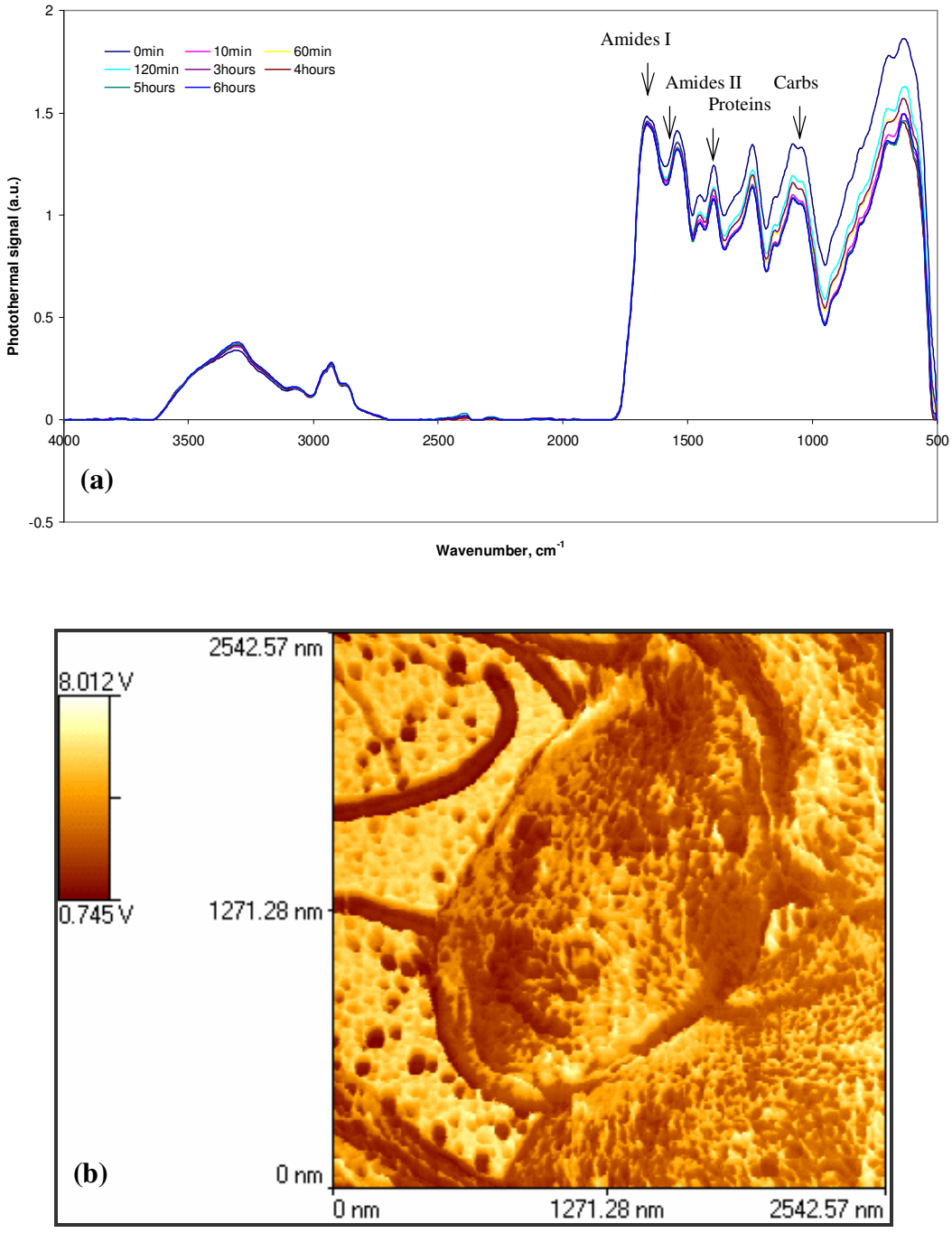

Figure 6.15 Photothermal spectra obtained with Wollaston wire probe of MG16 SS E.coli cells: before treatment with antibiotics (*24 h cell culture*) & example of the typical cell structure **(b)** observed with AFM. From the PTMS data it is clearly seen that the intensity of the peaks decreases as a function of time

From the photothermal data obtained from untreated E.coli cells, presented in **Figure 6.15**, it is evident that vibrational bands, associated with spectral regions, where significant differences of interest might occur can be identified; these include the amide I (1650 cm^{-1}), amide II (1540 cm^{-1}), glycoproteins and acyl chain of lipids (CH_3, 1380 cm^{-1}), amide III (1260 cm^{-1}), carbohydrates (C-O,1155 cm^{-1}), RNA (1120 cm^{-1}), phosphodiester of nucleic acids (PO_2, 1080 cm^{-1}), CO-O-C (1050 cm^{-1}), and glycogen (C-O, 1030 cm^{-1}) (Gazi *et al.*, 2004). Also of reported interest is the absorption peak at 970 cm^{-1}; which has been suggested to be indicative of the level of intracellular protein phosphorylation (Tobin *et al.*, 2004). Similar observations of the spectral regions of interest were also made by Hammiche *et al* (2005) who used Photothermal Microspectroscopy to investigate MCF-7 strain of cancer cells. An example of the data obtained in their experiment is provided in **Figure 6.16**.

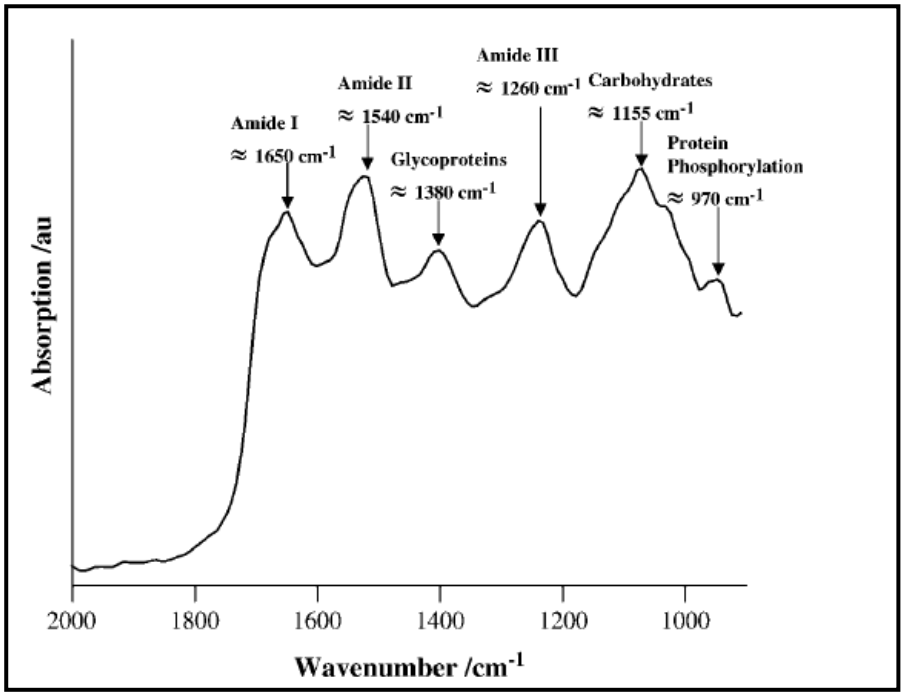

Figure 6.16 Spectral regions of interest, annotated in a typical absorption spectrum (2000–900 cm^{-1}) of MCF-7 cells after 24-h incubation. (*after Hammiche, 2005*)

From the experimental data presented in **Figure 6.15a** it is also evident that the intensity of the spectra decreases as a function of time. It has been suggested that such a reduction in the intensity of the spectra may be caused by starvation of the cells (**Figure 6.17**, Filip*, et al.,* 2008). However, in this case it is thought that the most likely cause for the observation of this effect is gradual dehydration of the cells that are attached to the Wollaston wire probe. Here it is also important to note that despite the occurrence of the dehydration effect, there were no changes in the spectra obtained suggestive of any structural changes of the E.coli bacterial cells.

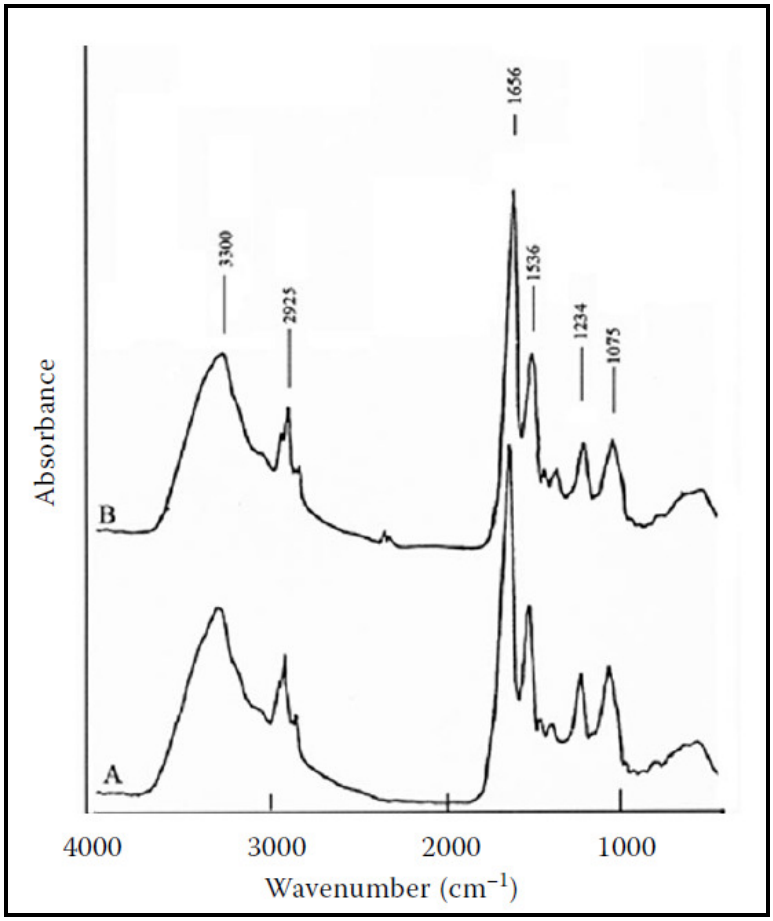

Figure 6.17 FT-IR spectra of E. coli cell mass harvested after 24 h cultivation A, and of a starved cell mass B (*after Filip et al., 2008*)

Figure 6.18 presents the Photothermal spectra (2000–900 cm^{-1}) obtained from *E.coli* after one week incubation period at a temperature of 4^0C. In exponentially growing cell populations marked variations in spectral intensities were observed at 24-h, which as described were most apparent in the intensity of the amide I band (1650 cm^{-1}) and the centroid position of the amide II band (1540 cm^{-1}). Such intrasample variations in IR signatures diminish in a time-related fashion with incubation (in this case one week incubation at 4^0C).

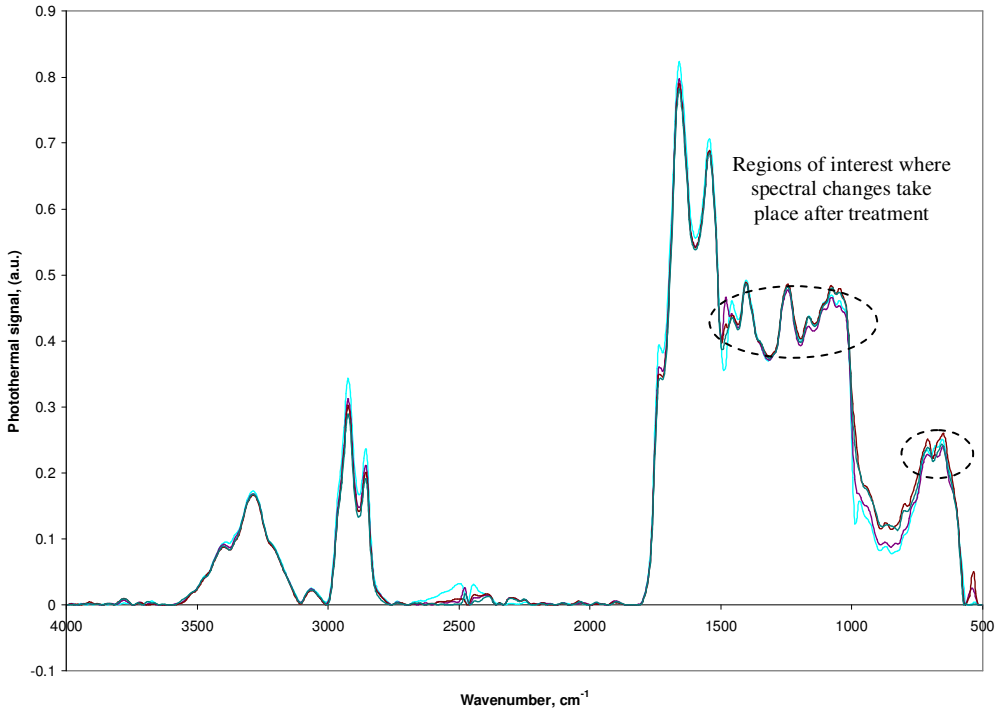

Figure 6.18 Photothermal spectra obtained with Wollaston wire probe of MG16 SS strain of E.coli cells after one week incubation at 4^0C

A time-related reduction in spectral intensity was observed in this region suggesting that, as cells transit from the exponential-growth phase into the more stationery phase

(**Figure 6.19**), bulk changes in intracellular biomolecules are spectrally observable and suggests that, although absorption spectra from exponentially growing cells after 24-h incubation are mostly similar, significant differences are observed throughout the spectrum as cell growth slows down. Hence, it would appear that the stage of the cell cycle may contribute to the variability of IR spectra of cells within apparently similar colonies (Tobin *et al.*, 2004). This would therefore suggest that IR spectra might be an alternative tool to monitor intracellular bulk changes as a cell progresses through the cell cycle.

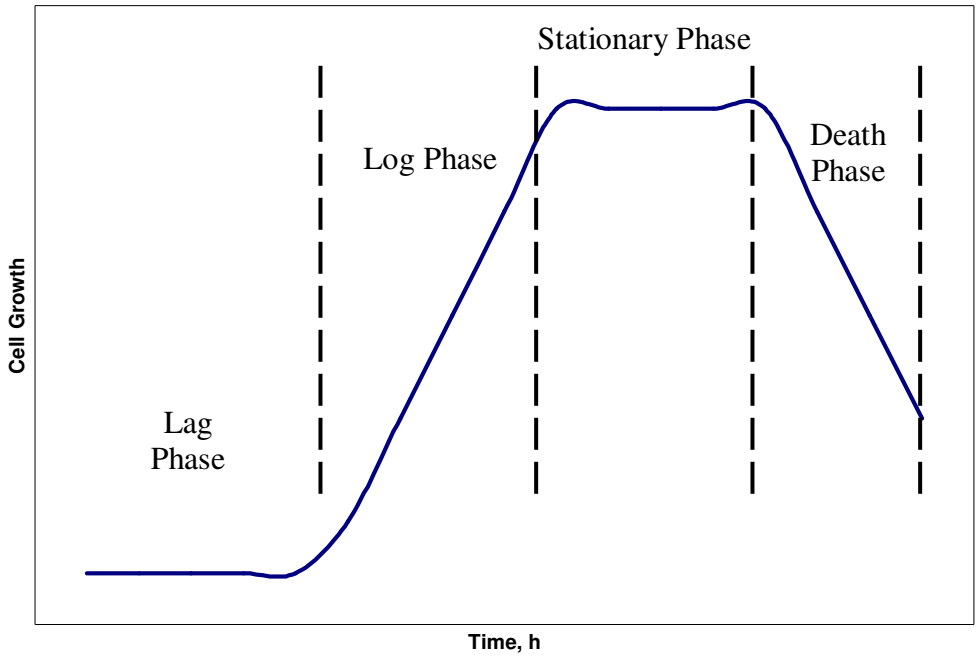

Figure 6.19 Typical Growth curve of E.coli bacterial cells

From the experimental data presented and discussed up to this point it was clearly demonstrated that the developed methodology can be successfully applied in the study of bacterial cells as they progress through their life cycle. The following part of

this chapter deals with the results from the measurements carried out on cells treated with antibiotics. As mentioned before, this was done with the aim to further investigate their interactions with pharmaceutically relevant material systems.

Figure 6.20 reveals the typical spectra obtained from E.coli bacterial cells treated with Ampicillin after 5h **(a)** and 12h **(b)** respectively. A representative image of the cell structure is also provided as an example (**Figure 6.20c**).

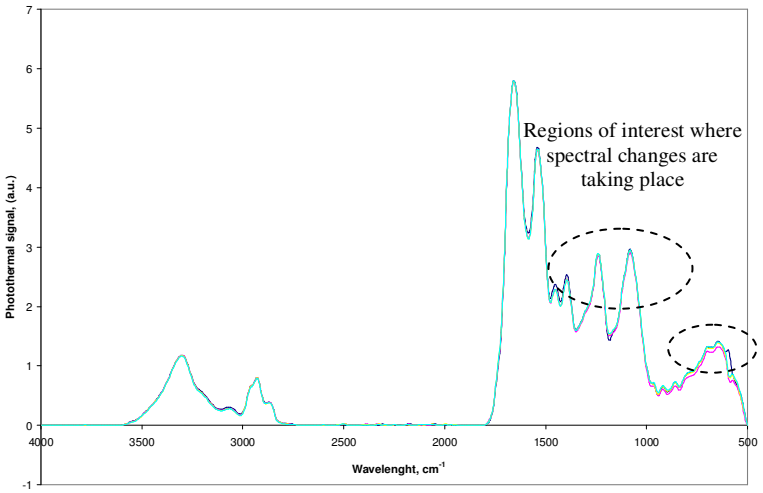

(a)

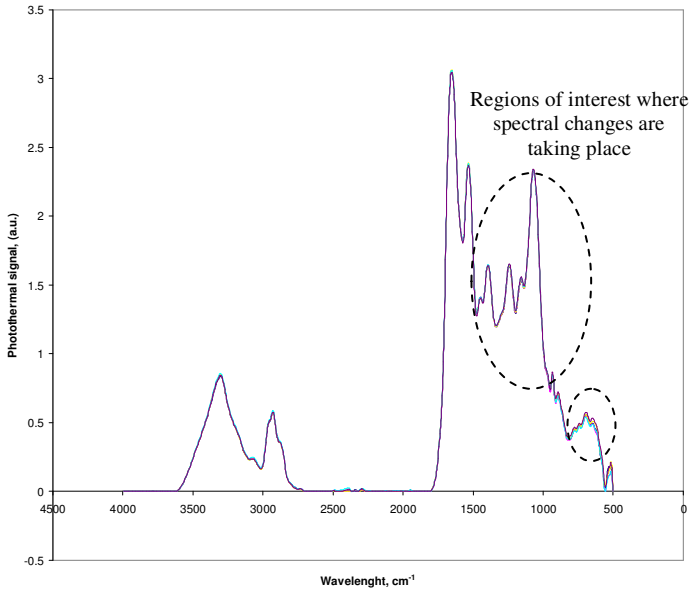

(b)

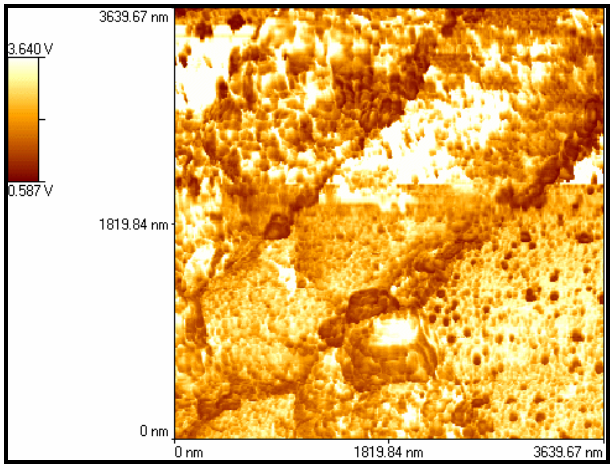

(c)

Figure 6.20 Photothermal spectra of MG16 SS strain of E.coli cells obtained after 5-h **(a)** and 12-h **(b)** incubation in the presence of Ampicillin. An example image of the cell structure is provided in **(c)**

From the spectra presented in the figure above it is evident that the are obvious changes in the spectral intensities in the presence of Ampicillin after 5 h and 12 hours of treatment, in comparison to the spectra obtained in the absence of this test agent. The differences appear to be situated primarily in the DNA/RNA spectral region (1490–1000 cm^{-1}). The reductions in spectral intensity also appear to be accelerated after 12-h treatment with Ampicillin, which is most probably the result of the E.coli cells being exposed for longer period of time to the effect of the antibiotic. This is in line with the observations made from the AFM images of the treated bacterial cells, discussed in detail in Chapter 4. Although Ampicillin-treated 12-h cultures exhibit the greatest overall reductions in spectral intensity, an increase in spectral variation was observed compared to untreated one week cultures. The band intensity at 970 cm^{-1} becomes less pronounced as cells transit from the exponential-growth phase into the

more stationery phase. A peak at this band has been associated with protein phosphorylation (Tobin *et. al.*, 2004); and as such it could be expected to be elevated in actively dividing compared to resting cells.

Furthermore, from the results it is also evident that there are significant changes in the spectral intensity in the carbohydrates regions. These can be associated with changes taking place within the outer membrane of the cell wall. This structural element, as described in the Materials & Methods chapter, is of great importance, as it has been shown that this layer is associated with the pathogenic capability of the bacteria (Salton & Kim, 1996). Therefore it can be suggested that the results from these experiments provide further evidence of the fact that antibiotics, such as Ampicillin, interact with gram-negative bacterial cells by combating the protective membrane layer of their walls (Woese, 1987). The actual detrimental effect of β-lactams on E. coli cells was recently investigated by Yang *et al.*, (2006) and discussed in detail in the Chapter Imaging of E.coli cells.

Overall, it can be said that the presented results clearly demonstrated that by employing Photothermal Microspectroscopy it is not only possible to monitor changes occurring in the cell-cycle, but also to study interactions between cells and pharmaceutically relevant materials, which would simultaneously provide additional information for structural changes taking place within the studied biological systems.

6.4.1. Summary of observations - E.coli cells

A methodology, combining the use of Atomic Force Microscopy and Infra Red spectroscopy, based on the original ideas of Hammiche *et al.*, 2004 was successfully developed and initially applied in the study of a model polymer system – polystyrene spheres. This was then applied in the study of E.coli bacterial cells. It was demonstrated that clear vibrational IR spectra could be obtained after the analysis of cellular material using PTMS. By using the developed methodology it was possible to observe spectral changes that were associated with cell-cycle kinetics; although it is noted that the full process that cells undergo is yet to be fully understood. The further reductions in spectral intensity seen after examination of cells after one week incubation and those treated with Ampicillin is suggestive that cell cycle effects & structural changes may be successfully monitored using Photothermal Microspectroscopy. The highly significant differences in spectral regions strongly suggest that significant structural changes within exponentially growing cells compared to stationary cells are also observable using this technique.

Undoubtedly the future of the technique will incorporate the development of a methodology for high resolution IR analysis (*e.g. sub-cellular*), which would require the use of probes with a much smaller sensing element (*nano probes*) than that used in this initial study, i.e., of the order of a few tens of nanometres. Also, it is important to note that PTMS permits a more direct measurement of temperature, an advantage which many techniques do not offer and hence suitable for further exploitation to

relevant systems. Furthermore, because detection is in the near-field, it allows, potentially, for a spatial resolution that is better than the diffraction limit.

In any way, it is strongly believed that the findings in this study provide conclusive evidence that PTMS may not only be used be used to examine cell cycle associated intracellular structural changes, but also interactions between cells and pharmaceutically relevant materials. Therefore, it is not unreasonable to suggest that such findings would constitute a novel approach in the use of Microspectroscopy.

6.5. PTMS studies on other biological systems

6.5.1. Introduction

In the earlier parts of this chapter it was clearly demonstrated that by developing a suitable methodology PTMS experiments can be successfully performed on polymer and biological systems. The final part of the chapter considers the results from an innovative collaborative research with the Institute of Food Research, Norwich, UK which was aimed at the further development and application of PTMS in the study of biological systems related to the food industry. This was done in an attempt to show that the above novel microspectroscopy technique can be used to provide high-resolution information of the intra- and inter-variability of both the chemical composition and the physical properties of the structures within the granules in wild and mutant type maize kernels. Mutant and wild type maize were chosen for this investigation as these two are widely studied systems in food science (Wellner *et al.*,

2010), because of the interest in their starchy structure and their possible applications in the pharmaceutical industry as new tablet excipients (Georget *et al.*, 2008). As with the E.coli data, here it is important to mention that there is no PTMS information available in the literature for the systems considered, which yet again emphasises the versatility of the characterisation technique used.

6.5.2. Maize and its structure

Prior to considering the structure of maize and its main means of studying, it is necessary to mention again that the primary aim of this experimental work was to investigate and in essence evaluate the possible use of Photothermal Microspectroscopy in the study of different types of maize, which would hopefully provide food scientists with an additional tool that may give further insight into their complex structure and composition. Hence, in this part of the chapter it was believed that only a basic background will provide sufficient cover of the issues addressed.

Maize grain is a caryopsis type of single seeded dry fruit (Vollmann & Rajcan, 2009). It is somewhat oval and flattened in shape (**Figure 6.21**). The flat surface on the narrower side shows a white triangular region, which is known as the embryo. The broad and yellowish region is called the endosperm.

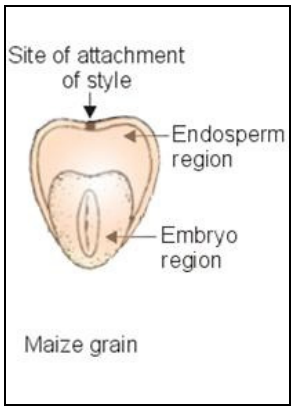

Figure 6.21 Structure of maize grain (*after Vollmann & Rajcan, 2009*)

The embryo of the maize grain is located beneath the endosperm. It is demarcated from the latter by a single layer of epithelial cells. The cells of the epithelial layer secrete digestive enzymes during seed germination which digest the nutrients in the endosperm and absorb them. These nutrients have been shown to help in the development and growth of the seedling.

The starchy endosperm occupies about 2/3 of the total seed and is located in the broader part of the maize grain. There is a continuous layer of large cubical cells situated immediately beneath the hull, called the aleuronic layer, which also contains protein granules. The rest of the endosperm consists of starch-laden cells, which are of particular interest to food scientists (Wellner *et al.*, 2010).

Starch is the basic source of energy for the majority of the world's population. In human nutrition, starch plays a major part in supplying the metabolic energy that enables the body to perform its different functions. Recent studies suggest that slowly

digestible starch and resistant starch have significant implications on human health (Han *et al*., 2006, Miao *et al*., 2009).

Two polysaccharides can be isolated from the starch present in the maize kernels: amylose and amylopectin. Amylopectin is a highly branched molecule and it is considered to comprise the crystalline structure within the granule: the branches of the amylopectin molecules are present as radially orientated crystalline lamellae within the granule. Amylose is an essentially linear molecule which is thought to be found predominantly in the amorphous regions within the starch granule. There is considerable interest in mapping the nature of the carbohydrate distribution within granules and various labelling procedures (Ridout *et al*., 2004, Capron *et al*., 2007) have been used in attempts to locate amylose or amylopectin structures, and to visualise the growth ring structures within starch granules for isolated intact granules, or within sectioned plant material. It has also been suggested that imaging of starch within seeds may also offer a way of screening starch varieties for novel structures, and for characterising any variability of intra- and inter-granule structure, arising from natural or induced mutations in biosynthesis (Matsushima *et al*., 2010).

Infrared microspectroscopy is commonly used to study plants and their mutants and to monitor changes during their development (Barron *et al*., 2005). Moreover, this technique gives unique information about the molecular structures and interactions of the major components in situ. However, as mentioned before, the use of this technique to study biological specimens at a more detailed level is generally diffraction limited to around 5-10 μm. Other recently developed techniques used for

studying starches include screening (Parker *et al.*, 2008) and staining (Wellner *et al.*, 2010).

6.5.3. PTMS studies on wild and mutant type maize

This part of the chapter presents the results from the PTMS experiments carried out on the wild and mutant type maize specimens. The experiments were carried out using the methodology developed and used on the model system – polystyrene spheres and the treated and untreated E.coli bacterial cells. Kernels of the wild and mutant type maise were obtained from the Institute of Food Research, Norwich, UK. As described before, these were chosen in order to characterise any variability in the granule structure induced by a mutation of the starch branching enzyme. The mutant maize is an isogenic mutant which gives rise to a high amylose starch. In studies on isolated mutant maize starches it is apparent that this simple mutation gives rise to a heterogeneous population of starch granules with novel physical properties (Chen *et al.*, 2006, Jiang *et al.*, 2010).

The images and spectra were obtained from endosperm areas, i.e. the starch containing parts, of non-sliced samples, e.g. whole grain of maize, as in a preliminary study it was established that using mica as a sample holder/substrate can greatly reduce the intensity of the photothermal signal because it acts as its own heat sink and so the thermal waves are attenuated. The data obtained from the PTMS experiments is compared to data acquired using conventional FTIR microscopy.

The results from the PTMS experiments are presented in the figures below. From the example topographical AFM images (**Figure 6.22** and **6.23**) of the studied maize types obtained with Wollaston wire probe and with contact mode tip it is evident that there are no significant differences in their microstructures. It is also clearly seen that the quality and contrast of the images in contact mode is much better compared to the ones obtained with the Wollsaton wire probes. As suggested previously, this difference in image quality is believed to be caused by the shape and size of the thermal probe. Nevertheless, the images obtained in this study are comparable to those available in the literature (Wellner *et al.*, 2010).

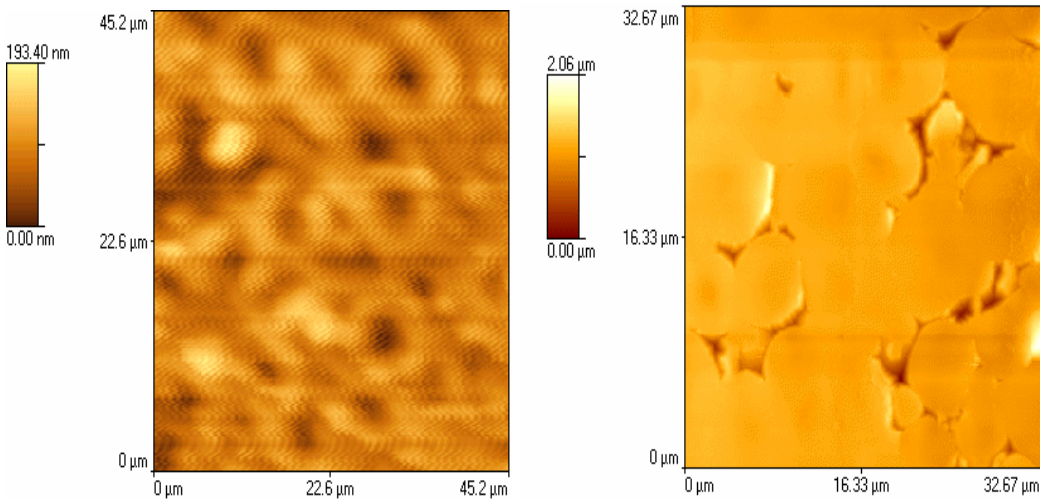

(a) **(b)**

Figure 6.22 Topographical AFM image of the endosperm of mutant maize with Wollaston probe **(a)** and **(b)** contact mode AFM image

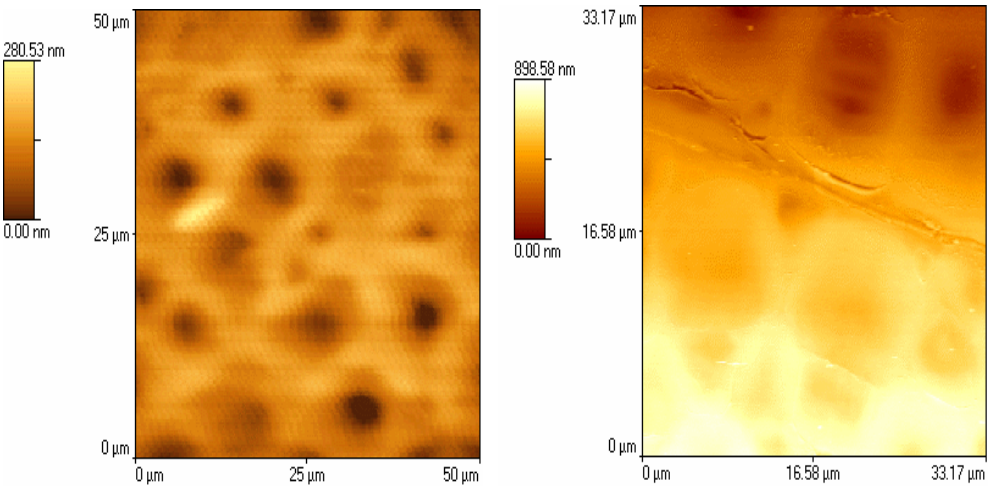

(a) **(b)**

Figure 6.23 Topographical image of the endosperm of wild type maize with Wollaston probe **(a)** and **(b)** contact AFM mode images

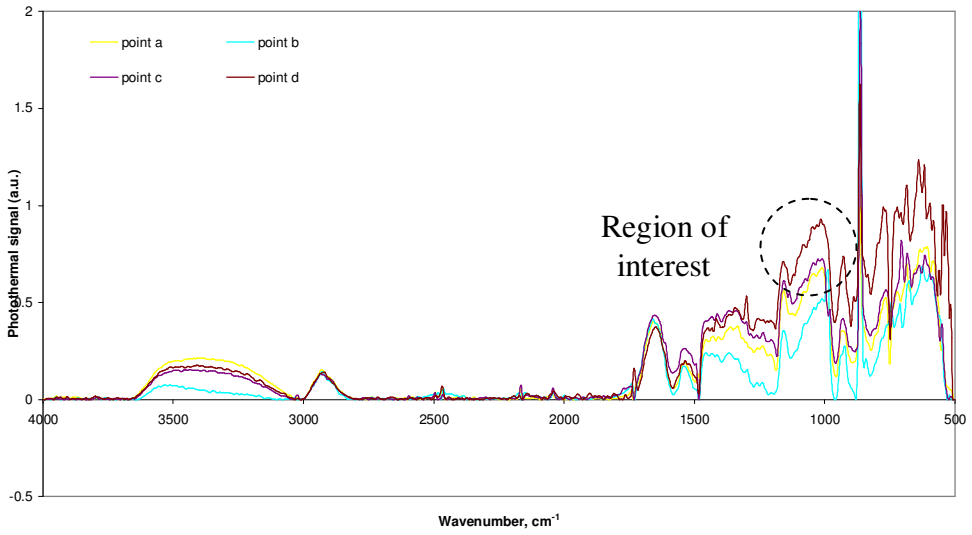

Figure 6.24 Photothermal spectra from 4 different points in the mutant maize endosperm sample. The region of interest where significant spectral differences can be seen has been highlighted

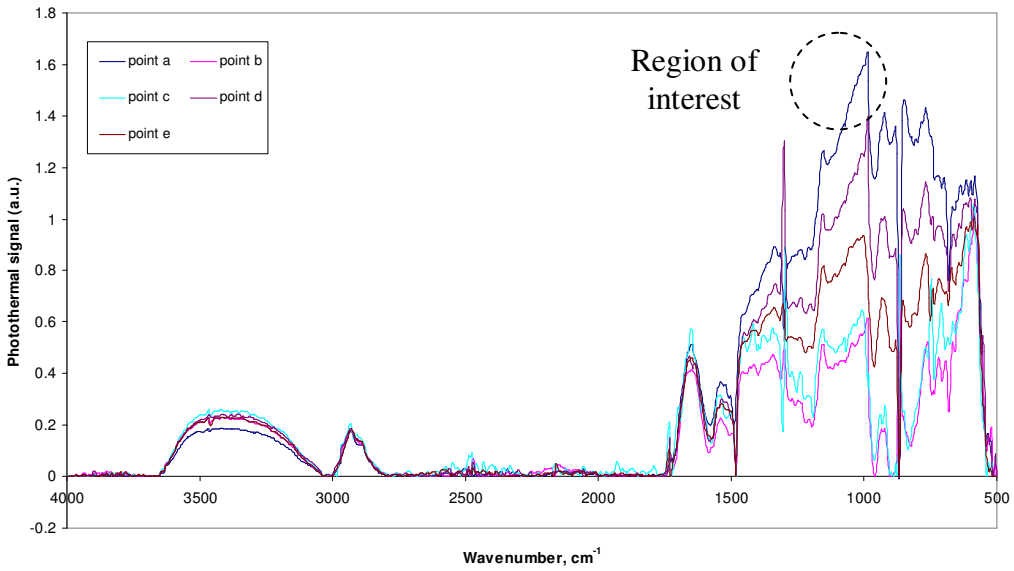

Figure 6.25 Photothermal spectra from 5 different points in the wild type maize endosperm sample. The region of interest where significant spectral differences can be seen has been highlighted

However, it is clearly evident that the preliminary data obtained with photothermal microspectroscopy, shown in **Figures 6.24** and **6.25**, have yielded very promising spectra from the maize starch granules. From the average spectra from mutant and wild-type maize seed sections that have been combined and shown in **Figure 6.26** it can be clearly seen that there is one marked difference in the starch bands: the 998 cm^{-1} component is noticeably higher in the mutants than in the wild type, and the main peak at 1022 cm^{-1} lower, whereas the other major starch bands were unchanged. The band at 1022 cm^{-1} is assigned to the amorphous phase, whereas granular starches are characterised by a band at 1000 cm^{-1}. However, here it is also important to mention that the ratio of these two bands can also be highly influenced by water content and may in this case indicate a different short-range order of helices (Capron

et al., 2007), because the 1047 cm^{-1} band which has been shown to be linked to starch crystallinity is almost unchanged.

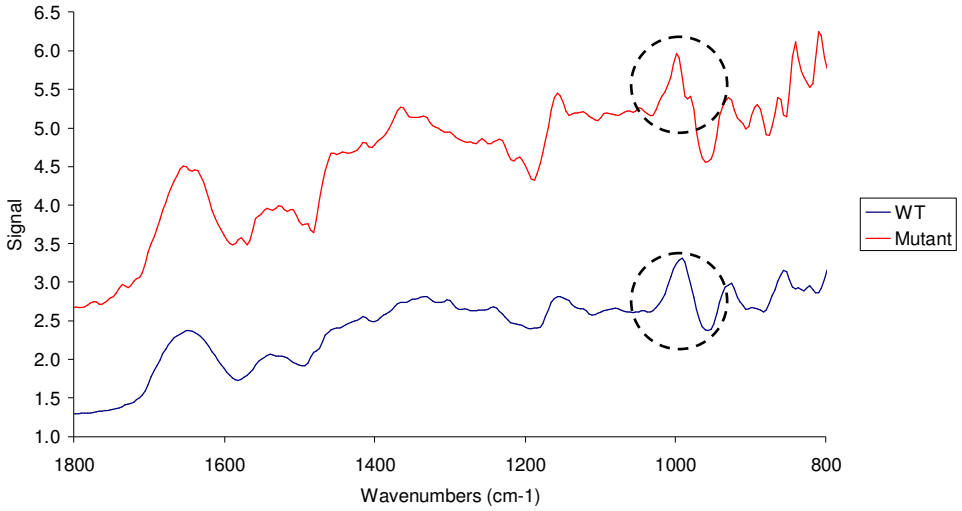

Figure 6.26 Average of photothermal spectra from 5 different points each in the wild type and mutant maize endosperm samples. The peaks of interest have been indicated by the circles in the graph above

The data obtained in this study is in complete agreement with the data obtained in a parallel study conducted by members from the IFR team, who examined the same specimens by means of conventional FTIR spectroscopy. The results presented in **Figure 6.27** show the same differences between the mutants and wild type material, although they do not appear as clear as the ones seen in the PTMS spectra. Nevertheless, they are also indicative of the fact that this variability may arise not just from chemical composition but also from physical differences between the granules. However, there is on big drawback in the FTIR methodology, which lies in the fact that by using it, it is not possible to focus on and thus obtain spectra exclusively from

individual starch granules, let alone different parts of individual granules, which the photothermal approach obviously offers.

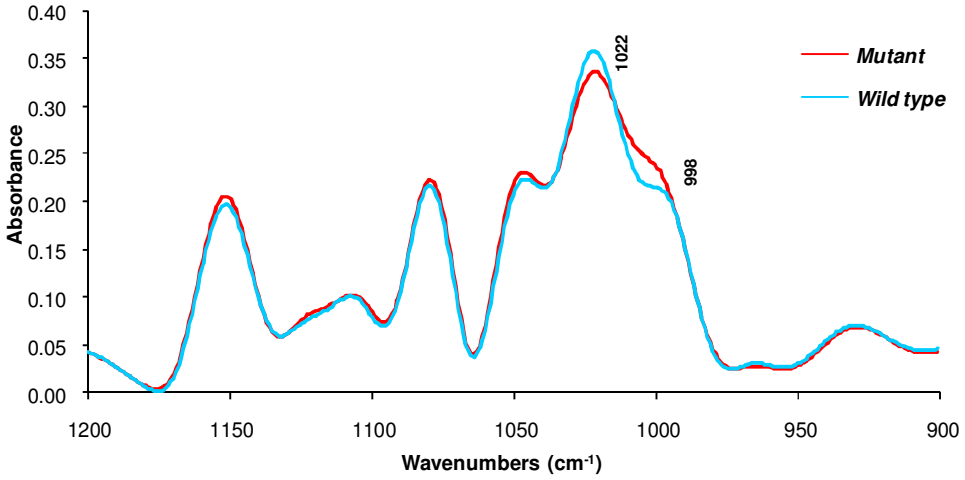

Figure 6.27 Starch bands in Fourier-deconvoluted average spectra of maize mutant and wild type seeds (*data kindly provided by Dr Klaus Wellner, Institute of Food Research, Norwich, UK*)

6.5.4. Summary of observations – maize samples

In summary, it can be said that the preliminary results of this proof of concept study clearly demonstrate that Photothermal Microspectroscopy (PTMS) can also be successfully employed in the study of other biological systems, such as different types of maize.

This principle of the methodology, as described before, is similar to photoacoustic spectroscopy except that the measurement is made at a point on the surface rather than as an average of the whole surface. The spatial resolution is not diffraction

limited, instead it is limited by the size of the tip of the thermal probe and the thermal diffusion length of the thermal waves created by the movement of the mirror of the interferometer.

These initial spectra, which represent the first attempt to apply this technique to plant tissues, are indeed very promising, but unfortunately they suffer from two very serious shortcomings: 1) Spectra from individual spots are quite noisy. Averaging over several spots can improve the signal to noise ratio, but that negates the desired mapping of spatial heterogeneity. 2) The signal originates from an area around the tip position which depends on tip size, optical setup, and thermal diffusion in the sample. In the current instrument this is still too large to measure individual parts of starch grains.

7. Conclusions and Suggestions for Further Work

Overall Conclusions

(1) Atomic Force Microscopy (*AFM*) in combination with Micro/Nano-Thermal Analysis and Infrared Spectroscopy (Photothermal Microspectroscopy) has been shown to be a unique set of experimental techniques that can be used not only for high-resolution imaging, but also to simultaneously study interactions between different material systems. These techniques have been successfully applied to a number of model systems, including Paracetamol & polystyrene spheres, but more importantly in the study of the interactions of bacterial cells (e.g. E.coli) with pharmaceutically relevant materials, such as antibiotics (e.g. Ampicillin).

(2) In this largely experimental research it was clearly demonstrated that the use of a lock-in amplifier leads to a significant reduction in the signal to noise ratio, which leads to an increase in the sensitivity of the probes used. It is strongly believed that this would undoubtedly provide greater confidence and improved consistency in any further measurements carried out using Microspectroscopy.

(3) The bacterial sample preparation and treatment technique employed in this study gave not only consistent results, but also offered the opportunity to generate images of excellent quality in all AFM modes used. It was found that the best contrast achieved in this study was in Pulse Force Mode (PFM), which is not commonly used for imaging of bacterial cells. PFM images of the studied bacterial system were also successfully obtained for the first time ever with heated nano probes. It was also

demonstrated that imaging at increased probe temperatures results in higher quality images compared to conventional ones. Based on the results, it is strongly believed that PFM imaging at elevated probe temperatures together with its ability to provide data for the mechanical properties of the studied biological system is indeed a unique methodology which would undoubtedly provide further insight to understanding the phenomenon of adhering of E.coli to surfaces, for example to hospital equipment. Finally, it was shown that Atomic Force Microscopy offers greater potential and flexibility for cell examination compared to an alternative Electron Microscopy technique.

(4) AFM was also successfully used in studying the effects of pharmaceutically relevant materials on bacterial cells. From the images of the Ampicillin treated E.coli cells it was evident that in the early stages of the treatment there were not any obvious changes to the structure of the individual cells. However, after approximately 8 hours of treatment it became apparent that changes to the cell wall began to occur; and after 12 hours of treatment the degradation of the cell wall and membrane had progressed to a very advanced stage so that it became difficult to distinguish individual cells. Two main reasons that account for the detrimental action of the antibiotic were considered: inhibition of cell division by the creation of nanopores at the apical ends of the E. coli cells and leakage of the cell contents. It can therefore be suggested that the damage to the cell wall structure would create an imbalance between the inner and outer osmotic pressures of the cell, resulting in the loss of inner contents and consequent cell death. It was also concluded that there may be a range of antibiotic concentrations that have similar effect when used on bacterial cells. Hence,

it seems plausible that AFM may also find useful application in the determination of the optimum antibiotic concentration needed for the treatment of for example bacterial infections

(5) Atomic Force Microscopy was successfully employed to measure the interactive forces between different types of probes and a variety of material systems. The developed methodology, initially applied in the study of a model system (Paracetamol tablets), was then used in the study of E.coli bacterial cells; where the use of heated probes was also successfully utilised for the first time ever. It was clearly demonstrated that the adhesive forces decrease with increase in temperature. It was proposed that this finding may be indicative of structural and/or compositional changes within the systems in question. From the shapes of the obtained curves it was evident that there was no long distance of detachment and sequential breaking which is indicative of a sudden break in contact. Therefore, there was no indicative continued stretching of the cell, localised stretching of cell surface regions still in surface contact, stretching and rupturing of adhesive molecules and the 'peeling' of the cell away from the surface. Undoubtedly, it can be concluded that the AFM force measurement capability offers great opportunities for further investigations into the properties and function of the microbial cell surface and their interactions not only on its own, but also for example with pharmaceutically relevant materials.

(6) Photothermal Microspectroscopy was developed and initially applied in the study of a model system - polystyrene spheres. The methodology was then successfully used to further investigate and characterise the complex interactions of E.coli

bacterial cells and the antibiotic system - Ampicillin. Vibrational bands, associated with spectral regions, where significant differences of interest might occur were successfully identified. The results obtained in this research clearly demonstrated that by employing Photothermal Microspectroscopy it is not only possible to monitor changes occurring in the cell-cycle, but also to study interactions between cells and pharmaceutically relevant materials, which would simultaneously provide additional information for structural changes taking place within the studied biological systems. The reductions in spectral intensity seen after examination of cells after one week incubation and those treated with Ampicillin is also believed to be further proof that cell cycle effects & structural changes may be successfully monitored using Photothermal Microspectroscopy. It was also demonstrated that PTMS can also be successfully employed in the study of other biological systems, such as maize.

Suggestions for Further Work

(1) AFM imaging of other biological systems

Atomic Force Microscopy with its wide range of applications, high spatial resolution and ability to image specimens in their natural state, with in many cases minimal sample preparation, will undoubtedly continue to be extensively used in the future for imaging of biological species. It is hoped that Pulse Force Mode imaging at both room at elevated temperatures will become more routinely used in everyday characterization, as it not only offers the possibility to image the surface of the specimen, but also to probe its mechanical properties. It is also strongly believed that the application of AFM in the study of other biological systems will also aid the

refining and further development of the instrumentation involved in this methodology.

(2) Further development of thermal probe techniques

The results in this research are thought to have laid the foundations of further developments in the area of thermal probe techniques that can be used in the study for the physical and chemical characterization of interactions between biologically and pharmaceutically relevant materials, e.g. bioadhesives. It is hoped that the future research will be focused in exploring the use of coated heated probes for measuring the adhesion between the coating and the surface that it is placed in contact with. In actual fact, here in a very brief pilot study, we were able to successfully produce a series of force distance curves for uncoated and HPMC-coated thermal probes, examples of which are provided in the figure below. It is evident that the uncoated probe showed very little detectable hysteresis on approach and withdrawal while it is clear that the coated probe shows a distinct and quantitative adhesion to the surface as measured by the pull-off force, thereby demonstrating that the coated tip is allowing for more accurate measurement of adhesion of the coating material with the substrate of interest. It is strongly believed that this approach may indeed provide an additional tool to scientists investigating, for example interactions between different types of drugs, carrier systems and cellular materials. The other advantage of this approach is that it allows data for these interactions to be obtained simultaneously as a function of temperature.

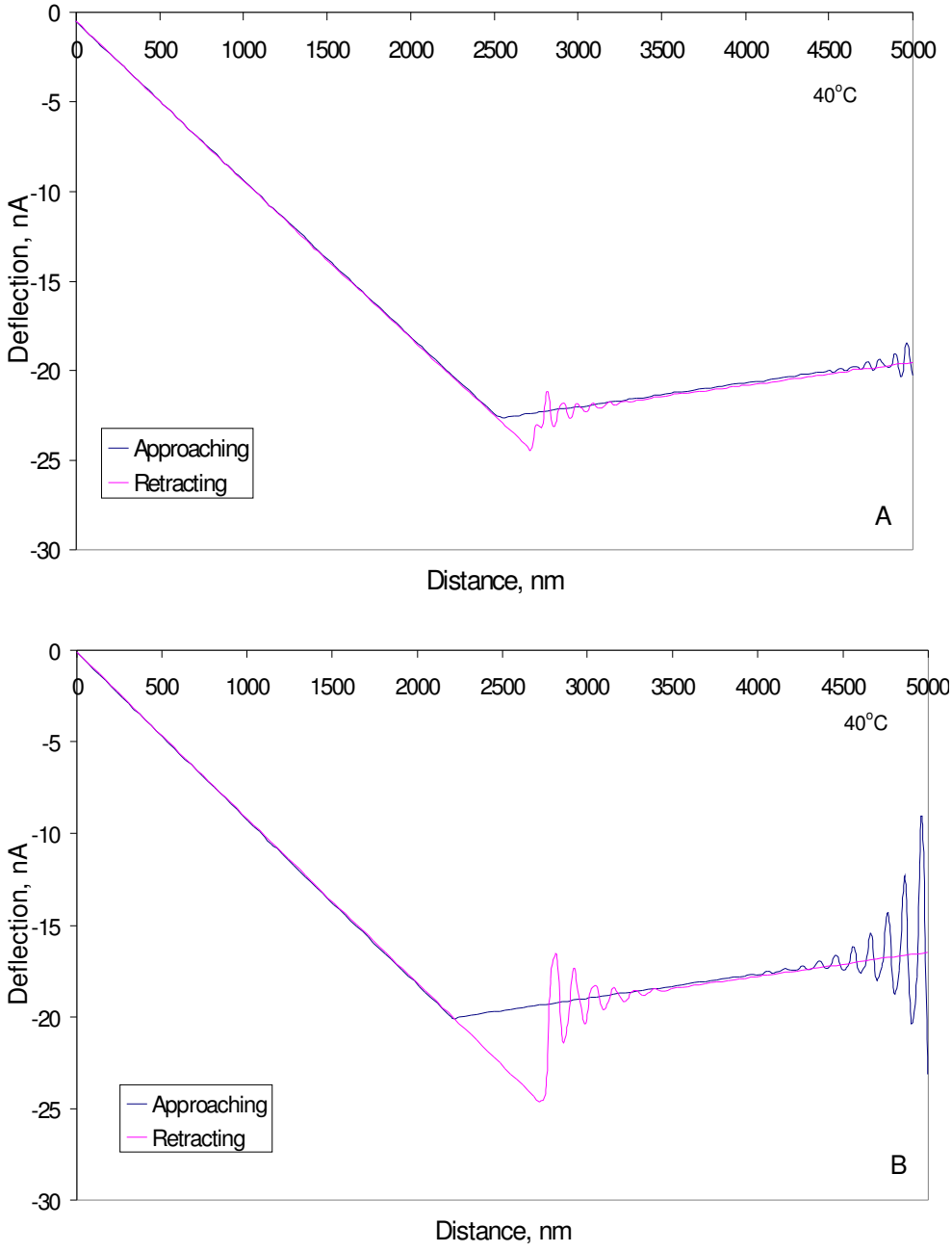

Example FDC on clean glass with uncoated (A) and hydroxypropyl methylcellulose (HPMC) - coated Wollaston tip (B)

(3) Further development of Photothermal Microspectroscopy

While in this research it was shown that the PTMS technique can address current experimental problems, for example associated with FTIR, the technique is far from routine and has various experimental problems, such as large tip size and low signal to noise ratio. To date all the published work has been carried out with a Wollaston wire probe, the tip of which is a loop of platinum 5 μm in diameter that has a contact area of about 0.5 μm squared. Over a number of years the equipment has been optimised for this probe in terms of maximising the signal to noise. There are now a number of commercially available thermal probes with much smaller tips that provide much higher spatial resolution, e.g. nano probes. To date no attempt has been made to optimise photothermal spectroscopy with these probes. We do not currently know what the best performance of the higher spatial resolution probes might be. Also, it might seem surprising that the current optics uses relatively small part of the beam. This arises because of the particular AFM used for all of the photothermal experiments to date; while the Explorer AFM has a number of positive attributes it has a very restricted optical access for the IR beam. It is believed that in the future this will be improved, for example by moving to a platform with much more open optical access from above and employ the use of more advanced AFMs which should enable to improve not only the beam power but the overall performance of the equipment. Finally, it is also believed that chemometric analysis will become vitally important for the data analysis, especially for biological samples, where the spectral differences as shown in this research are very small.

List of References

Adams, E.L., *PhD Thesis*, University of East Anglia, 2001.

Adya, A.K., Canetta, E., and Walker, G.M., *FEMS Yeast Res.*, **6**, 2006, p.120.

Ahimou, F., Denis, F.A., Touhami, A. and Dufrene, Y.F., *Langmuir*, **18**, 2002, p.9937.

Ahimou, F., Touhami, A. and Dufrene, Y.F., *Yeast*, **20**, 2003, p.25.

Alberts, B., Johnson, A., Lewis, J., Raff, M., Roberts, K., Walter, P., in *Molecular Biology of the Cell*, Garland Science, New York, 2002.

Amalaradjou, M.A.R., Hoagland, T. & Venkitataryanan, K., *Int. Journal of Food Microb.,* **141**(1-2), 2010, p.125.

Aoki, T., Hiroshima, M., Kitamura, K., Tokunaga, M., and Yanagida, T., *Ultramicroscopy*, **70,** 1997, p.45.

Arce, F.T., Avci, R., Beech, I.B., Cooksey, K.E. and Wigglesworth-Cooksey, B., *Biophys. J.*, **87,** 2004, p.4284.

Avravomivic, M., Petrovic, S.D., Kalman, E., Milosavljevic, T., Reljin, I., Reljin, B., Bogdanovic, G., Baltic, V.V., and Keresztes, Z., *J. Serb.Chem.Soc.*, **70** (6), 2005, p.823.

Bertani, G.*, J. Bacteriology,* **186**, 2004, p.595.

Beyer, T., Day, G. M. and Price, S. L., *J Am Chem Soc*, **123**, 2001, p.5086.

Bhushan, B., in *Introduction - Measurement techniques and applications. Hanbook of Micro/Nano Tribology*. B. Bhushan. Boca Raton, CRC Press, 1999.

Bialkowski, S. E., in *Photothermal spectroscopy methods for chemical analysis*, Logan, UT, USA, John Wiley and Sons, Inc, 1996.

Binning, G., Rohrer, H., Gerber, Ch., and Weidel, E., *Phys. Rev. Lett.*, **49**, 1982, p.57.

Binning, G., Quate, C.F., and Gerber, C., *Phys. Rev. Lett.*, **56**, 1986, p.930.

Boldyreva, E. V., Shakhtshneider, T. P., Ahsbahs, H., Sowa, H. and Uchtmann, H., *J. Therm. Anal. Cal.*, **68**(2), 2002, p.437.

Bolshakova, A.V., Kiselyova, O.I., Filonov, A.S., Frolova, O.Yu., Lyubchenko, Y.L., Yaminsky, I.V., *Ultarmicroscopy*, **86**, 2001, p.121.

Bolshakova, A.V., Kiselyova, O.I. and Yaminsky, I.V., *Biotechnol. Prog.*, **20** (6), 2004, p.1615.

Bond, L., Allen, S., Davies, M. C., Roberts, C. J., Shivji, A. P., Tendler, S. J. B., Williams, P. M. and J., Z., *Int. J. Pharm.*, **243,** 2002, p.71.

Bowen, W. R., Hilal, N., Lovitt, R. W. and Wright, C. J., *Colloids Surface A*, **136**(1-2), 1998, p.231.

Bozec, L., *PhD thesis*, University of Lancaster, 2003.

Braga, P.C. and Ricci, D., *Antimicro. Ag. Chemo.*, **42**, 1998, p.18.

Bruce Alberts, B., Johnson, A., Lewis, J., Raff, M., Roberts, K. and Walter, P. in *Molecular Biology of the cell*, 4th Edition, 2002.

Bustamante C., Erie, D.A., Keller, D., *Current Opinion in Structural Biology*, **4**, 1994, p.750.

Caliber Operations Manual, Veeco Instruments Limited, 2006.

Cameron, R. E. and Donald, A. M., *J. Microscopy*, **173**, 1994, p.227.

Canetta, E., Adya, A.K. and Walker, G.M., *FEMS Microbiol. Lett.*, **255**, 2006, p.308.

Cao, T., Tang, H., Liang, X., Wang, A., Auner, G.W., Salley, S.O. and Simon N, K.Y., *Biotechnol. and Bioeng.,* **94** (1), 2006, p167.

Chen, L., Shiming, L. and Lin, L., World *J. Microbiol. Biotechn.*, **22**, 2006, p.565.

Cooper, G.M. & Hausman, R.E., in '*The Cell*', 5th ed., Sinauer Associates, 2009.

Costa, K.D., *Disease Markers*, **19**, 2004, p.139.

Craig, D.Q.M., Kett, V.L., Andrews, C.S. and Royal, P.G., *J. of Pharm. Sci*., **91**(5), 2002, p.1201.

da Silva Junior A., and Teshke, O., *Biochim. Biophys. Acta*, **1643**, 2003, p.95.

da Silva Junior A., and Teshke, O., *W. J. Microbiol.Biotech*., **21**, 2005, p.1103.

de Wet, F. N., Gerber, J. J., Lötter, A. P., van der Watt, J. G. and Dekker, T. G., *Drug Dev. Ind. Pharm* **24**(5), 1998, p.447.

Di Martino, P., Conflant, P., M., D., Huvenne, J.P. and Guyot-Hermann, A. M., *J. Therm. Anal.*, **48**, 1997, p.447.

Di Martino, P., Guyot-Hermann, A.M., Conflant, P.M.D. and Guyot, J.C., *Int. J. Pharm.*, **128**, 1996, p.1.

Doktycz, M.J., Sullivan, C.J., Hoyt, P.R., Pelletier, D.A., Wu, S. & Allison, D.P., *Ultramicroscopy*, **97**, 2003, p.209.

Donald, A. M., *Nature Materials* **2**, 2003, p.511.

Drug Information, American Society of Health-System Pharmacists, 2006.

Dufrene, Y.F., Boonaert, C.J.P, van der Mei, H.C., Busscher, H.J. and Rouxhet, P.G., *Ultramicroscopy*, **86**, 2001, p.113.

Dufrene, Y.F., *J. Bacteriol*., **184**, 2002, p.5205.

Dufrene, Y.F., *ASM News*, **69**, 2003, p.438.

Dufrene, Y.F., *J. Bacteriol*., **186**, 2004, p.3283.

Dufrene, Y.F., *Nat. Rev. Microbiol*., **2**, 2004, p.451.

Eckert, R., Jeney, S. and Horber, J.K.H., *Cell Biol. Inter*., **21** (11), 1997, p.707.

Elkirat, K., Burton, I., Dupres, V., and Dufene, Y.F., *J. Microsc.*, **218** (3), 2005, p.199.

Erbe, E. & Pooley, C., in ARS Image Gallery, 2005; Rocky Mountain Laboratories, NIAID, NIH, 2005.

Explorer Operations Manual, Veeco Instruments Limited, 2000.

Filip, M., Back, P. & Vemfleteren, J., *Free Radical Biology & Medicine*, **45**(5), 2008, p.705.

Fullwood N.J., *Nat. Chem. Biol*., **3**, 2007, p.435.

Gad, M. and Ikai, A., *Biophys. J*., **69**, 1995, p.2226.

Gad, M., Itoh, A. and Ikai, A., *Cell Biol. Inter*., **21**, 1997, p.697.

Galop, M., *Pharm. Res.*, **22**(2), 2005, p.293.

Gazi E., Dwyer J., Lockyer N., Gardner P., Vickerman J. C., Miyan J., Hart C.A., Brown M., Shanks J. H., and Clarke N., *Faraday Discuss*., **126**, 2004, p.41.

German, M.J., Hammiche, A., Ragavan, N., Tobin, M.J., Cooper, L.J., Matanhelia, S.S., Hindley, A.C., Nicholson, C.M., Fullwood, N.J., Pollock, H.M. & Martin, F.L., *Biophysical Journal*, **90**(10), 2006, p.3783.

Giordano, F., Rossi, A., Bettini, R., Savioli, A., Gazzaniga, A. and Novak, C., *J. Therm. Anal. Cal.*, **68**(2), 2002, p.575.

Gordon, R.C., Regamey, C. & Kirby, W.M., *Antimicrobial agents and chemotherapy,* **6**, 1972, p.504.

Gradinaru, C.C., Martinsson, P., Aartsma, T.J., and Schmidt, T., *Ultarmicroscopy*, **99**, 2004, p.23.

Grandy, D. B., PhD thesis, Loughborough University, 2002.

Grude O., Hammiche A., Pollock H., Bently A.J., Walsh M.J., Martin F.L. and Fischer, H., *Macromolecules*, **38**, 2005, p.844.

Grude, O., Nakamura, T., Hammiche, A., Bentley, A.J., Martin, F.L., Pollock, H.M., Kinoshita, S. & Fullwood, N.J., *Vibrational Spectroscopy*, **49**(1), 2009, p.22.

Fullwood N.J., *Journal of Microscopy,* **228** (3), 2007, p. 366.

Hammiche, A., Hourston, D. J., Pollock, H. M., Reading, M. and Song, M., *J. Vac. Sci.Technol. B*, **14**(2), 1996, p.1486.

Hammiche, A., Price, D.M., Dupas, E., Mills, G., Kulik, A., Reading, M., Weaver, J.M.R., and Pollock, *J. Microsc*., **199**(3), 2000, p.180.

Hammiche, A., Reading, M., Grandy, D., Price, D., German, M., Bozec, L, Weaver, J.M.R., Stopford, P., Mills, G. and Pollock, H.M. in *Proc. 12th International Conference on Scanning Tunnelling Microscopy/spectroscopy and related techniques*, Eindhoven, The Netherlands, American Institute of Physics Conference Proceedings, 696, Melville, USA, 2003.

Hammiche, A., German, M.J., Hewitt, R., Pollock, H.M. and Martin, F.L., *Biophysical Journal*, **88**(5), 2005, p.3699.

Han, S.W., Nakamura, C., Obataya, I., Nakanura, N. and Miyake, J., *Biosensors and Bioelectronics*, **20**, 2005, p.2120.

Hanna, A., Berg, M., Stout, V. and Razatos, A., *Appl. Env. Microbiol*., **69** (8), 2003, p. 4474.

Hansma, H.G., Laney, D.E., Bezanilla, M., Sinsheimer, R.L., *Biophys.J*., **68**, 1995, p.1672.

Hansma, H.G., *J. Vac. Sci. Technol. B*, **14** (2), 1996, p.1390.

Harding, L., *PhD Thesis*, University of East Anglia, 2007.

Harding, L., Qi, S., King, W.P., Reading, M. & Craig, D.Q.M., *Pharmaceutical Research*, **24**(11), 2007, p.2048.

Harding, L., Qi, S., Hill, G., Reading, M. & Craig, D.Q.M., *International Journal of Pharmaceutics*, **354**(1-2), 2008, p.149.

Hashimoto, T. and Morikawa, *Jpn. J. Appl. Phys.*, **42** (2), 2003, p.706.

Hassan,E., Heinz, W.F., Antonik, M.D., D'Costa, N.P., Nageswaran, S., Schoenenberger, C. and Hoh, J.H., *Biophys. J.*, **74**, 1998, p.1564.

Hermansson, M., *Colloids and Surf., B, Biointerfaces*, **14**, 1999, p.105.

Hu, D., Micic, M., Klymyshyn, N., Suh, Y.D. and Lu, H.P., *J. Lumin.*, **107**, 2004, p.4.

Kasas, S. and Ikai, A., *Biophys. J.*, **68**, 1995, p.1678.

Kailas, L., Ratcliffe, E.C., Hayhurst, E.J., Walker, M.G., Foster, S.J., Hobbs, J.K., *Ultramicroscopy***, 109**(7), 2009, p.775.

Kajiyama, T., Tanaka, K., Ge, S.-R. and Takahara, A., *Prog. Surf. Sci*, **52**(1), 1996, p.1.

King, W.P., *J Micromech Microeng*, **15**, 2005, p.2441.

Lo, Y., Huefner, N.D., Chan, W.S., Stevens, F., Harris, J.M., and Beebe, T.P.Jr., *Langmuir*, **15**, 1999, p.1373.

Lo, Y., Zhu, Y. and Beebe, T.P., Jr., *Langmuir*, **17**, 2001, p.3741.

Lower, S.K., Tadanier, C.J., Hochella, Jr, M.F., *Geochim. Cosmochim. Acta*, **64**, 2000, p.3133.

Lund, W., in *The pharmaceutical codex - principles and practice of pharmaceutics*, London, The Pharmaceutical Press, 1994.

Machida, K., Agemato, H., Matsumoto, N., Fujii, Y., Kabumoto, H. & Doi, S., *Biotechnology, and Biochemistry Science***, 70**, 2006, p307.

Marler, B. in on-line *Journal of food poison*, 2009.

Marti, O., Stifter, T., Waschipky, H., Quintus, M. and Hild, S., *Colloid Surface A*, **154**, 1999, p.65.

Meredith, P. and Donald, A. M., *J. of Microscopy*, **181** (1), 1996, p23.

MicroThermal Analyzer - Operator's Manual, TA instruments, Inc., New Castle, DE, 2000.

Milani, M., Ballerini, M., Batani, D., Squadrini, F., Cotelli, F., Poletti, G., Pozzi, A., Eidmann, K., Stead, A. and Lucchini, G., *Eur. Phys. J. Appl.Phys.*, **26**, 2004, p.123.

Moffat J.G., Mayes A.G., Belton P.S., Craig D.Q.M., and Mike Reading, *Anal. Chem.*, **82**, 2010, p.91.

Moon I., Androsch, R., Chen, W. and Wunderlich, B., *J. Thermal. Anal. Cal.*, **59**, 2000, p.187.

Morris, V.J., Kirby, A.R., and Gunning, A.P., in *Atomic force microscopy for biologists*, Imperial College Press, London, 1999.

Morrow, J.B., Stratton, R., Yang, H.H., Smets, B.F. and Grasso, D., *Env. Sci. Technol.*, **39**, 2005, p.6395.

Murphy, J. R., Andrews, C. S. and Craig, D. Q. M., *Pharm. Res.*, **20**(3), 2003, p.500.

Murray, A., Lever, T., Reading, M. and Price, D. M., *Materials world*, **6**(10), 1998, p.615.

nanoTA User Manual, TA Instruments, Inc., New Castle, DE, 2006.

Nguyen, T.H., Choi, S.S., Kim, D.W., Kim, Y.U., *Journal of the Korean Physical Society*, **50**(6), 2007, p.1942.

Nichols, G. and Frampton, C. S., *J. Pharm. Sci.*, **87**(6), 1998, p.693.

Nojavan, S., Grassempour, A., Bashour, Y., Darbandi, M.K. & Ahmadi, S.H., *J. of Pharm. & Biomed. Analysis*, 36(5), 2005, p.983.

Oberringer, M., English, A., Heinz, B., Gao, H., Martin, T. and Hartmann, U., *Eur. Biophys. J.*, **32**, 2003, p.620.

Odlyha, M., Cohen, N.S., Foster, G.M., Aliev, A., Verdonck, E., and Grandy, D., *J. Thermal. Anal. Cal.*, **71** (3), 2003, p.939.

Ong, Y., Razatos, A., Georgiou, G. and Sharma, M.M., *Langmuir*, **15**, 1999, p.2719.

Oulevey, F., Burnham, N.A., Gremaud, G., Kulik, A.J., Pollock, H.M., Hammiche, A., Reading, M., Song, M., and Hourston, D.J., *Polymer*, **41**, 2001, p.3087.

Pasquali, F., Kehrenberg, C., Manfreda1., G & Schwarz, S., *Antimicrob. Chemotherapy,* 55 (4), 2005 p.562.

Patel, D., Smith, A.W., Grist, N., Barnett, P., Smart, J.D*., J. Control Release*, **61**, 1999, p.175.

Patel D, Smith J.R., Smith A.W., Grist N., Barnett P. and Smart J.D., *International Journal of Pharmaceutics*, **200**, 2000, p.271.

Pelling, A.E., Li, Y., Shi, W., and Gimzewski, K., *PNAS*, **102**, 2005, p. 6484.

Pelling, A.E., Sehati, S., Grala, E.B., Valentine, J.S., Gimzewski, J.K., *Science*, **305**, 2004, p.1147.

Pereira, R. and Geibel, J., *Mol. Cell. Biochem.*, **201**, 1999, p.17.

Perry, C.C., Weatherly, M., Tiffany, B. & Alexandrine, R., *Journal of the science of food and agriculture*, **89**(6), 2009, p.958.

Peterson, M. L., McIlroy, D., Mustonen, J. P., Oliveira, M. and Almarsson, Ö., *Cryst. growth design*, **3**(5), 2003, p.761.

Pfister, G., Stroh, C.M., Perschinka, H., Kind, M., Knoflach, M., Hinterdorfer, P. and Wick, G., *J.Cell Sci*., **118** (8), 2005, p.1587.

Pollock, H. M., Burnham, N. A. and Colton, R. J., *J. Adhesion* **51**, 1995, p.71.

Pollock, H.M., and Hammiche A., *J. Phys. D: Appl. Phys*., **34**, 2001, p.23.

Poole, K., Meder, D., Simons, K. and Muller, D., *FEBS Letters*, **565**, 2004, p.53.

Price, D. M., Reading, M., Hammiche, A. and Pollock, H. M., *Int. J. Pharm*, **192**, 1999, p.85.

Putman, C.A.J., van der Werf, K., Bart, G., Niek, F., van Hulst, F.B. & Segerink, J.G., *Ultramicroscopy*, **2**(42-44), 1992, p.1549.

Pylkki, R.J., Moyer, P.J., and West, P.E., *Jpn. J. Appl. Phys*., Part 1, **33**, 1994, p.3785.

Qi, S., Gryizke, A., Belton, P & Craig, D., *International Journal of Pharmaceutics*, **354** (1-2), 2008, p.158.

Ramachandran, V., Brady, M.F., Smith, A.R., Feenstra, R.M. and Greve, D.W., *Journal of Electronic Materials*, **27** (4), 1998, p.308.

Razatos, A., Ong, Y., Sharma, M.M., Georgiou, G., *Proc. Natl. Acad. Sci. USA*, **95**, 1998, p.11059.

Razatos, A., Ong, Y., Boulay, F., Elbert, D.L., Hubbell, J.A., Sharma, M.M. and Georgiou, G., *Langmuir*, **16**, 2000, p.9155.

Reading, M., Price, D. M., Grandy, D. B., Smith, R. M., Bozec, L., Conroy, M., Hammiche, A. and Pollock, H. M., *Macromol. Symp.*, **167**, 2001, p.45.

Reading, M. and Price, D. M., *United States Patent Application Publication*, 2003.

Rieti, S., Manni, V., Lisi, A., Giuliani, L., Sacco, D., D'Emilia, E., Cricenti, A., Generosi, R., Luce, M., and Grimaldi, S., *J. Microsc*., **213**, Part 1, 2004, p.20.

Robins-Browne, R. M., Bordun, A. M., Tauschek, M., Vicki, R., Bennett-Wood, J., Oppedisano, F., Lister, N. A., Bettelheim, K. A., Fairley, C. K., Sinclair, M. I. and Hellard, M. E., *Emerging Infectious Diseases*, **10**, 2004, p.1797.

Rodrigez, V.V., Busscher, H.J., Norde, W., Vries, J., Dijksta, R.JB., Stokroos, I. and van der Mai, H.C., *Appl. Env. Microbiol.*, **70**, 2004, p.5441.

Rolhion, N., Darfeuille-Michaud, A., *Inflammatory Bowel Diseases*, **13** (10), p.1283.

Rosa-Zeiser, A., Weilandt, E., Hild, S. and Marti, O., *Meas. Sci. Technol.*, **8**, 1997, p.1333.

Rotsch, C. and Radmacher, M., *Biophys. J.*, **78**, 2000, p.520.

Round, A.N., *PhD Thesis*, University of East Anglia, 1999.

Royall, P. G., Hill, V. L., Craig, D. Q. M., Price, D. M. and Reading, M. *Pharm. Res.*, **18**(3), 2001, p.294.

Royall, P. G., Kett, V. L., Andrews, C. S. and Craig, D. Q. M., *J. Phys. Chem. B* **105**, 2001, p.7021.

Salton, M.J.R. & Kim, K.S., *Structure.* in: *Baron's Medical Microbiology*, 4th ed., University of Texas Medical Branch, 1996.

Sanders, G.H.W., Roberts, C.J., Danesh, A., Murray, A. J., Price, D.M., Davies, M.C., Tendler, S.J.B. and Wilkins, M.J., *J. Microsc.*, **198**(2), 2000, p.77.

Schaer-Zammaretti, P. and Ubbink, J., *Ultramicroscopy*, **97**, 2003, p.199.

Seidel, K, in *Biological Control of Water Pollution*, University of Pennsylvania Press 1976.

Sezonov, G., Joselau-Petit, D. & Dari, R., *J. Bacteriol.*, **189**(23), 2007, p.8746.

Shao, Z.F., Yang, J., Somlyo, A.P., *An. Rev. Cel. Devel. Biol.*, **11**, 1995a, p.241.

Shao, Z.F.,Yang, J.,*Quart. Rev. Biophys.*, **28**,1995b, p.195.

Shao, Z.F., Mou, J., Czajkowsky, D.M., Yang, J., Yuan, J.Y., *Adv. Phys.*, **45**, 1996, p.1.

Sharma, S., Sen, P., Mukhopadhyay, S.N., Guha, S.K., *Colloids Surf. B: Biointer.,* **32**, 2003, p.43.

Shenai, M.B., Putchakayala, K.G., Hessler, J.A., Orr, B.G., Holl, M.M. and Baker Jr., J.R., *IEEE Transactions of Nanobioscience*, **3**, 2004, p.111.

Simon, A., Cohen-Bouhacina, T., Aime, J.P., Porte, M.C., Amedee, J. and Baquey, C., *Cell. Mol. Biol.*, **50**(3), 2004, p.256.

Six, K., Murphy, J., Weuts, I., Craig, D. Q. M., Verreck, G., Peeters, J., Brewster, M. and Van den Mooter, G., *Pharm. Res.*, **20**(1), 2003, p.135.

The Merck Index, Eds, Whitehouse station, NJ, Merck & Co., Inc., 2001.

Tobin, M.J., Chesters, M.A., Chalmers J.M., Rutten F.J.M., Fisher, S.E., Symonds I.M., Hitchcock, A., Allibone, R., and Dias-Gunasekara, S., *Faraday Discuss.*, **126**, 2004, p.27.

Tortora, G.J., Funke, B.R., Case, C.L., in *"Microbiology an introducrtion"* 9th Ed., Pearson Education, Inc, San Francisco, USA.

Touhami, A., Nysten, B. and Dufrene, Y.F., *Langmuir*, **19**, 2003, p.4539.

Touhami, A., Hoffmann, B., Vasella, A., Denis, F.A. and Dufrene, Y.F., *Microbiology*, **149**, 2003, p.2873.

Varki, A., Cummings, R. & Esko, J., in '*Essentials of Glycobiology*', Cold Spring Harbor Laboratory Press; 1999.

Velegol, S.B., Pardi, S., X.L., Velegol, D. & Logan, B.E., *Langmuir*, **19** (3), 2003, p.851.

Vollmann, J. & Rajcan, I., in *Handbook of Plant Breeding*, Oil Crops, Springer Science and Business Media, 2009.

Walker, G.M., in *Yeast Physiology and Biotechnology*, John Wiley & Sons, Chichester, West Sussex, 1998.

Walsh, M.J., Singh, M.N., Pollock, H.M., Cooper, L.J., German, M.J., Stringfellow, H., Fullwood, N.J., Paraskevaidis, E., Martin-Hirsch, P.L., & Martin, F.L., *Biochemical and Biophysical Research Communications*, **352**(1), 2007, p.213.

Walsh M.J., Hammiche, A., Fellous, T.G., Nicholson, J.M., Cotte, M., Susini, J., Fullwood, N.J., Martin-Hirsch, P.L., Alison, M.R. and Martin, F.L., *Stem Cell Research*, **3**, 2008, p.15.

Williams, D. H. and Fleming, I. in *Spectroscopy methods in organic chemistry*, London, McGraw Hill, 1997.

Woese, C.R., *Microbiological reviews*, **51**(2), 1987, p221.

Wong, C.S., Jelacic, S., Habeeb, R.L., Watkins, S.L., Tarr, P.I., *New England Journal of Medicine*, **342** (26), 2000, p.1930.

Wright, C.J. and Armstrong, I., *Surf. Interface Anal*., **38**, 2006, p.1419.

Wright, C.J. and Armstrong, I., *Microscopy Anal*., **21** (2), 2007, p. S11.

Yang, C., Keng. H. & Jia, C., *Biomedical Microdevices*, **9**(2), 2006, p.253.

Yang R., Xi, N., Fung, C.K.M., Lai, K.W.C., Seiffert-Sinha, K., Sinha, A.A., Zhang W., *Nano/Micro Engineered and Molecular Systems (NEMS)*, 2010, p.129.

Yu, M. and Ivanisevic, A., *Biomaterials*, **25**, 2004, p.3655.

Zalas-Wiecek, P. & Gospodarek, E., *Med. Dosw. Mikrobiol*., **61**(4), 2009, p.335.

Zammaretti, P., Fakler, A., Zaugg, F. and Spichiger-Keller, U., *Anal. Chem*., **72**, 2000, p.3689.

Zhao, C., Brinkhoff, T., Burchardt, M,, Simon, M., Wittstock, G., *Ocean Dyn*, **59**, 2009, p.305.

Zohar, O., Ikeda, M., Shinagawa, H., Inoue, H., Nakamura, H., Elbaum, D., Alkon, D.L., and Yoshioka, T., *Biophys. J.*, **74**, 1998, p.82.